INVESTIGATING FOAMING SOLUTIONS GENERATED BY NaOH EXTRACTION OF PLANT MATERIALS

by

Paul Ronald Hudson

A thesis submitted to

The University of Birmingham

for the degree of

Engineering Doctorate (EngD)

School of Chemical Engineering
University of Birmingham
September 2013

Abstract

Surfactants, often derived from crude oil, are included in laundry detergent formulations to clean oily and greasy stains. However, the level of surfactant included is higher than necessary for effectively cleaning clothes in order that foam is generated, as required by consumers, when products are used.

This thesis covers extraction from hay with NaOH to produce foaming solutions. Extraction time, temperature and NaOH concentration were found to have varying levels of influence on the properties of the extract solutions. Models were constructed to describe their effects on the % mass extracted from the hay, as well as extract solution absorbance, viscosity, and contact angle using response surface, experimental design methodology.

The hay extract foam was examined along with other types of foaming solutions, using cryogenic SEM. Hay, rice straw and horse chestnut leaf extract foams were found to be particle stabilised and interesting images were captured showing their microstructures. Foaming was found to be due to lignin-carbohydrate complexes in hay extract solutions and proteins in horse chestnut leaf extract solutions.

Finally correlations were sought between foaming of hay extract solutions and their other properties, *e.g.* Foaming of the hay solutions is due to lignin derivatives, hence solution absorbance correlates positively with foaming; and foaming is improved by increased solution viscosity hence its positive correlation with solution viscosity and % mass extracted from hay.

This thesis is dedicated to my fantastic parents, my brothers, my beautiful daughter Lillian and my wonderful wife-to-be Jenny.

Without your love, support and understanding this thesis would not have been possible.

Thank you all.

“This too shall pass”

- Unknown

Acknowledgements

I would like to thank my supervisors who have all helped me greatly during the course of my EngD. Professors Jon Preece and Zhibing Zhang have helped me to academically appraise and interpret my research then form a viable thesis. Whilst working within P&G the expertise, encouragement and supervision of Nigel Sommerville-Roberts and Alan Brooker helped me to work hard within the project and always strive to increase knowledge and understanding. I am also very grateful to Dr. Richard Greenwood for the input he gave many times during my EngD, and for his handling of the administrative side of the project.

On a personal note, every one of those listed above has been incredibly supportive throughout the time I worked on the project and I feel fortunate to have had such a great group of people to work with. Their expertise and knowledge has been invaluable but it is the encouragement they gave that allowed me the confidence to reach the end of my EngD, and this is something I shall always remember.

Others at P&G who I would like to thank are Nicola Tilt for her assistance in analysing and interpreting my data and Julian Martin for allowing me to work in his lab (for far longer than originally intended). I also acknowledge the support of P&G and EPSRC. Paul Stanley and Theresa Morris from the University of Birmingham's Centre for Electron Microscopy, were very helpful in capturing the SEM images in this thesis and I thank them also.

Finally I would like to thank my family and friends, especially my parents for their support throughout my education as well as my beautiful daughter Lillian and my wonderful fiancée Jenny. Without you all I would not have made it this far and I am lucky to have you all in my life.

Contents

List of Figures

List of Tables

Acronyms and nomenclature

Acronyms		Nomenclature	
P&G	Procter and Gamble	θ_{cL}	Contact angles on the left hand side of the droplet on the surface
LAS	Linear Alkylbenzenesulphonate	θ_{cR}	Contact angles on the right hand side of the droplet on the surface
FMCG	Fast Moving Consumer Goods	A	Absorbance
RSPO	Roundtable on Sustainable Palm Oil	Y_M	Model predicted % mass extracted from hay
UV	Ultra Violet	Y_A	Model predicted solution absorbance
CSTR	Continuous Stirred Tank Reactor	Y_V	Model predicted extract solution viscosity (Pa.s)
HLAS	Linear Alkylbenzene Sulphonic Acid	Y_S	Model predicted extract solution surface tension (mN m^{-1})
UV-vis	Ultra Violet – visible	Y_C	Model predicted extract solution contact angle (°)
SEM	Scanning Electron Microscopy	$*Y_C$	Model predicted extract solution contact angle - data 'screened' (°)
AFM	Atomic Force Microscopy	X_1	Coded reaction time parameter in the models
LCC	Lignin Carbohydrate Complex	X_2	Coded reaction temperature parameter in the models
LHC	Lignin Hemicellulose Complex	X_3	Coded NaOH concentration used parameter in the models
DMSO	Dimethyl Sulphoxide	β_0	Regression term value at the centre of the experimental design (*i.e*. the coded variables are 0, 0, 0)
RuBP	Ribulose-1,5-bisphosphate	$\beta_{n,m}$	Linear regression term in the models
% DM	% Dry Mass	β_{nn}	Quadratic regression term in the models
RPM	Revolutions Per Minute	β_{nm}	Interaction term in the models
RCF	Relative Centrifugal Force	Δz	The peak-valley height in AFM images (nm)
CMC	Critical Micelle Concentration		
PTFE	Polytetrafluoroethylene		
NSS	Not Statistically Significant		
RMS	Root Mean Square		
FWHM	Full Width Half Maximum (nm)		

Chapter 1 – Introduction

1.1 Project backdrop

Environmental concerns affect all aspects of modern life and reduced reliance on crude oil for fuels and as the basis of many widely used chemicals and products is becoming ever more important. In the future the price of crude oil is likely to increase (Shafiee and Topal, 2010) as availability decreases (Shafiee and Topal, 2009). Small molecule surfactants used in laundry detergent formulations *e.g.* linear alkylbenzene sulfonate (LAS), are expensive and derived from crude oil (or other unsustainable resources). The worldwide market for laundry detergents will develop in the future as economies such as China and India continue to grow (Euromonitor International, 2011a, 2011b). Growing demand for laundry detergents brings an opportunity for fast moving consumer goods (FMCG) companies to grow sales. However, manufacturers will be unable to produce enough current formulation laundry detergents to take advantage of this opportunity without significant cost increases due to scarcity of oil resources.

The expense of crude oil derived surfactants and the fact that they are environmentally damaging (Marcomini *et al.*, 1988, Warne and Schifko, 1999, Brandt *et al.*, 2001, Ying, 2006) means there is now an imperative to reduce use of oil based surfactants across the FMCG industry. Therefore this project was conceived to address this challenge by increasing the understanding of foaming solutions generated from renewable plant based materials. Ultimately these foaming materials might be included in sustainable laundry detergents to allow smaller amounts of oil based surfactants to be used and still maintain foaming properties.

1.2 The 12 Principles of Green Chemistry and Engineering

Anastas and Warner (1998) together pioneered the 12 Principles of Green Chemistry. The principles aimed to reduce/eliminate the use or generation of hazardous substances to give benign products or processes (Anastas and Kirchhoff, 2002). Green chemistry places sustainability and safety at its heart. Green chemistry does this through efficient use of materials and/or energy and minimising potential harm done to individuals or the environment. The 12 Principles of Green Chemistry in Table 1.1 are applicable to the research within this project.

Table 1.1. The 12 Principles of Green Chemistry (Anastas and Warner (1998)) .

1	**Prevention** - It is better to prevent waste than to treat or clean up waste after it has been created.
2	**Atom economy -** Synthetic methods should be designed to maximize the incorporation of all materials used in the process into the final product.
3	**Less hazardous chemical syntheses -** Wherever practicable, synthetic methods should be designed to use and generate substances that possess little or no toxicity to human health and the environment.
4	**Designing safer chemicals -** Chemical products should be designed to affect their desired function while minimizing their toxicity.
5	**Safer solvents and auxiliaries -** The use of auxiliary substances (*e.g.*, solvents, separation agents, *etc.*) should be made unnecessary wherever possible and innocuous when used.
6	**Design for energy efficiency -** Energy requirements of chemical processes should be recognized for their environmental and economic impacts and should be minimised. If possible, synthetic methods should be conducted at ambient temperature and pressure.
7	**Use of renewable feedstocks -** A raw material or feedstock should be renewable rather than depleting whenever technically and economically practicable.
8	**Reduce derivatives** - Unnecessary derivatisation (use of blocking groups, protection/deprotection, temporary modification of physical/chemical processes) should be minimized or avoided if possible because such steps require additional reagents and can generate waste.
9	**Catalysis** - Catalytic reagents (as selective as possible) are superior to stoichiometric reagents.
10	**Design for degradation** - Chemical products should be designed so that at the end of their function they break down into innocuous degradation products and do not persist in the environment.

11	**Real-time analysis for pollution prevention** - Analytical methodologies need to be further developed to allow for real-time, in-process monitoring and control prior to the formation of hazardous substances.
12	**Inherently safer chemistry for accident prevention** - Substances and the form of a substance used in a chemical process should be chosen to minimize the potential for chemical accidents, including releases, explosions, and fires.

To complement the 12 principles of Green Chemistry, Anastas and Zimmerman, (2003) compiled the 12 principles of Green Engineering which are reproduced in Table 1.2. These principles are more applicable to future large scale manufacturing of chemicals/products i.e. when the current research is used to develop a manufacturing route for foaming materials.

Table 1.2. The 12 principles of Green Engineering (Anastas and Zimmerman, 2003).

1	Designers need to strive to ensure that all material and energy inputs and outputs are as inherently non-hazardous as possible.
2	It is better to prevent waste than to treat or clean up waste after it is formed.
3	Separation and purification operations should be designed to minimize energy consumption and materials use.
4	Products, processes, and systems should be designed to maximize mass, energy, space, and time efficiency.
5	Products, processes, and systems should be “output pulled” rather than “input pushed” through the use of energy and materials.
6	Embedded entropy and complexity must be viewed as an investment when making design choices on recycle, reuse, or beneficial disposition.
7	Targeted durability, not immortality, should be a design goal.
8	Design for unnecessary capacity or capability (e.g., “one size fits all”) solutions should be considered a design flaw.
9	Material diversity in multicomponent products should be minimized to promote disassembly and value retention.
10	Design of products, processes, and systems must include integration and interconnectivity with available energy and materials flows.
11	Products, processes, and systems should be designed for performance in a commercial “afterlife”.
12	Material and energy inputs should be renewable rather than depleting.

As the current research is an investigation into the foaming of plant extract solutions rather than process design for manufacture of foaming solutions the Principles of Green Engineering are more appropriate when considering the restrictions/limitation placed on the extraction conditions. The paper by Anastas and Zimmerman, (2003) overlaps significantly with the requirements for a green process placed upon the current research e.g. separation and purification should be minimised, energy consumption should be minimised. The points raised by Anastas and Zimmerman, (2003) should certainly be considered in future scale up of the current research.

1.3 Improving the 'greenness' of FMCGs

The FMCG industry has already developed several green strategies for laundry products, one of which is compaction of detergents to increase the sustainability of products. Edser (2007) provides a discussion of the sustainability benefits of compaction of detergents, describing a 60% reduction in water usage during production, > 40% reduction in petrochemical based plastic packaging per bottle as well as reduced fuel required and emissions generated in transporting the products. Saouter (2002) gives a more in depth description of the benefits of compaction from a life cycle assessment point of view, describing considerable savings in raw materials, water and energy usage as well as reduction in emissions due to product use and disposal. Saouter is an employee of P&G hence the research demonstrates the efforts of the FMCG industry are actually making to understand how to effectively improve the sustainability of their products.

Reductions in material, water and energy use will certainly have a positive effect on the environmental impact of laundry detergent products. Consumers such as those using hand wash laundry detergents washing clothes in a river which they also use for drinking water may not find the discussion by Saouter very interesting. How sustainable a product is would

be less interesting than what the effect of the product might be on humans when ingested. Warne and Schifko (1999) describe the variable level of toxicity of Australian laundry detergent ingredients, which lists surfactants as being among the most toxic ingredients. The research does acknowledge, however, that the potential for acute toxic effects from secondary or tertiary laundry effluent (containing breakdown products from the detergents) is frequently low, but that primary effluent if released untreated could cause problems. Thus, whilst water treatment is widespread in some parts of the world, in some areas primary wash effluent may make its way into potable water sources. Their findings suggest that surfactant reduction in formulations is desirable in terms of reducing the potential effects of detergent toxicity. Interestingly Warne and Schifko (1999) acknowledge help from detergent manufacturers in compiling their data which again reinforces the view that the FMCG industry is making efforts to reduce the harmful effects of their products to people and the environment.

1.4 Palm oil based surfactants

One alternative raw material for use in surfactant production is palm oil (Edser, 2006). Production of surfactants from sources such as oil palm trees should in theory be less harmful to the environment than using crude oil based sources. Using plant raw materials would also seem to be inherently renewable at first glance, however, the situation is not as straightforward as a plant raw material being equivalent to a sustainable raw material.

Palm oil use has a negative image due to the environmental impacts associated palm oil plantations. Problems of deforestation are described by Koh and Wilcove (2009) and the associated destruction of animal habitats by Tan *et al.* (2009). Reduction in biodiversity and disruption of ecosystems mean palm oil has not been produced sustainably in the past. It is debated as to whether palm oil can in fact be produced sustainably in the future. Corley

(2009) published projections stating that palm oil demand will increase substantially in the future. A convincing case is made that meeting growing future demand for *edible* palm oil is possible without further environmental damage being caused. The article is less affirmative in its outlook on the impact of palm oil demand for use in biofuels (and biochemicals by logical extension of the argument). Corley (2009) states only that biofuel demand for palm oil and subsidies for production of fuel from palm oil could make future oil palm expansion 'difficult'. Wicke *et al.* (2011) discuss how expansion of palm oil production without land use change is only possible if growth in demand is not too great and if the expansion is properly managed.

Objections for expansion of palm oil tree plantations are raised even when deforestation is removed from the equation. Use of arable land for palm oil plantations to make fuel or for conversion to chemicals, versus using the oil as a foodstuff, or even allocation of the land for producing alternative types of food, is a contentious issue. Arguments both for and against the idea that biofuel production will affect food production exist in the literature (Cassman and Liska, 2007, De La Torre Ugarte and He, 2007, Stein, 2007, Rathmann *et al.*, 2010). Concerns of this type are not limited to palm oil, but also exist over the effect of land use for growing cereal crops/sugar cane/coconut trees for the purpose of converting them into biofuels/chemicals rather than as food for the world's growing population (Spiertz and Ewert, 2009, Ajanovic, 2011, Wetzstein and Wetzstein, 2011).

Use of palm oil and other plant derived resources for production of FMCG ingredients is not necessarily the primary concern in the literature due to the potentially very much larger scale of the future biofuels sector. The published information and discussion on palm oil use is still applicable to biochemicals such as surfactants, and should be examined when considering the environmental impact of such biochemicals. Expansion of palm oil

production for whatever purpose has the potential to do environmental harm and this is concerning. Given the anxieties associated with production of palm oil there is a movement in the consumer goods industry toward ensuring sustainable production/procurement of palm oil for the manufacture of surfactants. FMCG companies are making visible efforts in moving toward sustainably sourced palm oil by founding organisations such as the Roundtable on Sustainable Palm Oil (RSPO). The aim of the RSPO is "*promoting the growth and use of sustainable oil palm products through credible global standards and engagement of stakeholders"* (Rountable on Sustainable Palm Oil, 2012). Forming the RSPO is a step in the right direction and might help drive sustainable production of palm oil in the future, though the environmental damage caused by the palm oil industry in the past is inarguable. The future of palm oil production is unclear as there is uncertainty as to whether increased demand for palm oil will mean food insecurity and further environmental damage even in spite of efforts of the RSPO and similar parties.

The available literature underlines the need to generate sustainable alternatives to oil based surfactants in general. Ultimately these replacements must:

1. be environmentally benign in production, use and disposal.
2. not require the use of land which might otherwise be available for growing foodstuffs.
3. be cheap to produce.
4. give products which consumers enjoy.

Palm oil based surfactants do not meet all of these criteria and it is possible that they may never be completely sustainably produced if they are increasingly used for production of biofuels as well as other chemicals.

1.5 Biomass

Instead of growing crops such as palm oil trees or cereal crops on arable land to produce biofuels and chemicals such as surfactants, there is considerable work going on looking at using sustainable biomass feedstock. Biomass/lignocellulosic waste material is plant waste from:

1. rice/cereals crops *e.g.* straw/husk.
2. forestry activity *e.g.* bark, leaves, and wood shavings.

Alternatively biomass can be used directly for electricity generation through pyrolysis, gasification and combustion. Evans *et al.* (2010) describe the size of the contribution to energy demands made by burning of biomass on anything more than a local scale (*e.g.* to produce heat/electricity for a specific manufacturing plant) as likely to be small, variable by region and expensive compared to conventionally generated electricity.

With the potential contribution to energy needs from combustion of biomass being small, it is more sensible to convert biomass resources into value added chemicals or liquid biofuels. Liquid fuels offer flexibility in how and where they are used and chemical production increases the valorisation of biomass overall versus burning the solid raw materials. This opportunity to maximise profitability is why biomass utilisation is moving away from combustion to more complex processing and exploitation of the materials in future. If biomass residues become more valuable then they may move from being regarded as a process waste product to valuable by products. Future utilisation of biomass will mean increased revenues for both the companies producing the waste and those using the waste while reducing environmental harm, resulting in positive outcomes all round.

Examples of work to utilise plant raw materials in the FMCG industry exist in the patent literature (see Chapter 2). A particularly interesting patent submitted by Unilever (Batchelor *et al*., 2007) discloses alkali extraction of plant raw materials (agricultural waste) with solid particles from the extractions being incorporated into laundry detergent formulations to improve cleaning. The current research differs from the Batchelor patent in that it is concerned with understanding the properties of the liquid generated during alkali extraction of plant raw materials in order that it may ultimately be exploited as a laundry detergent ingredient. The liquid extracts from alkali treatment of plant materials are found to generate suds when agitated or sparged and it is the aim of P&G to utilise these liquid extracts to boost sudsing and increase foam stability in laundry detergent formulations which contain less surfactant.

The alkali plant extracts do not need any actual efficacy in terms of cleaning action, it was the objective of this project to more specifically understand the capacity for foam generation from alkali extracted plant raw materials and gain insight into the properties of the extracts/foams. The knowledge generated by the current research will be used in the future by P&G ultimately to facilitate incorporation of alkali plant extracts into laundry detergents. The function of any products made from alkali extraction of plant materials will be to increase the volume of suds generated per volume of surfactant in a formulation or increase the suds lifetime for low surfactant content products.

1.6 Laundry detergent formulations

Laundry detergents clean soiled fabrics by removing stains, dirt and smells which have a wide range of compositions/causes. Ingredients are selected and blended in proportions to maximise the effectiveness of the specific detergent product depending on the most important functions and cost base of the product. A premium product aimed at giving

consumers 'brilliant whites' for example will have larger proportions of cleaning ingredients whereas another product aimed at giving the consumer the best possible 'sensorial experience' will include greater proportions of fabric softening or perfume ingredients.

1.6.1 Ingredients and functions

Bleaches (which are often catalyst activated in modern formulations) oxidise molecules in soils reducing their ability to adhere to fabrics, increasing their solubility in the wash liquor and ultimately leaving fabrics clean (Burns *et al*., 2003, Wieprecht *et al*., 2003). Enzymes clean by breaking down stains using biologically catalytic activity. Enzymes used in formulations must be tailored for the soils they clean *i.e.* separate enzymes will be used for proteinaceous (Knorr *et al.*, 2001), fatty (Svendsen *et al.*, 1999) and carbohydrate (Bettiol *et al.*, 1998) based stains. Other ingredients used in laundry detergents include polymers, which modify fabric surfaces making stains less likely to stick and lighteners/whiteners which act to convert some UV light into visible light giving whites a more intense brightness. Another important class of ingredients in laundry detergents are surfactants (Rolfes, 1999, Brouwer and Wint, 2000, Hsu *et al.*, 2006).

1.7 Surfactants, cleaning and sudsing

Surfactants (surface active agents) act to remove oily and greasy stains from fabrics. Surfactants are amphiphilic which means they have affinity for both polar and non-polar substances. Surfactants, therefore, are attracted to fatty molecules and increase their water solubility resulting in their removal with wash liquor post rinsing. Surfactants reduce the surface tension of water and therefore stabilise bubbles (through the Marangoni effect, see section 9.1.3) which accumulate as suds/foams. Surfactants such as Linear Alkylbenzene Sulphonate (LAS), used in laundry detergents make up around 15 – 20% of formulations,

hence contribute a great deal to the cost of production as well as the environmental impact of products.

Consumers expect to see laundry detergents generate foam which is provided by surfactants, during use. The presence or absence of foam during a washing is not indicative of product efficacy, though foam provides a psychological cue for consumers which they associate with efficacy anyway (Kasturi *et al.*, 2005). Excessive amounts of surfactants are used in formulations to produce foam, compared to the amount required to deliver cleaning of fabrics only. It is desirable therefore to find new ingredients, in order to allow the reduction of the petrochemical surfactants concentration to levels used only for cleaning and not foaming.

An obvious question regarding laundry foam is: "Why not just educate consumers that foams do not indicate efficacy for laundry detergents?" This is a valid question and ultimately it may be that consumers realise the lack of need for suds when using laundry detergents. However, currently for a manufacturer of laundry detergents to maintain customer satisfaction and hence loyalty, which leads to success in the market, they must sell products which generate foam, otherwise the consumer may take a negative view of their laundry detergent products, and lose loyalty to the brand.

Another suggestion to solve the problem of consumers requiring foam from their laundry detergents is "Why not build washing machines without windows so consumers cannot see if suds are absent?" This question comes from a limited world view, without considering or necessarily understanding global variation in laundry methods. In Asia a lot of washing still takes place by hand, perhaps in a river or bucket of water. Hand washing means consumers have intimate contact with detergents and they touch and feel bubbles being generated as well as seeing them. Hand wash consumers require formulations that generate bubbles with

low energy input whilst washing, where bubbles persist throughout the wash process until they are rinsed away. Water quality for such hand washing may be low, with low volumes of water used which might be reused further degrading water quality. Therefore, hand wash laundry products sold into Asia must be robust enough to clean effectively and generate stable foam in these challenging conditions.

Washing habits in North America involve top loading washing machines being primarily used which require significantly more water (up to 35 litres of water per load). Top loading washing machines have increased energy input compared to hand washing and less foam is required by product users as too much might overwhelm the washing machine. Too much foam also becomes difficult to rinse away hence the level of foam produced by detergents must be just right. Finally in Europe it is usual to use front loading automatic washing machines which require around 13 litres of water for cleaning laundry. A front loading washing machine also inputs more energy into cleaning fabrics than hand washing, and too much foam could again damage washing machines. Hence front/top loading washing machines and hand washing all need different detergent formulations.

There is a wide variety of washing methods used globally with a wide range of detergent consumers having varying expectations, hence simply 'removing the window' will not solve the problem of foaming requirements for laundry detergent products universally. Products must also be effective in varying quality and volumes of water and in systems with higher and lower energy input into the wash. Laundry detergent formulations must behave as consumers, in the respective regions, require in order to be successful and bring profits to FMCG companies. Producing a 'one size fits all' formulation to satisfy all consumers is not possible and hence products are tailored for the respective consumers. Use of a sudsing agent to aid in producing and stabilising foam instead of using excess surfactant, should

allow the foam properties to be tailored to satisfy the variety of consumer needs. Foams generated by laundry products have a range of important qualities including their colour, texture, volume and stability, whilst being easy to rinse away, leaving no residue. The primary concern of the current research is to increase understanding of the foaming of alkali plant extracts in order that in the future this knowledge may be used to produce suds enhancers/stabilisers for incorporation into future detergent products.

1.8 Business drivers and expected benefits

Surfactants used in laundry detergent formulations contribute a large part of the financial and environmental cost associated with the products, hence using less petrochemical based surfactants would mean significant cost savings and environmental benefits. Cost savings in manufacturing could either be passed on to consumers in the form of lower prices or the benefit retained by the manufacturer in the form of increased profits.

Consumers are increasingly concerned about the environmental impact that their product choices are having, which presents an opportunity for P&G (and other FMCG companies) to develop environmentally friendly products. Improving the environmental profile of laundry detergent products means P&G could market greener products specifically toward consumers in the environmentally conscious 'niche' at a premium price. The production of detergents with better environmental profiles would benefit the reputation of P&G improving their image as a company that operates in a sustainable and ethical manner for more 'average' customers (with fewer environmental concerns) also. If greener products can be produced by P&G whilst maintaining current pricing structure and performance then P&G will meet the demands of the high proportion of customer who are identified as unwilling to trade off performance or value in order to be more sustainable (Procter and Gamble, 2012). Both environmentally conscious and 'average' consumers would be more

inclined to buy P&G products if their purchases were more environmentally friendly whilst maintaining effectiveness. Therefore the need for P&G to produce greener products is not a burden but a business opportunity.

Sustainability is at the core of the business drivers which affected the design of the process by which extraction of plant raw materials took place during the research in this EngD thesis. To ensure sustainability of potential processing routes for alkali extraction of plant materials, a number of requirements needed to be met to deliver a process addressing the criteria listed in Table 1.1.

1.8.1 Business drivers behind the simple alkali extraction process

- For an energy efficient process, extractions should be simple, not requiring energy intensive milling, heating nor as far as possible, separation techniques such as filtration and centrifugation. (Milling and separation was required during the current research to ensure consistent plant raw materials for the extractions and sample generation for analysis.)
- To ensure a green process, no harmful/volatile/expensive solvents should be used. Aqueous NaOH extraction of plant materials produces solutions which generate foam hence its suitability for the current research. Prior use of aqueous NaOH within P&G manufacturing plants means from a business perspective, the training and knowledge about its safe use is already in place, as well as a supply chain being available for future commercial exploitation of the research.

A sustainable and energy efficient process to produce foamability enhancing ingredients from extracted lignocellulosic materials within the constraints listed above would be advantageous for P&G as a business because:

- Manufacturing plants could be placed into geographical regions where lignocellulosic raw materials were locally, cheaply and abundantly available *(e.g.* farms where lignocellulosic waste material is generated and where residues from alkali extractions of lignocellulosics might be used as animal feed).
    - Cost benefit analysis and life cycle assessment would help understanding of how local sourcing of raw materials could lead to a greener, more cost effective supply chain with reduced CO_2 emissions/costs from transportation of raw materials. Incorporation of lignocellulosic wastes into animal feed is possible as alkali extraction increases biological digestibility of materials such as straw (see section 2.4).
- Operating simpler manufacturing plants is easier with decreased potential for breakdown than if complex/expensive equipment were required. *e.g.* if alkali extractions of plant materials took place in static tanks where the sudsing liquid was simply decanted off after the extraction period then potential problems of mechanical failure of equipment are low. Whereas extracting the materials in continuously stirred tank reactors (CSTRs) and passing the liquid through centrifuges to separate the solids after extraction leaves the possibility of breakdown of CSTR or centrifuge *etc.* which could halt the process and be costly to repair.
    - Minimising down time of production plants is important for cost effective and successful manufacturing. If more complex manufacturing plants were operated in remote areas, where expertise and equipment spares may not be readily accessible, the possibility of down time and loss of productivity in the event of equipment failure increases.

- Capital costs in construction of manufacturing plants are lower for simpler processes (*i.e.* a process without requirements for centrifuges/filter banks/vessels which must withstand high pressures or temperatures).
    - Simpler plants, being more cost effective would ultimately end up being more profitable for the business. Increased cost effectiveness and profitability means reduced time for return on investment from the manufacturing plant and decreased exposure to risk associated with new plant construction, for P&G.
- The NaOH used in the extractions might potentially be taken from and reincorporated back into, process streams in established laundry detergent manufacturing plants.
    - NaOH is used to neutralise linear alkylbenzene sulphonic acid (HLAS) to produce LAS surfactant in detergent manufacture so could potentially be used in extraction of plant materials before using it to neutralise HLAS. This would incorporate the extracts into the production process without the use of any extra solvents which might require separation and disposal. Not using extra solvents in the extraction process is another way to keep the process green and more cost effective as plant modification is limited.

1.9 Project objectives/questions

Specific questions identified before and during the course of the current research addressed within this thesis include:

(1) Which components of the plant raw materials are solubilised during alkali extraction?
    a. How do reaction conditions affect the extent of extraction of the materials?

b. What changes in the reaction product solution properties occur as reaction conditions change?

(2) What is the current state of the art regarding foaming by different materials (*e.g.* surfactants/proteins/particles)?

a. What is the current understanding of foaming mechanisms from the various sources?

b. Which methods are there for investigating foam production and microstructure and can they be applied in the current research?

(3) What others uses do plant raw materials of the kind examined during the project find within the literature?

a. Could the waste stream from any other industry/processes offer raw materials for sudsing agent production?

b. Could the waste stream from sudsing agent production be useful in any other application?

(4) Which are likely to be the important extracted components in terms of aiding foam formation from the alkali extract solutions?

a. What are the possible mechanisms by which the components aid foaming?

(5) What is the extraction mechanism of the materials into solution from the plant materials?

a. How can extraction from plant materials be optimised to better use the raw materials in producing sudsing agents?

(6) How is foam formed from the extracted materials?

a. What is the microstructure of the foams?

b. Can sudsing potential of alkali extracts from plant solutions be measured and modelled according to varying extraction conditions?

c. Do correlations exist that mean another solution property could be used as a proxy measurement of sudsing potential for alkali extract solutions?

1.10 Requirements for success in the current research

At the beginning of the project, little was known about foaming of the products of alkali extraction of plant materials beyond the fact that the liquid extraction products give foam when shaken. The literature was consulted and yielded some insights, though gaps in the knowledge exist which the current research aims to fill.

1.10.1 Alkali extraction of plant raw materials to produce sudsing agents

There is much research in the literature covering extraction of materials from plants for use in various areas (see Chapter 2), though little to no published research covering extraction of materials from plants for use as sudsing/foam enhancing agents exists. Understanding of the extraction of the various components of plant materials can be garnered from the established literature, though the reaction conditions used may not be optimal for suds generation, nor for sustainable/efficient production plant operation. Therefore, it was necessary to expand on the research in the literature by examining the changes in the physical properties of the reaction product solutions, including the foamability of the solutions from alkali extraction of plant raw materials.

1.10.2 The sudsing mechanism

There is much research literature describing foam formation by a variety of materials *via* a range of mechanisms including small molecule surfactants (*e.g.* LAS), protein and particle (Pickering) stabilised foams. However, after extensive searching, no prior research has been found to describe the microstructure of foaming by alkali extracted plant raw materials. To understand how solutions from alkali extracted plant raw materials generate foam,

experimentation and analysis was required to examine which components of plant materials are important in the foaming, and what the mechanism of foam formation and stabilisation.

Due to time constraints, extension of the research into the realms of how the alkali plant extracts might be specifically formulated within laundry detergents were not explored though work is on-going to incorporate the research into development of future P&G detergent products.

1.11 Thesis outline

1.11.1 Literature review - Chapter 2

Chapter 2 critically examines the state-of-the-art in the literature with regards extraction of components from plant raw materials and current knowledge and understanding of relevant foam microstructures. This chapter will give a broader insight into what are the important areas of research relevant to this project, and identify areas where gaps in the knowledge exist in the context of the current work.

1.11.2 Materials and methods - Chapter 3

Chapter 3 describes the materials and methods used to generate foaming solutions from plant raw materials. A description of each of the methods used for characterisation of the alkali extracts is given.

1.11.3 Single variable investigation of alkali hay extract solutions - Chapter 4

Single variable experiments were performed where hay was extracted with aqueous NaOH and reaction time, temperature and concentration of the NaOH were altered. The effect of varying these reaction conditions on the UV-vis absorbance of extract solutions, % mass of

hay components extracted and solution viscosity for the liquid reaction products are presented and discussed.

1.11.4 Modelling work as a continuation of the single variable work – Chapter 5

In this chapter the single variable work is expanded upon by applying designed experiments to various characterisations of the liquid alkali hay extracts. Using response surface methodology allowed the effect of reaction variables and their interactions on the hay extract solution properties to be investigated and models generated. The models give insight into the relative effect of changing the reaction variables and their interactions with each other, on various reaction product solution properties.

1.11.5 Examination of the microstructure of foams - Chapter 6

Chapter 6 examines the microstructure of the foam generated from the alkali extraction of plant materials. Cryogenic SEM was found to be a very useful tool in examining the foams and AFM was used to further probe the microstructure of dried alkali hay extract foam. Isolation and identification of particles observed in the foams was not possible during the research, though their possible origins and nature are discussed.

1.11.6 Correlating sudsing and other extract solution properties – Chapter 7

Part of the aim of using the combination of measured properties of the alkali plant extract solutions was to find how the various properties of the solutions would affect the ability of the solution to produce suds. It was the intention that a proxy indicator for sudsing potential (foamability) of the extract solutions might be found by looking for correlation between the various solution properties and foam production.

Finding an easy to measure proxy for foamability of the extract solutions was desirable as sudsing measurements of solutions are difficult. Foam production by the hay extract solutions was tested using a version of the Bikerman (1973a) sparging test. Attempts are described to model foaming of extract solutions with varying extraction conditions, then establish correlation of foaming with other measured solution properties.

1.11.7 Conclusions, reflections and further work - Chapter 8

Chapter 8 draws together overall conclusions from the research in the previous chapters. These conclusions summarise the knowledge generated by the research on the effect of alkali extraction on plant materials, the properties of the extract solutions, the microstructure of the foams generated from the solutions and correlation between the measurements of solution properties and foaming from the solutions. Recommendations are also given for future work.

1.12 Publications

1.12.1 Conference presentations

Paul Hudson, Nigel Sommerville-Roberts, Alan Brooker, Zhibing Zhang, and Jon. A. Preece, *"Green" Alternatives to Conventional Surfactant Foams in Laundry Detergents,* 15th Annual Green Chemistry & Engineering Conference, June 2011, Washington DC (USA)

Paul Hudson, Nigel Sommerville-Roberts, Alan Brooker, Zhibing Zhang, and Jon. A. Preece, *Sudsing Agents for Laundry Detergents from Lignocellulosic Materials,* 4th International IUPAC Conference on Green Chemistry, August 2012, Foz do Iguaçu (Brazil)

1.12.2 Patent

Neil Lant, Alan Brooker, Nigel Sommerville Roberts, Paul Hudson, 2009, *Cleaning composition containing hemicellulose*, European Patent EP 2 336 283 B1.

2 Chapter 2 – Literature review

2.1 Introduction: Overview of this chapter and its context with respect to this EngD thesis

This literature review will give an outlook on the current state-of-the-art in areas relevant to this project. The discussion will begin by describing lignocellulosic (plant) materials (which contain lignin, cellulose and hemicellulose, as well as protein) and their uses as described in academic journals and patent literature. Examination of the effect of pretreatment on the components of lignocellulosic materials follows, including describing the effect of alkali extractions as used within the research for this thesis. Literature pertaining to the exact materials (primarily hay but also horse chestnut leaves and rice straw) used in the present research was not extensive though similarities in the effects of pretreatment on lignocellulosic materials are discussed. Given the similarities in the behaviour of lignocellulosic material when processed in similar ways it is reasonable to examine research into materials other than those specifically used in the current investigations (*e.g.* hay and rice straw versus wheat straw *etc).* This literature review then concludes by examining foams and their microstructure.

2.2 The composition of lignocellulosic materials

A table outlining the proportions of cellulose, hemicellulose and lignin (see section 2.4 for descriptions of the components of lignocellulosic materials) in various sources of biomass was compiled by Sun and Cheng (2002) and is reproduced in Table 2.1. For a description of the structure of lignin see section 2.4.1, of hemicellulose see section 2.4.2 and for a description of the structure of cellulose see section 2.4.4.

Table 2.1. The proportions of cellulose, hemicellulose and lignin in a range of biomass sources. (Reproduced from Sun and Cheng, 2002).

Lignocellulosic materials	% Cellulose	% Hemicellulose	% Lignin
Hardwood stems	40 - 55	24 - 40	18 - 25
Softwood stems	45 - 50	25 - 35	25 - 35
Nut shells	25 - 30	25 - 30	30 - 40
Corn cobs	45	35	15
Grasses	25 - 40	35 - 50	10 - 30
Paper	85 - 99	0	0 - 15
Wheat straw	30	50	15
Sorted refuse	60	20	20
Leaves	15 - 20	80 - 85	0
Cotton hair seeds	80 - 95	5 - 20	0
Newspaper	40 - 55	25 - 40	18 - 30
Waste papers from chemical pulps	60 - 70	10 - 20	5 - 10
Primary waste water solids	8 - 15	NA	24 - 29
Swine waste	6	28	NA
Solids cattle manure	1.6 - 4.7	1.4 - 3.3	2.7 - 5.7
Coastal bermuda grass	25	35.7	6.4
Switch grass	45	31.4	12

'Straw' is the stem from cereal crops which themselves are types of grasses grown for food production. Table 2.1 also demonstrates that 'grasses' and 'straws' have compositions which are similar in terms of cellulose, hemicellulose and lignin content, hence research findings concerning wheat straw should be applicable to hay. For a more detailed description of the nature of the cellulose, hemicellulose, lignin and protein content of lignocellulosic materials and the effect of pretreatments see section 2.4.

2.3 Plant materials used within the current research

Throughout this thesis hay is used as a model plant material to represent 'biomass' raw materials generally. Some experiments were also performed using horse chestnut (*Aesculus hippocastanum)* leaves and rice straw (*Oryza sativa).*

2.3.1 Hay

Hay is a name given to mixed plant materials which are fed to animals. Hay is made up of *Poa* grasses (*Gramineae*) *e.g.* ryegrass (*Lolium*); and legumes (*Leguminosae*) *e.g.* alfalfa (*Medicago sativa*) and clover (*Trifolium*). Hay was chosen for use in the alkali extractions as it was considered important that the model plant material used in the experiments should have appreciable levels of cellulose, hemicellulose, lignin and protein. Grasses which make up hay are suitable as they are known to contain appreciable levels of cellulose (25 - 40%), hemicellulose (35 - 50%), lignin (10 - 30%) (Saidur *et al.*, 2011) and proteins (up to 20%) (Koschuh *et al.*, 2004).

2.3.2 Straw

The use of straw as a raw material has been examined as it is cheaply available (Deswarte *et al.*, 2007, Wang and Sun, 2012). Research exists demonstrating that it is possible to increase the nutritional value and digestibility of straw by increasing biological availability of the cellulose in the straw, through routes including the use of alkali treatment similar to the extraction in the current research (Harbers *et al.*, 1982, Arisoy, 1998, McCartney *et al.*, 2006).

2.3.3 Leaves

Little relevant research exists in the literature regarding potential uses for horse chestnut leaves. The composition of leaves is different from the hay and straw in that they do not contain lignin (see Table 2.1) which leads to increase the effectiveness of extraction of the other components such as hemicellulose and proteins (see sections 2.4.2 and 2.4.5) by NaOH.

2.4 Pretreatment of lignocellulosic materials

Alkali extraction of lignocellulosics is one of a range of methods used as a pretreatment in biofuels production (Hendriks and Zeeman, 2009, Binod *et al.*, 2010), or to increase the nutritional value of lignocellulosics (Drennan *et al.*, 1982). Ethanol can be produced by fermentation of glucose from within cellulose making lignocellulosics an attractive, potentially sustainable material for production of biofuel. Direct fermentation cannot take place as the glucose is 'bound' within cellulose fibrils. Cellulose requires enzymatic hydrolysis into glucose monomers before fermentation, however, this cannot simply be performed by applying appropriate enzymes to plant materials. Lignin protects the cellulose fibres in biomass such as straw and hay, from enzymatic breakdown, hence pretreatment of the material is required. The use of alkali has been reported in relation to pretreatment of lignocellulosics, using bases including lime (Holtzapple *et al*., 1997, Saha and Cotta, 2007, 2008), sodium hydroxide (Macdonald *et al.*, 1983, Fox *et al.*, 1987, Lapierre *et al.*, 1989, Sun *et al.*, 1995, Saulnier *et al.*, 1995) and ammonia (Lawther *et al.*, 1996a). Extraction/treatment of lignocellulosic materials by other routes such as acid treatment, steam explosion, organosolv or hydrothermal are also covered in the literature and reviews are available covering the range of pretreatments used (Sun and Cheng, 2002, Yang and Wyman, 2008, Thirmal and Dahman, 2012).

The pretreatment of lignocellulosic biomass reduces the recalcitrance of the materials to enzymatic hydrolysis by breaking down the lignin which encrusts the cellulose and removing hemicellulose. The biomass surface area is also increased and the crystallinity of cell-wall cellulose is decreased. After pretreatment, the remaining plant solids contain a higher proportion of accessible cellulose for enzymatic breakdown into fermentable glucose.

Pretreatment lowers a major hurdle to effective use of these materials in second generation biofuels (Sun and Cheng, 2002, Mosier *et al.*, 2005).

This thesis covers the use of sodium hydroxide for extraction of lignocellulosic materials and examines the physical properties and foaming ability of the solutions generated. As the aim of pretreatment is to reduce the recalcitrance of lignocellulosics to enzymatic breakdown, the changes in the physical properties of materials brought about by different pretreatment methods is similar. Therefore alternative pretreatment methods will potentially still give some insight into what is happening during alkali extraction of lignocellulosic materials.

Discussion of the effects of pretreatments on lignocellulosics will now follow and further investigation of compositional changes during extraction of lignocellulosics was not undertaken during the current research hence will not be covered elsewhere in this thesis.

2.4.1 Lignin

Lignin is a generally described as a heteropolymer made up of three monolignols: *p*-coumeryl, coniferyl and sinapyl alcohol (Jaramillo-Carmona *et al.*, 2008) as shown in Figure 2.1

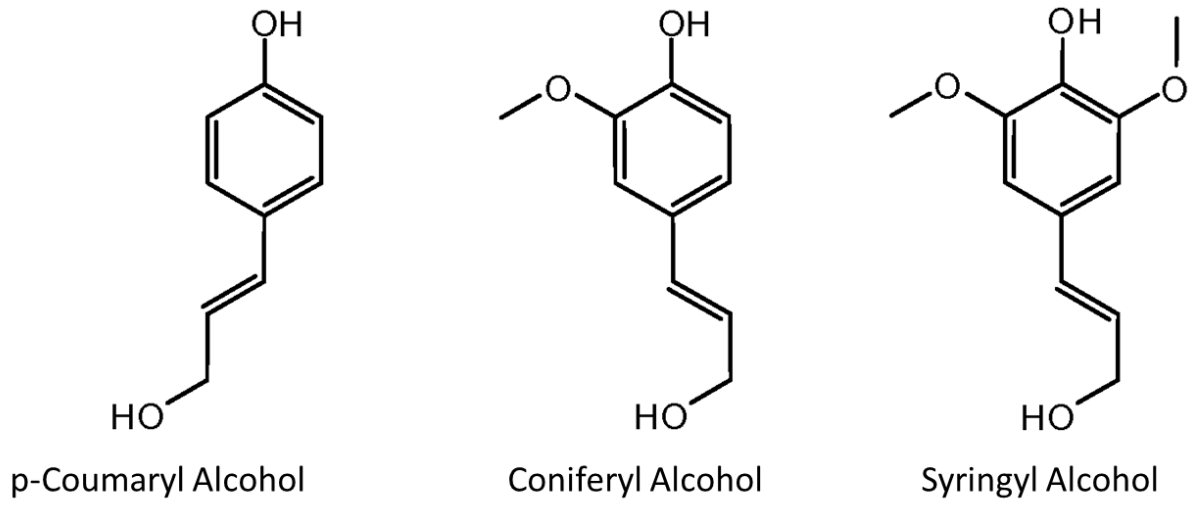

Figure 2.1. The monomers of lignin.

Some research does also exist describing lignin as having structures which incorporate more diverse monolignols than just these three (Vanholme *et al.*, 2008). Lignin is found in a wide variety of structures containing differing proportions of monolignols, varying according to plants species and tissue type. Lignin functions as a binding material within plant tissues giving some structural integrity to plants. Lignin also gives plants protection from parasite and enzymatic attack, as well as functioning in water transport as lignin is hydrophobic.

Elucidating the structure of lignin in plants is difficult due to its recalcitrance to breakdown. Though the research of Sun *et al.* (1997) looks at wheat straw rather than hay, the alkali treatment is similar to the extractions performed on hay in the current research. The paper describes a tentative structure of lignin including how lignin in wheat straw links to hemicellulose *via* hydroxycinnamic acids (*p*-courmeric and ferulic acids) through ester and ether bonds. It is the ester bonds which are cleaved during low temperature (< 170 °C) alkaline hydrolysis of wheat straw with the ether bond requiring higher temperatures for cleavage. The paper provides interesting and convincing insight into lignin structure and the effect of alkali extraction which due to the similarity in the composition of wheat straw and grasses which make up hay (see Table 2.1.) are relevant to alkali extraction of hay.

2.4.1.1 Lignin removal and redeposition

Kristensen *et al.* (2008) performed hydrothermal (hot water) pretreatment and steam explosion on wheat straw. Hydrothermal pretreatment involved heating pieces of straw (up to 5 cm long), in water at 80 °C for six minutes before passing through a continuous extractor (with average residence time of 6 minutes) containing water, heated using steam at 195 °C. Steam explosion involved impregnating the straw with SO_2 before heating materials in steam at pressure, then using rapid decompression (explosion) to disrupt the straw's structure.

Figure 2.2 shows the structural changes that occur in wheat straw after pretreatment as imaged using SEM and AFM (using amplitude images).

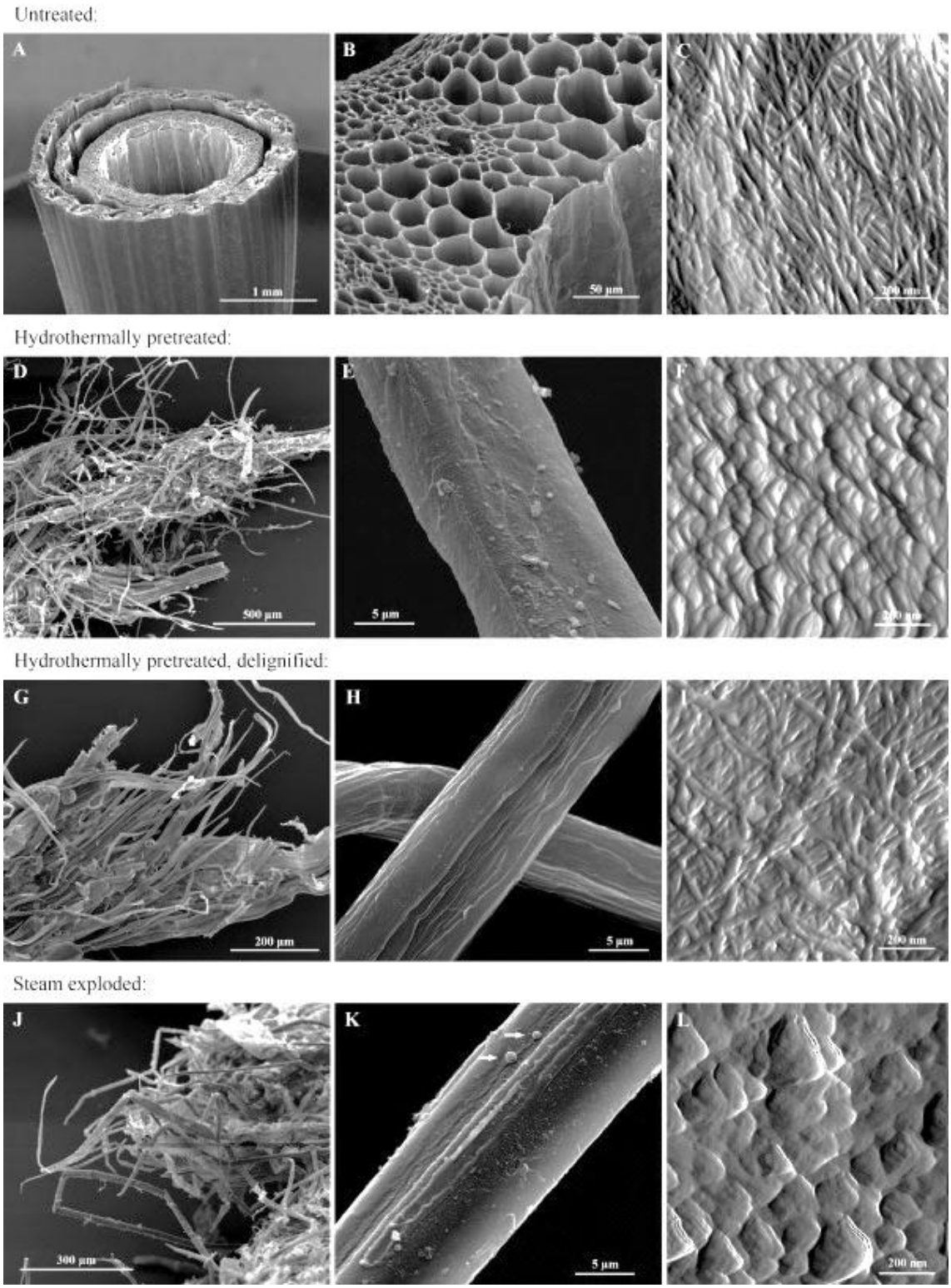

Figure 2.2. Structural changes seen in hydrothermally treated and steam exploded wheat straw as imaged by SEM and AFM (Reproduced from Kristensen *et al*., 2008).

Plates A – C in Figure 2.2 show untreated, D – F show hydrothermally pretreated, G – I show delignified, hydrothermally pretreated and J – L show steam exploded wheat straw.

Ordinary wheat straw surrounded by a sheath leaf which can be seen in plate A. Plate B

increases the magnification so that individual cells of the wheat straw wall can be observed. Plate C shows a high resolution AFM image (amplitude image) of a primary cell wall lining the straw cavity, where interwoven cellulose microfibrils, partially imbedded in non-cellulosic polymers are observable. Plate D shows how the hydrothermal pretreatment has caused the individual fibres to partially separate. There is a layer of debris visible on the surface of the straw fibres detailed in plate E.

An AFM scan (plate F - amplitude image) of the surface of a fibre shows 'globular' deposits characteristic of lignin, though no microfibrils are visible underneath the lignin globules.

Delignification was performed using glacial acetic acid and sodium chlorite on pretreated fibres and caused no further separation of fibres (plates G and H). Delignification did remove most of the surface layer/deposits seen in plate E and the surface of the straw fibre in plate H looks smoother. Cellulose lamellae/agglomerates are visible with the lignin removed. An AFM scan (plate I) shows that delignification exposes intact, interwoven cellulose microfibrils which look similar to the fibrils seen in plate C before disruption of the lignin within the straw.

Steam explosion is observed to cause partial separation of fibres with 90° compression bends visible in plate J. A surface layer with debris and droplets can be seen in plate K with the surface appearing similar to that seen in plate E where lignin has been ‘re-deposited’ as globules onto the surface. Lignin globules are indicated with arrows. The AFM image shows globular surface deposits in plate L, which when compared to plate F demonstrate similarity in the effect of hydrothermal and steam explosion pretreatment on the lignin in wheat straw.

Overall the research of Kristensen *et al.* very effectively demonstrates that lignin is disrupted during hydrothermal pretreatment and steam explosion. They suggest that the lignin is removed and redeposited on the straw with the reattachment of the lignin potentially being weaker than when it was bonded to the material through its native bonds. The pretreatments also have the effect of defibrating the materials, increasing their surface areas.

Ibrahim *et al.* (2011) have published research comparing steam explosion and alkali pulping of rice straw to prepare the material for enzymatic hydrolysis and subsequent fermentation to produce bioethanol. Though the starting materials are different (Ibrahim *et. al*. using rice straw) and they did not use SO_2 impregnation, their research had similar findings for steam explosion of straw as Kristensen *et al.* (2008). Straw fibres were found to be well separated and upon closer inspection are observed to have 'holes' in their surface due to disruption of the rice straw. Alkali pulping of the straw is found to separate the fibres in the material, but leaves the surface smooth and without holes, but with lignin globules present similar to those described by Kristensen *et al.* (2008).

Lignin droplet formation *via* pretreatment is also described by Selig *et al.* (2007) though they use corn stover and yet another pretreatment method (H_2SO_4 extraction at 150 °C for 20 minutes). The Selig paper describes an elegant and thorough experiment which demonstrates solubilising of lignin derivatives from corn stover, their removal from the plant matrix into solution, then redeposition onto cellulose substrates. The cellulose substrates having, lignin droplets attached to their surfaces, and the corn stover were then imaged using SEM and AFM and similar droplets were found. The SEM images of the corn stover showed hemispherical formations emanating from the corn stover cell wall (as indicated by

the green arrows) and near perfect spheres (indicated by the blue arrows) attached to the surface of the corn stover and cellulose substrates as shown in see Figure 2.3.

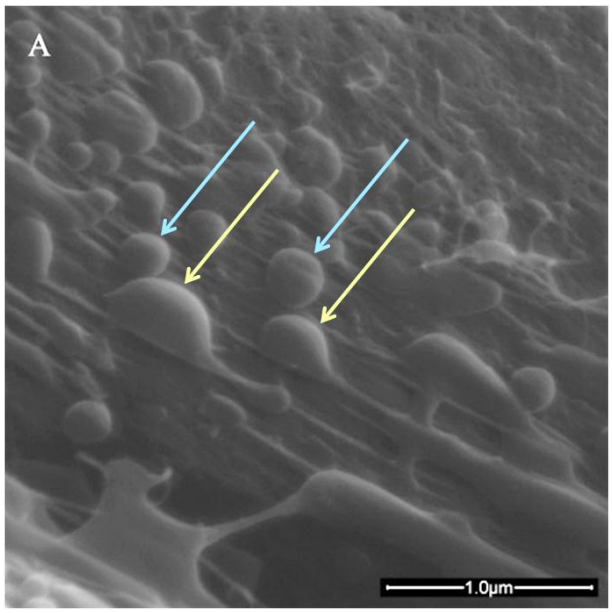

Figure 2.3. Lignin emanating from corn stover cell walls and attaching to the surface of the corn stover. (Reproduced from Selig *et al.*, 2007)

These spherical formations are ascribed as being due to lignin from the raw material. The theory of lignin droplet formation by thermochemical treatment of lignocellulosic material is further strengthened by perhaps the most convincing work investigating lignin extraction by Donohoe *et al.* (2008) who performed acid pretreatment of corn stover at elevated temperature (150 °C). It was found that lignin extraction from lignocellulosics occurs if the lignin is heated above its phase transition temperature (120 °C) at which point the lignin becomes fluid. Temperatures above 120 °C were found to be effective for lignin extraction even over short time periods. The fluid lignin migrates and droplets agglomerate outside of the plant cell wall matrix before redepositing on the material. The Donohoe *et al.* research covers a range of analytical techniques including SEM imaging of the droplets. Figure 2.4 (a) shows lignin droplet formation, and droplet growth as they combine. Different morphologies of the lignin droplets can be observed including roughened surfaces (as seen

in Figure 2.4 (b)) attributed potentially to carbohydrate shells making the droplets effectively covered in lignin-carbohydrate complexes.

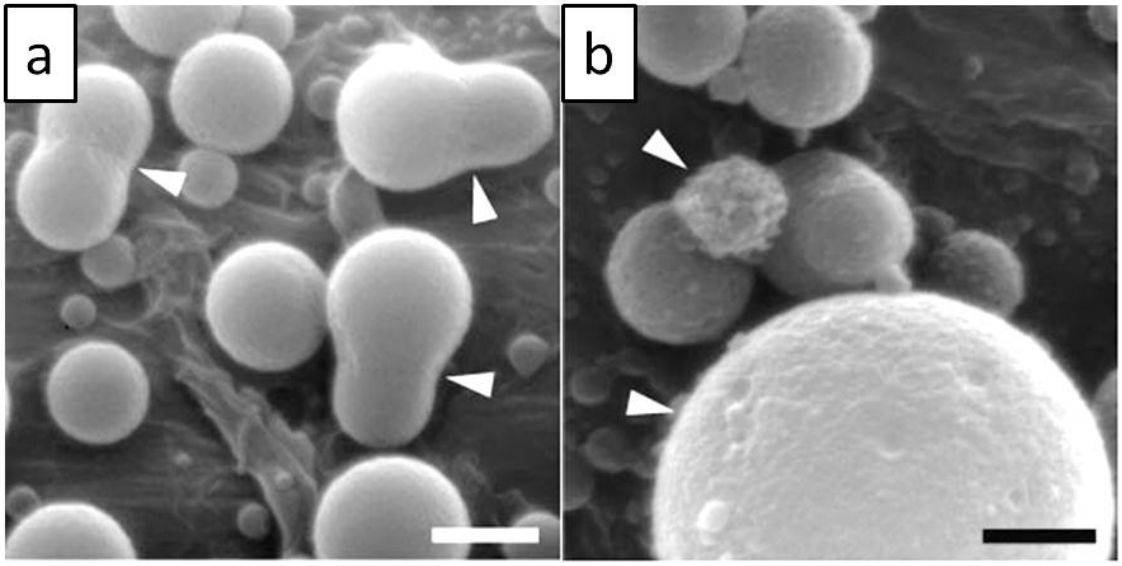

Figure 2.4. Lignin droplet formation from lignocellulosic materials. (a) Shows lignin droplets forming and combining. (b) Shows the roughened surface of some of the lignin droplets. The scale bar = 0.5 µm. (Reproduced from Donohoe *et al.*, 2008)

FTIR comparison of the droplets from corn stover and lignin control materials demonstrates that the droplets are composed of lignin. Nuclear magnetic resonance (NMR), antibody application (using antibodies sensitive to syringyl guaiacyl propane epitopes) and staining (using $KMnO_4$) provide even more evidence that the droplets were indeed lignin derived. These findings are among the most compelling and convincing for the formation of lignin droplets upon pretreatment of lignocellulosic material.

2.4.2 Hemicellulose

Hemicellulose differs from cellulose in that it is a heterogeneous, branched polymer composed of monomers including xylose, mannose, galactose and arabinose. The branching includes other organic compounds as well as saccharides and prevents hemicellulose chains from aggregating, as cellulose does, therefore increasing its solubility (Collins and Ferrier, 1995). Hemicellulose is situated between cellulose fibrils and lignin in plant tissues.

Hemicellulose is removed during pretreatment of lignocellulosic materials and removal is necessary to achieve effective enzymatic hydrolysis of cellulose in lignocellulosic materials. Hemicellulose composition varies with plant type though xylose is the most common monosaccharide in hemicellulose. Xylan forms the hemicellulose backbone, similarly to cellulose being made up of β(1→4) linked xylose sugars (Hirst, 1962). An example structure for hemicellulose is given in Figure 2.5.

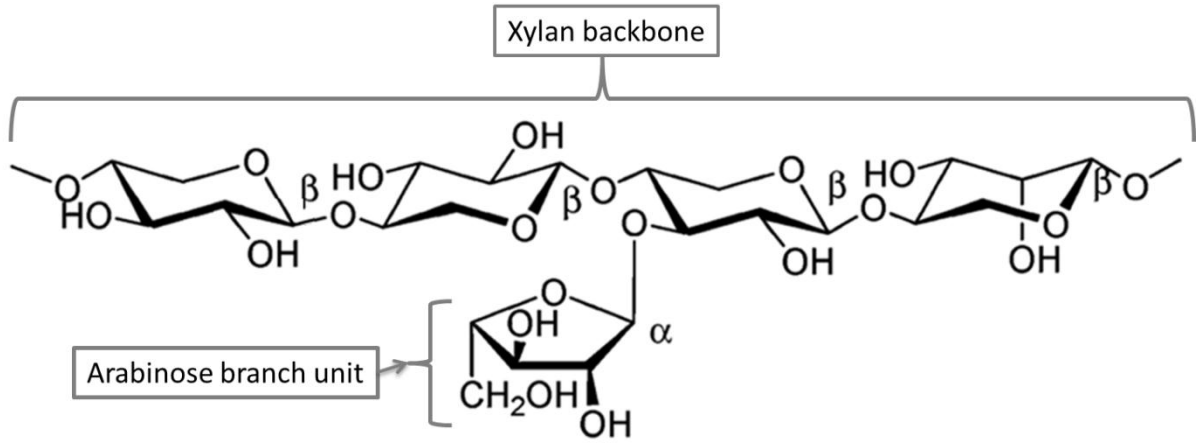

Figure 2.5. An example structure for hemicellulose (adapted from Dutta *et al*., 2012).

Chaudhry *et al.* have a number of publications in this area and though their research is performed using NaOH of lower concentration than that used in the current research, they consistently find that NaOH treatment of straw increases its digestibility through removal of hemicellulose (Chaudhry and Miller, 1996, Chaudhry, 1998, 2000). Removal of lignin/hemicellulose gives increased digestibility of straw as these materials encrust cellulose (Foyle *et al*., 2007), protecting it from breakdown by gut enzymes in animals, which is also why pretreatment of lignocellulosic materials is required in biofuel production.

Hemicellulose and lignin are removed together due to the association between them within plant materials. Alkali treatment acts to cleave lignin-hemicellulose covalent bonds and therefore, leads to removal of lignin and hemicellulose derivatives, as well as lignin-carbohydrate complexes.

2.4.3 Lignin-carbohydrate complexes

The hydrophobic nature of lignin and hydrophilic nature of carbohydrates means that lignin-carbohydrate complexes potentially have surfactant-like properties. This amphiphilicity makes them potential candidates for foaming agents from plant materials. Lignin-carbohydrate complexes from perennial grasses (*Lolium perenne/multiflorum*) have been studied by Morrison *et al.* and research published in a number of papers (Morrison, 1973, 1974a, 1974b).

Morrison (1973) describes the extraction of lignin-carbohydrate complexes using aqueous NaOH. Some pretreatment of the grasses was performed to remove lipids, low molecular weight phenols and de-wax the samples before alkali extraction of lignin-carbohydrate complexes. It is reported that 'some' of the samples required ball milling for 7 days prior to extraction in order to successfully extract significant yields of the complexes. It is not made clear, however, which samples benefitted from ball milling or indeed if all samples underwent the same ball milling procedure or not.

The procedure given for the NaOH extracted sample involved mixing the grass with 1 $molL^{-1}$ aqueous NaOH overnight by rolling in sealed bottles before filtering the solids, precipitating the lignin-carbohydrate complexes then analysing the precipitated extracts. Alkali extraction was found to produce complexes containing the largest amount of lignin of all of the extraction methods examined in this research (13% of lignin within the carbohydrate complexes which were isolated). It was found that the carbohydrate composition of the alkali extracted lignin-carbohydrate complexes isolated by Morrison is similar to the composition of grass hemicelluloses. The carbohydrate composition of the complexes found by Morrison is given in Table 2.2:

Table 2.2. Carbohydrate content of lignin-carbohydrate complexes extracted from grass. (From Morrison, (1973))

	Arabinose	Xylose	Mannose	Galactose	Glucose
% carbohydrate in hydrosylate	17.6	72.4	-	4.8	5.2

Morrison (1974a) furthered his investigation of grasses and carbohydrate complexes by trying to better understand the structure of lignin-carbohydrate complexes in different parts (leaf, leaf sheath and stem) of diploid (S23) and tetraploid (Barpastra) ryegrass plants. Extraction with dimethyl sulphoxide (DMSO) was performed before extraction with aqueous NaOH in order to extract what were referred to by Morrison as the lignin-carbohydrate complexes ('LCCs' - corresponding to the cell walls) before extracting what Morrison refers to as the lignin-hemicellulose complexes ('LHCs'), associated with the hemicellulose content of the grass. It is acknowledged within the article however, that if the DMSO step had not been performed then some of the LCCs would be extracted by the alkali treatment step. Another difference in the methodology for the alkali extraction step used by Morrison in this paper is that the concentration of aqueous NaOH used was 0.1 $molL^{-1}$ which is 10 fold more dilute than that used in his previously mentioned publication (Morrison, 1973).

The diploid and tetraploid varieties of grass showed little difference in the results generated between their respective samples. The amount of lignin found in stem tissue > sheath leaf tissue > leaf. It was also found that virtually all samples had greater lignin content in the LHC than LCC indicating that the lignin is associated with the hemicellulose content of plant material (predominantly containing xylose) rather than the 'carbohydrate' content (predominantly glucose containing). Therefore, although the extractions by Morrison are not perfectly matched to the conditions examined in the present research, the NaOH extraction of grasses is relevant hence the extraction and identification of lignin-carbohydrate or lignin-hemicellulose complexes is relevant.

Complementing the research by Morrison is research by Sun *et al.* (1997) which attempts to suggest a structure for wheat straw lignin by a well designed and thorough sequential fractionation of wheat straw hemicellulose and lignin in a multistage process. Aqueous NaOH was used to extract lignin and hemicellulose, then the hemicellulose precipitated by ethanol and lignin precipitated by adjusting the solution to pH 1.5.

The paper intelligently describes the attachment of ferrulic acid and *p*-coumeric acid between hemicellulose and lignin *via* ester or ether bonds. Ester linkages are described as being the 'alkali-labile' covalent bonds which Morrison (1974a) described, while ether linkages are 'acid labile'. Alkali hydrolysis of ester bonds was described as occurring at room temperature, with 1 $molL^{-1}$ aqueous NaOH being used in a 16 hour reaction. The ether bonds required high temperature (170 °C) and concentration of NaOH (4 $molL^{-1}$) indicating the increased stability of ether bonds to alkaline conditions. A tentative structure for lignin is given which is a helpful in visualising the ester and ether linkages in a potential lignin structure (see Figure 2.6).

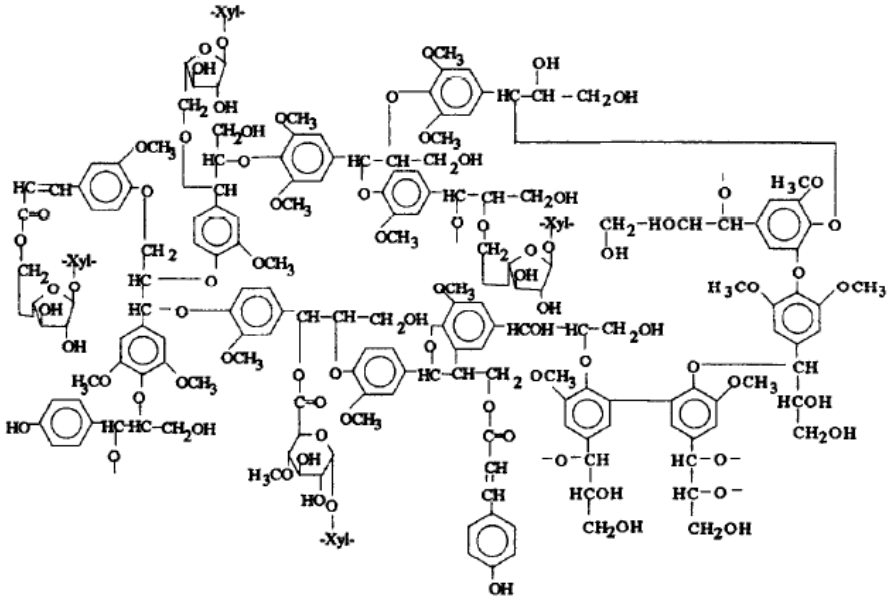

Figure 2.6. A tentative structure for wheat straw lignin. (Reproduced from Sun *et al.*, 1997)

2.4.4 Cellulose

Cellulose makes up the largest proportion of lignocellulosic materials and is the most abundant naturally occurring polymer on Earth. Cellulose is a polysaccharide made up of glucose monomers linked *via* β(1 → 4) glycosidic bonds in chains hundreds to thousands of units in length as shown Figure 2.7.

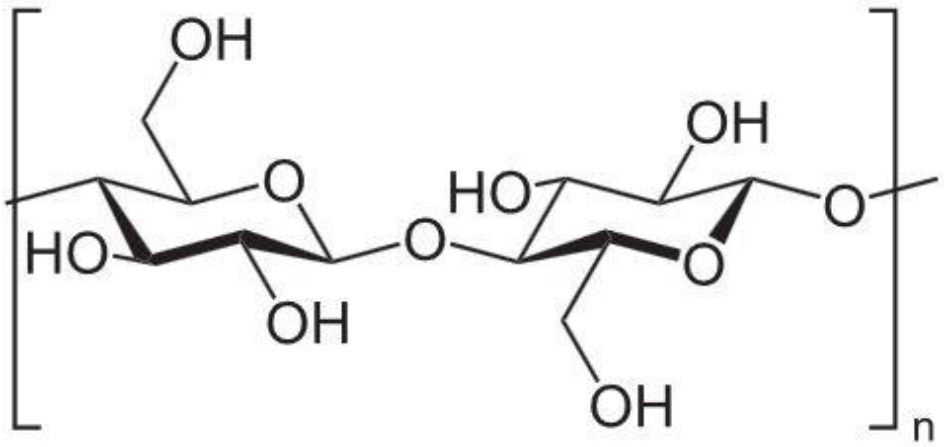

Figure 2.7. The structure of cellulose polymer.

Cellulose polymers interact forming larger bundles of fibres held together by hydrogen bonds, which are found in the plant cell walls. Cellulose polymers help impart strength and rigidity to plants (McMurry, 2004).

Knill and Kennedy (2003) have published an extensive, thorough and informative review on understanding mechanisms for cellulose dissolution and degradation under alkaline conditions. They state that the glycosidic (1→4) linkages between glucose units in cellulose are stable at temperatures < 170 °C. Significant degradation to produce D-glucoisosaccharinic acids can be obtained if cellulose is boiled in dilute NaOH as well as significant weight loss from dissolution of short-chain material within the cellulose. The rate of cellulose degradation (by all modes) depends on the degree of crystallinity of the cellulose with more crystalline cellulose degrading more slowly. In chemical attack on cellulose (such as by alkali) the reaction rate limiting steps are from the rate of scission of mid-chain parts of

the cellulose, or reaction end groups in the cellulose which are inaccessible due to encrusting of the fibres by lignin/hemicellulose or bundling of the molecules into fibres.

Degradation at lower temperature is due to competing reactions. 'Peeling' is degradation due to dissolution of short chain material attached to reactive (reducing) end groups on the cellulose. If peeling reactions were to continue without something to halt their progression then whole polymer chains would be dissolved resulting in complete dissolution of the material. Complete dissolution does not occur due to 'stopping' reactions where alkali stable cellulose derivatives (substituted D-glucometasaccharinic acids) are produced which prevent further degradation of a particular cellulose molecule.

These reactions will continue to occur with accessible/reactive portions of the cellulose until they are exhausted, then the degradation rate will be limited by the generation of new reactive portions of the cellulose (reducing end groups) by random mid-chain scission which a much slower process. Overall, the Knill and Kennedy review demonstrates that cellulose is degraded under alkaline conditions such as in the current research and in pretreatment for biofuel production. The reactions described explain how alkaline extraction of plant materials could lead to dissolution of cellulose from the materials.

2.4.5 Protein

Plants contain protein which make up plant enzymes such as those involved in photosynthesis (RuBP and Rubisco) (Kanai and Edwards, 1999) as well as structural elements within plants. Chiesa and Gnansounou (2011) have reviewed the extraction of protein from biomass for use in animal and human nutrition. Extraction of protein from biomass within a 'bio-refinery' would help maximise the utilisation of biomaterials and increase the valorisation of biomass overall. Plant protein content can vary dramatically with Nagy *et al.* (1978) listing a range of tropical and subtropical leaves ranging from 20 - 61% DM (% dry

matter) and tropical forage grasses having protein content of around 10 - 12% DM. Extraction of plant protein from fresh biomass is more effective than dried biomass. Nutritive protein extraction from dry biomass is problematic because it requires harsh conditions (high temperature and pH) which are not suitable for effective extraction of high quality protein without degradation. Protein extraction can be performed by pulping leaves (without pH modification) and extracting the juices, but extraction is improved under alkaline conditions away from the isoelectric point of the proteins (Betschart and Kinsella, 1973).

Lestari *et al.* (2010) describe protein extraction from an oilseed crop (*Jatropha Curcas)* and is particularly interesting as it states that protein extraction can be enhanced using pH 11 or higher (as in the current research), which has the effect of denaturing and dispersing the protein to expose polar and apolar groups. Lestari *et al.* (2010) perform extractions at room temperature as denaturation or hydrolysis of proteins can occur due to the effect of temperature and it is stated that cooling or extraction at room temperature is favourable where protein quality is important. High pH is, however, described as the most effective method of protein extraction without mention of protein hydrolysis/degradation by Fernández *et al.* (1999).

When considering extraction of leaf biomass it is worth noting that tannins in leaves can bind to proteins. Tannin-protein binding is in fact described as a mechanism by which leaves protect themselves from consumption by herbivores, as tannin association with proteins decreases their digestibility (Muetzel and Becker, 2006). Tannins are responsible for the brown coloration of leaves in autumn when chlorophyll production in leaves ceases and their green coloration desists. The strong coloration of tannins and their association with

protein does offer the possibility that any foaming agent made from leaf proteins may be strongly coloured which might make them unsuitable for use in laundry detergent products.

2.5 Foams

This section aims to give an insight into the literature regarding foam formation and foam stabilisation where relevant to the alkali extracted plant solutions examined in the current research. An attempt will be made to explain the importance of some of the components of the plant raw materials solubilised during extractions in relation to forming stable foam. For basic, background information on more conventional small molecule type surfactants, the Marangoni effect, foam formation and foam coarsening/disproportionation, see section 9.1. Increasing foam stability by manipulating bubble size distribution and solubility of the gaseous phase in the foam is not possible in laundry foaming systems hence discussion of these will not be covered here.

Foam formation and foam stabilisation may occur due to the effect of different materials in solution as is described by Schmidt *et al.* (2010) where foaming is caused by proteins and the foam is stabilised by dissolved saccharides. Formation of viable foam comes from rapid and extensive coverage of the air-water interface by foaming materials. Slow adsorption of large foaming species at the interface means stable film formation required for bubble formation is not as easy as for small molecule surfactants. The molecules extracted into solution which would be responsible for foaming of alkali plant extract solutions would likely be large. Lignin-carbohydrate complexes are a possible source of foaming and those extracted by (Morrison, 1973) were found to have molecular weight ≥ 150000 $gmol^{-1}$. Proteins extracted from plant materials would be expected to have high molecular weights also, whereas linear alkylbenzene sulphonate (LAS) has a much lower molecular weight. Martinez *et al.* (1989) studied toxicity of LAS by molecular size, working with molecular weight LAS from

232 - 250 $gmol^{-1}$. Hence foam formation by lignin-carbohydrate complexes or proteins would involve large molecules and slow adsorption at the interface which would result in foams having quite different properties to small molecule surfactant foam.

Foam stabilisation comes from changing the solution properties within the liquid films around bubbles in the foam. A discussion follows regarding foam formation potential for lignin-carbohydrate complexes and proteins in plants followed by the potential for foam stabilising effects of extracted saccharides from plants.

2.5.1 Foaming solutions from lignin derivatives

This author has trawled the literature for research covering foaming of solutions containing lignin derivatives/lignin-carbohydrate complexes, however, no research was found. What was found was research covering the use of lignin derivatives in rigid foams such as starch-lignin foams for packaging containers (Stevens *et al.*, 2010) or polyurethane foams containing lignin (Nadji *et al.*, 2005, Silva *et al.*, 2009) for use in construction or the automotive industry, for example. Research by Rojas *et al. (2007)* looked at the emulsifying effects of lignin based materials (lignin sulphonates from kraft pulping black liquor) and found that the 'unmodified' lignins in solution reduce surface tension. Shulga *et al.* (2011) found that modified (oxidised) softwood sulphate lignin also had a surface tension reducing effect on aqueous solutions. The effect of reduction of liquid surface tension by lignin is interesting as it implies that lignin may be able to assist in foam generation.

However this author was unable to find any research covering surfactant behaviour of solutions containing lignin-carbohydrate complexes produced from alkaline extraction of lignocellulosic materials in the literature. Within the current research any alkali plant extract solutions produced would contain unrefined, unpurified and unmodified materials. The nature of the alkali plant extract solutions, being complex mixtures of multiple solubilised

components, further separates the current research from that performed on purified lignin derivatives. Surfactant properties would be expected for lignin-carbohydrate complexes as for lignosulphonates, as lignin is hydrophobic and carbohydrates hydrophilic. Lack of publications covering surfactant properties of lignin-carbohydrate complex containing solutions from alkaline extracted plant raw materials suggests a gap in the knowledge which the current research contributes towards.

2.5.2 Foam formation by proteins

Alkali extraction of plant materials leads to solubilisation of proteins as discussed in section 2.4.5, hence proteins are another potential candidate which could be responsible for generation of foams from the extract solutions (see section 6.4 for further insight). It is considered useful therefore to present some of the relevant literature regarding proteinaceous foams.

Proteins have surfactant properties as within the same molecules, some side chains from the amino acids forming the proteins are hydrophilic (*e.g.* Arginine, Histidine, Lycine *etc.*) and some are hydrophobic (*e.g.* Alanine, Valine, Isoleucene, Leucine *etc.*) The mechanism by which proteins stabilise foam is debated in the literature. Wierenga and Gruppen (2010) discuss both the 'loop-train model' for the stabilisation of foam (which treats proteins adsorbing at the interface as random coils) and the colloidal-particle foam stabilisation mechanism (which treats adsorbing proteins as colloidal particles).

2.5.2.1 The 'loop-train' model

Wierenga and Gruppen (2010) acknowledge the lack of a unifying theory in terms of the microstructure of proteinaceous foams. They discuss the loop-train and colloidal models of protein foam formations in a very interesting and well-constructed paper. In the loop-train model, proteins are regarded as polymeric coils with a specific three dimensional structure.

During adsorption at an interface this 3D protein structure is changed and the protein said to be denatured (Graham and Phillips, 1979, Beverung *et al.*, 1999, Holt *et al.*, 2000).

Denaturation of proteins at the interface minimises their energy when adsorbed, giving the most stable conformation whereby the hydrophobic side chains of the protein become orientated toward the air at the interface (loops) while the hydrophilic side chains of the proteins orientate to the aqueous region (trains). Figure 2.8 (a) is a schematic showing adsorption of random coil proteins at an interface and undergoing conformation change leading to the loop and train appearance of the protein as seen in Figure 2.8 (b).

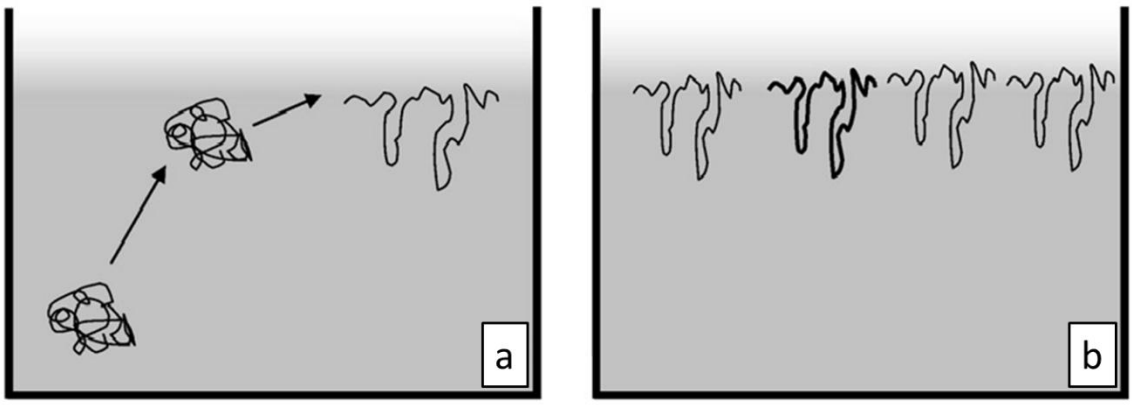

Figure 2.8. Schematic showing (a) proteins acting as random coils adsorbing at the interface during the initial stages and (b) at saturation. (Reproduced from Wierenga and Gruppen, 2010).

Compared to conventional surfactant foam, the formation of protein foam requires greater energy input (through whipping, sparging or other agitation) and longer times to allow protein adsorption at the interface. In the loop-train model protein foam formation is slow compared to small molecule surfactants as proteins are transported to the interface more slowly and protein unfolding taking time. The protein denaturation and reorganisation at the air-water interface, of the hydrophilic and hydrophobic side chains of the protein provides a system of lower energy. The long and flexible nature of proteins is said to convey a viscoelasticity to the interface giving it stability against distortion and making rupture of the bubble film less likely when the interface is deformed or disturbed. Elasticity of the

interface is thought to come from proteins forming a gelled network when adsorbed at the interface with the foam stability being dependent on how quickly the protein can change conformation at the interface and the formation of a gelled network (Martin *et al.*, 2002).

Wierenga and Gruppen (2010) point to convincing evidence presented by Husband *et al.* (2001) and Jorgensen *et al.* (2004) among others (Lu *et al*., 1998, 1999, Meinders and De Jongh, 2002, Kudryashova *et al*., 2003) which challenges the idea that proteins undergo significant conformational changes when adsorbing at the interface. Instead it is suggested that the tertiary structure may be disrupted with the secondary structure being less altered than the loop train view of protein adsorption might suggest. The supporting evidence presented, such as the measured enthalpy change for protein denaturation being similar for both adsorbed and 'free' protein makes the idea of limited denaturation of proteins at bubble interfaces quite convincing.

2.5.2.2 Colloidal proteins/particle stabilisation of foams

Evidence of lack of protein conformational change at the interface leads Wierenga and Gruppen (2010) to discuss evidence that adsorption of proteins at an interface can be considered as adsorption of charged particles as shown schematically in Figure 2.9.

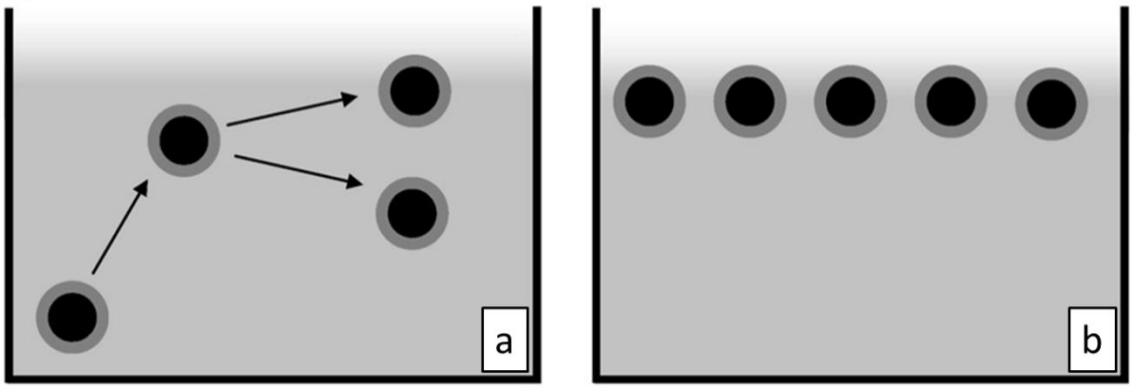

Figure 2.9. Schematic showing proteins acting as colloidal particles adsorbing at the interface. (a) Arrows indicate how proteins approach the interface and can either be adsorb if there is a space available or diffuse back into the solution. (b) Shows the interface when it has become saturated with adsorbed particles. (Reproduced from Wierenga and Gruppen, 2010).

Figure 2.9 (a) shows how protein particles approach the interface and either adsorb or diffuse back into the solution. Adsorbed proteins form a layer covering the interface which is associated with the stabilising effect of proteins on foams. Protein stabilising of foams may also be attributed to gelling or 'jamming' of these particles within the confined area of the interface. This could lead to an increase in the apparent viscosity of the liquid in turn increasing foam stability (Sethumadhavan *et al.*, 2001, Wierenga *et al.*, 2009). Proteins adsorb at interfaces and the rate of adsorption increases with protein hydrophobicity (Wierenga *et al.*, 2003). Small effective particle size is also important (as for Pickering stabilisation). Finally the net charge on a protein has an effect on how quickly it adsorbs at the interface. Higher net charge on adsorbed proteins results in repulsion between them which provides a barrier to more particles adsorbing at the interface, and leads ultimately to less protein adsorbing at the interface, and less foaming.

There are two important things to note when considering adsorption of particles at an interface. The first is the irreversible adsorption of particles; the second is that the rate of adsorption decreases as coverage of the interface by particles increases. The irreversible nature of adsorption of particles at an interface is discussed by Binks (2002) and is attributed to very high energy of detachment for particles at the interface. The energy of detachment is high compared to small molecule surfactants, though very small particles of the size comparable to most surfactant molecules (< 0.5 nm in radius) are easily detached. If a particle stabilised bubble shrinks then the overall bubble surface area would decrease and accommodate fewer particles however, the high energy of detachment of particles means bubbles are more stable to shrinkage as particles are effectively permanently bound. Difficulty in removing the particles impedes shrinking of the interface and contributes to the high stability found for particle foams.

The slowdown in adsorption at an interface as coverage increases is examined by Talbot *et al.* (2000) in some depth using mathematical modelling (which is beyond the scope of this discussion) to describe random sequential adsorption (RSA) of particles. Slowdown of adsorption is perhaps most easily described by the car parking analogy discussed by Talbot *et al.* whereby a car enters a car park similar to a particle approaching an interface. The car moves around looking for a space to occupy, which in an empty car park it finds and fills quickly. Similarly for a particle approaching an interface, if there is a gap the particle will occupy it. The car park becomes more full as more cars enter hence there are fewer available spaces so the car might approach a space, find it full and move on. Similarly a particle will approach the interface and if it is occupied the particle will diffuse away and continue moving around until it finds an available space. The probability of finding an empty space for the car decreases as the car park becomes fuller, hence the slowdown in parking rate for the cars. Similarly as the interface becomes increasingly filled with particles, the probability of a particle approaching an empty space decreases and it takes longer for the particle to find an empty space and adsorb at the interface. The approach and adsorption or diffusion away from the interface by a particle is shown in Figure 2.9 (a) with the resulting coverage of the interface by particles shown in Figure 2.9 (b).

Over time a bubble interface becomes saturated and no more protein particles can be adsorbed. Saturation is not necessarily when the interface is completely covered by close packing of particles since charge repulsion of particles also plays a role in the packing density. Therefore, the packing density will be smaller at saturation for charged particles than if they were uncharged. Although simplistic, the RSA model is a useful aid in understanding slow adsorption of proteins acting as particles at the interface.

Wierenga and Gruppen (2010) present convincing evidence of the behaviour of proteins as particles rather than as random coils when they adsorb at an interface. Considering the particle size, hydrophobicity and charge with the RSA model of particles at the interface, the colloidal model of protein adsorption offers a plausible explanation of protein adsorption at interfaces and the corresponding requirement for more time for protein particles to adsorb compared to small molecule surfactants. This slower adsorption offers a potential explanation of the difficulty in forming foam by shaking/agitating plant extract solutions should they be composed of proteins or other particles.

Due to the large size of lignin-carbohydrate complexes, this author considers it plausible that similar effects to those described for proteinaceous particles could potentially be applicable to adsorption of lignin-carbohydrate complexes acting as particles at interfaces.

2.5.3 Solution viscosity and saccharide extraction from plant materials

Aside from their nutritional value, saccharides in biological systems interact with water to give some degree of structure to aqueous solutions whereby increased saccharide concentration in solution increases the solution viscosity. Banipal *et al.* describe the effect of increasing solution viscosity with concentration of saccharides in two interesting papers (Banipal *et al*., 2010, 2011) as do Pal and Chauhan (2009). Though these papers are related to the study of saccharide interactions with other molecules in aqueous solution, the measurements made for blank solutions (saccharide and water only) are useful as they demonstrate increasing solution viscosity with saccharide concentration increase. Alkali extraction of plant raw materials solubilises hemicellulosic saccharides which increase the solution viscosity as more saccharides are solubilised. The increase in solution viscosity from solubilised saccharides will in turn have an effect on the stability of foams produced from the solutions as discussed in the following sections.

2.5.4 Foam stabilisation and the relevance of solution viscosity

Film drainage occurs under gravity when the liquid held within a bubble film drains down through the film. As film drainage occurs, the volume of liquid within the film decreases therefore the film thins. If film thinning progresses too far 'critical film thickness' will be reached, which is where film rupture occurs (Sheludko, 1967), and foam collapse will follow.

Wang and Narsimhan (2007) have published research which describes liquid film rupture. They give a good explanation of why liquid films in foams rupture describing how the surfaces of liquid films undergo random perturbations caused by thermal fluctuation and movement of air *etc.* These perturbations could be imagined as waves travelling across the inner/outer surfaces of the film making up a bubble, varying in amplitude according to the size of the perturbations. If the amplitude of the perturbation is equal to or greater than one half the film thickness then the film will rupture as shown schematically in Figure 2.10.

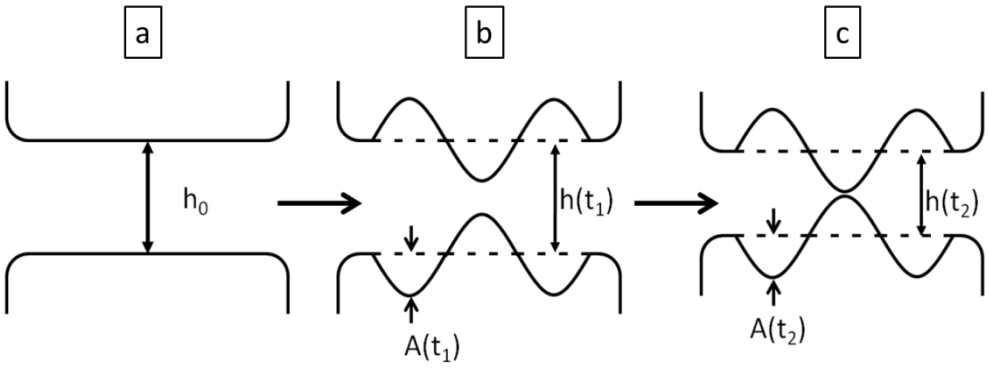

Figure 2.10. Film rupture due to random perturbations on the film surfaces of a draining film. (a) Non-equilibrium film with an initial thickness of h_0. (b) Growth of surface perturbation and decrease in film thickness. (c) Rupture of the film when the amplitude of the perturbations is equal to half of the film thickness, which at this point is the critical film thickness for the amplitude of the perturbations. (Adapted from Wang and Narsimhan, (2007))

In Figure 2.10 h_0 is the equilibrium liquid film thickness, $h(t_1)$ and $h(t_2)$ are the liquid film thicknesses at time t_1 and t_2; $A(t_1)$ and $A(t_2)$ are the amplitude of the perturbations at times t_1 and t_2. Figure 2.10 (a) shows the liquid film at equilibrium, (b) shows the liquid film being perturbed whilst the film thickness reduces and (c) shows the situation when the film

ruptures – when the perturbations are equal to half the liquid film thickness (and the film thickness = the critical film thickness).

Wang *et al.* state that rupturing of liquid films from thinning is reduced if the viscosity of the liquid within the film is higher. Higher viscosity liquid in the thin films forming the bubbles will reduce the rate of thinning hence the amplitude of the perturbations are less likely to lead to rupture the film. The effect of foaming by proteins being improved by foam stabilisation due to interaction between proteins and dissolved saccharides is discussed by Schmidt *et al.* (2010). In the context of the current research adsorption of particles (possibly proteins/lignin-carbohydrate complexes acting as particles) at the interface and the interactions between them would have the effect of increasing the surface viscosity of the film. Increased surface viscosity would have the effect of damping the surface perturbations and hence meaning it would be more difficult for the amplitude of the perturbations to increase to one half of the film thickness hence the film/bubble/foam would be more stable.

2.6 Literature review conclusion

As outlined within this chapter, the literature contains insight into the plant based materials used within the current research including their composition and the effects of NaOH extraction on them. This chapter has also discussed the established research covering foaming by a range of materials/mechanisms. What is not covered in the established literature is the foaming of solutions made by NaOH extraction on plant materials. The research within this thesis attempts to generate knowledge of foaming of alkali extracted plant materials and this makes the current research novel. The following Chapters will present the research conducted and results obtained during the research.

3 Chapter 3 – Materials and methods

3.1 Introduction

This chapter describes the process of alkali extraction of plant raw materials, analysis of the extracts, techniques to investigate foaming ability of the extracts and a discussion of the methodology of the *response surface and factorial experimental designs* used in Chapters 5 and 7 respectively.

3.2 Raw materials

All plant raw materials were dried and milled before alkali extraction (see section 3.3). Milling was required to ensure proper mixing of the solids in the NaOH solution, though milling will not be used in any process derived from the current research if possible.

3.2.1 Hay

A single bale of hay was used for all of the experiments in this research, with the exception of the repeated sparging experiments in Chapter 7 (for data set 2) because the original hay bale had been consumed.

Hay incorporates grass (*e.g.* ryegrass: *Lolium Perenne*), legumes (*e.g.* clover: *Trifolium*) and herbaceous plants (*e.g.* alfalfa: *Medicago sativa).* Hay has natural variability in composition which is affected by the type of plants incorporated into the hay, how the hay was managed during growth, maturity of the plants at the time of harvest and the time of year the hay was harvested.

3.2.2 Horse chestnut leaf

Horse chestnut (*Aesculus hippocastanum*) tree leaves were collected from trees in Stewart Park, Middlesbrough, U.K. (latitude and longitude +54° 32' 34.36", -1° 12' 13.74") on

25/08/2009. The dried/milled material (section 3.3) was sealed in plastic zip lock type bags at ambient temperature, out of direct sunlight, until required for use.

3.2.3 Rice Straw

Rice straw is the dried shafts of rice plants (*Oryza sativa*) and bales were acquired from farmer Jerry Uhland, Marysville, California in September 2010.

3.2.4 Other materials

The NaOH pellets were purchased from VWR and ultra-high purity water (having resistivity of 18 MΩ cm^{-1}) was used to make up the aqueous NaOH solutions. Aqueous hydrochloric acid (1.18 specific gravity) used for pH adjustment of solutions was purchased from VWR.

3.3 Plant material drying and milling

The plant raw materials were oven dried at 60 °C for 24 hours (to constant mass) before use. The loss on drying for the materials is listed in Table 3.1.

Table 3.1. The % mass loss on drying for the plant raw materials.

Material	% Mass loss when dried at 60 °C for 24 hours	Observations post drying
Hay	12	Darker in colour and more brittle when dried.
Horse chestnut leaves	75	Dried leaves were very thin and crisp, with a strong earthy smell.
Rice straw	11	The rice straw appearance did not change after drying.

After drying the hay and rice straw were chopped into 2 – 3 cm long pieces to fit into the coffee grinder for milling. The brittle, dried horse chestnut leaves were broken down by hand whilst putting them in the grinder. Milling took place using two similarly designed coffee grinders - a Delonghi KG49 and a Krupps F203. 1 – 2 kg of plant material at a time was chopped and milled in small quantities of around 10 – 15 g. The amount of material milled

was such that the grinding cup was approximately ⅔ full each time. Milling took place for approximately 30 seconds. The aliquots of milled material were mixed in a large bag to achieve homogenisation before use in extractions.

Plant materials have inherent variability and it was understood that the samples of plant raw materials used during alkali extractions should be representative of the plant material generally. The plant raw materials were gathered over a large area during bailing/leaf collection which helped ensure representative sampling of the raw materials. Sub-sampling/milling of small amounts of the dried plant materials before recombining and mixing increased the assurance that each sample used in alkali extraction was representative of the respective plant raw material.

A simpler and more attractive prospect would have been to mill the whole of the available amount of each of the plant materials in a single batch. This would have more easily ensured that the material was fully mixed and homogenised to ensure better representative sampling. However, large scale equipment was not available to achieve this. Images of dried hay before and after drying and milling can be seen in Figure 3.1.

Figure 3.1. Hay (a) before and (b) after drying and milling.

3.3.1 The reaction scheme

The reaction scheme used in this research is shown in Scheme 1.

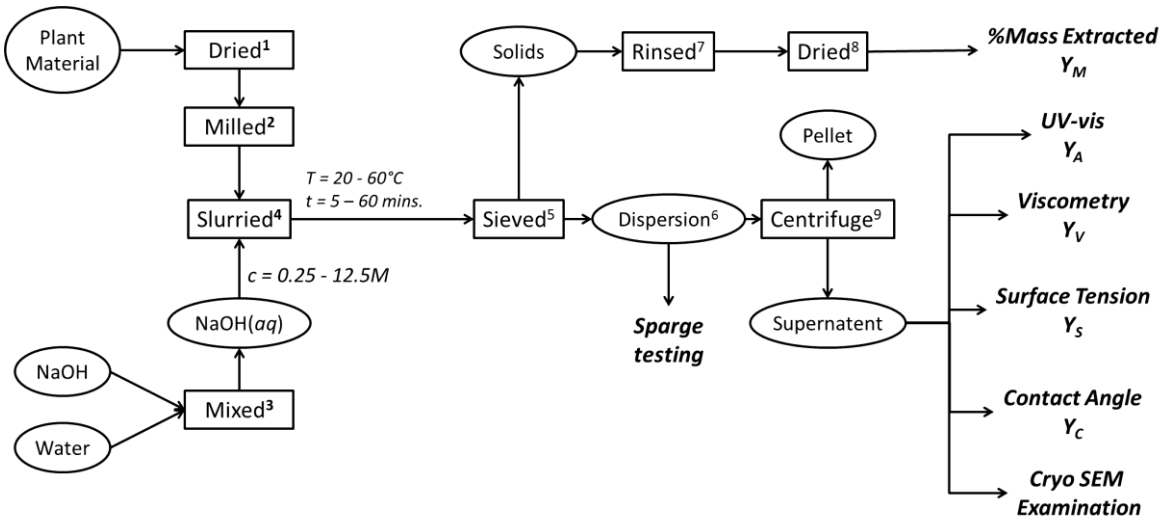

Scheme 1. Reaction scheme used for the experiments in this research. [1]Plant material was dried for 24 hours at 60 °C. [2]Milling was carried out for 30 seconds in a coffee grinder. [3]NaOH pellets were dissolved in ultra-high purity water. [4]The plant material/aqueous NaOH slurry was mixed using a magnetic stirrer. [5]A 100 µm sieve was used to separate the solids from the extract solution. [6]Dispersion sparged with particles < 100 µm present. [7]The separated solids were repeatedly rinsed with tap water then [8]dried (60 °C/24 hours) before weighing and calculating the % mass of material extracted. [9]Centrifugation at 2445 g relative centrifugal force (RCF) for 60 minutes was performed on the sieved extract solution which separated out the < 100 µm particulates into a solid pellet from the aqueous extract leaving the supernatant which was then analysed.

Dried and milled hay, horse chestnut leaf or rice straw were added to aqueous NaOH (concentrations up to 12.5 $molL^{-1}$) at a ratio of 6 g solids to 100 ml liquid. Greater solids loading made it difficult to disperse the hay/straw into the reaction slurry without more milling, which was not desirable. For all experiments except the large scale sparging experiments (see section 3.4), 100 ml of NaOH and 6 g of solids produced sufficient volumes of extract solutions for all measurements (UV-vis, Viscometry, Surface Tension, Contact Angle, and SEM).

The plant material tended to float on the NaOH and was difficult to disperse. Dispersion was achieved by first stirring the material into the aqueous NaOH using a spatula, then stirring the slurry with the magnetic stirrer at a speed which kept the solids dispersed. The dispersions were mixed at room temperature (~20 °C), 40 °C or 60 °C using a hotplate, for 5 - 60 minutes. The exact extraction conditions are given in the relevant chapters.

After extraction with the aqueous NaOH, the larger solids were removed using a 100 µm sieve. In order to keep the alkali extraction process simple, the samples for sparging testing

were only sieved, not centrifuged or further filtered. Hence the foaming of the solutions was tested with particles < 100 μm still present in the liquids. This was acceptable as foaming of the solutions was unaffected by centrifugation of the solutions when tested. Samples to be examined by other analytical methods were centrifuged before analysis as the presence of solids would have adversely affected the test methods by clogging the gap during viscosity measurements or blocking the needle during surface tension/contact angle measurement. The centrifuged solution was used for UV-vis measurement also as centrifugation was found to have no effect on the UV-vis measurements.

3.4 Sparging solution preparation

For sparging experiments in Chapter 7, 800 ml of aqueous NaOH and 48 g of hay were required to produce 450 ml of sparging solution. The remainder of the solution was removed with the separated solids during sieving when preparing the solution.

3.5 Solids removal from the product slurries

3.5.1 Sieving

Various solid/liquid separations were attempted including filtering with papers and sintered glass filters. Filtration was impossible due to the filters clogging. Sieving was found to be effective at separating the larger particles from the slurries. The reaction slurries were passed over a 100 μm stainless steel sieve and the solid/liquid portions retained. Sieving was still slow as the sieve would frequently be blinded by the viscous solution and the large particles. Gentle 'scraping' of the sieve surface using a spatula cleared the sieve apertures and ensured the liquid passed through the sieve. Careful squeezing of the solids retained on the sieve mesh maximised the liquid separated out from the solids.

3.5.2 Centrifugation of the solutions for analysis

Where required, the solutions were centrifuged in disposable plastic sample tubes for 60 minutes at 4400 RPM using a Centaur 2 centrifuge with a 34117-6034 angle rotor and 46156 - 602 buckets fitted, generating 2445 g relative centrifugal force (RCF) or using a Sigma 6-15 centrifuge fitted with a 12165 - 8 x 85 ml sample holder set to generate the same RCF.

3.6 Analytical techniques applied to the centrifuged supernatant

3.6.1 UV-vis measurement

See Appendix section 9.2.2 for background information on UV-vis spectrometry. UV-vis absorbance has been used in the literature to examine solutions which contain lignin derivatives produced by extraction of lignocellulosic materials *via* a range of methods including aqueous NaOH extraction (Morrison, 1973, Nadji *et al.*, 2009). Absorbance at 278 - 282 nm comes from non-conjugated phenolic groups (aromatic rings) in lignin such as sinapyl alcohol, coniferyl alcohol, and a small amount of absorbance by *p*-coumaryl alcohol. Absorbance at 316 - 318 nm is due to conjugated phenolic groups in *p*-coumaric and ferulic acids (Sun *et al.*, 2000, 2001, Akin, 2008, Xu *et al.*, 2008). Figure 3.2 (a) shows a comparison of UV-vis spectra recorded for solutions containing lignin extracted from wheat straw in the literature (Xu *et al.*, 2008) and a spectra generated from a solution made by extraction of hay with NaOH (b).

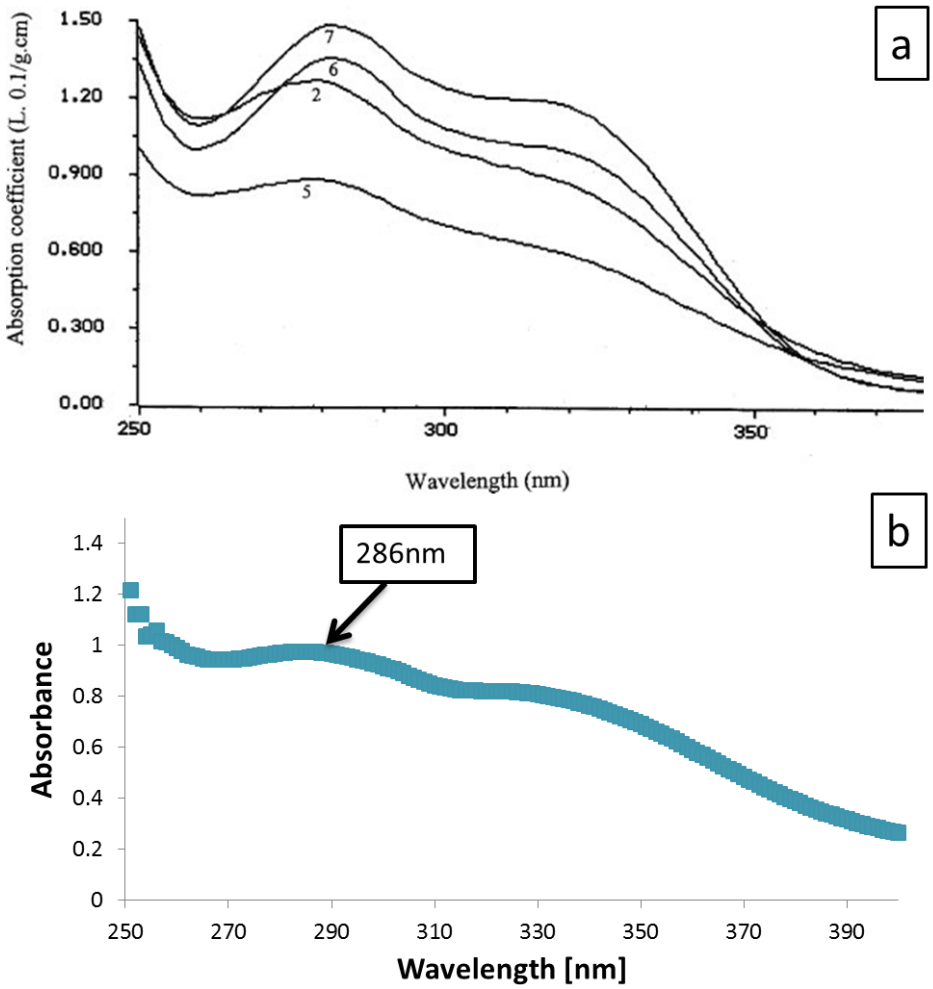

Figure 3.2. (a) UV-vis spectra showing absorbance of lignin extracted from wheat straw obtained by Xu *et al.* (2008); (b) UV-vis spectrum typical of those recorded for NaOH extracted hay solutions in the current research.

The absorbance spectrum recorded for NaOH extracted hay solution in Figure 3.2 (b) is typical of the spectra for hay/NaOH extract solutions. The absorbance at 286 nm was used in the current research as the absorbance maxima for the extract solutions. The variation in absorbance between 279 nm and 289 nm for the spectrum in Figure 3.2 (b) is 0.3% therefore any error associated with the simplification of recording the solution absorbance values at 286 nm rather than a value between 278 and 282 nm was negligible. This was found to be typical of the hay extract solution spectra.

Method

Alkali extract solutions were diluted by adding 30 µl of the centrifuged supernatant to 3 ml of ultra-high purity water in a disposable polystyrene cuvette then shaking. The UV-vis spectra of these solutions were measured on either a Cary 5000 or a Cary 50 UV-vis spectrometer (both spectrometers were found to be consistent). Measurements were taken across the range 250 – 600 nm with 1 nm increments. The source change over for the measurement lamps was at 393 nm. Each solution was measured three times and the average absorbance is reported in the results. The results of UV-vis absorbance measurements are presented in Chapter 5.

3.6.2 Viscosity measurement

Rheology is the study of flow of materials when shear forces are applied to them and how the magnitude of shear force/time/temperature all affect the viscosity of the materials. Rheology has importance in process engineering as when forces are applied to a material it may behave in very different ways depending on how large the force is, or how long it is applied for as it is processed in a plant (Barnes *et al.*, 1991). Changes in solution viscosity when materials are mixed or pumped has implications in the processing of materials generated by a particular process.

The viscosity of the reaction product solutions in the current research varied according to how much material was extracted by aqueous NaOH into solution from the hay. The viscosity of a foaming solution is important not just from the point of view of processing the solutions, as viscosity also influences the stability of foam produced from that solution (see section 2.5.3). More viscous foaming solutions result in slower drainage of liquid within the films between bubbles in foam, which in turn results in increased stability of the foam. Due

to the importance of solution viscosity in foam stabilisation, measurement of viscosity was performed for solutions produced under each set of reaction conditions.

Method

Solution viscosities were measured on a Bohlin CVO rheometer and a 40 mm, smooth, stainless steel, parallel plate geometry set-up is shown in Figure 3.3.

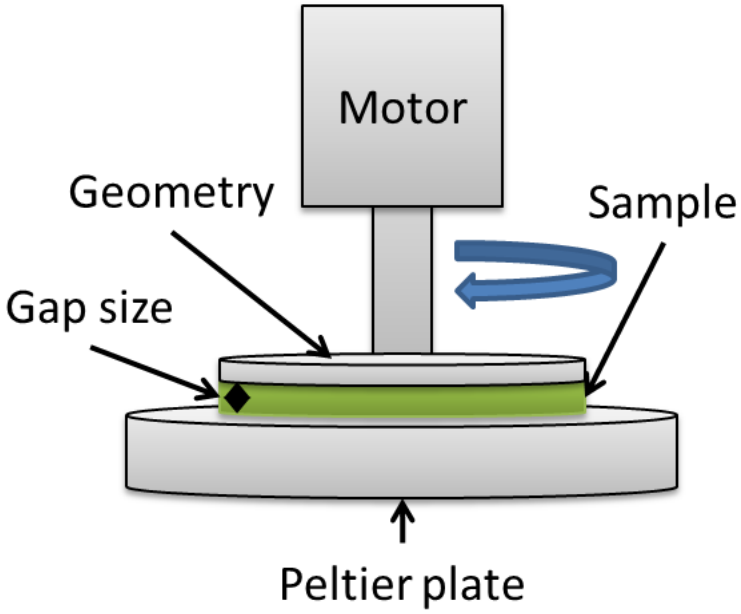

Figure 3.3. The parallel plate rheometer set up used for measurement of extract solution viscosities

A shear rate sweep (0.1 – 1000 s^{-1}) was used to look at extract solution viscosity change with shear rate. It was found that the solution viscosity did not vary much above 30 s^{-1} (see 9.2.3) hence solution viscosities were measured at 94 s^{-1}.

Solutions were dispensed onto the sample stage using disposable plastic Pasteur pipettes. The gap size for the measurements was 150 µm. Each measurement involved the solution viscosity being recorded 5 times whilst the solution was sheared at 94 s^{-1} over approximately 72 seconds. The viscosity of each solution was measured in this way three times and the

average viscosity from the three measurements reported. The results of solution viscosity measurements are presented in Chapter 5.

3.6.3 % Mass of hay components extracted in to solution

To measure the % mass of hay components extracted into solution, the solids were sieved from the reaction slurry then transferred to a 5 litre beaker and stirred for 5 seconds in 3 litres of tap water using a spatula. The solids were then separated from the rinsing water using the 100 µm sieve. This rinsing procedure was repeated 3 times, then the retained solids were squeezed by hand over the sieve mesh to remove excess water. The damp solids were oven dried for 24 hours at 60 °C before recording the dried weight and calculating the % mass extracted during the reaction according to Equation 3.1.

Equation 3.1. % Mass of the hay components extracted into solution.

$$\%\ \text{Mass extracted} = \left(1 - \frac{\text{mass of rinsed solids retained after reaction}}{\text{initial mass of plant raw material used}}\right) \times 100$$

Solids having a particle size < 100 µm were not weighed with the residues to simplify the experiments and increase throughput. In order to weigh the particles < 100 µm from every extraction, the extract solution would have required centrifugation after sieving then rinsing the solids and centrifuging again before drying. In practice this was found to be very difficult. The extra steps needed to isolate the < 100 µm particles would have added considerably to the time required to process samples hence the decision was made to simplify the experiments by only weighing the solids retained on the sieve *i.e.* those > 100 µm. It was found that this simplification in measurement of % mass extracted from hay by NaOH did not preclude effective modelling of the % mass extracted (see Chapter 5).

3.6.4 Surface tension measurement

Surface tension is the energy required to increase the surface area of a gas-liquid interface by one unit. Surface tension comes about because molecules in solution interact with each other through forces acting in all directions in the bulk of the solution, but at the surface these forces only act from within the bulk perpendicular to the interface. This leads to an imbalance of the forces acting on the molecules at an interface which manifests itself as surface tension. The surface tension of a liquid (*e.g.* water) is decreased by dissolution of surfactant in the liquid up to the critical micelle concentration (CMC) of the surfactant in solution. Beyond the critical micelle concentration (CMC) for the surfactant, the surface tension remains virtually constant. Despite this, examination of surface tension was still deemed useful in the current research due to its importance in foam generation and the fact that it was unknown if the surfactant concentration in solution would be above the CMC for the solubilised surfactants. Surfactants facilitate stable bubble formation through variation of surface tension across a bubble surface *via* the Marangoni effect. (see section 9.1.3 for further explanation).

Surface tension was measured in the current research to examine the effect of extraction conditions on the amount of dissolved surfactant present in the alkali plant extract solutions. As a control, the surface tension of aqueous NaOH of varying concentrations was measured. The surface tension was measured as 69 - 70 mN m^{-1}, slightly lower than pure water (71.9 mN m^{-1}). The pendant drop method used for measuring surface tension of the extract solutions involves forming a droplet of liquid hanging in a 'teardrop' shape under gravity at the end of a needle as shown in Figure 3.4.

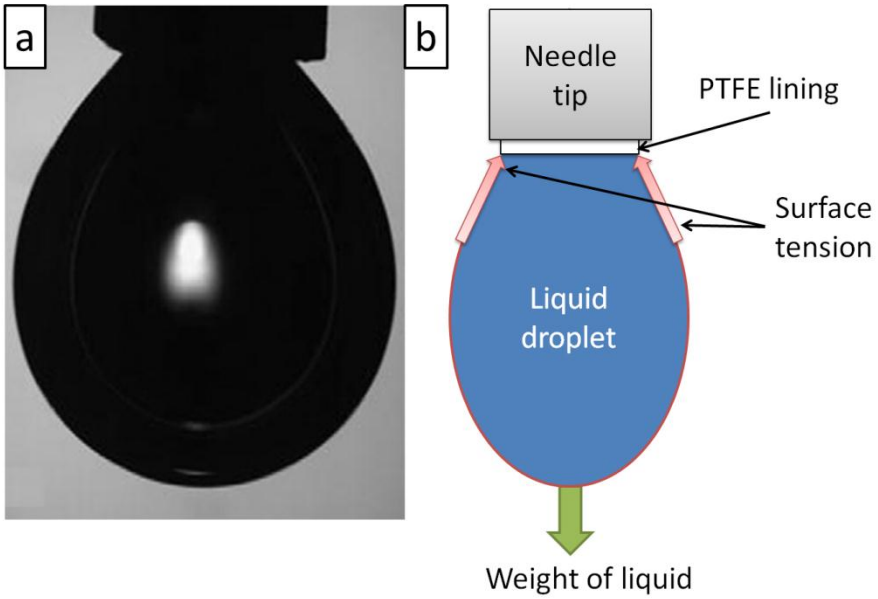

Figure 3.4. Pendant drop method of surface tension measurement. (a) Photograph of a suspended liquid droplet (reproduced from Alvarez *et al*., 2009). (b) Schematic demonstrating the forces involved in pendant drop liquid surface tension measurement.

A high speed camera captures images of the droplet and computer software analyses the droplet shape in the images to calculate the surface tension of the liquid. Figure 3.4 shows how surface tension in the liquid droplet acts to make droplets spherical by minimising the surface area and gravity elongates the droplet due to its mass. Therefore, variation in the magnitude of surface tension of the liquid gives different droplet shapes, which can be analysed by software to calculate the surface tension of the liquid.

Software analyses the outline of the droplet and compares its shape to theoretical shapes for varying surface tension values. The more spherical a droplet is, the more difficult it becomes to measure surface tension accurately as pointed out by Saad *et al.* (2011) and Hoorfar *et al.* (2005). Long equilibration times for the extract solutions in the current research caused problems in using the pendant drop method for measuring surface tension of the solutions. Long equilibration times meant the droplet shape was likely to continue to change until the surfactant adsorbed at the interface was at equilibrium. Long equilibration times were not compatible with the pendant drop surface tension measurement method as

evaporation from the droplet occurs, which ultimately leads to shrinkage of the droplet hence measurement over long time periods was impossible.

Method

The solution to be measured was drawn into a 10 ml syringe with a 25G X 1 gauge, polytetrafluoroethylene (PTFE) lined, flat tipped needle. Air was expelled and the syringe/needle mounted on a FTA200 device. The camera was set up and calibrated against the measured needle diameter on the FTA32 software (version 2.1). A single droplet of the solution was dispensed manually until it hung in a tear drop shape in view of the camera. An image was taken of the droplet just before detachment from the needle (the point at which it is as far from spherical as possible) and the image analysed by the software. The average of three surface tension measurements was calculated per extract solution and the results are discussed in Chapter 5.

3.6.5 Contact angle measurement

Contact angle of solutions is a measure of the wetting ability of the solution on a surface. Surfactants affect solution surface tension which in turn affects the contact angle hence contact angle is another measure which can give insight into the presence of surfactants in the reaction product solutions. The presence of surfactants in the hay extract solutions is important as more surfactant in the solutions should enable them to generate more foam.

Contact angle was measured because variation in the reaction conditions used during the alkali extractions of hay by NaOH would lead to variation in the concentration of surfactants in the extract solutions. Changes in the concentration of surfactant in the extracts would affect the surface tension of the solutions which in turn affects the contact angle of the solutions on a surface according to the Young's equation.

Equation 3.2. Young's equation which relates solution contact angle to surface tension.

$$\cos\theta_C = \frac{\gamma_{SL} - \gamma_{SG}}{\gamma_{LG}}$$

Where γ_{SL} = the solid-liquid interfacial energy; γ_{SG} = the solid-gas interfacial energy and γ_{LG} = the liquid-gas interfacial energy (this is the surface tension of the liquid) as represented in Figure 3.5.

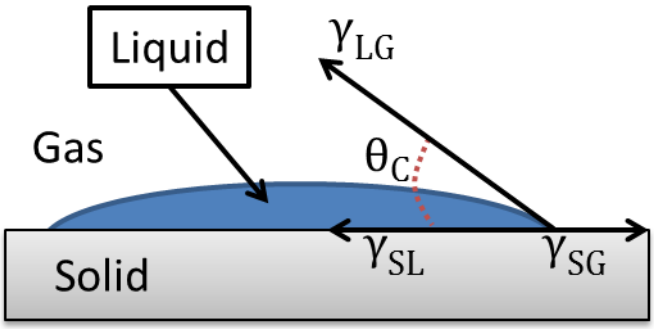

Figure 3.5. Schematic representation of Young's equation.

Young's equation demonstrates that as surface tension increases, the cosine of the contact angle decreases (hence the contact angle increases).

Where the reaction conditions increased extraction of surfactant materials, the surface tension of the solution would be reduced and the contact angle of the solutions would be lowered. Hence the aim was to use measurements of contact angle of the solution to allow the effect of changing reaction conditions on the amount of extracted surfactant to be examined. Contact angle was measured in addition to extract solution surface tension to look at surfactant extraction from the hay, due to difficulty in measuring the surface tension using the pendant drop method.

3.6.5.1 Selection of the surface

A polystyrene surface was used to measure the contact angle of the alkali extract solutions as the reaction conditions were varied. A hydrophobic surface was necessary as the contact

angle of the solutions on glass (a hydrophilic surface) was so low that it was not always possible to measure it. The contact angle was much higher on the hydrophobic polystyrene.

The contact angle of the solutions was measured on a new surface each time on the side of a polystyrene cuvette. Assumption that surfaces on different cuvettes were equivalent is valid because the contact angle of solutions on surfaces of the same materials, manufactured by the same routes, should be consistent according to the research of Chen *et al.* (2012a). Consistency of the surfaces means variation in the contact angle of the solutions on the surfaces could be attributed to changes in the alkali hay extract solutions caused by variation in the extraction conditions.

Method

The supernatant from the centrifuged alkali hay extract solution to be measured was drawn into a 10 ml syringe which was then fitted with a 25G x 1 gauge, PTFE lined, flat tipped needle. PTFE lined needles were required as they are hydrophobic which allowed a droplet to be more easily formed.

Air was expelled and the syringe mounted on a FTA200 device. A droplet of solution was dispensed onto the surface from a height of approximately 1 cm. Images were captured using a monochrome high speed camera at a rate of 15 frames per second as the droplet spread on the surface. Analysis of the images by FTA32 software (version 2.1) allowed the contact angle of the liquid on the surface to be measured on both sides of the droplet and an average of the two values was recorded for each frame (see Figure 3.6).

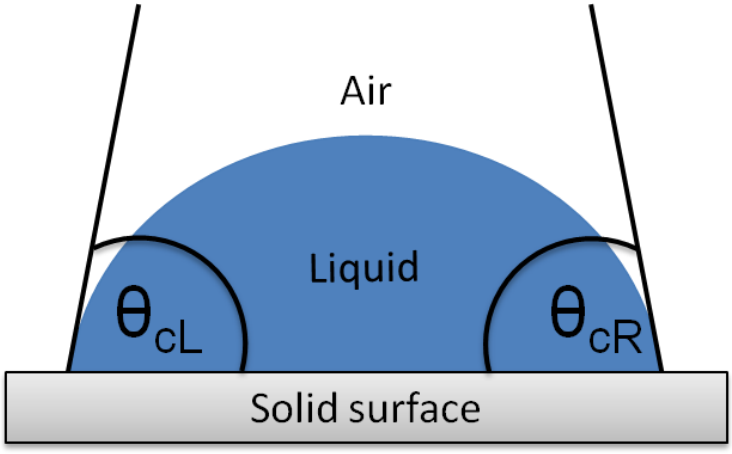

Figure 3.6. Contact angle measurement on the left hand (θ_{cL}) and right (θ_{cR}) sides of a liquid droplet on a solid surface, in air.

θ_{cL} and θ_{cR} in Figure 3.6 refer to the contact angles on the left and right hand side of the droplet on the surface. The measured angles are tangents to the droplet at the contact points between the liquid and the surface. The contact angle measurements were performed in triplicate for each solution and the average of the three measurements is reported.

The contact angle of the droplet on the polystyrene surface after 25 seconds was used to represent the contact angle of the solution. This time limit was imposed because the equilibration time of the solution droplet on the surface was found to be very long. The contact angles were still changing as the liquid crept outward across the surface as the measurement time approached 30 minutes. Data processing of the images over more extended times became impossible due to computation limitations, when longer equilibration times were attempted. Evaporation was an issue over longer equilibration times and this also meant that the contact angle measurement time had to be restricted.

3.6.6 Cryogenic scanning electron microscopy of foam

See section 9.2.4 for background discussion of scanning electron microscopy (SEM).

Method

Foam was generated by shaking the respective solutions in a sealed 500 ml plastic sample bottle. Foam was extracted from the bottle using a wide mouthed (tip diameter ~2 mm) plastic Pasteur pipette. Foam was dispensed slowly and carefully onto a clean, dry brass sample stage which was used to present samples for cryo SEM examination. The foam was rapidly frozen by plunging the sample stage into liquid nitrogen slush to maintain its microstructure. The frozen sample was sealed in an evacuated chamber then immediately transferred to the nitrogen cooled cryo SEM chamber. The frozen foam sample was fractured using a spike to expose fresh surface. The fresh, fractured surface was coated with Pt under vacuum for SEM examination.

Generating a viable sample for cryo SEM examination by freezing the foam using this method was difficult as the foams tended to collapse and were often destroyed during the freezing process. Even when successfully frozen, the foam would often fall off the sample stage before being placed into the SEM as the foam did not stick well to the sample stage. Multiple attempts at foam preparation were required for each sample in order to ensure the frozen foam persisted through the preparation process and hence could be examined.

Cryo-SEM images were obtained using a FEI XL-30 FEG-ESEM microscope, fitted with a Polaron PP2000T cryo-transfer system. Spot size 3 was used and the potential set to 3 keV in order to minimise sample degradation which occurred when higher energy electrons were used. ImageJ software (version 1.46r) was used to analyse the microstructure of foams. The SEM images generated are presented in Chapter 6.

3.6.7 Atomic force microscopy

See section 9.2.5 for background discussion of atomic force microscopy (AFM).

Method

Foam was generated by shaking a sample of hay extract solution in a sealed bottle then a wide mouthed Pasteur pipette was used to obtain some of the foam as for the cryo SEM sample preparation. The foam was dispensed onto a piece of blue roll and after draining for around 2 seconds, a clean mica microscope cover slip was gently pressed against the foam before it collapsed completely, which transferred a foam 'print' onto the mica slide. The slide was placed into a closed petri dish and allowed to dry overnight at ambient temperature.

AFM imaging was performed by the author assisting Martin Munz of the Analytical Science Division, National Physical Laboratory (UK). The AFM system used was a Cypher from Asylum Research and an AFM cantilever made of Si with resonance frequency ~325.9 kHz and quality factor: ~460.3. The results of AFM examination of the dried alkali hay extract foam are presented in Chapter 5.

3.7 Sudsing capacity measurement

3.7.1 Sparging

Foamability of the alkali extract solutions was examined by measuring the foam volume produced when blowing air through a porous glass frit (sparging) into the solutions at a constant air-flow rate and monitoring foam production with time. This method is similar to dynamic foamability measurements described by Bikerman (1973b). Sparging solutions is preferable to using mechanical agitation to generate foam *e.g.* whipping or shaking; as approximately uniform bubbles are formed in a controlled manner. Also when sparging gas into liquid extract solutions, bubbles rise though the liquid meaning surfactants in solution have more time to adsorb at the gas-liquid interface than in mechanical agitation. Sufficient

time for adsorption is especially important for higher molecular weight surfactants or particles where the rate of adsorption at the interface is lower than for small molecule surfactants.

3.7.2 The sparging rig

The sparging rig is shown in Figure 3.7. A 1 cm increment scale was marked up the side of the tube with the zero point on the scale being level with the bottom of the vertical tube. The sparging nozzle (see section 9.2.1) was pushed through the hole at the centre of the base to blow air through the solutions.

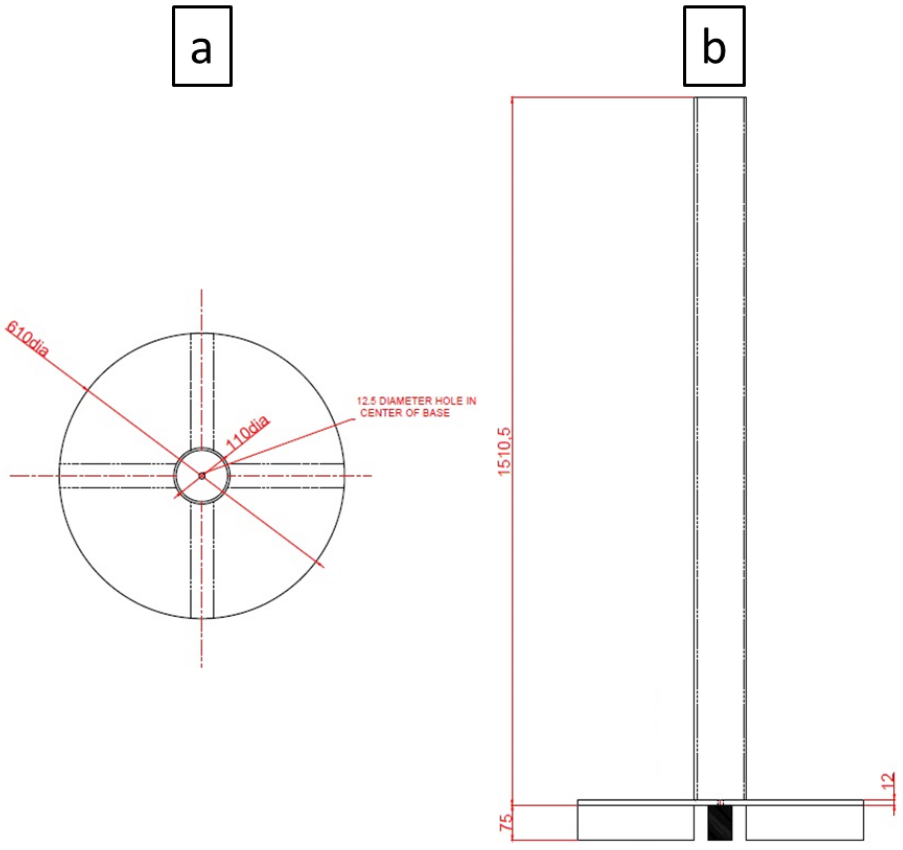

Figure 3.7. Schematic of the sparging rig used for solution testing. (a) A top down view. (b) A side profile view (dimensions are given in mm).

The diameter of the rig was 110 mm as this meant that for even very effective foaming solutions, the foam should not climb the tube too rapidly, which would have made frequently reading the foam height more difficult.

The height of the rig was 1510 mm as it allowed large volumes of foam to be accommodated. Another reason for large sparging rig height and diameter was to allow an attempt to reach equilibrium between foam production and collapse as described by the Bikerman method. However equilibrium was never reached for some of the extract solutions hence the use of *initial* foaming rate (rate of foaming in the first 7 minutes of foaming) in the data analysis for the sparging technique as presented in Chapter 7.

3.7.3 Sparging method

The hay extract solution (450 ml) was poured carefully into the top of the tube whilst it was tilted at a shallow angle to minimise foam generation. The tube was stood was vertically again before sparging and the air flow (2 $Lmin^{-1}$) was turned on. The foam height was recorded every 30 - 60 seconds during sparging.

4 Chapter 4 - Single variable experiments to investigate alkali extraction of hay

A note on presentation of data

Where data is compiled into graphs within this chapter, error bars show the standard error for the repeated measurements of the responses. Standard error is calculated as:

Equation 4.1. Standard error calculation.

$$standard\ error = \frac{measurement\ standard\ deviation}{\sqrt{n}}$$

Where n = the number of measurements which were averaged to generate the data point. The standard error is used in this thesis as it is an estimate of how closely the measured sample mean represents the population mean (the 'actual' value) for the response.

4.1 Introduction

Single variable experiments were performed to gain initial insight into the effects of changing reaction conditions for NaOH extraction of hay on the reaction products. Reaction time, temperature and aqueous NaOH concentration (the variables) were altered and changes in the % mass of the hay extracted and physical properties of the product solutions were measured (the responses). The range of the variables investigated in this chapter was broader than in subsequent research. The experimental findings of this chapter helped decide the limitations on the range of the variables used in further research (see Chapter 5).

Figure 4.1 shows changes in physical appearance of hay during extraction with NaOH.

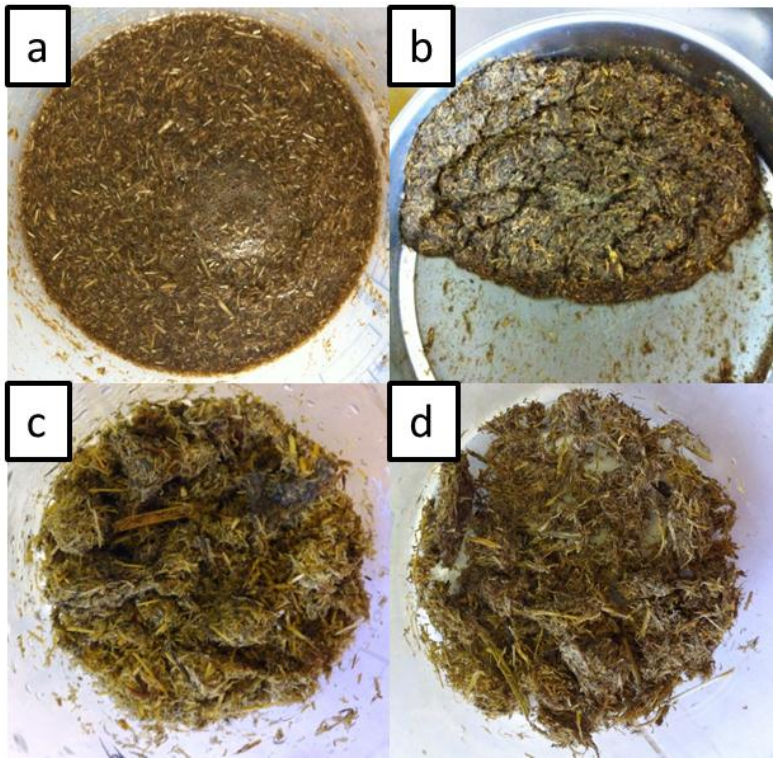

Figure 4.1. Changes in the physical appearance of hay during processing. Hay was extracted with 3.75 molL^{-1} NaOH at ambient temperature (~20 °C) for 30 minutes. (a) Hay/NaOH slurry. (b) Hay residue removed from slurry by sieving. (c) Hay post reaction residue after rinsing. (d) Hay post reaction residue after rinsing and drying at 60 °C for 24 hours.

Figure 4.1 (a) shows that the solution darkened during extraction and the hay became softer and darker in colour, which Sun *et al.* (2005) attribute to hemicellulose removal from plant material. (b) The sieved hay solids were softer after extraction and after rinsing (c) the hay again appeared fibrous though remaining softer than it was before extraction. (d) After drying the hay was fibrous and less brittle than before extraction.

4.2 Absorbance at 286 nm of hay alkali extract solution

Absorbance of the hay extract solutions at 286 nm was used as a measure of the amount of lignin derivatives extracted from hay into solution (see section 3.6.1). Absorbance of the extract solutions at 286 nm (which will be referred to simply as 'the solution absorbance' from this point onward) was measured versus varying reaction time (5 – 60 minutes), temperature (ambient ~20 °C – 60 °C) and concentration of aqueous NaOH (0.25 molL^{-1} - 12.5 molL^{-1}).

Alternative measurements of lignin by chemical methods such as thioacidolysis/alkaline nitrobenzene oxidation *etc.* which are used in the literature (Billa *et al.*, 1998) could have been used for monitoring lignin extraction. UV-vis absorbance was chosen as it was a simpler technique which gave adequate information to examine changes in reaction products with varying reaction conditions.

4.2.1 Absorbance versus reaction time

Absorbance was measured periodically for extraction of hay with NaOH performed at ambient temperature (approximately 20 °C) for 60 minutes using 20% wt/vol (5 $molL^{-1}$) NaOH. Samples of the reaction slurry were passed over a 100 µm mesh sieve to remove the solids before triplicate UV-vis measurements at 286 nm of 30 µl of extract diluted in 3 ml of ultra-high purity water. The solids and any excess reaction solutions were returned to the reaction vessel. The average of three measurements was recorded and absorbance versus reaction time is shown in Figure 4.2.

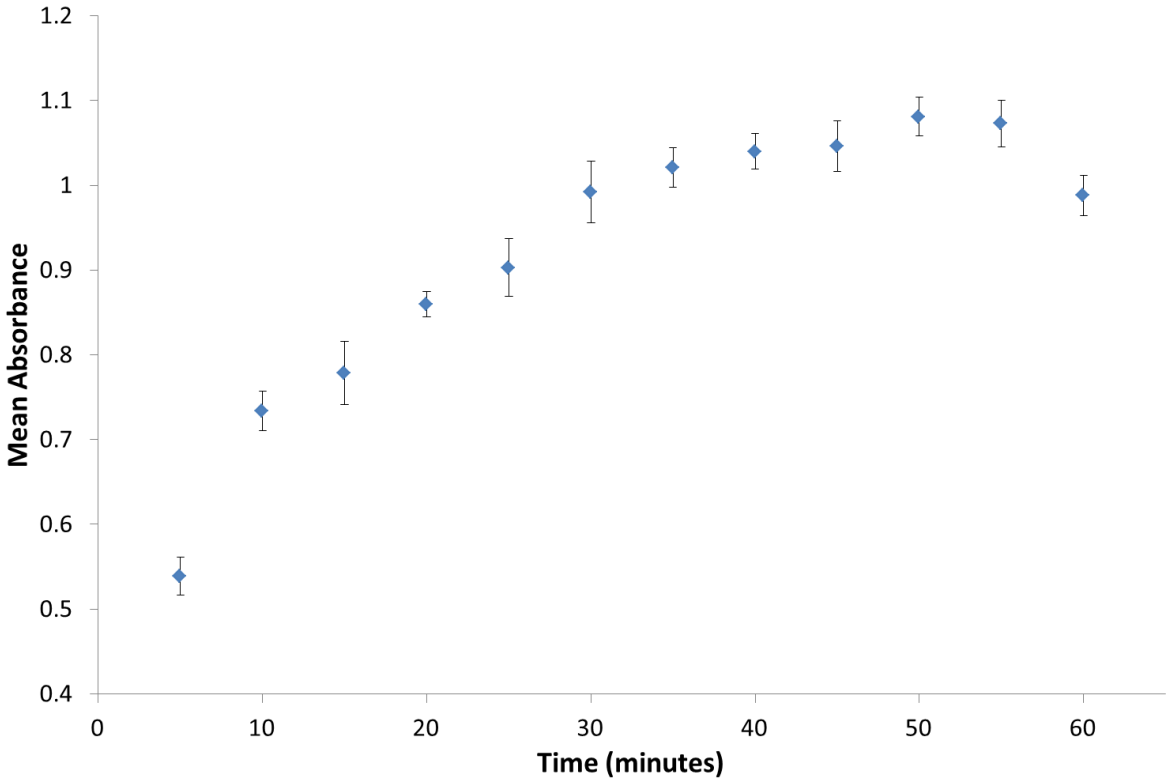

Figure 4.2. Absorbance at 286 nm with reaction time (reactions performed at room temperature using 5 molL^{-1} NaOH).

Figure 4.2 shows that in the first 25 - 30 minutes the extract solution absorbance increases with the extraction time then becomes flat between 30 - 60 minutes.

During the first 30 minutes of reaction the most easily extracted lignin derivatives are solubilised from the hay. If the most easily extracted materials are removed then the more insoluble lignin derivatives remain in the residue, requiring more extreme reaction conditions for removal, hence the absorbance of the extract solutions effectively plateauing longer extraction times. Investigation of the effect of reaction time on any of the other measured reaction product solution properties was not performed at this stage in the research. Further experiments designed to examine the effect of reaction time on extract solution properties are presented in Chapter 5.

4.2.2 Absorbance versus concentration of NaOH

When examining the effect of aqueous NaOH concentration, the absorbance of the reaction product solutions was measured for extractions performed at room temperature (~ 20 °C) for 30 minutes. The absorbance of the solution versus aqueous NaOH concentration is shown in Figure 4.3.

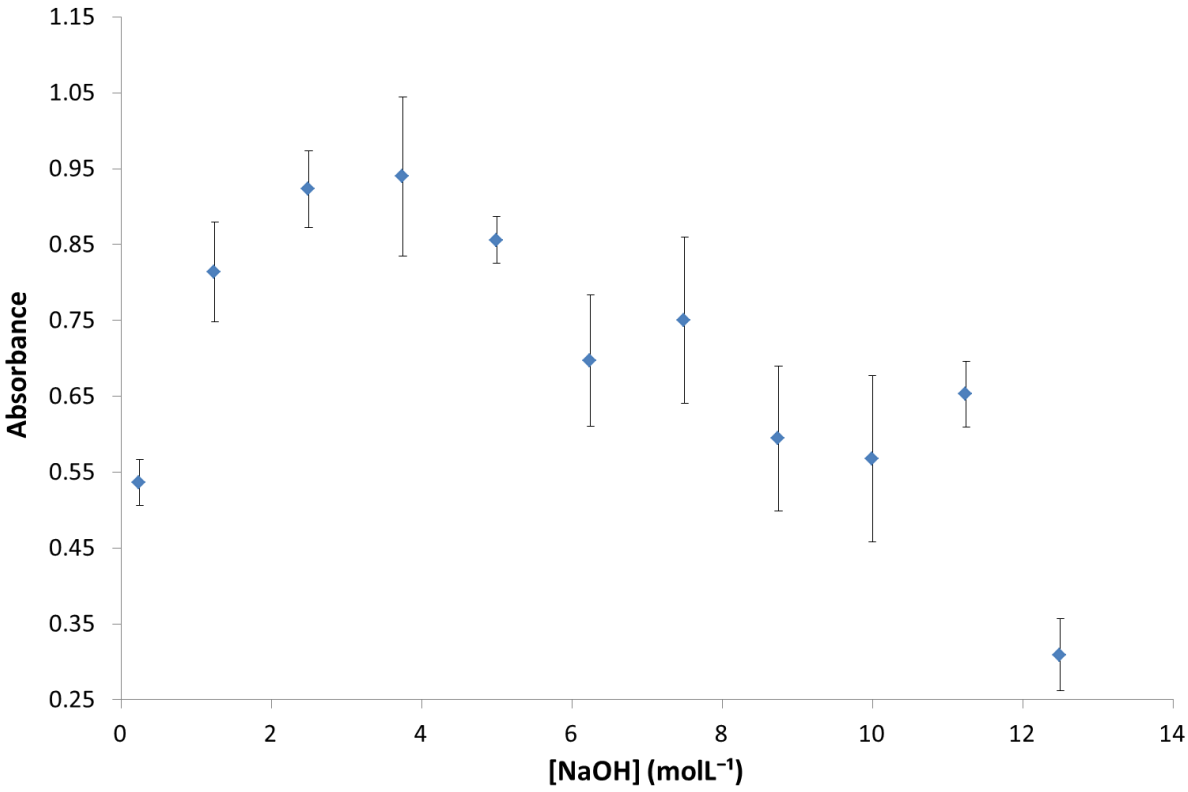

Figure 4.3. Absorbance at 286 nm with concentration of NaOH used in the reactions (reactions performed at room temperature for 30 minutes).

Figure 4.3 shows that the absorbance (A) of the hay/NaOH extract solutions increases with aqueous NaOH concentration from 0.25 $molL^{-1}$ (A = 0.54) up to 2.5 $molL^{-1}$ (A = 0.92). The absorbance then remains steady up to 5 $molL^{-1}$ (A = 0.86) as indicated by the overlap of the error bars for the absorbance of the solutions between 1.25 and 5 $molL^{-1}$. As the aqueous NaOH concentration increases to 6 $molL^{-1}$ the absorbance is seen to drop (A = 0.70) and the error bars for the values at 1.25 $molL^{-1}$ and 6 $molL^{-1}$ NaOH overlap. As the concentration of NaOH is increased beyond 6 $molL^{-1}$ up to 12.5 $molL^{-1}$, an overall trend of decreasing

absorbance is seen though the error bars for aqueous NaOH concentrations between 6 $molL^{-1}$ and 11.25 $molL^{-1}$ show overlap. The product solution absorbance when 12.5 $molL^{-1}$ aqueous NaOH was used is less than all solutions made with lower concentration NaOH, without overlap of their respective error bars.

Overall the absorbance of the extract solutions increases from low concentration of aqueous NaOH to intermediate concentrations, then decreases from intermediate to high concentration of aqueous NaOH. That absorbance increased when aqueous NaOH concentration went from low to intermediate, is not surprising as using stronger base during extractions would be more effective at hydrolysing the bonds within the hay. Cleavage of 'alkali labile' ester bonds in lignin carbohydrate complexes contained in ryegrass is described by Morrison (1973). Sun *et al.* (1997) give a more detailed description of hydrolysis of the ester bonds between hydroxycinnamic acids and lignin in wheat straw leading to dissolution of lignin-carbohydrate complexes. Increased cleavage of ester bonds by alkali leading to increased amounts of solubilised lignin derivatives would explain the increase in the absorbance of the extract solutions with initially increasing NaOH concentration during extraction of hay.

It is interesting that the product solution absorbance shows a downward trend when using intermediate to high aqueous NaOH concentrations in the extractions at room temperature. It might have been expected that solution absorbance would continue to increase with higher NaOH concentration as hydrolysis of the hay raw material became even more effective with stronger NaOH. It was also a possibility that the excess of NaOH increasing beyond some point, might result in plateauing of the solution absorbance as further aqueous NaOH concentration increase would not drive the reaction any further or faster. However,

neither continual increase nor plateauing of the absorbance with increasing NaOH concentration is observed in the data.

Decreasing extract solution absorbance might be explained as being due to high concentrations of NaOH being generally less effective at solubilising the hay if the overall % mass of material extracted from the hay decreased in a similar fashion to the solution absorbance (see section 4.3.1).

4.2.3 Absorbance versus changing reaction temperature used in the extractions

Absorbance of hay/NaOH extract solutions was measured for extractions performed for 30 minutes, 5 $molL^{-1}$ aqueous NaOH with reaction temperature varying from ambient (~ 20 °C) to 60 °C. The absorbance of the hay extract solutions versus varying reaction temperature is shown in Figure 4.4.

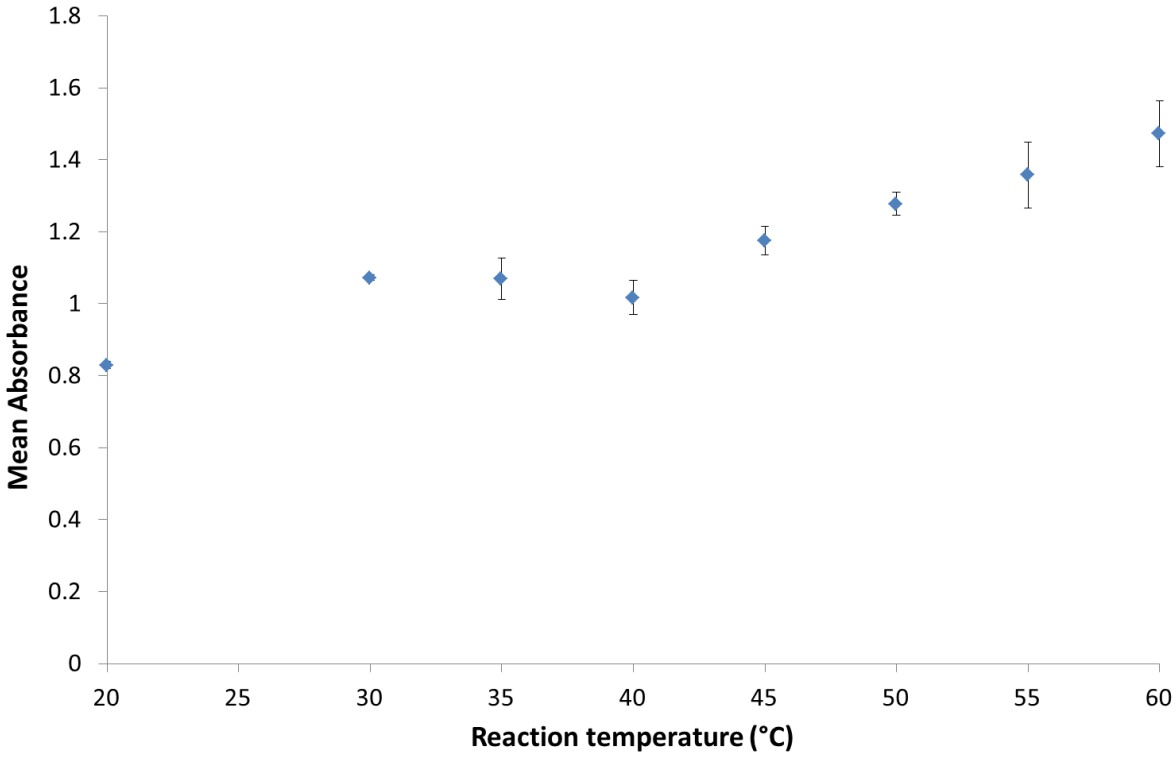

Figure 4.4. Absorbance at 286 nm with reaction temperature (reactions performed using 5 molL^{-1} NaOH for 30 minutes).

Figure 4.4 shows increasing absorbance with increased extraction temperature in the hay/NaOH extraction solutions. When examined more closely, it appears from the data that the absorbance of the solutions increases from 20 - 30 °C but that no further increase is observed until the reaction temperature reaches 45 °C. Above 45 °C the absorbance of the product solutions does increase further with overlap in the data for absorbance at temperatures from 50 °C to 60 °C.

Donohoe *et al.* (2008) examined lignin coalescence and migration through maize cell walls observing that lignin would migrate to the surface of the plant material if it were heated above 120 °C, attributing this migration to lignin becoming fluid as the temperature became higher than its phase transition. As far as the current research is concerned this effect of increasing mobility of lignin with increasing temperature might be involved even though the reaction temperatures do not get close to 120 °C. Though not described by Donohoe *et al.*,

if lignin underwent softening as it was warmed at temperatures < 120 °C, this could aid the extraction of lignin from the hay.

The work of Donohoe *et al.* compliments the current research and it is possible that the alkali extract solution absorbance would be very much higher if the reaction was performed above the phase transition temperature of lignin (120 °C according to Donohoe *et al.*) If the reaction were performed above 120 °C lignin mobility would be increased and as the droplets migrated out of the hay, they would be more easily dissolved in the alkaline solution due to the high surface area lignin droplets. If the sudsing of the extract solutions occurred due to the presence of lignin in solution then foaming potential of the solutions would be expected to be increased by performing the extractions at temperatures > 120 °C for the same reason, which offers an opportunity for further research in the future.

4.3 % Mass of hay components extracted during the reactions of hay and aqueous NaOH

The % mass of hay component extracted during reaction with NaOH is interesting in the context of the current research as it indicates how effectively the reactions with NaOH solubilise hay which is important because increased solubilisation should mean increased foaming of the extract solutions.

4.3.1 % Mass of hay components extracted vs. concentration of NaOH

Changes in the % mass of hay components extracted were measured for extractions performed at room temperature (~20 °C), for 30 minutes using 0.25 – 12.5 $molL^{-1}$ aqueous NaOH. The % mass extracted from hay during extraction with varying aqueous NaOH concentration is shown in Figure 4.5 with the graph of absorbance versus NaOH concentration from Figure 4.3 reproduced for comparison, which is discussed in section 4.4.1.

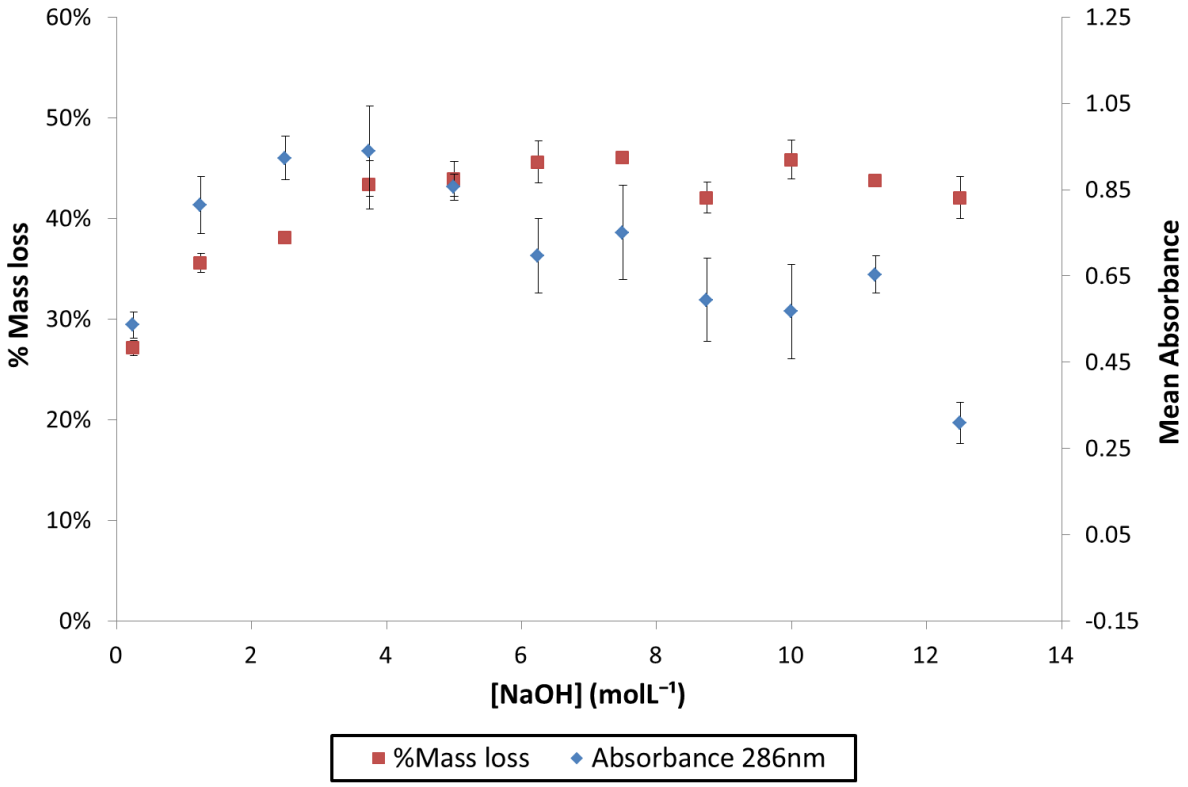

Figure 4.5. % Mass of hay components extracted and extracts solution absorbance at 286 nm versus concentration of NaOH used in the extractions (extraction performed at ambient temperature for 30 minutes).

Figure 4.5 shows that % mass of the hay components extracted during reaction with NaOH increases as the concentration of aqueous NaOH increases from 0.25 to 3.75 $molL^{-1}$. As the concentration of aqueous NaOH is increased beyond 3.75 $molL^{-1}$ to 12.5 $molL^{-1}$, the mass of hay components extracted appears to plateau. The reason for this plateau could be that the most accessible material which can be extracted from the hay in a 30 minute reaction at room temperature is extracted by 3.75 $molL^{-1}$ aqueous NaOH.

Simão *et al. (2008)* described a 'critical alkali concentration' which was the concentration up to which the NaOH rapidly consumed at the beginning of the reactions made a relevant contribution to the reaction. Though they studied alkali extraction of wood pulp, it is conceivable that a similar 'critical concentration' of NaOH might exist in alkali extraction of hay above which, NaOH concentration increases does not lead to increase of the outcome of the extraction, in this case, the % mass extracted from the hay. From the data for % mass of

hay extracted by NaOH of varying concentrations at room temperature, the critical concentration of NaOH is between 2.5 and around 5 $molL^{-1}$. Section 4.3.2 discusses the possibility that in order to increase the amount of material extracted from the hay the extraction temperature must be increased.

4.3.2 % Mass of hay components extracted during the reactions vs. changing reaction temperature used in the extractions

The % mass of hay components extracted was measured for extractions performed for 30 minutes using 5 $molL^{-1}$ NaOH at varying temperatures (ambient (~ 20 °C) to 60 °C). The % mass of hay components extracted versus reaction temperature is shown in Figure 4.6 with the data from Figure 4.4 included for comparison with the effect of reaction temperature on solution absorbance which is discussed in section 4.4.2.

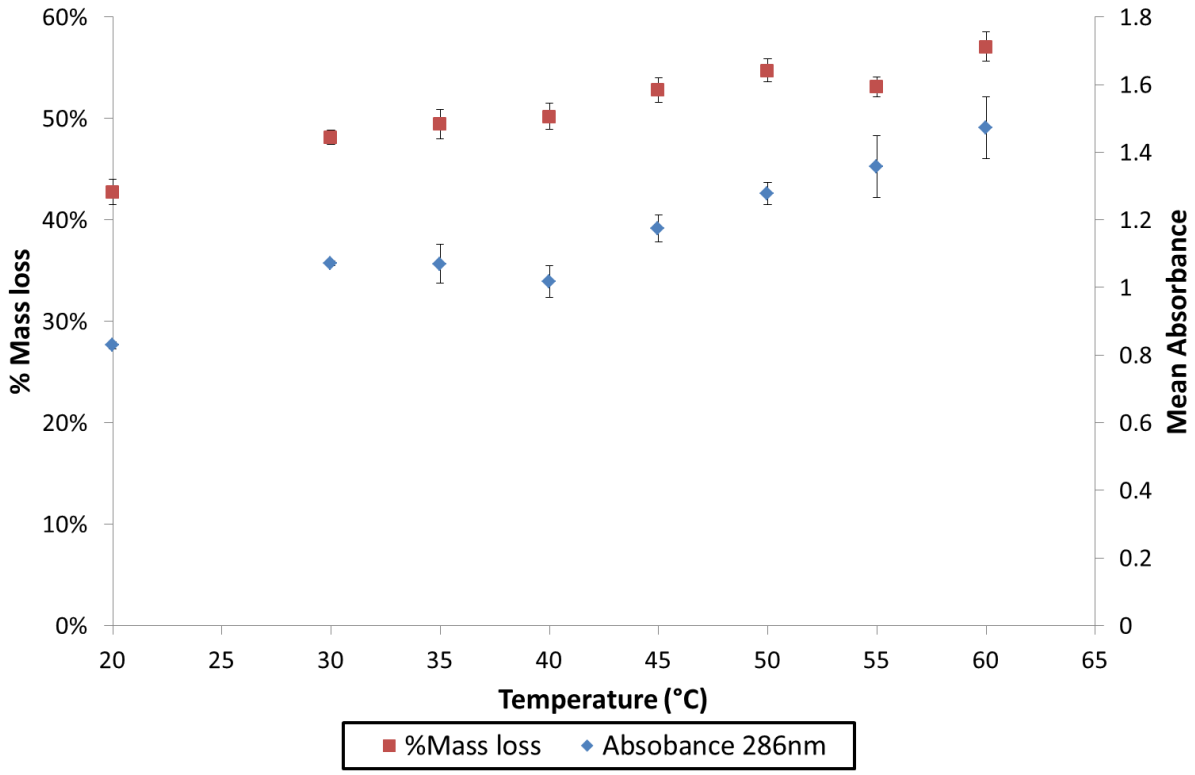

Figure 4.6. % Mass of hay components extracted and extract solution absorbance at 286 nm versus reaction temperature (reactions performed for 30 minutes using 5 $molL^{-1}$ NaOH).

Figure 4.6 demonstrates an increase in the % mass of hay components extracted as reaction temperature increases which is approximately linear up to 60 °C. It is possible that % mass may have increased further still at even higher temperatures which would be understandable if higher extraction temperatures lead to improved lignin and cellulose dissolution. The mass of hay components extracted at 60 °C using 5 $molL^{-1}$ (57%) is higher than when using any other concentration of NaOH at room temperature (maximum = 46%) hence increased temperature appears to improve solubility of lignin more than increasing NaOH concentration.

4.4 The effects of reaction temperature and aqueous NaOH concentration on extraction of hay

4.4.1 The effect of aqueous NaOH concentration on % mass extracted from hay extract solution absorbance

Increasing NaOH concentration up to 3.75 $molL^{-1}$ leads to increasing % mass of hay components extracted at which point the amount of hay components extracted levels out and does not change significantly up to 12.5 $molL^{-1}$ NaOH. In contrast the product solution absorbance increases up to around 3.75 $molL^{-1}$ of aqueous NaOH, then shows an apparent decreasing trend at concentrations > 3.75 $molL^{-1}$.

When considered in isolation from the % mass extracted results, a possible explanation of the decrease in hay/NaOH extraction solution absorbance at the higher concentrations of aqueous NaOH could be that it is an artefact of the extraction procedure itself. When 12.5 $molL^{-1}$ aqueous NaOH was used for extraction of hay, the NaOH solution was viscous and effective dispersion of the hay was difficult. Dispersion was maintained by using high stirring speed during extraction to ensure the solids remained suspended. These steps ensured that the extraction took place with effective mixing of the solids/liquids and

minimised potential problems due to poor dispersion of the hay during extraction. If inadequate mixing of the slurry were responsible for the decrease in the solution absorbance at high NaOH concentration then it would be expected that the % mass extracted from the hay would be decreased at higher NaOH concentrations also. The % mass of hay components extracted does not decrease with high NaOH concentration which suggests something other than inadequate mixing is responsible for the absorbance decrease.

No research demonstrating similar trends of decreased solution absorbance with higher NaOH concentrations used in extraction of plant materials was found in the literature. The use of UV-vis absorbance to monitor lignin from alkali extraction of plant materials is commonly used in the literature (Morrison, 1973, Lawther *et al.*, 1996b, Bikova and Treimanis, 2004, Hromadkova *et al.*, 2005, Nadji *et al.*, 2009). However, the concentration of NaOH used in extractions of lignocellulosic materials within other research is generally lower than in the current research. The low temperatures of reaction used in the current research are also not compatible with the research in the literature which is predominantly done at higher temperatures.

As the % mass of hay components extracted increases, the amount of lignin derivatives in solution would be expected to increase which would in turn lead to higher extract solution absorbance. However, the solution absorbance was found to decrease at higher concentrations of NaOH even though % mass extracted from the hay does not decrease. This suggests that higher concentrations of NaOH do continue to effectively extract material from the hay. It seems reasonable to assume that as the amount of material extracted from the hay overall does not decrease, then the amount of lignin extracted would not decrease. What appears to have occurred is breakdown of lignin chromophores in solution leading to

reduced extract solution absorbance even when the amount of material extracted into solution overall is increased or at least the same for a set of reaction conditions. One theory to explain this is that high concentrations of aqueous NaOH might be able to breakdown lignin chromophores extracted from hay. In her thesis, Olarte (2001) described mechanisms by which lignin is degraded using alkaline solutions. The reactions reported in her thesis, however, were performed under different reaction conditions than those used in the current research (160 - 350 °C, using 2.78 $molL^{-1}$ NaOH). When considering the research of Olarte, it seems one possible route through which the solution absorbance might decrease is that lignin is oxidised in the presence of NaOH when the reaction is performed in air. The current author acknowledges that this is made less likely however, as the reaction temperatures used in the current research are very much lower than those used by Olarte. Further experimentation would be required to confirm oxygen degradation of NaOH extracted lignin at low temperature and simply requires experiments performed in air/under a nitrogen atmosphere to look at the change in solution absorbance with NaOH concentration variation again.

The change in the extract solution absorbance with varying NaOH concentration up to 3.75 $molL^{-1}$ is investigated further in Chapter 5.

4.4.2 The effect of extraction temperature on % mass extracted from hay and extract solution absorbance

Increasing extraction temperature when reacting hay with aqueous NaOH increased both the absorbance of the extract solutions and the % mass of hay components extracted during the reactions. This means that increasing extraction temperature up to 60 °C increases the overall amount of material (including lignin chromophores) extracted into solution but does not affect destruction of the lignin chromophores responsible for the solution absorbance.

The implication of this is that though lignin derivatives may be broken down by very concentrated aqueous NaOH, they are not by increased extraction temperature up to 60 °C.

4.5 The effect of NaOH concentration on the viscosity of hay extract solutions

Extractions were performed at room temperature (approximately 20 °C) for 30 minutes with varying concentrations of NaOH. The solution rheologies were found to be Newtonian at shear rates > 30 s^{-1} (see Appendix section 9.2.3) and the viscosity of the extract solutions was measured at 94 s^{-1}. The viscosity of the hay extract solutions is plotted versus aqueous NaOH concentration used in the extractions in Figure 4.7.

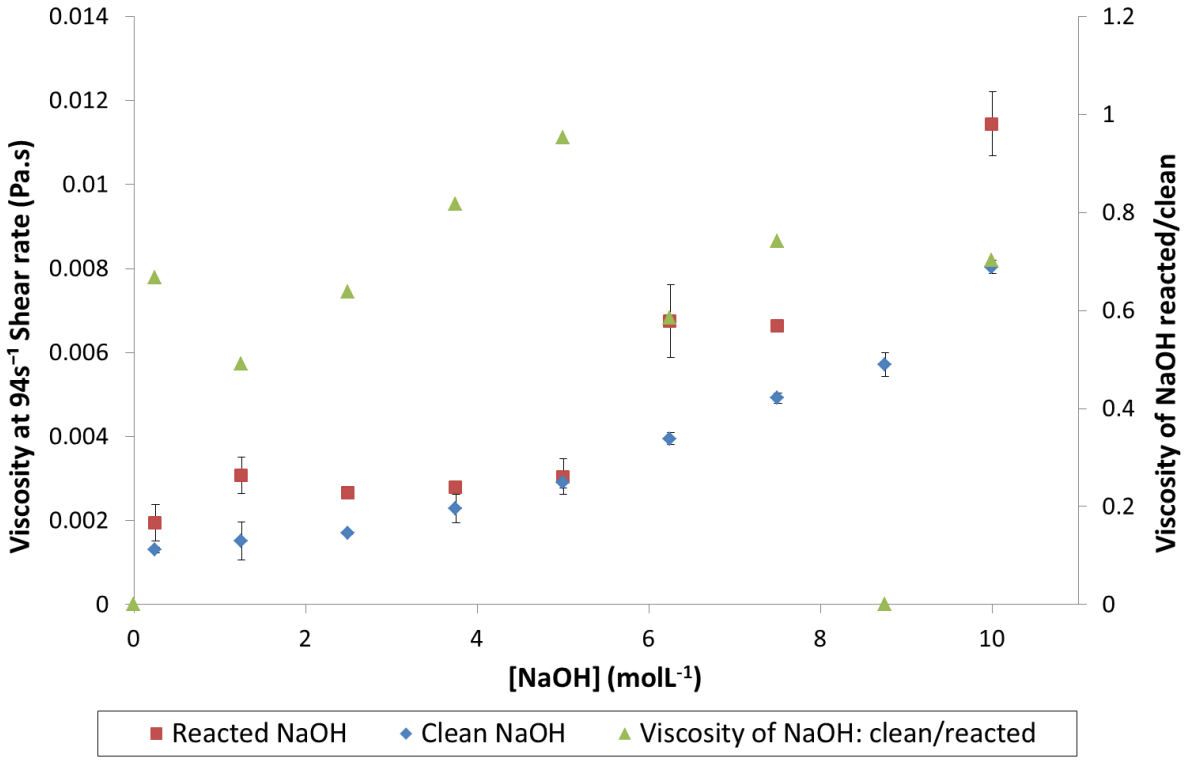

Figure 4.7. Hay extract solution viscosity vs. NaOH concentration used in the extractions (reactions were performed at ambient temperature for 30 minutes).

Figure 4.7 shows the viscosity of unreacted NaOH and the corresponding hay extract solution generated with aqueous NaOH of the same concentration. The viscosity of the unreacted aqueous NaOH increases with increasing concentration. The viscosity of the extract solutions also increases with increasing NaOH concentration used in the extractions, in a

similar fashion. The hay extract solutions have higher viscosity than the corresponding unreacted NaOH solutions indicating that dissolution of hay components increases the viscosity of the extract solutions as expected. The ratio of the unreacted NaOH/extract solution viscosities shows no obvious trend with increasing NaOH concentration *i.e*. it cannot be stated that higher concentration NaOH used in the extractions leads to larger relative increase in extract solution viscosity. Extract solution viscosity increase was due to dissolution of saccharides from the hay which would 'give structure' to the solutions as discussed in section 2.5.3.

It was considered possible that mass transfer limitation due to more concentrated NaOH being increasingly viscous might impede diffusion of the NaOH into the hay, and hydrolysis products out of it during extractions. Simão *et al.* (2008) include alkali viscosity in their model to describe mass transfer during alkali extraction of wood chips, which acts to reduced diffusivity of the alkali. This would lead to reduced mass transfer during the reaction of the wood chips with more viscous alkali which would in turn impede the hydrolysis reaction, extracting less material into solution.

The findings of Simão *et al.* regarding viscosity of the NaOH used affecting extraction of wood chips are interesting and NaOH viscosity may have a role to play in affecting extraction from hay. However, the extractions that Simão *et al*. performed were under very different extraction conditions to the current research, in that they used a mixture of sodium hydroxide, sulphide and carbonate; the reaction temperature was higher (80 – 165 °C) than in the current research (< 60 °C) and the dimensions of the wood chips were much larger (6 mm thick chips versus < 1 mm thick hay strands). Lower reaction temperature will mean the reaction is slower and the NaOH more viscous, but the significantly smaller dimensions of the hay are likely to mean diffusion of the NaOH into the hay is less restricted. The

magnitude of the influence of the viscosity of the NaOH used in the extractions on the properties of the extracts solutions is unclear and further research would be needed to draw any firm conclusions.

Alkali hay extract solution viscosity is investigated further in Chapter 5 with the effect of extraction time and temperature examined as well as NaOH concentration. Section 7.3 then looks at correlation between extract solution viscosity and other extract solution properties.

4.6 Process considerations and experimental findings

4.6.1 NaOH concentration

During extraction of sudsing materials from lignocellulosics it is desirable to maximise the amounts extracted hence improving efficiency whilst minimising costs associated with running the process. Using very high concentration NaOH would not be 'green' and would make the process less economical. Destruction of any of the extracted components as indicated by the drop in extract solution absorbance at high NaOH concentrations (see Figure 4.3) is undesirable. Also, using high concentrations of NaOH has not been found to offer any benefit in terms of increasing the amount of materials dissolved into solution during extraction of hay (see Figure 4.5). Hence it was decided that during further research, the NaOH concentration used in hay extractions would be limited to a 3.75 $molL^{-1}$ maximum as extract solution absorbance and % mass extracted from the hay were found to be maximised around this concentration.

It was unnecessary to consider processing implications raised by viscosity increase of reaction product solutions at this stage of the research into foam enhancing materials even though extract solution viscosity does potentially affect foaming. Change in the viscosity of the extract solutions with extraction conditions is investigated further in Chapter 5.

4.6.2 Reaction temperature

Increased extraction of lignin derivatives occurs at higher reaction temperatures. Extending the current research to using higher extraction temperatures however, was not desirable even when higher yields from extractions were potentially possible. Higher extraction temperatures are undesirable as operating a manufacturing plant at high temperature would increase the risks and hazards associated with the extraction of hay with aqueous NaOH. Heating the process would also be necessary which would add to the complexity and cost of a building and running a plant. Working with NaOH at elevated temperatures may require corrosion/pressure resistant vessels which would significantly add to the capital cost of a manufacturing plant. Finally, if the lignocellulosic raw materials were chosen correctly then maximising efficiency of extraction from them would not be critical as the residues from the process might find use elsewhere *e.g.* feeding to cattle. A life cycle assessment of any potential industrial extraction process would help decide if the use of process residues elsewhere meant that maximising the amount of extracted material was less important than the plant having low energy requirements in terms of overall sustainability of the process. Finding that 60 °C extraction temperature increased effectiveness of extractions together with the desire for a green/low energy /safe process meant extraction temperatures would be 60 °C or less for the research which followed, as presented in Chapter 5.

4.7 Extension of the single variable work

The research within this chapter provides insights into the effect of reaction time, temperature and aqueous NaOH concentration as individual variables on some of the properties of the product solutions from hay/NaOH extractions. However the insights from single variable experiments do not give information as to which reaction variables is most/least important in affecting the different extract solution properties nor can they give

information on the interactions between the variables. Improved experimental design and data analysis methods are needed to better understand the relative effect of each of the reaction variables and their interactions on the extract solutions. Experiments further examining hay/NaOH extract solution absorbance, viscosity as well as the % mass of the hay components extracted will be discussed in Chapter 5. The hay extract solution surface tension and contact angle changes with the hay/NaOH reaction variables are also investigated as these may be influencing foaming of the hay extract solutions.

5 Chapter 5 – Modelling physical properties of alkali hay extract solutions

This chapter builds upon the research in Chapter 4 by using response surface methodology experimental design to increase understanding of the relative effect of each reaction variable and their interactions on the hay extract solutions. The results of the experiments and models developed from them to describe the effects of reaction variables on the measured responses will be discussed in section 5.4. The relationship between the models and the results of Chapter 4 will then be discussed in section 5.5. Correlation between the properties of the alkali hay extract solutions with each other and the foaming ability of the solutions is explored in section 7.3.

Response surface methodology is used to examine the effect of changing multiple variables on reactions/products. Many examples of the use of response surface methodology can be found in the literature where it has been applied to extraction of a variety of components from a variety of plant materials, *e.g.* protein from oat bran (Guan and Yao, 2008), peanut (Ma *et al.*, 2010), red pepper seed (Firatligil-Durmus and Evranuz, 2010), polysaccharides from pomegranate peel (Zhu and Liu, 2013) and mushrooms (Guo *et al.*, 2010, Chen *et al.*, 2012b) amongst others.

The same methods used to measure the responses examined in Chapter 4 (% mass extracted from the hay (Y_M), the solution absorbance (Y_A) and the solution viscosity (Y_V) were used in this chapter as well as extract solution surface tension (Y_S) and contact angle (Y_C and $^*Y_C$). The solution contact angle and surface tension are both indicative of the presence of surfactants in solution. Surfactants dissolved during the alkaline extraction of hay are important as they would affect the ability of the extract solutions to produce stable bubbles hence generate foam.

The range of reaction parameters was selected according to conditions identified as favourable during the single variable investigations (see section 4.6) and through consideration of desirable production plant processing conditions (see section 1.8.1 for further discussion of these considerations).

5.1 The experimental design

A 16 experiment central composite response surface design was used for the three independent variables; reaction time in minutes (x_1), temperature in °C (x_2) and concentration of NaOH used in $molL^{-1}$ (x_3). The three variables were set at three levels (low, centre point and high, coded as -1, 0 and 1 respectively). Quadratic polynomial models describing the measured responses were developed by analysis of the experimental data using JMP® software (Version 9.0.2, SAS Institute Inc., Cary, NC, 2010). The full experimental protocol is shown in Table 5.1.

Table 5.1. The experimental matrix used for this investigation.

Expt.	Coded variables			Uncoded variables		
	X_1	X_2	X_3	x_1	x_2	x_3
	Reaction Time (mins.)	Reaction Temp. (°C)	[NaOH] ($molL^{-1}$)	Reaction Time (mins.)	Reaction Temp. (°C)	[NaOH] ($molL^{-1}$)
1	1	0	0	30	40	2
2	-1	-1	1	5	20	3.75
3	0	0	1	17.5	40	3.75
4	-1	-1	-1	5	20	0.25
5	1	1	-1	30	60	0.25
6	1	1	1	30	60	3.75
7	0	0	0	17.5	40	2
8	0	0	0	17.5	40	2
9	-1	1	1	5	60	3.75
10	1	-1	-1	30	20	0.25
11	-1	0	0	5	40	2
12	-1	1	-1	5	60	0.25
13	0	1	0	17.5	60	2
14	0	0	-1	17.5	40	0.25
15	0	-1	0	17.5	20	2
16	1	-1	1	30	20	3.75

The experiments were performed in a randomised order to minimise bias and the response measurement data (and standard errors associated with the measurements) used in generating the models is given in Table 5.2 overleaf. Note the % mass extracted data does not have an associated standard error as this was a single measurement per extraction.

Table 5.2. Response surface experimental design measurement data used in generating the models for each of the responses.

Reaction variables			Measured response								
Time (mins.)	Temperature (°C)	[NaOH] ($molL^{-1}$)	Y_M % Mass of hay extracted	Y_A Absorbance at 286 nm	Y_A STD Error	Y_V Viscosity at $94s^{-1}$ (Pa.s)	Y_V STD Error (Pa.s) $x10^{-5}$	Y_S Surface Tension ($mN\ m^{-1}$)	Y_S STD Error ($mN\ m^{-1}$)	Y_C Contact Angle on Polystyrene (°)	Y_C STD Error (°)
30	40	2.00	49.0	1.012	0.024	0.00283	2.20	31.07	0.14	45.51	0.69
5	20	3.75	30.4	0.398	0.019	0.00231	2.83	45.69	0.06	71.18	0.33
17.5	40	3.75	50.8	0.955	0.094	0.00328	6.91	41.81	0.16	65.36	0.74
5	20	0.25	26.3	0.266	0.013	0.00104	2.43	44.38	0.08	60.12	1.14
30	60	0.25	42.7	0.985	0.021	0.00171	3.60	41.73	0.09	61.06	0.79
30	60	3.75	53.2	1.270	0.140	0.00453	0.00	35.88	0.47	61.75	0.71
17.5	40	2.00	46.5	1.000	0.156	0.00258	2.68	39.80	0.23	54.55**	1.28
17.5	40	2.00	45.7	0.938	0.108	0.00241	4.03	39.39	0.13	53.09	0.69
5	60	3.75	48.6	0.836	0.071	0.00329	6.93	36.19	0.24	61.79	1.20
30	20	0.25	42.5	0.429	0.021	0.00121	3.53	35.88	0.47	58.71	0.67
5	40	2.00	33.6	0.757	0.043	0.00195	3.27	31.70	0.16	39.47	0.58
5	60	0.25	31.2	0.498	0.017	0.00119	4.05	40.91	0.17	62.34	0.36
17.5	60	2.00	55.4	1.162	0.014	0.00312	7.42	28.75	0.08	33.76	0.76
17.5	40	0.25	42.4	0.585	0.024	0.00211	70	45.85	0.09	64.25	0.47
17.5	20	2.00	34.7	0.675	0.022	0.00181	3.80	42.05	0.12	51.79	0.57
30	20	3.75	42.3	0.855	0.053	0.00279	6.49	42.47	0.12	67.22	0.70

**This data point was excluded from the data analysis for the *Y_C model in order to try and improve the Y_c model, see section 5.3.2.

5.2 The model coefficients

The models proposed for describing the measured responses (Y_i) in terms of the reaction variables were based on the second order polynomial Equation 5.1.

Equation 5.1 The second order polynomial model used to describe the responses measured in the experiments.

$$\mathbf{Y_i = \beta_0 + \sum_{n=1}^{3} \beta_n X_n + \sum_{n=1}^{3} \beta_{nn} X_n{}^2 + \sum_{n \neq m=1}^{3} \beta_{nm} X_n X_m}$$

Where $\mathbf{Y_i}$ ($\mathbf{i}$ = M, A, V, S, C) is the predicted response for the measurable, $\boldsymbol{\beta_0}$ is the value of the fitted response at the centre of the experimental design (*i.e*. the coded variables are 0, 0, 0), $\boldsymbol{\beta_n}$ and $\boldsymbol{\beta_m}$ are the linear, $\boldsymbol{\beta_{nn}}$ the quadratic and $\boldsymbol{\beta_{nm}}$ the interaction regression terms respectively for the independent variables used in these experiments. $\mathbf{X_{n,m}}$ refers to the coded values for the parameters used in the experiments ($\mathbf{n}$ and $\mathbf{m}$ refer to the reaction variables where $\mathbf{n}$,$\mathbf{m}$ = 1 = reaction time, 2 = reaction temperature, 3 = aqueous NaOH concentration used during extraction) *e.g.* β_1 = reaction time regression term coefficient, β_{12} = the interaction term for time x reaction temperature, X_1 refers to the reaction time parameter *etc.* The reaction variables were coded according to Equation 5.2:

Equation 5.2. The coding of the variables.

$$\mathbf{X_i = \frac{x_i - \bar{x}_i}{\Delta x_i}}$$

Where $\mathbf{X_i}$ is the coded (dimensionless) value of the variable $\mathbf{i}$, $\mathbf{x_i}$ is the actual value of the variable $\mathbf{i}$, $\mathbf{\bar{x}_i}$ is the value of the variable $\mathbf{i}$ at the centre point and $\mathbf{\Delta x_i}$ is the step change value of the variable $\mathbf{i}$ (from low to centre point or centre point to high values) *e.g.* coding for reaction time 30 minutes:

Equation 5.3. Example of coding of 30 minutes extraction time.

$$X_{t=30} = \frac{30 - 17.5}{12.5} = 1$$

The model coefficients generated by analysis of the experimental data are given in Table 5.3 overleaf.

Table 5.3. Estimated coefficients and their significance based on p-values, of the second order models for the responses.

	% Mass extracted from hay (Y_M)		Abs 286 nm (Y_A)		Viscosity (Y_V)		Surface Tension (Y_S)		Contact Angle (Y_C)		**Contact Angle ($*Y_C$)	
Term	Estimate	p-value	Estimate	p-value	Estimate	p-value	Estimate	p-value	Estimate	p-value	Estimate	p-value
β_0	45.9	<0.0001	0.924	<0.000	0.00239	<0.0001	35.5	<0.000	49.8	<0.000	44.71	<0.0001
β_1	5.96	0.0002	0.180	<0.000	0.00032	0.006	-1.183	0.278[b]	-0.00491	0.973[b]	-0.0614	0.971[b]
β_2	5.49	0.0004	0.213	<0.000	0.00046	0.0005	-2.70	0.027	-0.142	0.139[b]	-2.84	0.114[b]
β_3	4.02	0.0032	0.155	<0.000	0.00089	<0.0001	-0.673	0.528[b]	1.19	0.268[b]	2.08	0.233[b]
β_{11}	-5.94	0.0058	NSS[a]	>0.05	NSS[a]	>0.05	NSS[a]	>0.05	NSS[a]	>0.05	NSS[a]	>0.05
β_{22}	NSS[a]	>0.05	NSS[a]	>0.05	NSS[a]	>0.05	NSS[a]	>0.05	NSS[a]	>0.05	NSS[a]	>0.05
β_{33}	NSS[a]	>0.05	-0.216	0.0002	NSS[a]	>0.05	5.617	0.0271	5.56	0.0001	18.7	<0.0001
β_{12}	NSS[a]	>0.05	NSS[a]	>0.05	NSS[a]	>0.05	NSS[a]	>0.05	NSS[a]	>0.05	NSS[a]	>0.05
β_{13}	NSS[a]	>0.05	NSS[a]	>0.05	NSS[a]	>0.05	NSS[a]	>0.05	NSS[a]	>0.05	NSS[a]	>0.05
β_{23}	3.00	0.0275	NSS[a]	>0.05	0.00025	0.0365	NSS[a]	>0.05	NSS[a]	>0.05	NSS[a]	>0.05

[a] These coefficients were statistically not significant (NSS) based on the p-value from the student t-test (*i.e*. p >0.05); [b] These parameters are retained in the model despite p >0.05 as they were the variables used in the experiments and as such it makes sense to retain these terms. **This model for Y_c is developed having excluded a single data point in an attempt to improve the model for Y_C (see section 5.4.4 for further explanation).

The data in Table 5.3 can be used to construct the respective models. Using the % mass extracted from hay model (Y_M) as an example, the full form of the model is shown in Equation 5.4:

Equation 5.4. The predictive model describing the % mass loss from the hay during the alkali extractions written out in full.

$$\%\ \text{Mass Loss} = 45.9 + 5.96 \times \left(\frac{\text{Time} - 17.5}{12.5}\right) + 5.49 \times \left(\frac{\text{Temperature} - 40}{20}\right) + 4.02 \times \left(\frac{[\text{NaOH}] - 2}{1.75}\right) - 5.94 \times \left(\frac{\text{Time} - 17.5}{12.5}\right)^2 + 3.00 \times \left(\frac{\text{Temperature} - 40}{20}\right) \times \left(\frac{[\text{NaOH}] - 2}{1.75}\right)$$

The terms in the brackets for the model in Equation 5.4 code the respective variables in the predictive equations, as in Equation 5.2 and Equation 5.3.

The columns are coloured in Table 5.3 only for easier reading. The 'coefficient' column shows which coefficient of Equation 5.4 the value in the 'estimate' column refers to. The p-values give an indication of the confidence level for the estimate of the coefficient. $p < 0.05$ indicates statistical significance of the estimate of the estimate. $p < 0.05$ gives > 95% confidence in the value being correct and that the value did not occur by chance.

When constructing the models, terms in the equations which were not statistically significant (where $p > 0.05$) were removed sequentially in order of decreasing p-value *i.e*. the term having the highest p-value was removed first, the model re-run then the term having the next largest p-value removed and so on, until only significant terms were left in the models. This meant the models became simpler and more reliable as regression terms which were not statistically significant were removed. Each time a term which was not statistically significant was removed from the model, the p-values for the other terms and overall model were altered; hence values of the insignificant terms are not listed nor their associated p-values unless otherwise stated. Response surfaces to graphically illustrate the

effect of the reaction variables and their interactions on the models are presented in sections 5.4.1 to 5.4.3.

5.3 ANOVA of the models

Analysis of the variance of the models (ANOVA) involves examining the fit of the model to the experimental data (Dejaegher and Vander Heyden, 2011) and was performed using JMP® (Version 9.0.2) software. The results of the ANOVA are listed in Table 5.4 (overleaf) and are discussed in this section. Specific discussion of each of the models will follow in sections 5.4.1 - 5.5. Where the values in the ANOVA table are not discussed, they are included for completeness. Further explanation of the meaning of values in the ANOVA table can be found in the Appendix section 9.2.6.

Table 5.4. ANOVA analysis of the model data for the responses Y_M, Y_A, Y_V, Y_S, Y_C and $*Y_C$ (see section 5.3.2 for discussion of $*Y_C$).

	% Mass extracted from hay (Y_M)		Abs 286 nm (Y_A)		Viscosity (Y_V)		Surface Tension (Y_S)		Contact Angle (Y_C)		Contact Angle ($*Y_C$)	
Source	DF	Sum of Squares	DF	Sum of Squares	DF	Sum of Squares	DF	Sum of Squares	DF	Sum of Squares	DF	Sum of Squares
Model	5	1022	4	1.195	4	1.176×10^{-5}	4	209.8	4	1210	4	1285
Lack Of Fit	9	108	11	0.0628	10	1.023×10^{-6}	10	200.4	10	347.3	-	-
Pure Error	1	0.32	15	0.00206	1	1.462×10^{-8}	1	0.0824	1	1.167	10	267.9
C. Total	16	1131	15	1.26	15	1.280×10^{-5}	15	410.3	15	1559	14	1553
R^2	0.90		0.95		0.92		0.51		0.78		0.83	
R^2 adjusted	0.86		0.93		0.89		0.33		0.70		0.76	
Model prob. > F	<0.0001		<0.0001		<0.0001		0.074		0.0014		0.0008	
Lack of fit Prob.> F	0.13		0.42		0.29		0.05		0.14		-	

5.3.1 R^2 and p-values

R^2 values in Table 5.4 indicate how well variance in the experimental data is explained by the model, hence as R^2 tends to 1 the better the ability of the model to describe the experimental data. $R^2 = 0.8$ was deemed to represent a satisfactory model before experimentation began. $R^2 = 0.8$ indicates that 80% of the variance in the experimental data is explained by the model. 'R^2 adjusted' makes R^2 more comparable between models with different numbers of parameters. Similarity between R^2 and R^2_{adj} indicates a more robust model as the model R^2 value is not artificially improved by using more parameters in its calculation. For the current research a difference between R^2 and $R^2_{adj} < 0.1$ was accepted as indicating the model was satisfactory and that it was not artificially improved by inclusion of unnecessary terms.

Plots of the experimentally measured responses versus those predicted by the models (see Appendix section 9.3.1, Figure 9.10 - Figure 9.15) show a good fit of the experimental and model predicted values for the responses Y_M, Y_A, Y_V,Y_C and $^*Y_C$. Residual plots for the models (included in section 9.3.2, Figure 9.16 - Figure 9.21) have a random appearance which suggests that differences between measured and model-predicted values for the responses arises from random fluctuations in the measurements, rather than systematic flaws in the models or response measurements.

The models represent the experimental data well with a high degree of statistical significance in most cases. The models describing % mass of the components extracted from the hay during reaction (Y_M), UV-vis absorbance of the extract solution at 286 nm (Y_A) and the viscosity of the extract solutions (Y_V) responses are statistically significant with $p < 0.0001$. High values of R^2 for Y_M, Y_A and Y_V, being respectively 0.90, 0.95 and 0.92

(R^2_{adj} = 0.86, 0.93, 0.89 respectively) suggest that the models for Y_M, Y_A and Y_V offer a good fit to the experimental data as well as being highly statistically significant.

5.3.2 The Y_C and $*Y_C$ models

The Y_C model was significant at p = 0.0014 with R^2 = 0.78 (R^2_{adj} = 0.70) hence this model is not as robust as those for Y_M, Y_A and Y_V as $R^2 < 0.8$. It is worth noting that the terms for reaction time, temperature and NaOH concentration are retained in the model for Y_C despite these terms being insignificant (as shown in the Y_C column of Table 5.3). These terms were included as they are reactions variables and removing them did not significantly improve the Y_C model. When the terms are removed, the model has p = 0.0002, R^2 = 0.72, R^2_{adj} = 0.68. This means removal of the not statistically significant terms related to reaction time, temperature and NaOH concentration in the model improved the p-value, which indicates increased statistical significance of the model. However, the ability of the model to describe the variation in the experimental data is slightly lowered as R^2 decreases (which represent the variation in the measured response explained by the regression equation, see section 5.4.4 for further discussion).

The experimental data was examined to investigate why the R^2 for the Y_C model indicated an unsatisfactory model, and an outlying data point was identified and removed (for the reaction coded as 0, 0, 0 and is highlighted in Table 5.2 and in Appendix section 9.3.1, Figure 9.15). Removal of this data point was successful in improving the model both in terms of the significance of $*Y_c$ (p = 0.0008) and the ability of the model to describe the experimental data (R^2 = 0.82 and R^2_{adj} = 0.76) as shown in Table 5.4. The 0, 0, 0 data point in the models for the other responses was not an outlier hence the models were not improved by screening the data and removing this data point. This improvement in the Y_C model and not the other models, indicates that the contact angle measurement for the reaction at 40 °C,

17.5 minutes using 2 molL^{-1} NaOH is problematic rather than something being wrong with the hay extract solution produced under these conditions. Therefore the Y_C model would be improved by repeating the 0, 0, 0 experiment and measuring the extract solution contact angle again. Unfortunately due to time constraints during the current research, this experiment was not performed.

5.3.3 Model lack of fit

Lack of fit measures the failure of the model to represent the experimental data at points which are not included in the regression (Montgomery, 1997). A value of $p > 0.05$ means the lack of fit between the experimental data and the values predicted for the corresponding experimental conditions by the model, is not statistically significant hence the model describes the experimental data well. The lack of fit for Y_M, Y_A, Y_V and Y_C models was insignificant with $p > 0.05$ in all cases. There is no lack of fit for the model $*Y_C$ as repeated experiments under the same reaction conditions are required to generate the lack of fit and the data point removed during the data screening for $*Y_C$ was for one of the repeated experiments.

5.3.4 The Y_S model

The model describing the extract solution surface tension (Y_S) response has $p = 0.074$ indicating lack of statistical significance of the model, *i.e.* it cannot be said with confidence that the model describes the experimental data. The Y_S model has $R^2 = 0.51$ and $R^2 = 0.33$, indicating poor fitting of the model to experimental data. Finally the $p = 0.0499$ value for lack of fit for the surface tension model indicates statistical significance of the lack of fit of the experimental data to the model, again demonstrating that the model is not acceptable in describing the experimental data. In the case of the Y_S model the R^2 and p-value are so poor that the model cannot be improved by screening the data.

The surface tension response measured by the pendant drop method is not well modelled when considering the extraction time, temperature and concentration of aqueous NaOH used in the reaction of hay and NaOH. Pendant drop surface tension measurements as used in these experiments can be made difficult by evaporation of water from the solution droplets during measurement over extended times. It is possible that during the measurement of the surface tension of hay extract solutions, evaporation from the air-droplet interface would adversely affect the accuracy of the measurement. To mitigate against evaporation from the liquid droplet during measurement, the measurement time was kept short. Short time for the pendant drop measurement may not have allowed the surfactant in the bulk solution/at the interface to reach equilibrium when the image was captured and the surface tension calculated, due to long equilibration times. The hay extract solution droplet not being at equilibrium could have adversely affected the accuracy of the data and impeded building a strong model to describe the surface tension of the hay extract solutions. Another possibility in explaining the inability to generate a useful model to describe the effect of reaction time/temperature and NaOH concentration on solution surface tension is that the concentration of surfactant in solution was above the CMC for at least some of the measurements. If the surfactant concentration was above the CMC then the surface tension would not vary, making construction of a usable model to describe the surface tension variation impossible.

The fact that an acceptable model for the hay extract solution contact angle could be constructed increases the likelihood that the weakness of the Y_S model being due to problems in accurately measuring surface tension than due to the surfactant concentration greater than the CMC. If the surfactant concentration being greater than the CMC caused

the failure to generate a model for Y_S then the contact angle model would also be expected to be very poor which was not observed.

5.4 Examination of the individual models

Considering all points described here it is concluded that the models given for Y_M, Y_A and Y_V represent the data well for the respective responses examined in these experiments with the model for Y_C not being as strong. A satisfactory model for the surface tension response could not be constructed using the pendant drop method for surface tension measurement applied during these experiments when varying the reaction time/temperature and aqueous NaOH concentration.

5.4.1 % Mass of hay components extracted during reaction

If more material is extracted from the hay during reaction with NaOH it is plausible to consider that the amounts of surfactant type species extracted would be increased which in turn means the extract solutions would have a higher potential for producing stable foams. Increased extraction of material from hay into solution also leads to increased viscosity of the extract solutions (see section 5.4.3) which improves the stability foams generated from the solutions. Table 5.3 shows reaction time, temperature, concentration of aqueous NaOH and reaction time squared are all statistically significant terms in the model describing the % mass extracted from the hay during reaction with NaOH as all terms have $p < 0.05$. The inclusion of the square of reaction time indicates a non-linear relationship between the response and reaction time (see section 5.4.1.2 for further discussion). The interaction between temperature and aqueous NaOH concentration is also shown to have a significant effect on the % mass extracted from hay during reaction indicating even greater extraction from hay when both NaOH concentration and temperature are increased together.

A Pareto plot is a way of visually representing data, used widely in such things as quality control for identification of the relative importance of causes of defects in products for example (Leland, 2006). The plots rank factors in order of their contribution to the 'problem' under investigation and allow an intuitive method for examining the relative contribution of each of the factors under consideration. Within this thesis Pareto plots are used to demonstrate the relative significance of the effects of the significant reaction variables and their interactions on the various measured responses. The value of the t-ratio used in the Pareto plots indicates the relative significances of the terms in the regression equations. The t-ratio lists the test statistics for the hypotheses that regression term estimates (β_n, β_m, β_{nn} or β_{nm}) are zero hence the associated reaction variables (or interaction of the variables) are insignificant in the model. The t-ratio is calculated by JMP® as the ratio of the regression term estimate to its standard error *i.e*. a large estimated regression term and relatively small standard error indicates significance of the regression term. A t-ratio greater than 2 is judged as indicating significance of the regression term as it indicates that the regression term is greater than twice the magnitude of the standard error which approximates the $p < 0.05$ significance level.

The orange lines in the Pareto plots within this chapter (Figure 5.1, Figure 5.4, Figure 5.7, Figure 5.9 and Figure 5.11) indicate the minimum t-ratio values required to show significance of the reaction variable or interaction terms (where $p < 0.05$) in the Pareto plots. The Pareto plots only include those terms within the models which are statistically significant unless otherwise stated. Positive values of t-ratios indicate that the regression term is positive and would act to increase the predicted value of the response, negative values indicate negative regression terms which act to decrease the value of the predicted response.

5.4.1.1 Pareto plot for % mass extracted from hay (Y_M) response

A Pareto plot in Figure 5.1 shows the relative effect of the reaction variables and their interactions on the % mass extracted response.

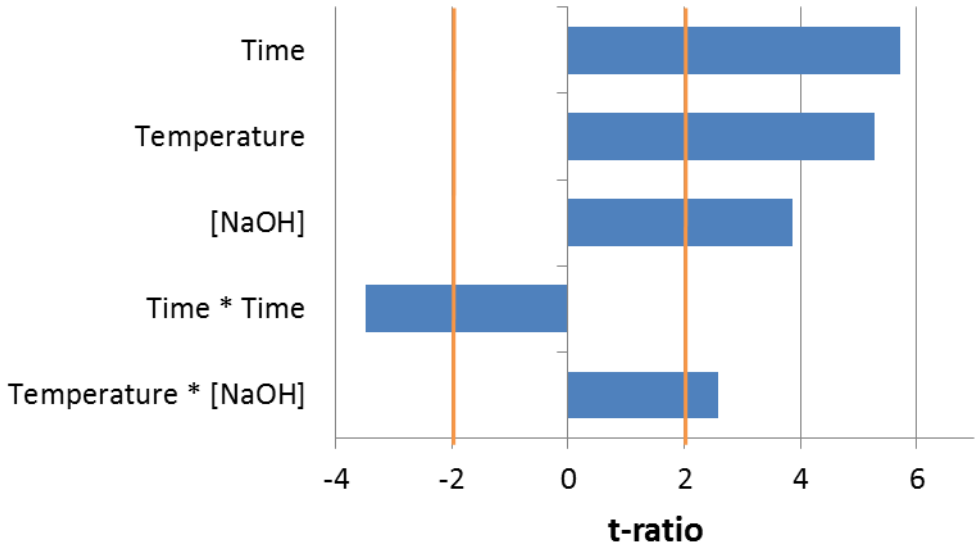

Figure 5.1. Pareto plot showing the relative effect of the reaction parameters and their interactions on the % mass of hay components extracted into solution by NaOH.

Figure 5.1 shows reaction time; temperature then NaOH concentration have progressively smaller significance in the model describing the % mass extracted from hay by NaOH. The significance of (extraction Time)^2 is next smallest with the interaction between reaction temperature and NaOH concentration having the smallest significant effect on the % mass extracted from hay response.

5.4.1.2 Surface plots for % mass extracted from hay (Y_M) response

Surface plots generated by the JMP software to visualise the effect of each of the reaction variables and their interactions on the % mass of the hay components extracted by NaOH are given in Figure 5.2 a-c.

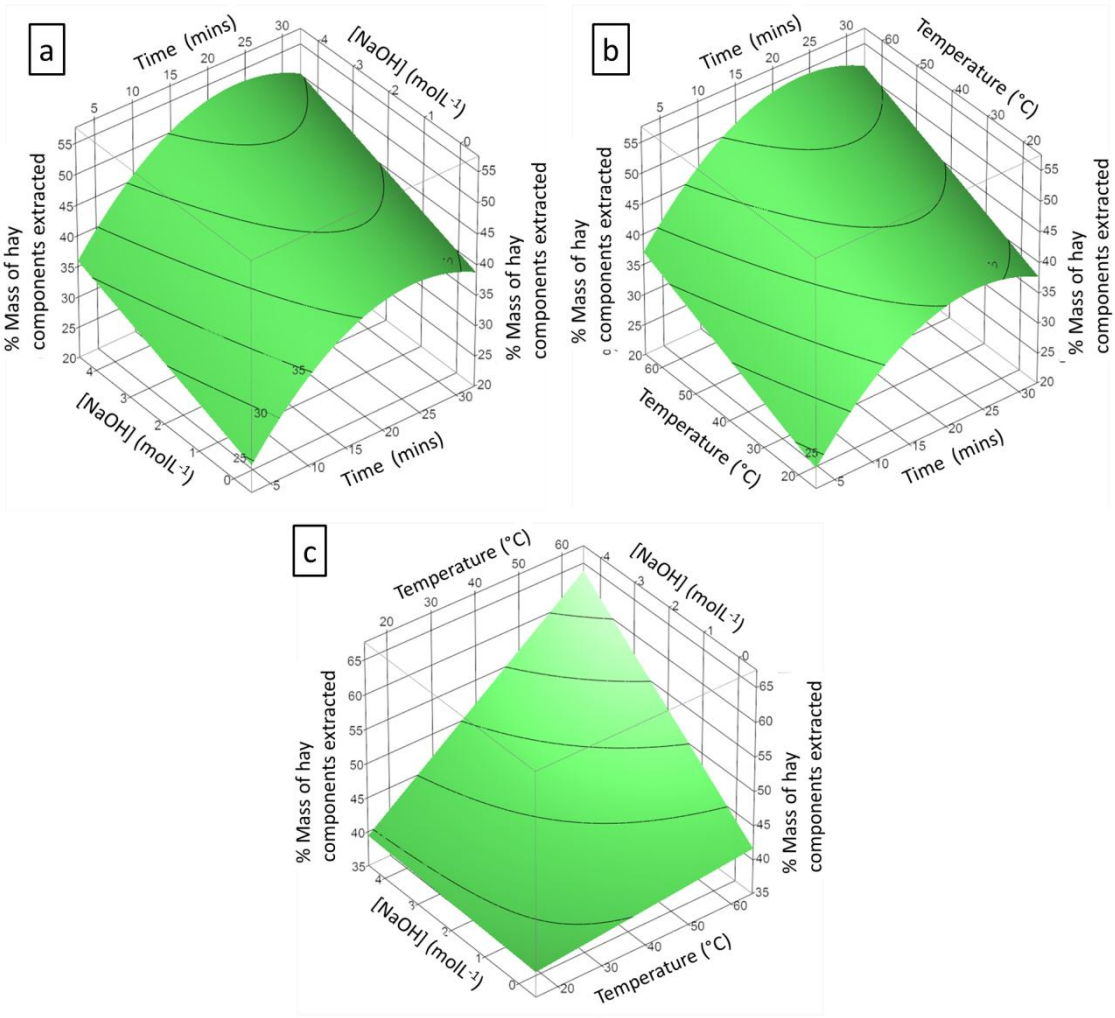

Figure 5.2. Surface plots for % mass extracted from hay using aqueous NaOH (a) Effect of aqueous NaOH concentration and time (extraction temperature = 40 °C); (b) Effect of reaction temperature and reaction time (aqueous NaOH concentration = 2.0 molL^{-1}); (c) Effect of aqueous NaOH concentration with temperature (extraction time =17.5 min).

Figure 5.2 (a) shows the linear effect of increasing aqueous NaOH concentration giving an increase in % mass extracted from hay during the reaction with aqueous NaOH which can be seen as increasing NaOH concentration on the *y*-axis leads to increasing % mass of hay extracted on the z-axis. Extraction time has a positive quadratic effect of increasing % mass extracted from hay during the reaction with aqueous NaOH, with the response reaching what appears to be a shallow maximum after 17.5 minutes (actually peaking at 23.8 minutes). No interaction between the NaOH concentration and reaction time variables is observable as indicated by the consistency in the surface shape at both low and high NaOH concentration and reaction times seen in Figure 5.2 (a).

The shallow maximum in mass extracted with increasing reaction time is hypothesised as actually being plateauing of the % mass response with reaction time. Plateauing of the % mass response with reaction time is not obvious from looking at the surface plot for the response in (a) and (b), however, if the response did come to a shallow maximum (not a plateau) then it would imply that beyond 17.5 minutes the % mass extracted would decrease. A decrease in the % mass response with extended reaction times is not logical as it would require re-deposition of material over extended reaction times. The % mass extracted from hay, response plateauing with reaction time can be seen more clearly in Figure 5.3 which is a reproduction of the relevant portion of the 'prediction profiler' output from the JMP software.

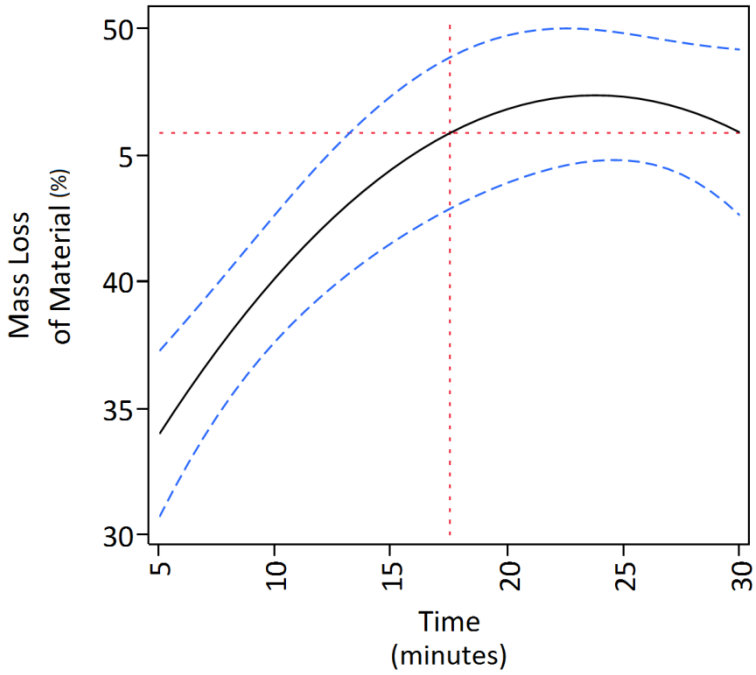

Figure 5.3. The change in % mass extracted from hay change with time potentially plateaus around 17.5 minutes (reaction temperature = 40 °C; [NaOH] = 2 molL^{-1}).

In Figure 5.3 the red dashed line rising from the *x*-axis indicates 17.5 minutes extraction time and the horizontal red dashed line indicates the corresponding % mass loss of the hay for the reaction (45.9%). The value of the 95% confidence intervals at 17.5 minutes reaction time are 42.9% and 48.9% and are shown as the blue dashed lines.

Figure 5.3 shows that within the confidence 95% confidence intervals the % mass extracted from the hay by NaOH response cannot be confidently described as reaching a shallow maximum then decreasing. Between 17.5 minutes and 30 minutes there is no statistically significant change in the % mass extracted from the hay within the 95% confidence intervals. The curve shows only how the JMP software interpreted the data for varying reaction times not necessarily a true decrease in the response at longer reaction times. The appearance of Figure 5.3 is combined with the knowledge of the solution absorbance showing a genuine plateau over extended times of reactions, beyond 30 minutes (as shown in Figure 4.2). The suspected plateau in the % mass extracted response model would be consistent with the observed plateau in extract solution absorbance response at longer extraction times seen in Chapter 4. This is the best available evidence with the current data set as % mass extracted with varying reaction times was not examined for Chapter 4.

Figure 5.2 (b) shows that an increasing reaction temperature gives a linearly increasing % mass extracted from hay during the reaction when using 2 $molL^{-1}$ aqueous NaOH. The positive quadratic effect of extraction time on % mass extracted from hay during the reaction with aqueous NaOH is evident as before. Again no interaction between the reaction temperature and the reaction time is observable.

Figure 5.1 shows that NaOH concentration used in the extractions and extraction temperature are both statistically significant in the % mass extracted from hay model. The effect of these terms individually is not as obvious in Figure 5.2 (c) though it is still the case that as aqueous NaOH concentration used in the extractions increases, % mass extracted from hay increases. Extraction temperature gives linearly increasing % mass extracted from hay also. The reason these effects are difficult to observe in Figure 5.2 (c) is that the interaction of NaOH concentration and reaction temperature has a significant effect on the

% mass extracted from the hay during reaction (as shown by Figure 5.1 also). Changing the NaOH concentration has a much larger effect on the % mass extracted response at high temperatures than low temperatures.

5.4.2 UV-vis Absorbance at 286 nm (Y_A)

Understanding the amount of lignin derivatives extracted into solution using UV-vis spectrometry is of value to the current research as lignin derivatives may be responsible for sudsing of the solutions (see section 5.5.2 and 6.4.2 for further discussion).

Table 5.3 shows that the extraction time, temperature and concentration of aqueous NaOH used in the extraction are all statistically significant (their regression terms have p-value < 0.05). Increase in these reaction variables acts to increase the UV-vis absorbance at 286 nm of the extract solutions. The square of aqueous NaOH concentration is also statistically significant in the model of the UV-vis absorbance of the hay extract solutions meaning that aqueous NaOH concentration has a quadratic rather than linear effect on the absorbance response. Though the coefficient for the NaOH concentration squared regression term is negative the effect of NaOH concentration variation is to increase the solution absorbance with increasing concentration up to a point where the increase in solution absorbance peaks (see section 5.4.2.2 for further explanation).

5.4.2.1 Pareto plot for solution absorbance at 286 nm (Y_A) response

A Pareto plot in Figure 5.4 shows the relative significance of the effects of the reaction variables and their interactions on the extract solution absorbance response.

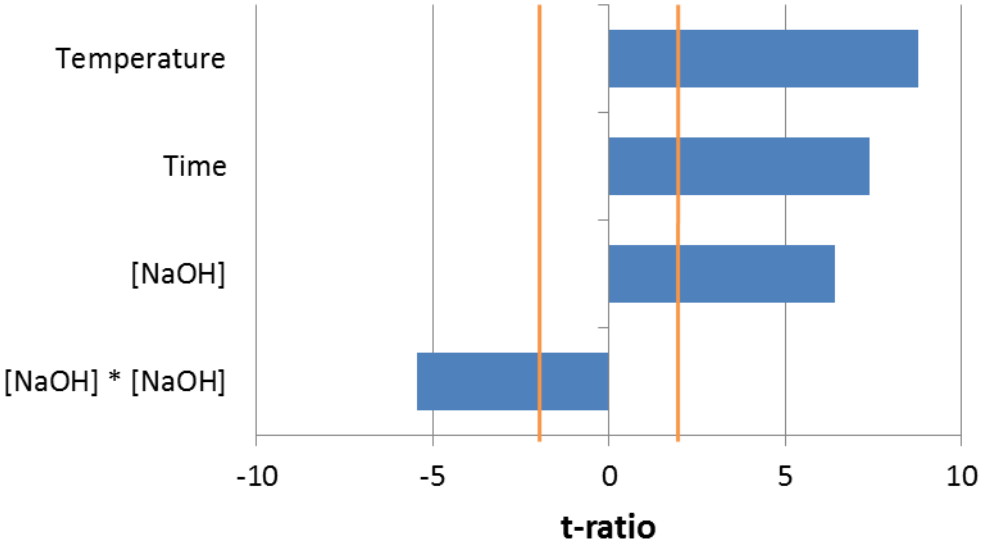

Figure 5.4. Pareto plot showing the relative effect of the reaction parameters and their interactions on the extract solutions absorbance at 286 nm.

Figure 5.4 shows that the reaction variables of reaction temperature, time and NaOH concentration have progressively decreasing statistically significance on the solution absorbance response with $[NaOH]^2$ being smallest.

5.4.2.2 Surface plots for solution absorbance at 286 nm (Y_A) response

Surface plots generated by the JMP software to help visualise the effect of each of the reaction variables and their interactions on the absorbance at 286 nm of the hay extract solutions are given in Figure 5.5 (a) – (c).

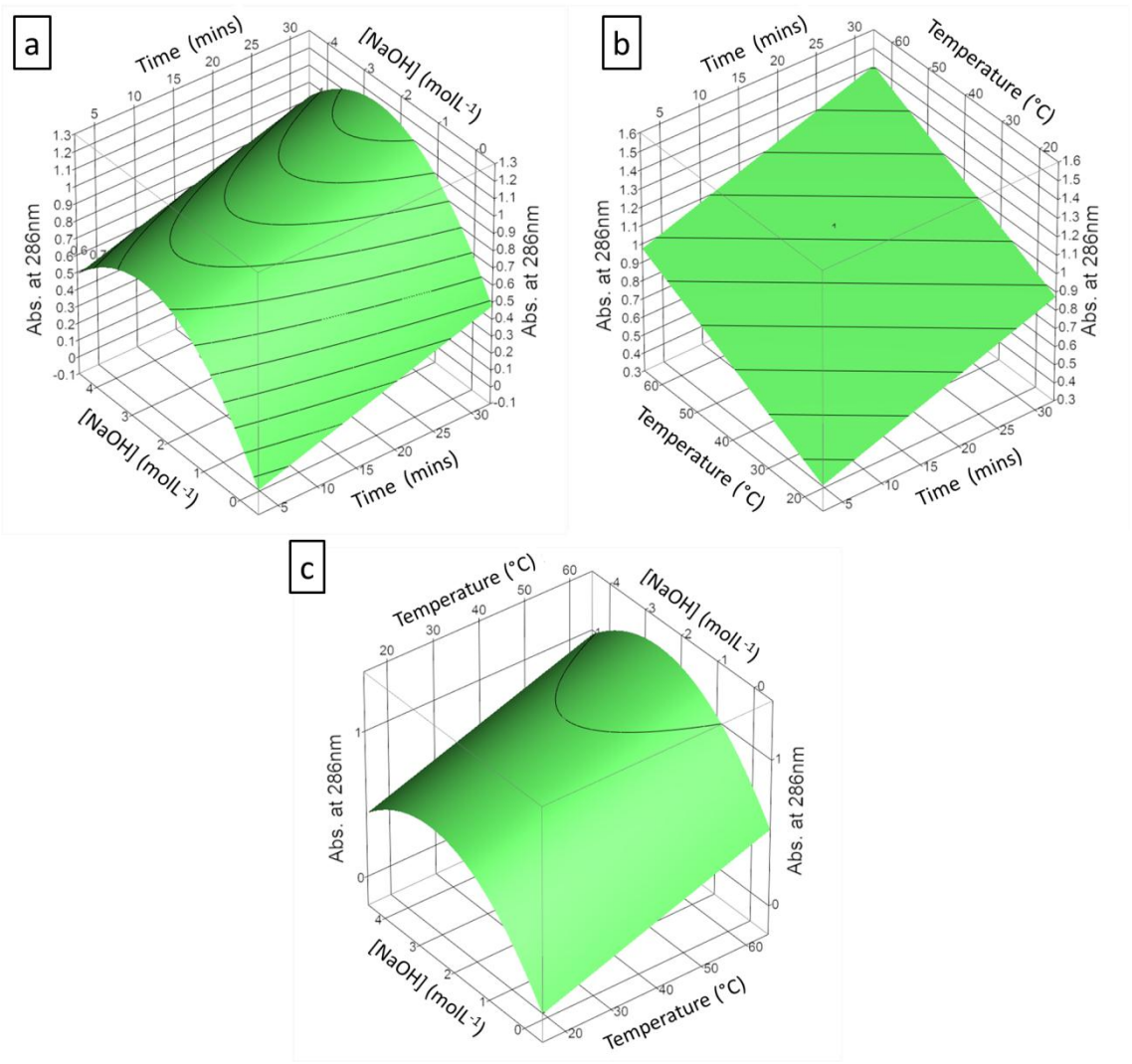

Figure 5.5. Surface plots for hay extract solution absorbance at 286 nm (a) Effect of aqueous NaOH concentration and time (extraction temperature = 40 °C); (b) Effect of reaction temperature and reaction time (aqueous NaOH concentration = 2.0 molL^{-1}); (c) Effect of aqueous NaOH concentration with temperature (extraction time = 17.5 minutes).

The effect of aqueous NaOH concentration and reaction time on the absorbance at 286 nm of the hay extraction products is shown in Figure 5.5 (a). The positive quadratic effect of aqueous NaOH concentration on the absorbance of the solutions at 286 nm is observable as indicated by the curved surface in the *y*-plane. The solutions absorbance at 286 nm appears to peak between 2 and 3 molL^{-1}. This peaking of absorbance can be seen more clearly in Figure 5.6 which is a reproduction of the relevant portion of the prediction profiler output from JMP.

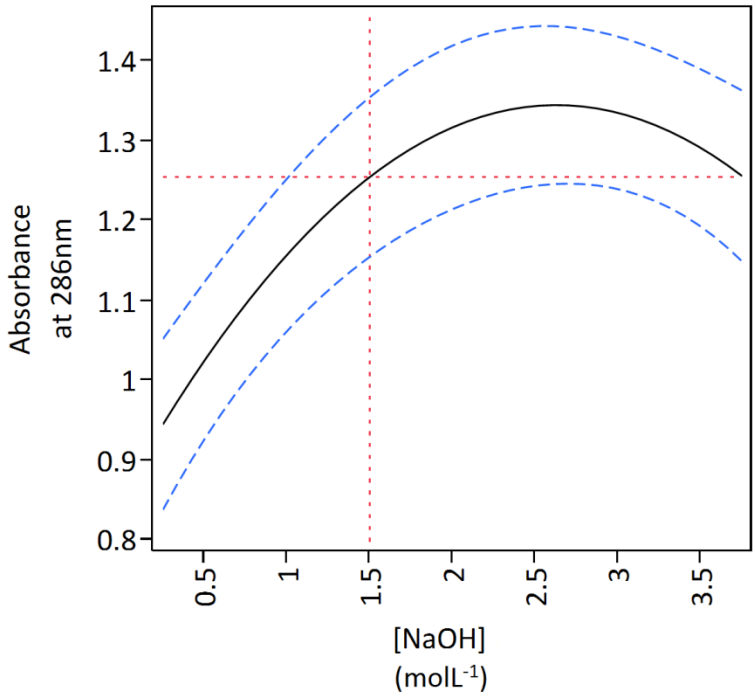

Figure 5.6. The change in extract solution absorbance (A) at 286 nm with NaOH concentration peaks at some concentration > 1.5 molL^{-1} NaOH.

Figure 5.6 shows that at 1.5 molL^{-1} the absorbance at the 95% confidence intervals = 1.15 - 1.35 as shown by the blue dashed lines. The in extract solution absorbance at 286 nm increases initially with increasing NaOH concentration then peaks somewhere after 1.5 molL^{-1} (appearing to peak at a NaOH concentration of 2.63 molL^{-1} in Figure 5.6). That the absorbance of the hay extract solution peaks at some concentration after 1.5 molL^{-1} is not unexpected when considered with the findings presented in Figure 4.3, where a maximum in absorbance was observed around the same NaOH concentration before decreasing with NaOH of increasing concentration. This is potentially explainable if lignin is broken down by high concentrations of NaOH as discussed in section 4.4.1. Conclusive identification of the concentration at which the absorbance peaks is not possible when examining Figure 5.6 as there is no statistically significant difference in the solution absorbance within the 95% confidence interval at concentrations > 1.5 molL^{-1}. The lack of significant difference in the solution absorbance at > 1.5 molL^{-1} is indicated by the fact that the horizontal red dashed line is within the 95% confidence interval for all concentrations > 1.5 molL^{-1}.

Figure 5.5 (b) shows how increasing reaction temperature and time (as seen previously in Figure 5.5 (a)) both gave linearly increasing hay extract solution absorbance with no interaction between the reaction variables apparent. Figure 5.5 (c) again shows aqueous NaOH concentration having a quadratic effect on the absorbance of the solution. Increasing reaction temperature again gives a linearly increasing reaction solution absorbance without significant interaction seen between the reaction temperature and aqueous NaOH concentration variables.

5.4.3 Viscosity (Y_V)

The viscosity of the hay extract solutions is important in the current research because reduction in drainage rate in bubble liquid films caused by increased viscosity of the liquid within the films, improves foam stability. Table 5.3 shows that the most statistically significant factor in increasing viscosity of the hay extract solution is increasing the concentration of the aqueous NaOH used during the extraction (p-value < 0.0001). Reaction time and temperature also have statistical significance in the hay extract solution viscosity model (p = 0.006 and p = 0.0005 respectively). The interaction term between reaction temperature and aqueous NaOH concentration has statistical significance and results in a more marked increase in hay extract solution viscosity when both extraction temperature and aqueous NaOH concentration are at high levels than would be gained from increases in either of the variables in isolation.

The link between viscosity of the hay extract solution and the concentration of aqueous NaOH reagent used is due to increased amounts of solubilised materials in the reaction products. It is also noted that solutions of higher concentration aqueous NaOH are more viscous than solutions of lower concentration aqueous NaOH (as demonstrated by Figure 4.7) hence this also contributes to extract solution viscosity increase with NaOH

concentration. The results presented in section 4.5 confirm that though NaOH is more viscous at higher concentrations, there is an effect of increasing the viscosity of the hay extract solutions due to the solubilisation of material from the hay on top of the viscosity increase seen with higher NaOH solution concentration.

5.4.3.1 Pareto plot for solution viscosity (Y_V) response

The Pareto plot in Figure 5.7 clearly shows the relative statistical significance of the effects of the reaction variables and their interactions on the model of hay extract solution viscosity response.

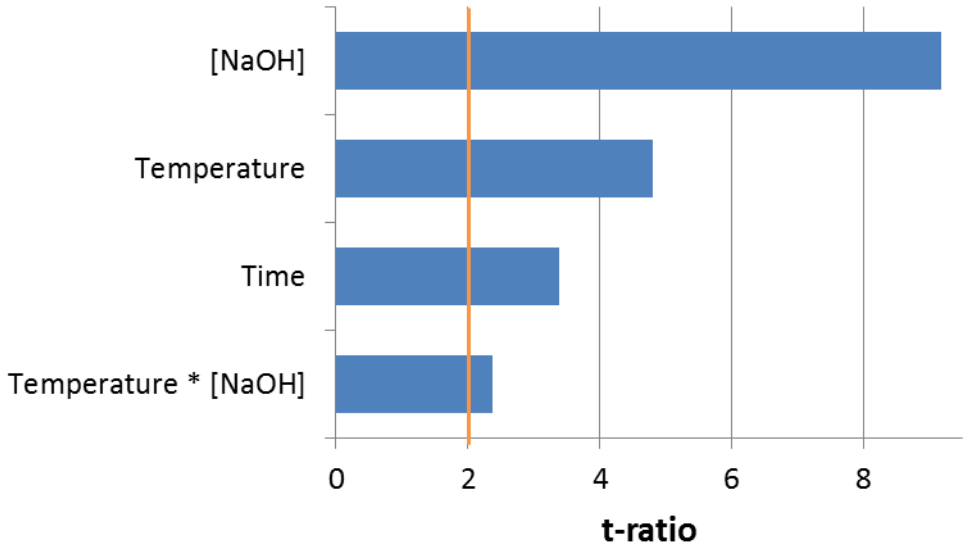

Figure 5.7. Pareto plot showing the relative effect of the reaction parameters and their interactions on the extract solutions viscosity.

Figure 5.7 shows that aqueous NaOH concentration used in the extraction, extraction temperature, time and the interaction term between extraction temperature and NaOH concentration have progressively smaller significance in the model describing the viscosity of hay extract solutions.

5.4.3.2 Surface plots for solution viscosity (Y_V) response

Surface plots were generated by the JMP software to help visualise the effect of each of the reaction variables and their interactions on viscosity of the hay extract solutions and these plots are given in Figure 5.8 (a) – (c).

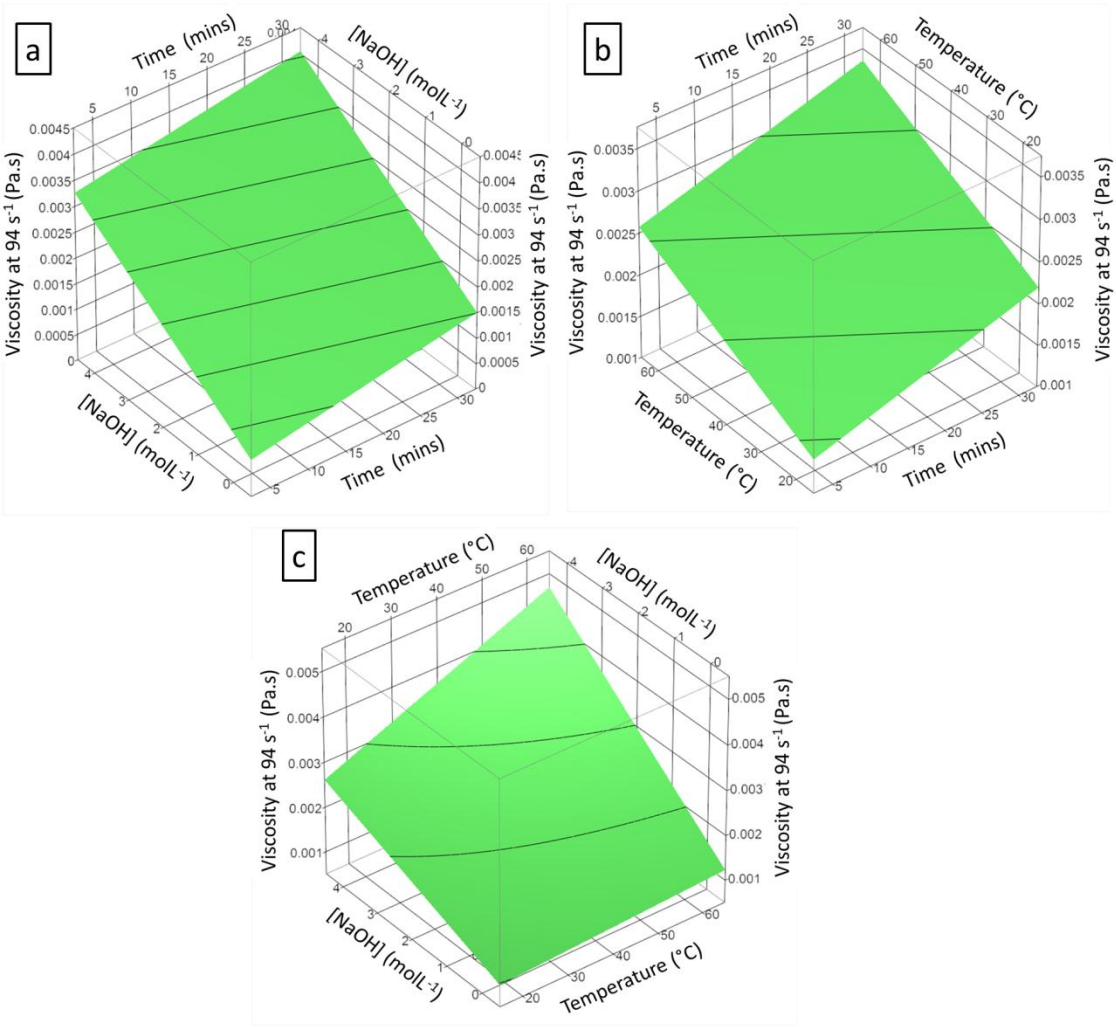

Figure 5.8. Surface plots for solution viscosity (a) Effect of Aqueous NaOH concentration and time (extraction temperature = 40 °C). (b) Effect of reaction temperature and reaction time (aqueous NaOH concentration = 2.0 molL^{-1}). (c) Effect of aqueous NaOH concentration with temperature (extraction time = 17.5 min).

Figure 5.8 (a) shows hay extract solution viscosity increases linearly with aqueous NaOH concentration and (to a lesser extent) extraction time. No interaction between the NaOH concentration and reaction time is observable.

Figure 5.8 (b) shows increasing reaction time gives a linearly increasing hay extract solution viscosity, though to a lesser extent than increasing reaction temperature without any significant interaction between the two parameters.

Figure 5.8 (c) shows aqueous NaOH concentration increase gives a linearly increasing hay extract solution viscosity and increased extraction temperature gives a smaller linearly increasing product solution viscosity at low aqueous NaOH concentration. Due to the statistically significant interaction between NaOH concentration and extraction temperature the effect of higher extraction temperature leading to increased product solution viscosity is more evident at higher aqueous NaOH concentrations.

5.4.4 Contact Angle Measurement (Y_C and $^*Y_C$)

Table 5.3 shows that the only statistically significant term in the model for contact angle of the hay extract solutions is the square of aqueous NaOH concentration, though the terms for extraction time and temperature as well as NaOH concentration are still retained in the model as these are reaction variables. The same reasoning for inclusion of all reaction variables is true for the $^*Y_C$ model also.

5.4.4.1 Pareto plot for the hay extract solution contact angle response

A Pareto plot demonstrates the relative statistical significance of the effects of the reaction variables and their interactions on the extract solution contact angle response is shown in Figure 5.9. The Pareto plot for the $^*Y_C$ model is included in the figure to demonstrate the similarity in the Y_C and $^*Y_C$ models.

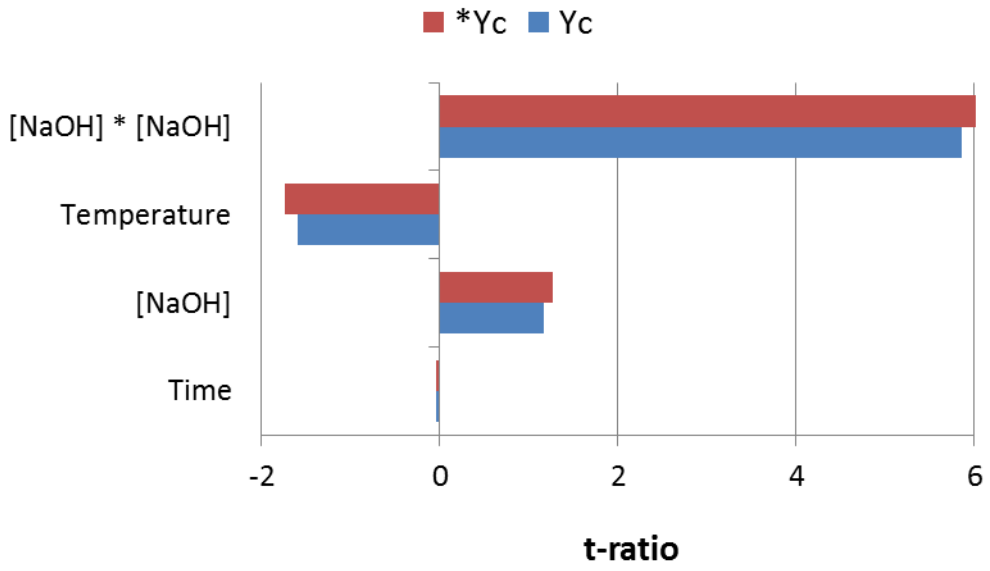

Figure 5.9. Pareto plot showing the relative statistical significance of the reaction variables and their interactions on the models describing hay extract solutions contact angle on a polystyrene surface (Y_C and $*Y_C$). (Note: In the case of this Pareto plot, only the [NaOH] * [NaOH] term is actually statistically significant for both models).

The Pareto plots of the Y_C and $*Y_C$ response models shown in Figure 5.9 demonstrate that removing the single data point for contact angle of the extract solution generated by the reaction variables coded to 0, 0, 0 to generate the $*Y_C$ model; did not dramatically change the nature of the model for Y_C. NaOH concentration squared is still the only significant term in the $*Y_C$ model and the statistical significance of that term is not changed dramatically by removing the single data point. The relative statistical significance of the other reaction variables and their interactions in the model are also unchanged. This similarity in the two models justifies the decision to screen the data and remove a data point as it did not affect the nature of the models much.

As there is only one significant term in the model for the extract solution contact angle response (both Y_c and $*Y_C$) it is not useful to look at the full set of surface plots for the reaction variables and their interactions. The minimising of product solution contact angle with varying concentration of NaOH can be seen clearly in Figure 5.10 which is a

reproduction of the relevant portion of the prediction profiler output from JMP for the solution contact angle response vs. the NaOH concentration used in the extraction.

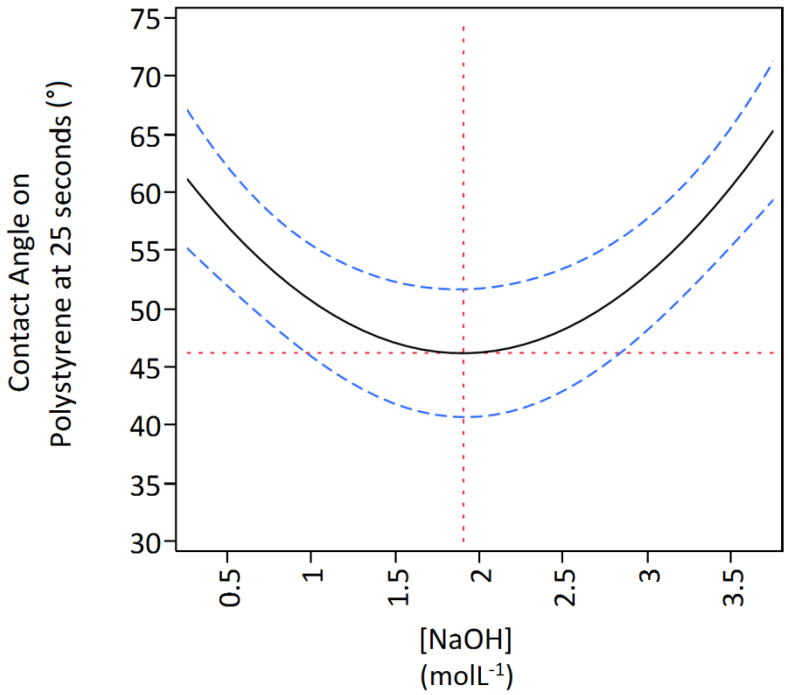

Figure 5.10. The change in hay extract solution contact angle with NaOH concentration reaches a minimum around 1.9 molL^{-1} NaOH.

Figure 5.10 demonstrates the quadratic effect of NaOH concentration on the measured hay extract solution contact angle response. At low to intermediate NaOH concentration (0.5 - 1.9 molL^{-1}) the contact angle of the extract solution decreases with increasing NaOH concentration. This indicates that the surface tension of the solution is decreasing which in turn indicates that the amount of surfactant at the interface is increasing.

At Intermediate to high NaOH concentration (1.9 – 3.75 molL^{-1}) the solution contact angle increases. Increasing contact angle of the solution indicates less surfactant is present at the interface which causes higher surface tension which is responsible for the increased contact angle. Knowing that more material overall is extracted from the hay at the higher NaOH concentration used in this chapter, and if higher concentrations of NaOH were expected to extract more surfactants from the hay, then it might be expected that surface tension would

decrease with higher NaOH concentrations hence contact angle would decrease. The increasing hay extract solution contact angle with higher NaOH concentration could be related to the maximum reached in the extract solution absorbance discussed in section 5.4.2.2. The potential relationship between hay extract solution contact angle and absorbance is discussed in section 5.5.2.

5.5 Comparison of the models

5.5.1 Discussion of the models

The Pareto plots showing the relative magnitude of the effect of the reaction variables and their interactions for the models of Y_M, Y_A, Y_V and Y_C are combined for easy comparison in Figure 5.11. (*Y_C is so similar to Y_C that it is not included).

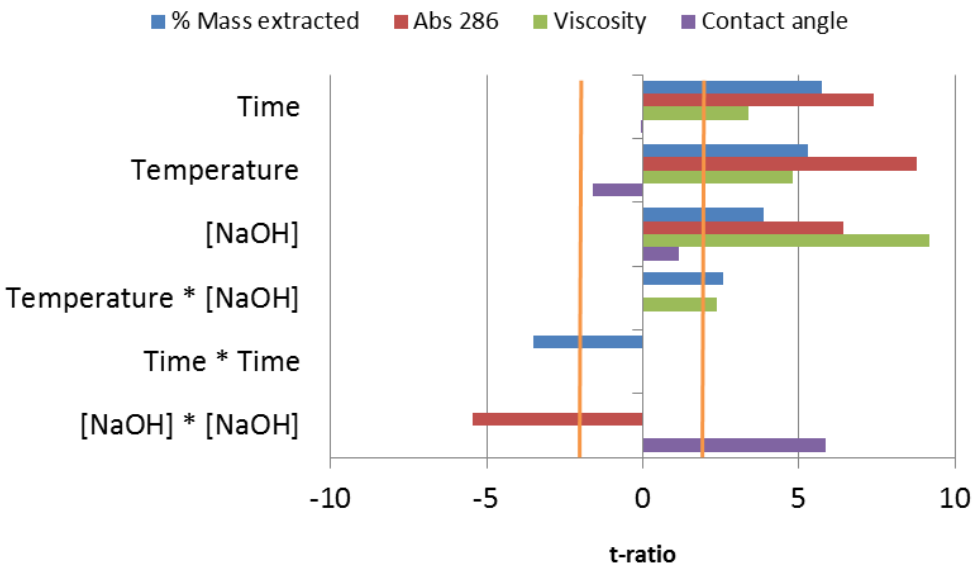

Figure 5.11. Pareto plot comparisons between the reaction variables and their interactions by response.

Figure 5.11 shows that % Mass of hay components extracted (Y_M), extract solution absorbance at 286 nm (Abs 286; Y_A) and extract solution viscosity (Y_V) models all have statistically significant positive contributions from increased reaction time, temperature and NaOH concentration variables.

That the models for Y_M, Y_A, Y_V and Y_C all have statistically significant terms in them for reaction time, temperature and NaOH concentration is not surprising as all of these would be expected to affect reaction extent or kinetics which in turn affect the measured responses. It is considered that similarities between the models could arise due to some of the responses being related such as increased % mass extracted from hay leading to increased viscosity of the extract solutions which explains why the same temperature * [NaOH] interaction term is statistically significant in both the Y_M and Y_V models.

The model for Y_M includes a negative quadratic term from the reaction time. By examination of the response surface plots (Figure 5.2) and the response profiler output for % mass extracted vs. time (Figure 5.3) as well as the observed plateau in the extract solution absorbance response with increasing reaction time seen in section Figure 4.2, it is hypothesised that the % mass of hay components extracted plateaus at longer reaction times used in the current research. The implication of the result is that as the reaction time increases, the amount of material extracted from the hay correspondingly increases at first, then peaks with no more material extracted as reaction time increases beyond around 17.5 minutes.

Though the responses are related, the % mass extracted from the hay plateauing in time is not consistent with the effect of extraction time on the extract solution viscosity, which increases linearly with increasing reaction time (see Figure 5.8 (a) and (b)). This is a puzzling result which suggests that viscosity builds with increasing extraction time without there necessarily being a corresponding increase in the % mass extracted from the hay. The reason that viscosity would continue to increase with extraction time without the % mass

extracted from the hay also increasing is unknown, though it offers an opportunity for further research to generate understanding of this phenomenon.

Finding that % mass extracted from hay during the reactions plateaus in time agrees with the result found previously where measured solution absorbance plateaus with reaction time (Chapter 4, section 4.1.1). That both % mass extracted and absorbance were found to plateau with increasing extraction time is in agreement with the idea that increased % mass extracted overall from the hay would be consistent with increased lignin derivative extraction. Figure 4.2 demonstrates that hay extract solution absorbance did not increase (indicating no more lignin chromophores were extracted into solution) when the reaction time went beyond 30 minutes for reactions at room temperature. The fact that the time to reach a plateau in % mass extracted in the experiments performed in this chapter is shorter may be due to reaction kinetics, as the extractions examining the effect of time were effectively performed at 40 °C which is higher than the experiments in Chapter 4.

Figure 5.2 (a) and Figure 5.2 (c) show that % mass extracted from the hay during the reaction increases linearly with aqueous NaOH concentration. The UV-vis absorbance of the solution does not demonstrate the same linear trend with NaOH concentration increase as seen in Figure 4.3. The reason that UV-vis absorbance peaks at some NaOH concentration > 1.5 $molL^{-1}$ may be that higher NaOH concentrations do not necessarily extract more lignin-hemicellulose chromophores, but increasingly extracts more of the other components of the hay (*e.g.* increased cellulose extraction with higher NaOH concentration as discussed in section 2.4.4). If higher NaOH concentrations did actually extract more lignin derivatives as part of the increased overall mass extracted from the hay, then it would be necessary that the chromophores were broken down by higher concentrations of NaOH. The possibility of lignin breakdown at higher NaOH concentration is discussed in section 4.4.1. It is

hypothesised that the actual explanation of this disagreement between linearly increasing % mass extracted from hay and the apparent plateauing of extract solution absorbance at the higher NaOH concentrations used in this chapter (which was shown to decrease at even higher NaOH concentrations in Chapter 4), is likely to be a combination of effects. Increased extraction of non-chromophores such as cellulose, and a degree of chromophore break down by high concentration NaOH would explain the observed effects though confirmation of this by further research is required.

5.5.2 A clue as to the origins of foaming from the alkali extract solutions from hay?

Section 5.4.2.2 shows that solution absorbance increases with NaOH concentration until it peaks. The peaking solution absorbance occurs at NaOH concentration between 1.5 and 2.5 $molL^{-1}$ within the 95% confidence limits of the model (see Figure 5.6). Figure 5.10 demonstrates that the solution contact angle decreased with NaOH concentration increase to around 1.9 $molL^{-1}$. With this in mind it is conceivable that the maximum hay extract solution absorbance and minimum contact angle occur at the same NaOH concentration. The solution absorbance increasing is due to more lignin derivatives being extracted from the hay and the solution contact angle decreasing is due to more surfactant being present in the extract solutions. This indicates a potential relationship between the solution absorbance increasing and the amount of surfactant in solution increasing. It is hypothesised that the lignin derivatives which increase solution absorbance, have surfactant properties hence are responsible for the decreased surface tension of the solutions leading to decreased contact angle at higher NaOH concentrations. The implication of this is that lignin derivatives solubilised from the hay would be responsible for foaming of the extract solutions. The hypothesis that lignin derivatives, being responsible for solution absorbance,

could also be responsible for foaming of the solutions was tested and is discussed in section 6.4.2 and the correlation between solution absorbance and foaming of hay extract solutions is examined in section 7.3.

5.5.3 Maximising the 'desirability' of the responses using the models

When analysing the models using the JMP® software (Version 9.0.2) it is possible to find the optimum values for the parameters used in the models (the reaction variables) in order to maximise the desirability of each of the responses modelled. Specifically it was desirable to maximise the % mass extracted from the hay, solution absorbance and solution viscosity and minimise the solution contact angle. This would be potentially very simple if the responses had linear relationships to the reaction variables in all cases. As some of the responses have quadratic terms for reaction variables, maximising desirability is less straightforward. The 'prediction profiler' in JMP was used to test the models and predict the best achievable values for the responses which are given in Table 5.5 along with the error and the reaction conditions predicted in order to achieve them.

Table 5.5. Reaction conditions to maximise the desirability of each of the responses.

			Reaction conditions		
Response	Optimised Response Value	Error (±)	Time (mins.)	Temp. (°C)	[NaOH] ($molL^{-1}$)
% Mass loss	59.9	4.9	23.8	60	3.75
Abs 286	1.35	0.099	30	60	2.63
Viscosity (Pa.s)	0.00433	0.00048	30	60	3.75
Contact angle (°)	43.4	7.5	30	60	1.89

The data in Table 5.5 for the % mass loss response highlights the quadratic of the relationship between the response and the reaction time variable as it is not simply a case of using the highest value for the reaction variable. The same is true for the NaOH

concentration reaction variable in its effect on the extract solution absorbance and contact angle responses. The extraction conditions for optimisation of the responses measured in the research for this chapter vary by response hence a choice might have to be made as to which response is most important when selecting extraction conditions.

5.5.4 Using the models to understand foaming of hay extract solutions

If the models generated in the research for this chapter can be used to find correlation with foamability of the alkali hay extract solution then it might be possible to identify which of the responses measured in this chapter could be used as a proxy to indicate which hay extract solutions might have high foamability. If the responses with the strongest correlations to foamability are known then it becomes a simpler task to find the most appropriate values of the reaction variables to maximise the appropriate extraction solution property which correlates with foamability. This would allow alkali hay extract solutions to be generated with better potential foamability without necessarily performing numerous difficult foaming measurements on individual solutions. Research to find correlations between foamability of alkali hay extract solutions and the responses measured in this chapter is presented in Chapter 7.

6 Chapter 6 – Examination of foam from alkali plant extract solutions using cryo SEM and AFM

6.1 Introduction

Cryogenic Scanning Electron Microscopy (cryo SEM) has been used to explore foam microstructures. As well as hay extract foam, other relevant foams were examined in order to compare their microstructures. Linear alkylbenzene sulphonate (LAS) foam was examined (section 6.2.1) as an example of a surfactant whose future use in laundry detergents will be reduced by application and extension of the research in this thesis. Examination of gelatin foam allowed comparison of the alkali plant extract foams to a pure protein foam (section 6.2.2). Foam from Guinness stout (section 6.2.3) and Kronenbourg lager (section 6.2.4) were also examined as these foams originate from proteins/polysaccharides providing another useful comparison with the microstructure of alkali hay, horse chestnut leaf and rice straw extract foam microstructures (sections 6.2.5 to 6.2.9).

Rather than discussing the meaning of each observed feature in each foam, discussion of the similarities and differences in the SEM images will be covered in section 6.3.

It was hypothesised that the plant extract foams might be proteinaceous or lignin derivative based, hence it was useful to compare protein based solutions with the plant extract solutions to look for similarities and differences. Section 6.4 describes attempts to identify the specific cause of foaming in plant extract solutions using simple experiments which aimed to disrupt the foaming of solutions in ways which gave conclusive evidence as to the origin of foaming.

6.2 Cryo SEM images of various foams

The resolution possible when examining the foams using cryo SEM was limited by the delicate nature of the samples. Using high energy electron beams to generate higher magnifications resulted in sample degradation and electrostatic charging, which made higher magnifications than those achieved in the following images impossible. The limited resolution of the SEM images that was achievable meant that particle size measurements were made difficult. Particles observed in the images may be agglomerates of smaller particles and it is not possible to positively identify this in the images hence the particle sizes indicated are approximate.

Etching was only used in examination of the hay extract foams as the effect of etching on the samples was, unfortunately, not well understood at the time of capturing the images hence its value was overlooked. Energy dispersive X-ray microscopy (EDX) was attempted to look at the foam composition during SEM imaging of the samples but yielded no useful data.

Consistency in observations of foam microstructures in terms of the presence of adsorbed particles, their shape, size and agglomeration behaviour, were seen across the respective range of images captured for each foam. Therefore only a representative selection of images is reproduced within this chapter.

Examination of the bulk solutions to look for evidence of particles proved impossible as the frozen solutions were too hard so could not be fractured to expose internal structures. Useful images of the bulk solution surfaces could not be generated as they were extensively covered in ice crystals.

6.2.1 Linear alkylbenzene sulphonate (LAS)

LAS foam was particularly fragile when frozen (being considerably more delicate than the other foams examined) and generating a viable frozen foam sample for SEM examination

was difficult. For this reason SEM examination of a fractured portion of frozen LAS foam was not possible as it was mostly destroyed during freezing. Therefore SEM images could only be captured of un-fractured foam hence the preparation method for the LAS foam was somewhat different to the other foams. That said cryo SEM examination of the LAS foam was still useful and images are included in Figure 6.1.

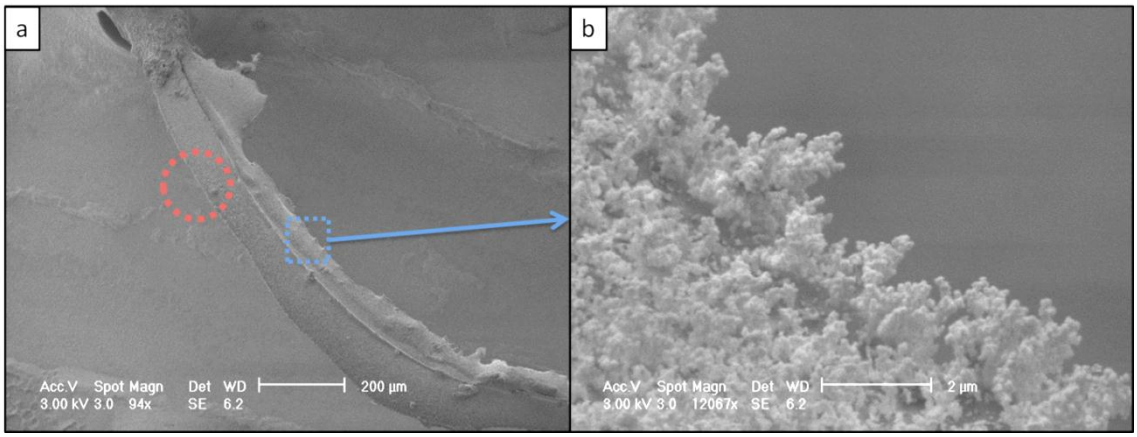

Figure 6.1. Cryo SEM images showing bubbles in LAS foam at a) 47x; b) 12067x magnification.

Figure 6.1 (a) shows a LAS bubble approximately 2.5 mm across with the red circle indicating the bottom 'edge' of the bubble as it would have sat upon the aqueous LAS solution, which appears as a line around the bubble. Upon closer examination, this line merely represents the edge of the bubble and did not contain anything particularly interesting *e.g.* particles. Figure 6.1 (b) is a magnified look at the edge of the liquid film in the region indicated by the blue dashed box in Figure 6.1 (a).

Figure 6.1 (b) shows ice crystals on the bubble film which formed during freezing of the foam. Ice crystals are not evident in the plant extract foam images that follow, as these samples were successfully fractured before SEM examination which removed the problem of ice crystal formation by exposing the subsurface foam microstructure. The ice crystals appear to be the only interesting feature seen in the SEM images of the LAS foam as expected for a solution only containing water soluble LAS.

6.2.2 Gelatin

Gelatin is a protein prepared by boiling animal skin, bone and connective tissue. Gelatin solution was made up in water, not as an alkaline solution as the plant extracts were. Gelatin was of interest as it generates voluminous, stable foam from a pure protein source which allows the plant NaOH extracted foams to be compared to known protein foam. Gelatin cryo-SEM images are shown in Figure 6.2.

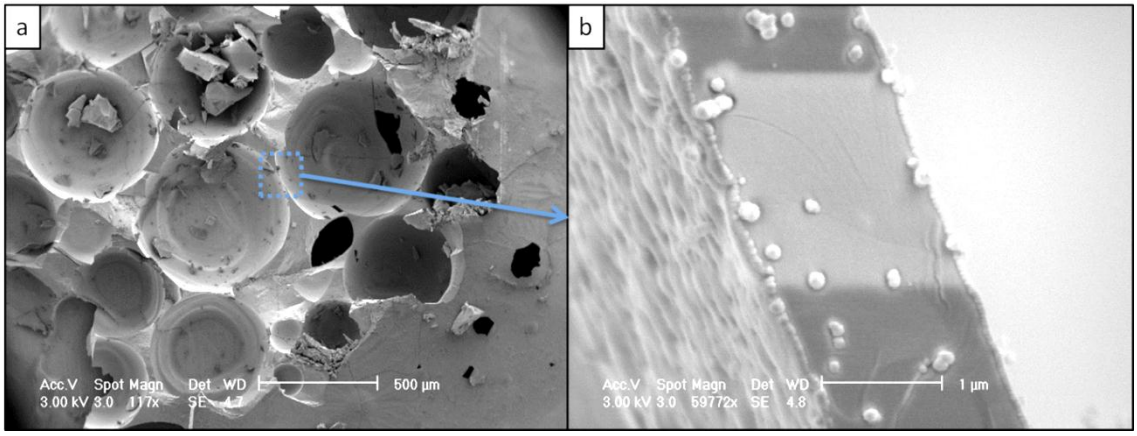

Figure 6.2. Cryo SEM images showing bubbles in gelatin foam at a) 117x; b) 59772x magnification.

Figure 6.2 (a) shows many closely arranged bubbles with dimensions in the size range 0.12 - 0.64 µm. The blue dashed box highlights the approximate region which was more closely examined in see Figure 6.2 (b).

The liquid film between the adjacent bubbles in Figure 6.2 (b) is approximately 1.5 µm across. It can be seen that the liquid continuous phase in the film between the gelatin foam bubbles has a relatively smooth fractured surface. The smoothness of the fractured surface of the liquid film indicates few particles are present and this smoothness is consistently seen in the gelatin foam in regions away from the bubble gas-liquid interfaces. A small number of globular sub-micron particles are visible in the fractured liquid film region with many more particles adsorbed on both surfaces of the bubble interface. The particles in the liquid film have an average size of 99 nm (averaged over 20 particles, with a standard deviation of 27 nm) and similarly sized and shaped particles are observed consistently in the SEM images

of gelatin foam. The particles adsorbed at the interface appear potentially smaller than those seen in the liquid film between the bubbles. The internal surface of the gelatin bubble in (b) is not smooth, having an undulating appearance.

6.2.3 Guinness

Guinness is a popular Irish stout drink known for its creamy foam 'head'. Like the consumer expectation of foam when using laundry detergents, consumers expected to see thick, creamy foam on top of a glass of Guinness as well as other beers/lagers. Guinness/lager are interesting in the context of the current research as the foams are known to be generated by proteins, specifically lipid transfer protein (Mills *et al.*, 2009). Saccharides increase foam stability in drinks such as Guinness/lager when they couple to proteins, increasing the solution viscosity local to foam films, decreasing film drainage rate and helping maintain an increased distance between adjacent bubbles (Evans and Bamforth, 2009). This aids foam stability by limiting film rupture and disproportionation which leads to foam coarsening and eventually foam collapse.

Cryo SEM was used to examine Guinness foam and the images captured are shown in Figure 6.3.

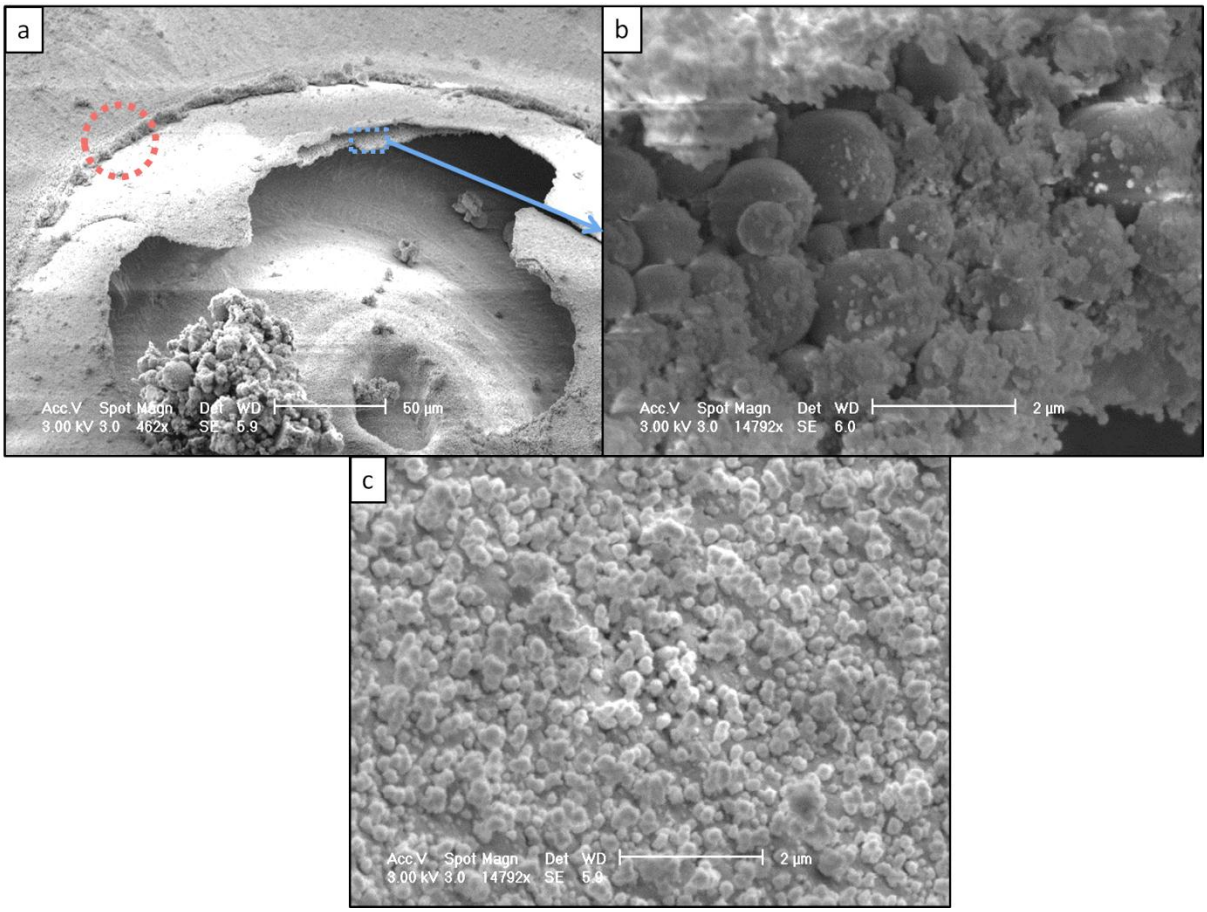

Figure 6.3. Cryo SEM images showing bubbles in Guinness foam at (a) 462x; (b) 14792x; (c) 14792x magnification.

Figure 6.3 (a) shows an interesting image of a bubble approximately 350 µm in diameter. The surface of the liquid has a rough appearance, though this sample was fractured hence this roughness is not due to ice crystals. The red dashed circle in (a) indicates a thick 'halo' seen around the bubble base which was a region of densely packed particles (a closer look at a similar halo of particles around a rice straw bubble is shown in Figure 6.10 (d).) Halos such as this were a consistent feature of the bubbles in the Guinness foam.

Due to the angle from which the bubble is observed it is particularly interesting to examine the region where the liquid film appears to have 'opened' and exposed the internal microstructure of the film. Figure 6.3 (b) gives a higher magnification look at the region

indicated by the dashed blue box in (a). The outer film interface in the upper left portion and inner film interface in the lower right portion of image (b), are both extensively covered with smaller adsorbed particles. The particles within the liquid film are almost spherical and are much larger than those on the internal and external liquid film interfaces. The larger particles within the liquid film have an average approximate diameter of 1.13 μm (the largest being ~1.8 μm, smallest ~0.55 μm, with the average calculated from 20 particle measurements, with a standard deviation ~0.4 μm). Accurate measurement of the particle sizes was made difficult by the particles being located at different depths within the liquid film, the perspective from which the image was captured and considerable variation in the particle size.

Figure 6.3 (c) shows the particles adsorbed at the bubble surface which at first glance appear to resemble ice crystals (as seen in Figure 6.1), however, these are in fact globular particles which densely cover the bubble surfaces. These globular particles are seen consistently covering the liquid surfaces in the SEM images of Guinness foam. The particles in Figure 6.3 (c) are in the size range 98 nm – 248 nm with the approximate average size being 160 nm (measured from 20 particles with standard deviation ~40 nm). Accurate particle size measurement is again made difficult as the particles tend to agglomerate and due to the limited image resolution particles might be measured which are not identifiable as being agglomerates.

6.2.4 Kronenbourg

Kronenbourg is a lager which also requires a (proteinaceous) foam head when served to consumers in order to meet their expectations. Cryo SEM images of Kronenbourg lager foam are shown in Figure 6.4.

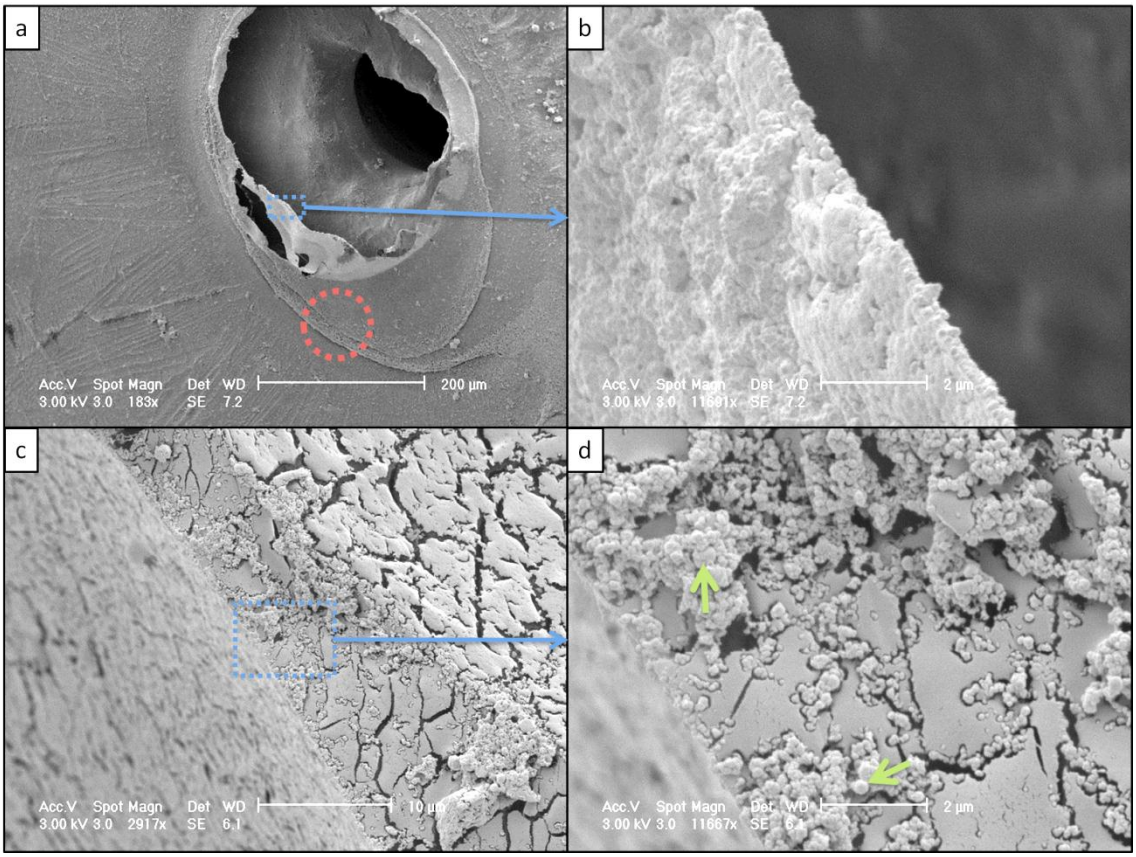

Figure 6.4. Cryo SEM images of Kronenbourg foam at a) 183x; b) 11691x; c) 2917x and d) 11667x magnification.

Figure 6.4 (a) shows a bubble in Kronenbourg foam approximately 460 µm x 330 µm. This bubble again has a 'halo' of particles (indicated by the red dashed circle) at its base. The blue dashed box indicates a region on the edge of the fractured bubble film which is more closely examined in Figure 6.4 (b).

Figure 6.4 (b) shows globular sub-micron particles adsorbed at the fractured bubble interface. As with the Guinness bubbles (section 6.2.3) the surface of the Kronenbourg bubble is densely covered by particles and this is consistently seen in images of other bubbles in the Kronenbourg foam.

Figure 6.4 (c) shows the interface between two adjacent bubbles in the fractured region of the Kronenbourg foam. Globular particles are observable within the liquid film between adjacent bubbles though the particles are more dispersed than those seen adsorbed at the interface in (b). This could be due to the bubble in Figure 6.4 (c) being in the process of

expanding at the point of the sample being frozen which would increase the separation of the particles. In contrast the bubble in Figure 6.4 (b) might have been static or contracting, which would result in the observed closer packing of the particles as the area of the interface decreased. The cracks in the surface of the fractured region in Figure 6.4 (c) and (d) are artefacts of the SEM imaging process and are caused by degradation of the sample by the electron beam. The blue dashed box in Figure 6.4 (c) indicates a region at the bubble interface examined more closely in Figure 6.4 (d).

Figure 6.4 (d) shows that as with the Guinness foam the submicron particles within the Kronenbourg foam are globular and have a tendency to agglomerate. The agglomerates display a tendency to accumulate at the interface rather than being dispersed evenly in the liquid making up the bulk of the sample. The particles are around 100 - 250 nm in diameter though better evaluation of the particle sizes is again difficult due to the limited SEM image resolution possible in examining the Kronenbourg foam. The green arrows indicate larger particles which were sporadically observable in the SEM images of the Kronenbourg samples. These larger particles were again difficult to accurately measure, but had sizes approximately 300 – 600 nm across.

6.2.5 Alkali hay extracts – non etched

SEM images captured by examination of frozen/fractured hay extract foams are shown in Figure 6.5.

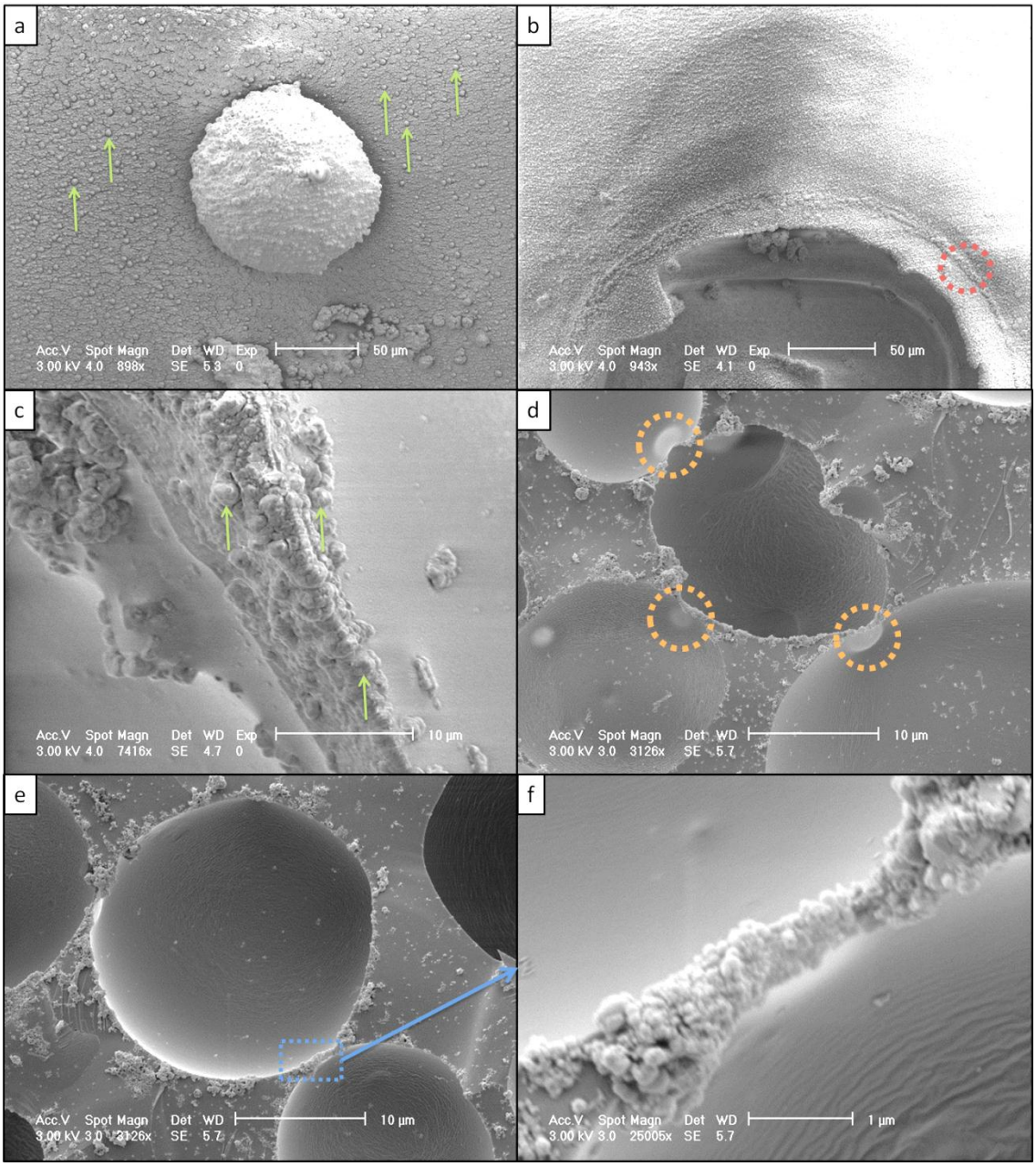

Figure 6.5. Cryo SEM images showing features observed in the microstructure of foam made using alkali hay extract solution prepared by extracting with 3.75 molL^{-1} NaOH at ambient temperature (~20 °C) for 30 minutes. a) 898x; b) 943x; c) 7416x; d) 3126x; e) 3126x and f) 25005x magnification.

Figure 6.5 (a) shows a hay extract foam bubble approximately 100 µm across coated with particles giving a textured appearance to the bubbles surface. The green arrows indicate some of the larger particles adsorbed on the bubble surface having diameters of approximately 5 µm. It is suspected that these particles may be agglomerates of smaller particles.

Figure 6.5 (b) shows another hay extract foam bubble, which fractured during freezing of the sample (some of the fractured bubble film is visible in the lower-centre part of the image). The surface of the bubble again appears textured due to particle adsorption. The red dashed circle indicates a 'halo' of particles around the base of the bubble. Figure 6.5 (c) shows a Plateau border between two adjacent bubbles and an accumulation of particles within the Plateau border. The green arrows indicate larger particles which again may be agglomerates of smaller particles.

Figure 6.5 (d) shows a bubble which has formed by the rupture of the film between two adjacent bubbles leading to the non-spherical shape of the bubble cavity in the centre of the image. The orange dashed circles indicate regions where bubbles sat adjacent to each other and particles can be observed within the Plateau borders between these bubbles. The orange dashed circles also indicate where bubbles of different sizes have bulged into their neighbours. The internal surface of the centre bubble is rippled rather than smooth.

Figure 6.5 (e) shows a bubble which is ~22 μm in diameter having two nearest neighbours with which it shares liquid films. Particles are observable adsorbed around the rim of the central bubble indicating adsorption at the interface of the bubble. Particles are again observed accumulated in the Plateau borders between adjacent bubbles and the Plateau border indicated by the blue dashed box is more closely looked at in Figure 6.5 (f).

Figure 6.5 (f) more clearly shows the particles within a Plateau border and allows a better indication of the size of the globular sub-micron particles. The average particle size measured from a sample of 20 particles is 171 nm with a standard deviation of 72 nm. Yet again the bubble interface in the lower right of the image is not smooth but has rippling/waviness to it.

6.2.6 Alkali hay extracts – etched

Etching of the foam samples by sublimation of the water within the sample was performed on some of the hay extract foam samples prior to platinum coating and SEM examination. Etching exposed the arrangement of particles in the extract foam and gave more insight into the internal microstructure of the foam without the particles being obscured by the water present in the sample as is the case in the other foam SEM images. This is why etching the hay foam gave SEM images (as shown in Figure 6.6) which had a very different appearance to those obtained without etching the foam.

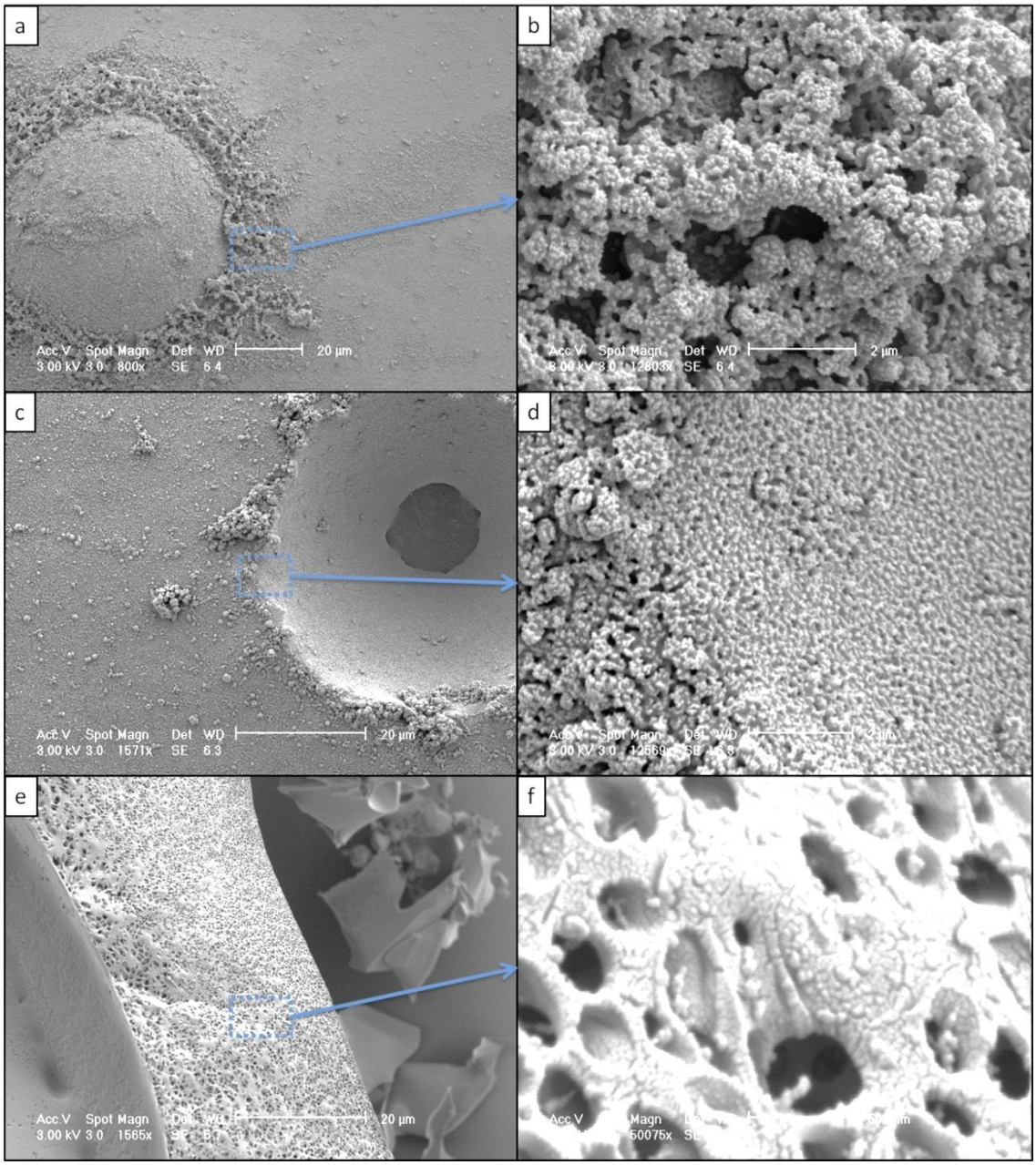

Figure 6.6. Cryo SEM images showing features observed in the microstructure of etched hay extract solution foam solution prepared by extracting with 3.75 molL^{-1} NaOH at ambient temperature (~20 °C) for 30 minutes. a) 800x; b) 12803x; c) 1571x; d) 12569x; e) 1565x and f) 50075x magnification.

Figure 6.6 (a) shows a whole bubble with a 'halo' of particles around the base of the bubble even more obvious than the particle halos seen previously. The blue dashed box indicates an approximate area in the particle halo for closer examination. Figure 6.6 (b) shows the agglomerated network of particles in the halo surrounding the bubble which was exposed when the water was removed by etching.

Figure 6.6 (c) shows a bubble in the fracture region of the foam sample where the bubble has effectively been cleaved horizontally exposing an internal view of the lower hemisphere of the bubble. Particles can be seen adsorbed at the bubble interface and these are visible in the region around the bubble rim. The particles adsorbed at the interface are of varying size due to agglomeration of smaller particles.

Figure 6.6 (d) shows a closer look at the particles at the bubble rim and those adsorbed on internal surface of the hay extract bubble. The larger particles adsorbed at the edge of the bubble can be more clearly seen as agglomerates of smaller particles in this image. The interface itself has a roughened appearance. The surface appears rough because etching has exposed the adsorbed particles and it can be seen that an extensive network of agglomerated particles is present across the whole bubble interface. Figure 6.6 (e) shows the liquid film between two adjacent bubbles and the effect of etching on the sample has been to generate holes/channels in the liquid film.

Figure 6.6 (f) looks more closely at the film between the bubbles and the holes/channels formed by etching the sample. A network of agglomerated particles is observable and the holes/channels in the liquid film can be seen to have formed within the film where the water has been removed leaving only the network of particles. The approximate average particle size measured from a sample of 20 particles is 67 nm with a standard deviation of ~10 nm. The smaller measured particle size in the etched foam image indicates that individual particles are more easily resolvable (though some difficulty remains in discerning the exact particle outlines as before hence particles could still be agglomerates).

6.2.7 AFM of dried hay foam

Use of high energy electrons during SEM imaging gives increased magnification in images which would have allowed imaging of the microstructure of agglomerated particles. The

image resolution possible using cryo SEM for examination of foams was limited by the fragility of the samples. It was found that using high electrons led to electrostatic charging of samples which resulted in images blurring due to movement of the samples. Higher energy electron beams also lead to rapid sample degradation which meant the samples would have been destroyed before useful images were captured. Evidence of sample degradation is still seen in some images as cracks in the samples.

AFM was identified as a technique which might allow closer examination of the particles in the alkali hay extract foam, as it does not result in sample degradation during imaging. A limitation in the application of AFM to the examination of alkali hay extract foam particles was that it could only be performed on dried samples of the foam rather than in its native form or as a frozen sample due to limitations on the equipment available. Some of the AFM images of dried alkali hay extract foam are reproduced in Figure 6.7 and Figure 6.8.

AFM image notes: 'Δz' denotes the peak-valley height, *i.e*. the maximum height difference across the image; 'rms' denotes the root mean square height which is a measure of the surface roughness in the area examined; FWHM = full width half maximum which measures the width of the scan profile at half the maximum height for the scan profile; the AFM image scan width = 5x the scale bar shown.

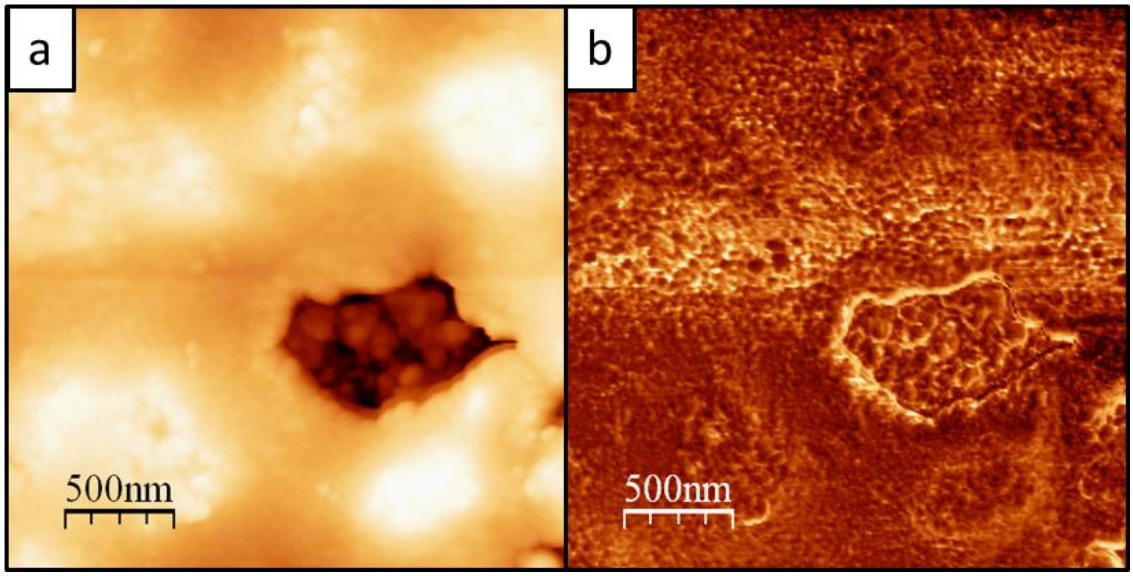

Figure 6.7. AFM of dried hay extract foam (solution prepared by extracting with 3.75molL^{-1} NaOH at ambient temperature (~20 °C) for 30 minutes). Δz ~359 nm, rms ~62 nm. (a) topography map (b) the phase map for an area of the sample.

Figure 6.7 shows a 'crater' observed in the otherwise relative level looking surface of the sample. The presence of the crater is the reason for the relatively high Δz value which occurred as the probe stepped down into the crater. Figure 6.7 (a) shows the sample topography which gives an impression of the overall shape/texture of the surface, the crater and the particles in it. It can be seen that the surface is fairly level with the dark region represented by the crater being at a lower height than the rest of the surface in the image.

Figure 6.7 (b) shows the phase image which gives an indication of the outline of the particles at the surface of the sample and those within the crater. (The phase image is generated using the change in the force constant of the free cantilever vs. that of the cantilever interacting with the surface). Particles can be seen clustered close together as well as the outline of particles on the sample surface outside the crater also being discernible. The particles have a round outline and combined with the topography observation in Figure 6.7 (a) suggests the particles are globular in shape. The area within the crater was examined more closely using the AFM to give a better indication of the topography of the particles and

allow particle size measurements. Some representative images and scan profiles used for particle size measurements are given in Figure 6.8.

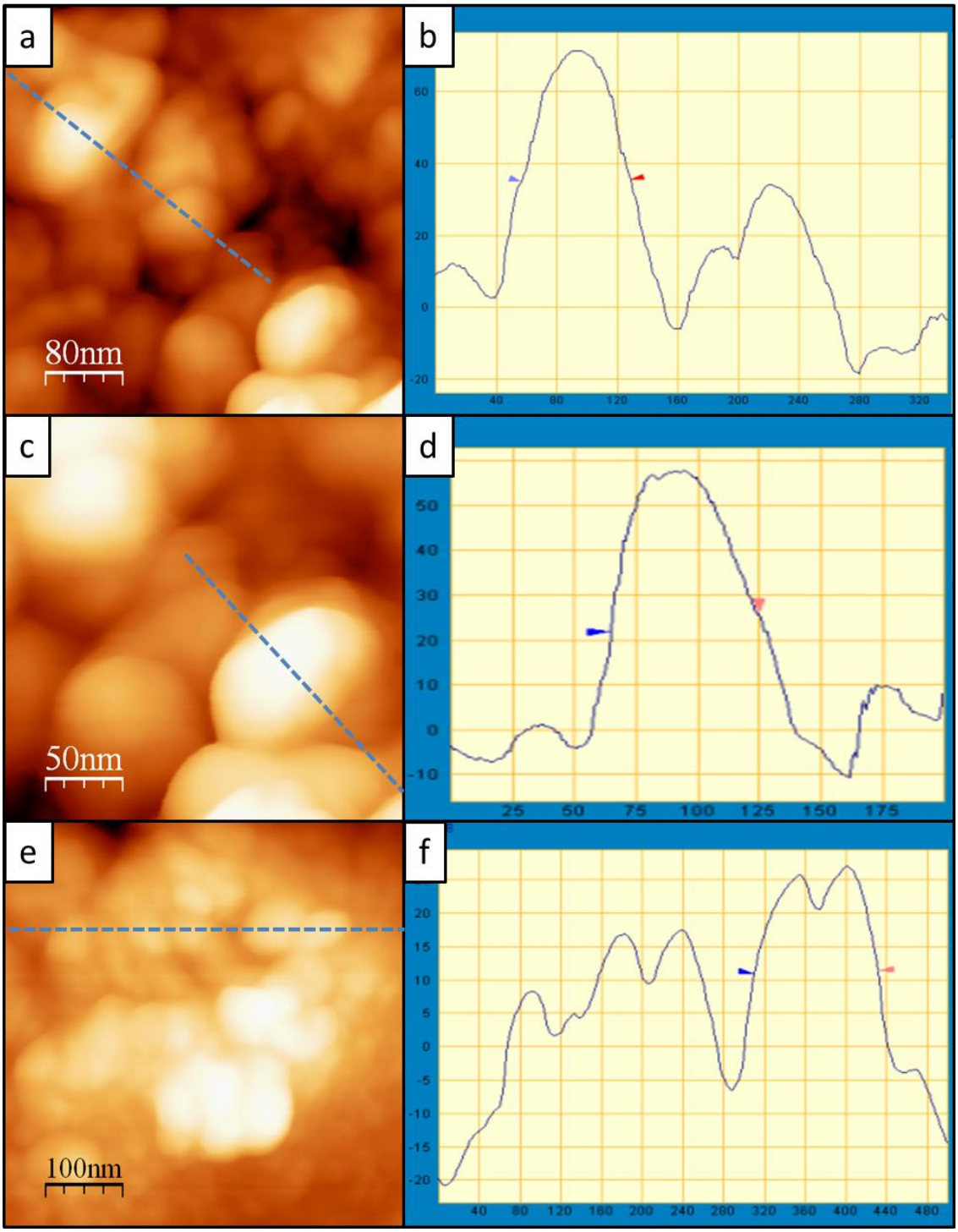

Figure 6.8. AFM scans of dried, alkali hay extract foam on mica slides. The solution was prepared by extracting hay with 3.75 molL^{-1} NaOH at ambient temperature (~20 °C) for 30 minutes. (a), (c) and (e) show the topography and (b), (d) and (f) show the profiles generated for cross sections along the line indicated by the blue dashes in the corresponding topography images. (a) Δz ~123 nm, rms ~27 nm; (b) measurement of an individual particle ~60 nm FWHM; (c) Δz ~140 nm, rms ~26 nm; (d) measurement of an individual particle ~72 nm FWHM; (e) Δz ~125 nm, rms ~21 nm; (f) measurement two agglomerated particles ~122 nm FWHM.

Figure 6.8 shows a more detailed examination of the particles in the crater identified in Figure 6.7. Within the crater the peak valley height is lower for all areas examined (~123 - 140 nm) and the surface roughness is lower also (~21 – 27 nm) than the image in Figure 6.7. The lower peak valley height and surface roughness indicates the flatter, smoother region within the crater compared to the step down into the crater from the elevated, rough surface surrounding it. Images (a), (c) and (e) demonstrate how the AFM allowed examination of the particles in the dried foam at resolutions beyond that possible with cryo SEM. Many globular particles can be observed in the topography images in (a), (c) and (e) with the probe being used to scan profiles of the surfaces in each image as indicated by the blue dashed lines. The respective profiles generated for the sample surface in images (a), (c) and (e) are shown in (b), (d) and (f). The particles which were measured are indicated in each of the profiles given in (b), (d) and (f), between the blue and red arrow heads. In images (b) and (d) consistency of the particle sizes is shown with the particles having sizes ~60 nm and ~73 nm FWHM respectively. An interesting feature on the right hand side of profile (b) is the double peak due to two agglomerated particles, which can also be seen around the centre of the blue dashed line showing where the profile was measured in (a). The two agglomerated particles each appear to have similar sizes to the measured particle in (b).

Image (f) shows further evidence of particle agglomeration in the profile and the measured distance indicated between the arrow heads corresponds to 122 nm for the two approximately equally sized particles. This gives the particles an average approximate size of ~61 nm across which would give these particles a size consistent with the individual particles measured in (b) and (d).

More agglomerated particles are observable in the same cross section to the left of the measured region in profile (f). Though these other particles/agglomerates are not measured, they appear to have particle sizes similar to the previously measured individual/agglomerated particles in (b) and (d). The agglomerates identified in the images presented are typical of those seen throughout the AFM images generated, with agglomerates being made up of particle with sizes typically in the range ~55 – 75 nm.

6.2.8 Alkali horse chestnut leaf extracts

NaOH extraction of dried and milled horse chestnut leaves generated foaming solution which was shaken in a sealed bottle to generate foam for cryo SEM examination. A selection of the images capture is shown in Figure 6.9.

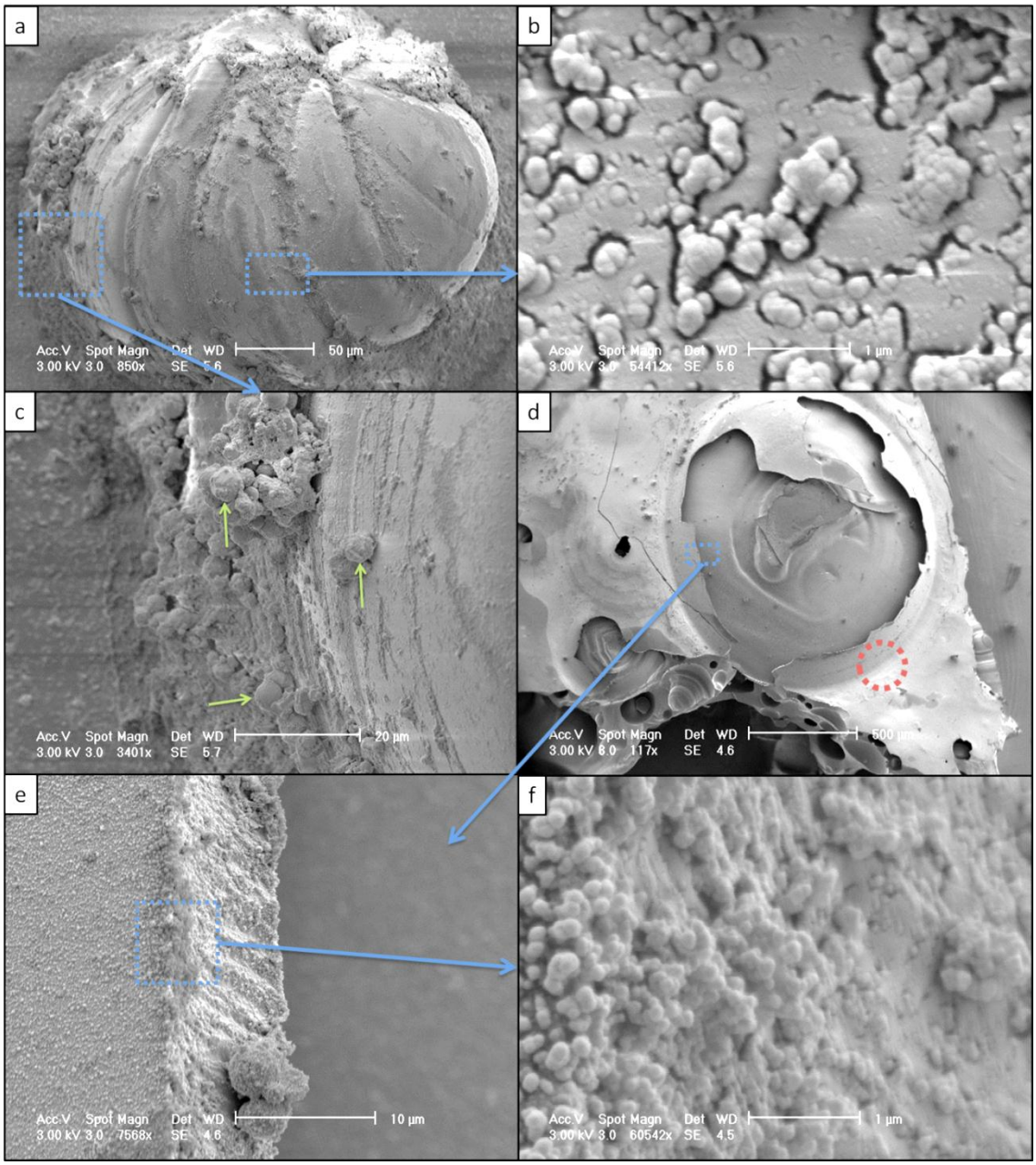

Figure 6.9. Cryo SEM images of horse chestnut leaf extract foam (solution prepared by extracting with 3.75 molL^{-1} NaOH at ambient temperature (~20 °C) for 30 minutes). (a) 850x; (b) 54412x; (c) 3401x; (d) 117x; (e) 7568x and (f) 60542x magnification.

Figure 6.9 (a) shows a particle stabilised bubble of diameter approximately 300 - 330 µm across. The surface of the bubble has a textured appearance due to particles of varying size being adsorbed across the entire interface. The blue dashed boxes indicate areas more closely examined in Figure 6.9 (b) and (c).

Figure 6.9 (b) shows the particles adsorbed at the bubble interface are globular and approximately 197 nm across (averaged over 20 particles with standard deviation of 31 nm).

Irregularly shaped particle agglomerates of smaller particles can be seen as well as individually identifiable particles. The liquid phase is visible between the particles/agglomerates adsorbed at the bubble interface. Many of the visible particles are submerged to different depths in the liquid region between the agglomerates/particles adsorbed at the bubble top surface.

Figure 6.9 (c) shows an increased magnification image of larger, almost spherical particles (indicated by the green arrows) attached to the outside of the bubble in (a). Accurate measurement of size for these larger particles is made difficult as the perspective means the bubble surface is sloping away hence the particles are potentially at different relative distances. With this difficulty in mind however, it was found that the particles have approximate sizes of 1.8 – 4.9 µm. These larger particles have a rougher appearance than the smaller particles indicating that they might be agglomerates of smaller particles.

Figure 6.9 (d) shows an entire bubble approximately 1.3 mm in diameter which has been frozen and fractured. The red dashed circle indicates a halo of particles at the base of the bubble. Though the bubble film fractured during freezing, a portion of the film remains intact and was examined more closely in the area indicated by the blue dashed box (see Figure 6.9 (e)).

Figure 6.9 (e) shows adsorption of particles on both the interior (right hand edge of the film in the image) and exterior (left hand edge of the film) surfaces of the bubble liquid film as well as particles dispersed within the continuous liquid phase sandwiched between the layers of adsorbed particles. The adsorbed particles again give the surface of the fractured film and liquid phase within the film, a textured appearance similar to images Figure 6.9 (a) and (b).

Figure 6.9 (f) shows higher magnification examination of the fractured bubble film allowing regions in the continuous liquid phase to be observed which are smoother than at the surface of the bubble similar to image (b). Particles are observable both at the surface of the fractured film and submerged to different depths within the film.

6.2.9 Alkali rice straw extracts

NaOH extraction of dried and milled rice straw generated foaming solution which was shaken in a sealed bottle to generate foam for cryo SEM examination. A selection of the images captured can be seen in Figure 6.10.

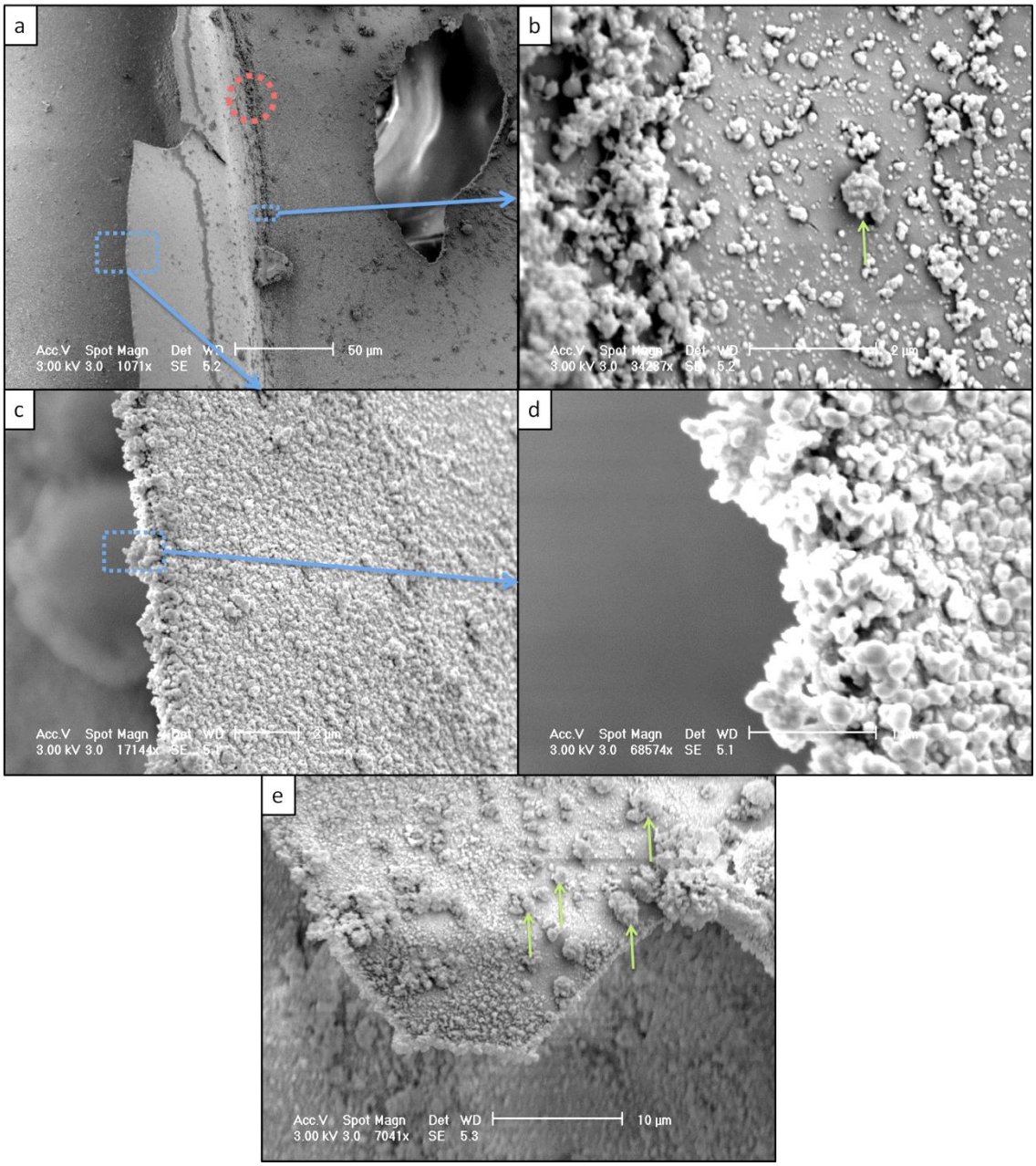

Figure 6.10. Cryo SEM images showing globular submicron particles in liquid films made using rice straw extracts (solution prepared by extracting with 3.75 molL^{-1} NaOH at ambient temperature (~20 °C) for 30 minutes). (a) 1071x; (b) 68574x; (c) 17144; (d) 68574x and (e) 7041x magnification.

Figure 6.10 (a) shows a bubble having dimensions approximately 1.1 x 1.3 mm in alkali rice straw extract foam. A halo of particles at the base the fractured bubble can be seen in the red dashed circle in the centre of the image. The blue dashed boxes indicate a region of the halo more closely examined in (b) and the edge of the fractured bubble film examined in (c).

Figure 6.10 (b) looks more closely at the particles in the halo around the base of the bubble. Similar to the particle halos observed in the SEM images of hay extract (Figure 6.5) and horse

chestnut leaf extract (Figure 6.9) foams there are individual and agglomerated particles visible as well as particles submerged in the liquid film to varying depths. The network of agglomerated particles in the halo seen in the left hand side of Figure 6.10 (b) appears similar to the image of the bubble halo in the etched hay foam sample in Figure 6.6 (d). Agglomerates are extensively observable in Figure 6.10 (b), with an almost spherical particle, which is clearly an agglomerate of smaller particles indicated by the green arrow. Particles submerged to different depths within the liquid film are also visible.

Figure 6.10 (c) shows the fractured bubble film with particles extensively adsorbed at the interface. The liquid film in this image appears to be thinner than the horse chestnut leaf extract bubble film seen in Figure 6.9 (e). The rice straw bubble film might be thinner due to the bubble being closer to rupture as a result of film drainage and thinning or it is possible that the horse chestnut leaf extract can sustain thicker bubble films than rice straw extract solution. Examination of other SEM images of rice straw extract bubbles does suggest that the liquid films are thinner for rice straw extract bubbles than horse chestnut leaf extracts in general. The blue dashed box indicates the region more closely examined in (d).

Figure 6.10 (d) shows that the particles adsorbed at the rice straw extract bubble interface have a similar size and shape to those observed in and around the particle halo at the base of the bubble suggesting that the particles at the interface and in the halo are the same type of particles. The liquid film in Figure 6.10 (d) is sloping away from the viewing position hence particle size measurement using this image is difficult though particles are present which have sizes typical of the particles seen in the other images (approximately 150 – 250 nm). The globular particles exhibit the same tendency to agglomerate as seen in the other foams.

Figure 6.10 (e) shows another region in the frozen rice straw extract foam where the bubble liquid film has fractured. Larger agglomerated particles, having approximate sizes

0.8 - 1.5 µm are visible adsorbed at the bubble interface (some indicated by green arrows), similar to those seen in the hay and horse chestnut leaf extract foams.

6.3 Discussion of the SEM images of the foams

Observations have been made of the cryo SEM images across the various foams examined in this chapter. This section will discuss the observations made of when examining the cryo SEM images of foams already presented. An attempt will be made to identify similarities and differences observed in the various foam microstructures

6.3.1 Linear alkylbenzene sulphonate foam

No particles were observed in the LAS foam SEM images, which is unsurprising as it was a pure solution of dissolved surfactant used to generate the foam that was examined. LAS generates foam *via* a well understood mechanism of surfactancy leading to surface tension reduction which leads to stable bubbles forming though the Marangoni effect (see Appendix section 9.1.3 for discussion of the Marangoni effect). The images of LAS foam show a very simple microstructure with nothing particularly interesting being observed which is very different to the images of the foams from the other sources presented subsequently.

6.3.2 Gelatin foam

The gelatin foam examined using cryo SEM was from a 'pure' protein solution which contained no other materials that would have caused foaming; leaving no doubt that it was protein foam being examined. The images of the gelatin foam showed faint particles in the liquid film and adsorbed at the bubble interfaces in Figure 6.2 (b). Observing proteins assembled into sub-micron particles was unexpected and very interesting. The appearance of particles covering the gelatin bubble interface contrasts with the relative lack of particles observed in the surface of the fractured region in the sample which represents the liquid film between adjacent bubbles. Preferential adsorption of particles at the bubble interface

suggests the proteins are acting as particles imparting Pickering stabilisation on the bubble (background on Pickering stabilisation is available in Appendix section 9.1.6).

Protein adsorption at the interface is described by Wierenga and Gruppen (2010) as possibly being due to the proteins acting as colloidal particles (as in Pickering stabilisation) or as random coils which rearrange their structure as they adsorb at the interface (discussed in section 2.5.2). Adsorption of proteins acting as particles or as random coils could both potentially explain the 'particles' observed in the cryo SEM images of the protein foam (Figure 6.2). If the adsorbing proteins are behaving as straightforward particles then the particles observed at the interface would be those with appropriate net charge, hydrophobicity and size. As gelatin is made by rendering animal parts it would be expected that the proteins in the gelatin solution would have varied properties hence adsorption of some protein particles with the correct properties at the interface. The 'free' particles in fracture region of the liquid film might simply have not migrated to the interface but have been in the process of migrating to the interface at the point of freezing the foam.

If the varied proteins in the aqueous gelatin solution were acting as random coils then when they adsorb at the interface, they denature which offers the potential for the proteins to coagulate. Such coagulation of many random coil proteins could lead to the formation of particles which could then be observed in the cryo SEM images. The appearance of particles in the gelatin foam was unexpected and interesting as was the non-smooth appearance of the interface in the gelatin foam was similar to rippling of the alkali plant extract bubble interfaces.

The protein solution foam differed in appearance to the other foams examined as the gelatin foam SEM images did not show the same obvious and extensive coverage of particles at the interface. Larger agglomerated particles as seen in the plant extract foams were also not

observed in the gelatin foam. Lack of large particles seen in the gelatin foam might be because the purely proteinaceous solution prohibits protein coagulation into larger particles, such as those seen in the plant extract foams which are potentially composed of a mixture of materials.

6.3.3 The presence of particles at the interface

Globular submicron particles indicating Pickering stabilisation were consistently observed adsorbed at bubble interfaces upon SEM examination of brewed foams (Figure 6.3 and Figure 6.4) and hay, horse chestnut leaf and rice straw extract foams (Figure 6.5, Figure 6.9 and Figure 6.10 respectively). Globular particles were also observed at the interface in gelatin foam (Figure 6.2 (b)) and though the interface was not perfectly smooth, the roughness indicating particles extensively covering the interface as for the bubbles from other sources was not observed in gelatin foam. The particles at the gelatin bubble interface appeared to be consistently submerged to greater depth than particles in the plant extract and brewed foams. If the particles in the gelatin foam were more hydrophilic than those in the plant/brewed foams this would explain why they are consistently more deeply submerged in the liquid within the bubble film. Joining together of the meniscus of liquid around these submerged protein particles at the interface might explain the uneven appearance of the interface in Figure 6.2 (b).

Bubbles are energetically unstable therefore foams tend collapse. Gas diffusion out of bubbles causes smaller bubbles to shrink as gas moves into larger bubbles which ultimately rupture. Particles adsorbed at bubble interfaces have high energy of detachment (Binks, 2002) hence remain adsorbed as bubble sizes reduce due to gas diffusion out of the bubbles. Due to the high energy of detachment of particles at the interface, as bubbles shrink the interface must deform in order to maintain enough surface area to accommodate the

attached particles resulting in rippling/wrinkling of the interface. Such deformation of the interface in hay extract foam would explain the observed non-smooth texture of the interface in Figure 6.5 (f) which was also observed in bubbles from the other sources.

Pickering stabilised bubbles, having gas-liquid interface covered in particles have been described as 'armoured' in the literature by Subramaniam *et al.* (2006). The current research differs from theirs and other studies on particle stabilised foams found in the literature as the adsorbed particles were not manufactured then introduced into the solution to stabilise bubbles. The stabilising particles in the current research were spontaneously generated during NaOH extraction of plant materials (or during the brewing process for the stout/lager) subsequently adsorbing onto the gas-liquid interfaces. Drawing conclusions as to the nature of the spontaneously generated particles/foams is therefore more difficult than if they were 'model' particles with well characterised hydrophobicities and size distributions. Research in the literature does assist in understanding the properties of the particles adsorbed at the interfaces in the foams examined in this chapter. The particles adsorbed at the interface will have contact angles with water > 90° making them somewhat hydrophobic. Hydrophobicity of these particles increases the probability of finding the particles adsorbed on top of the liquid interface, which increases the interaction between the particle and the air in the bubble and reduces the interaction with the water in the liquid film (Binks, 2002).

The plant materials used to generate the foaming solutions in this research have similarities in their compositions, each containing varying amounts of polysaccharides, lignin and proteins. In this sense the plants used in the NaOH extractions are compositionally similar to the grains used in brewing the stout/lager. The brewed foams potentially contain less polyphenols (similar to lignin in the plant extract foams) as these are removed during the

brewing process due to them being detrimental to the quality/palatability of the end product.

Similarities in composition of the plant raw materials used in making the foaming solutions examined here, contribute to stable foam formation of the solutions and similarities in the observed foam microstructures. Biopolymer nanoparticles/micro-particles can be formed by proteins and polysaccharides and such particles have been researched by Jones and McClements (2011). Their paper describes formation of protein-polysaccharide particles from well characterised raw materials under controlled conditions. The current research differs from theirs in that particles are formed spontaneously during extractions of plant materials and hence the composition of these particles is not known. The presence of particles in the foaming solutions examined in this chapter might be a result of biopolymer particle formation. Biopolymer particles might come from proteins in the brewed solutions/leaf extracts or lignin in the hay/rice straw extracts forming complexes with extracted polysaccharides hence the relevance to the work of Jones and McClement.

An obvious difference between the plant extract and brewed solutions is the pH of the solutions with the plant extract solution being generated and subsequently examined by SEM as alkaline solutions. The pH of the plant extract solution was not found to significantly affect the ability of the solutions to generate foam however; as the solutions continued to generate foam when their pH was adjusted to pH 5.5 (see section 6.4 for more details). The composition of the plant raw materials and the subsequent solutions generated from them, imparts foamability on the solutions which is unaffected by pH, hence comparison between the brewed foams and plant extract foams is sound despite their pH difference.

6.3.4 The particle sizes observed in the foams

The size of particles observed in the various foams was difficult to measure due to limitations on the resolution possible in capturing the SEM images, as well as problems due to surfaces in the images sloping away from the viewer's perspective. Particle size measurement in the plant extract solutions were attempted unsuccessfully using laser diffraction and photon correlation spectroscopy/electrophoretic light scattering. Therefore particle size measurement using the SEM images was the best available method during the current research. Research indicating the likely size of the particles which might be observed in alkali plant extract solutions was not found after extensive examination of the literature. The approximate sizes measured for the particles in the various foams are summarised in Table 6.1.

Table 6.1. Approximate particle sizes observed during SEM examination of various foams. The observed particles have been classified as large particles (> 1 µm or where the particles are obviously agglomerates in the SEM images) and small particles (< 1 µm) according to SEM observation of the particles.

Foam source	Observed approximate particle sizes (± values indicate the standard deviation for the measurement)	
Hay extract (non-etched)	Large particles	~5 µm
	Small particles	171 nm ± 72 nm*
Horse chestnut leaf extract	Large particles	1.8 µm – 4.9 µm
	Small particles	197 nm ± 31 nm
Rice straw extract	Large particles	0.8 µm – 1.5 µm
	Small particles	150 nm – 250 nm
Guinness	Large particles	0.55 µm – 1.8 µm
	Small particles	160 nm ± 40 nm
Kronenbourg	Large particles	300 nm – 600 nm
	Small particles	100 nm – 250 nm

*Particle size was 67 nm ± 10 nm in the etched hay foam SEM images and 55 nm - 75 nm by AFM examination of dried hay extract foam.

6.3.4.1 Plant extract foams

Large particles were observed in the SEM images of plant extract foams and are defined as particles with size > 1 µm or where the particles are obviously agglomerates, such as those indicated by green arrows in Figure 6.5 (a) and (c), Figure 6.9 (c) and Figure 6.10 (b). Small

particles were also observed and are defined as particles which were not discernible as agglomerates in the highest magnification images available, or those having size < 1 µm. Particles between the two sizes specified as 'large' or 'small' were observed though clearly identifying them as individual particles or agglomerates was difficult.

The larger particles seen in the hay (Figure 6.5 (a) and (c)) and horse chestnut leaf (Figure 6.9(c)) extract foams were up to approximately 5 µm diameter. Larger particles were also observed in rice straw extract foam (Figure 6.10 (b)) however these particles were only 0.8 - 1.5 µm diameter. Larger particles generally appeared rougher and more spherical than the smaller particles in the respective foams suggesting that they were agglomerates of smaller particles. It is plausible to consider that larger particles take longer to form during alkali plant extraction, or that they form by agglomeration of smaller particles. The hydrophobicity of the particles means that they are likely to aggregate in the aqueous phase which can slow or impede their ability to adsorb rapidly at an interface according to Murray and Ettelaie (2004). Gradual build-up of smaller particles into larger more spherical particles explains the irregular shape of the non-spherical larger particles. This common origin means the larger and smaller particles would be expected to have broadly similar compositions hence similar hydrophobicity and net charge in solution, which affects their affinity to the interface and their ability to stabilise foams.

6.3.4.2 Brewed foams

The Guinness foam showed large spherical particles completely submerged within the observed bubble liquid films (Figure 6.3 (a) and (b)). The larger particles being completely submerged in the liquid film is unlike any of the observed large particles in the plant extract foams. The large particles within the Guinness liquid films appear smaller (0.55 – 1.8 µm)

and smoother with few small particles attached to their surfaces than large particles observed in the plant extract foams.

Small particles are observed in the Guinness foam adsorbed at the gas-liquid interface. The smoothness of the large particles within the Guinness liquid film suggests that these large particles are not necessarily agglomerates of the smaller particles. The large smooth Guinness foam particles might be formed during the brewing process as discrete particles with different compositions to the smaller particles. The particles completely submerged within the liquid film will be hydrophilic and have contact angles < 90°; with those smaller particles adsorbed at the gas-liquid interface being more hydrophobic, having contact angles > 90° (Binks, 2002). The brewing process takes longer and involves more steps than the alkali extraction performed on the hay, horse chestnut leaves and rice straw. The difference in generating brewed foaming solutions might mean larger, discrete, hydrophilic particles can be formed alongside smaller hydrophobic particles during brewing when it might not be possible during alkali extraction of plant materials.

The Kronenbourg foam did contain some larger particles (indicated by the green arrows in Figure 6.4 (d)) though overall in the Kronenbourg SEM images there appears to be fewer present than in the Guinness foam and the plant extract foams. The reduced number of the large particles compared to Guinness could be due to differences in the composition of the brewed solutions arising from differences in the brewing methods. The Kronenbourg foam contained many smaller particles as seen in the alkali plant extract foaming solutions. Overall the particles observed in the Kronenbourg foam exhibited similarity in appearance and tendency to agglomerate as those seen in the Guinness and alkali plant extract foams.

6.3.5 Cryo SEM vs AFM measurement of particle sizes in hay foam

Cryo SEM examination of frozen foams allowed inspection of their microstructure essentially in their native form. AFM images could only be used to examine the foam in a dried state meaning there is the potential that the structure and properties of the particles in the foam were altered. Though this potential weakness is acknowledged, AFM was still used to capture some interesting images and measurements, which gave potential insight into the particles in hay foam (see section 6.2.7).

AFM topography images in Figure 6.7 (a) and Figure 6.8 (a), (c) and (e); show particles with apparently similar globular shapes to the particles seen in the hay foam cryo SEM images in Figure 6.5 and Figure 6.6. The particle size (~67 nm) measured during cryo SEM examination of etched hay foam in Figure 6.6 (f) was similar to that measured by AFM (~55 - 75 nm) which implies that the drying process required for AFM imaging of the particles in the hay extract foam may not have been destructive. The particle sizes measured in the SEM images of foams which were not etched is much larger due to the inability to resolve finer detail in particles in the non-etched hay foam due to the presence of water.

Cryo AFM is described by Shao and Zhang (1996) and this technique might allow examination of frozen foam (*i.e*. foam in its native structure) to test the hypothesis that the particles seen in cryo SEM of etched hay foam are the same as those seen by AFM of dried hay foam. Unfortunately cryo AFM was not available during the research for this thesis, though it does offer a potential opportunity for further into alkali plant extract foam research in the future.

6.3.6 Particle stabilised foams microstructure

The research of Limage *et al.* (2010) describes stabilisation of water-in-paraffin oil emulsions by surfactant and by silicon oxide particles. Water sublimation (etching) was used to capture images of the microstructure of the network of particles within the droplets as shown in Figure 6.11.

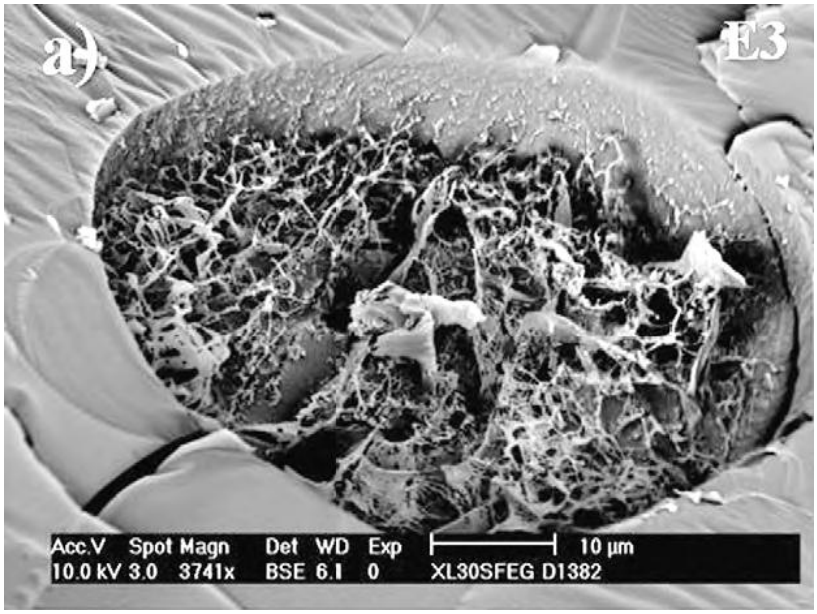

Figure 6.11. The internal microstructure of a particle stabilised emulsion droplet exposed by etching the sample before cryo SEM examination. (Reproduced from Limage *et al.*, 2010).

The appearance of the internal structure of the droplets (as seen in Figure 6.11) had similarity to the network of agglomerated particles observed in etched hay extract foam in Figure 6.6. This similarity confirms that etching offered insight into the microstructure of the hay extract foam, though at the time they were captured, the etched foam images were not understood and it appeared that the sample had been degraded. Had the publication of Limage *et al.* (2010) been found prior to the SEM image capture then etching would have been used more extensively than was the case during the current research.

Figure 6.6 (a) shows the halo around a hay extract foam bubble in the etched sample. The halo in this image looks rough/coarse due to the removal of water exposing the network of agglomerated particles adsorbed at the bubble base. Figure 6.6 (b) shows more clearly the

network of agglomerated particles at the base with channels visible where water has been removed. Figure 6.6 (c) shows the lower hemisphere of a fractured bubble and Figure 6.6 (d) takes a closer look at the internal surface of the bubble. The surface of the bubble looks rough due to a structured network of agglomerated particles adsorbed at the bubble interface. This image gives a clear view of the complete coverage of the bubble interface by particles and hence confirms the particle stabilisation of the bubble/foam by particles. This image demonstrates that the particles seen in the non-etched hay extract foam images extensively cover the entire surface of the bubble, hence are responsible (at least in part) for the stabilisation of the bubbles in the foam. The network of particles covering the bubble surface is obscured by the presence of water in the non-etched samples.

Figure 6.6 (e) and (f) show the liquid film between two bubbles in the etched alkali hay extract foam. In these images a network of agglomerated particles is visible within the liquid film between the bubbles. The extensive network of particles within the liquid film would increase the apparent viscosity of the liquid within the film which would decrease the rate of liquid drainage from the film. Slower film drainage would result in the film thickness reducing more slowly which would resist film rupture due to perturbation of the film (discussed in section 2.5.4) as well as shrinkage of the bubble due to gas diffusion out of the bubble.

Figure 6.9 (b) shows particles and agglomerates adsorbed at the gas-liquid interface of a bubble in (non-etched) alkali extracted horse chestnut leaf foam as well as submerged to varying degrees within the liquid film. The image of the fractured horse chestnut extract bubble in Figure 6.9 (e) and (f) shows the bubble as being covered in particles on the internal and external surface of the bubble and confirms the presence of particles dispersed throughout the liquid within the bubble film. The particles observed adsorbed at the

internal and external interfaces of horse chestnut leaf extract bubbles, and within the liquid film making up the bubbles indicates that a network of agglomerated particles was present in the liquid film as seen in the etched hay foam. This network of particles would stabilise the horse chestnut leaf extract bubbles by increasing the viscosity of the liquid within the film and by resisting bubble shrinkage. Saccharides dissolved during the alkali extractions of plant materials or brewing of the Guinness/Kronenbourg would also act to increase the viscosity of the solution within the bubble films hence would also have a stabilising effect on the foams.

It is reasonable to hypothesise that foam stabilisation by a network of agglomerated particles as seen in the hay and horse chestnut leaf extract foams would also stabilise the rice straw extract and possibly the brewed foams. Similarities in all of the images of the particle stabilised foams suggest that the microstructure responsible for foam stabilisation would be similar for all the foams. It is unfortunate that this was not explored further by applying etching to other frozen foam samples during their cryo SEM examination. Further use of etching to examine all of the foams discussed in this chapter would allow testing of the hypothesis of that foam stabilisation occurs due to networks of agglomerated particles adsorbed at the interface and within liquid films surrounding bubbles in all of the foams examined in the current research.

The networked arrangement of particles on and within the bubble films is similar to the structure of colloidal particles which stabilise emulsions discussed by Dickinson (2010) covering the research of Arditty *et al.* (2005) and Gautier *et al.* (2007). Dickinson describes a particle stabilising structure for oil-water emulsions where a disordered layer/network of particles adsorbs to the emulsion droplet interfaces, with the whole structure held together by attractive inter particle forces. Hunter *et al.* (2008) state in the conclusion to their review

on the role of particles as surfactants, that conclusive evidence of network formation by particles involved in stabilising emulsions/foams is difficult to obtain. The bubbles in Figure 6.6 (e)/(f) and Figure 6.9 (e)/(f) certainly appear to have similar emulsion/foam stabilising structures to those Dickinson describes and may contribute toward the conclusive evidence of network formation by particles in stabilising emulsions/foams sought after by Hunter *et al.*

6.3.7 Bubble halos

The halo of particles at the base of bubbles in the cryo SEM examined frozen foams is another consistently observed feature. A particle 'halo' is indicated by red dashed circles in Figure 6.3(a), Figure 6.4 (a), Figure 6.5 (b), Figure 6.9 (d) and Figure 6.10 (a). Though a line around the base of the bubble is indicated in the LAS foam SEM image in Figure 6.1 (a), closer examination of this region did not find particles present. The observed line is merely the boundary formed as the bubble protrudes from the liquid surface. A particle halo was also not observed at the base of gelatin bubbles.

The particle halos in the foam cryo SEM images appear to be composed of the same particles as those adsorbed at the bubble interface. Accumulation of these particles at the bubble bases would have occurred due to gas diffusion out of the bubble, leading to volume decrease and smaller interfacial area. Decreasing interfacial area would mean the adsorbed particles were forced closer together, ultimately accumulating at the bubble base as a halo. As no cryo SEM images of particle stabilised bubbles were found during literature searching, such halos have not been discovered in any other published research.

6.3.8 Plateau border clogging

The hay SEM images in Figure 6.5 (c), (d), (e) and (f) show particles accumulating within the Plateau borders between adjacent bubbles in hay extract foam. These particles would have

moved into Plateau borders as liquid flowed from the liquid films through the Plateau border. This clogging of the Plateau border by particles would then decrease the rate at which liquid could flow from the liquid films into the borders by increasing the apparent viscosity of the liquid in the Plateau border. This would lead to more stable foam as film thinning was retarded. Cryo SEM images of Plateau border clogging were only captured for hay extract foam and not the other particle stabilised foams examined during the current research. This does not mean that Plateau border clogging was absent in the other foams; it may simply be that it was missed during the capture of the cryo SEM images of the other foams or that lack of bubbles in close proximity within the frozen samples meant the effect was missed.

6.3.9 Bulging bubbles due to Laplace pressure differences

The Laplace pressure inside smaller bubbles is higher than in larger bubble which causes disproportionation of bubbles leading to foam coarsening and collapse of foams (see Appendix section 9.1.5 for further discussion of disproportionation). Differences in the Laplace pressure in bubbles means smaller bubbles adjacent to larger ones would bulge into the larger bubbles. Images showing this bulging of smaller bubbles into larger bubbles can be seen as the lighter regions within the orange dashed circles in Figure 6.5 (d). This image again provides a real-world example of theoretical foam microstructure.

6.4 Identification of the cause of foaming in plant extract solutions

Simple experiments were conducted to identify which materials were responsible for foaming in hay and horse chestnut leaf extract solutions. Early in the research it was hypothesised that foaming of the extract solutions might be caused by proteins extracted from plant materials during reaction with NaOH. Hay extract foam samples were analysed using the Bradford protein assay (Bradford, 1976), and elemental analysis (looking for

nitrogen) to detect proteins. Proteins were not detected during these analyses which led to the conclusion that the foaming of hay extract solution was not necessarily caused by proteins. It was considered possible that the level of protein in the extract solutions was too low to be detectable. Hence the hay extract solution was sparged then the foam dried to concentrate it before analysing for proteins, which were still not found. Lack of detection of proteins in the hay foam meant it was hypothesised that lignin-carbohydrate complexes might cause foaming. Hay extract foam and rice straw extract foam would both contain lignin derivatives according to research in the literature covering extraction of lignocellulosic materials (see section 2.4). As horse chestnut leaves do not contain lignin (see Table 2.1) it was hypothesised that the horse chestnut foam might be caused by proteins rather than lignin-carbohydrate complexes. Instead of analysing horse chestnut leaf extract foam for protein and the hay extract foam for lignin, simple experiments were performed to disrupt the foams and identify what was responsible for foaming of the solutions.

6.4.1 Is protein responsible for foaming in plant extract solutions?

Gelatin solution (450 ml) was prepared in 3.75 $molL^{-1}$ NaOH. 150 ml of this solution was sealed in a plastic sample bottle. The pH of the remaining 300 ml of the solution was reduced to pH 8.8 using HCl then 150 ml of this solution was sealed in a second sample bottle. A catalytic amount of protease was added to the final 150 ml of the gelatin solution to confirm the destruction of foaming ability in protein solutions by protease. The pH 13 solution was necessary as this is the same as the plant extract solution pH, which proved protein foaming occurred in high pH solutions. The pH 8.8 solution was needed as the protease might have denatured at pH 13 and not digested the protein in solution.

The three solutions were shaken to observe their foaming ability which is shown in Figure 6.12.

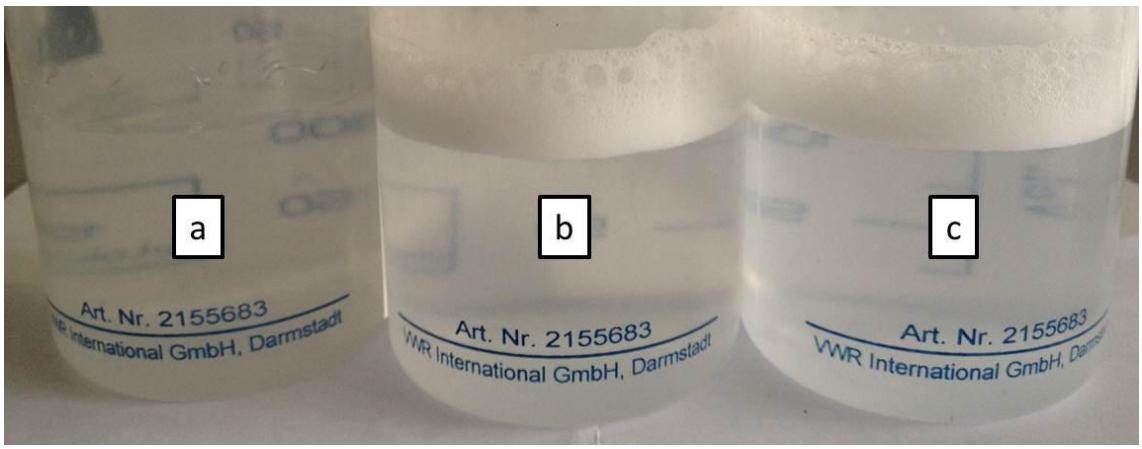

Figure 6.12. Gelatin solutions simultaneously shaken to attempt to produce foam. (a) pH 8.8 solution with protease added; (b) pH 8.8 solution with no protease added; (c) pH 13 gelatin solution.

Figure 6.12 (a) demonstrates that protease suppressed foaming in the pH 8.8 gelatin solution. (b) Demonstrates that foam was produced by the gelatin solution at pH 8.8 with no protease present and (c) shows that the gelatin solution generates foam at pH 13 without protease present. The solutions in Figure 6.12 prove that foaming in proteinaceous gelatin solution occurs at pH 13 and is still possible after reducing the pH to pH 8.8 using HCl. It also proves that protease addition to the pH 8.8 solution rapidly supresses foaming. The protease acts to breakdown the protein in solution which removes the ability of the solution to generate foam. It is this action of the protease which was used to see if protein was responsible for foaming in hay, horse chestnut leaf and rice straw extract foams.

Hay, rice straw and horse chestnut leaf extract solutions were prepared *via* the same extraction method as used throughout this thesis (see section 3.3.1) with the reaction conditions being 30 minutes extraction time, ambient temperature (~20 °C) and 3.75 $molL^{-1}$ NaOH. 450 ml of extract solution was prepared in total with 150 ml being retained in a sealed 250 ml sample bottle. HCl (1.18 specific gravity) was used to achieve pH 8.8 for the other 300 ml of extract solution and 150 ml of this sealed in another sample bottle. A catalytic amount of protease was added to the final 150 ml of the pH 8.8 extract solution which was sealed in a sample bottle also.

The extract solutions were shaken in the sealed sample bottles and the resulting foaming is shown for hay extract solution in Figure 6.13.

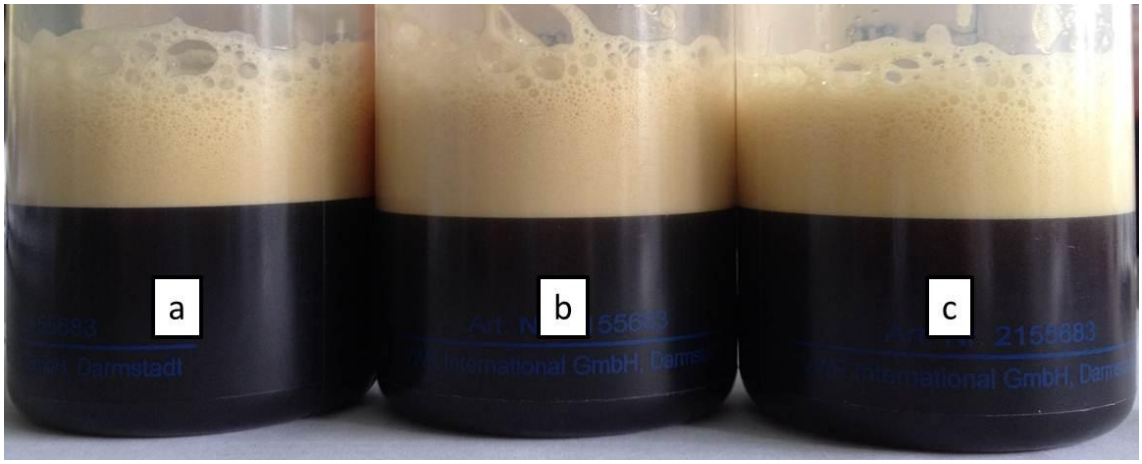

Figure 6.13. Hay extracts solutions simultaneously shaken to produce foam. (a) pH 8.8 solution with protease added; (b) pH 8.8 solution with no protease added; (c) pH 13 gelatin solution.

The hay extract solution foaming was not affected by protease addition (a) or by using HCl to achieve pH 8.8 for the solution (b), the foaming of the original extract solution is seen in (c). The effects of pH adjustment and protease addition were the same for rice straw extract solution. The continued ability of hay and rice straw extract solutions to produce foam indicated that it was not protein which was responsible for foaming in these solutions as predicted after finding that protein was not detected in concentrated hay extract foam.

The foaming of horse chestnut leaf solutions, however, was reduced after addition of protease as seen in Figure 6.14 solution (a).

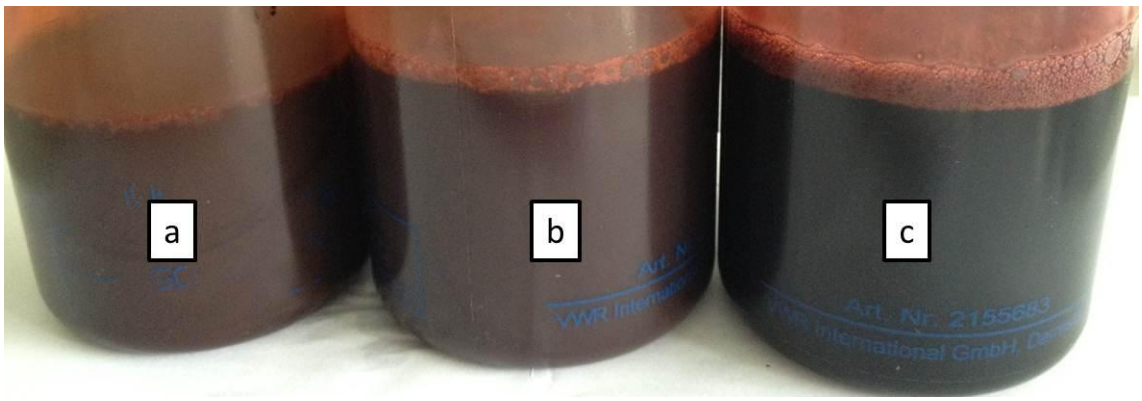

Figure 6.14. Horse chestnut leaf extract solutions shaken to produce foam. (a) pH 8.8 solution with protease added; (b) pH 8.8 solution with no protease added; (c) pH 13 gelatin solution.

Upon shaking the pH 8.8 and pH 13 solutions without protease present, foams were generated (as demonstrated in Figure 6.14 (b) and (c) respectively) though foaming occurred to a lesser extent than for the hay and rice straw solutions. It appeared that decreasing the pH had an effect of reducing the lifetime of the foam generated by horse chestnut leaf extracts which explains why the foaming in Figure 6.14 (b) is lower than (c). Protease addition to the solution gave a more pronounced effect of reducing the foaming of the solution than pH adjustment. The destruction of foaming ability by protease in horse chestnut leaf extract solution confirmed that protein was responsible for the foaming of the horse chestnut leaf extract solution. Fernández *et al.* (1999) extracted protein from leaves using high pH, finding that higher pH is better for extraction, but it is also assumed that high pH would result in the extracted proteins undergoing denaturation. Denaturation is not an issue in the current research, and may in fact be of benefit in generating sudsing or suds boosting materials for the research within this project. Such denaturation may also explain the appearance of proteins as particles at the interface as discussed previously (see section 6.3.2).

6.4.2 What is causing foaming in hay/rice straw extract solutions?

The hypothesis that lignin-carbohydrate complexes were responsible for causing the foaming in these solutions was tested after establishing that protein was not responsible for foaming of hay and rice straw extract solutions. Testing this hypothesis was achieved by removing the lignin from the hay extract solution using a method described by Xiao *et al.* (2001). Removing the lignin from the hay extracts solution involved adjusting the pH of 100 ml of the hay extract solution using 6 $molL^{-1}$ HCl to pH 5.5, with the resulting solution shown in Figure 6.15 (a).

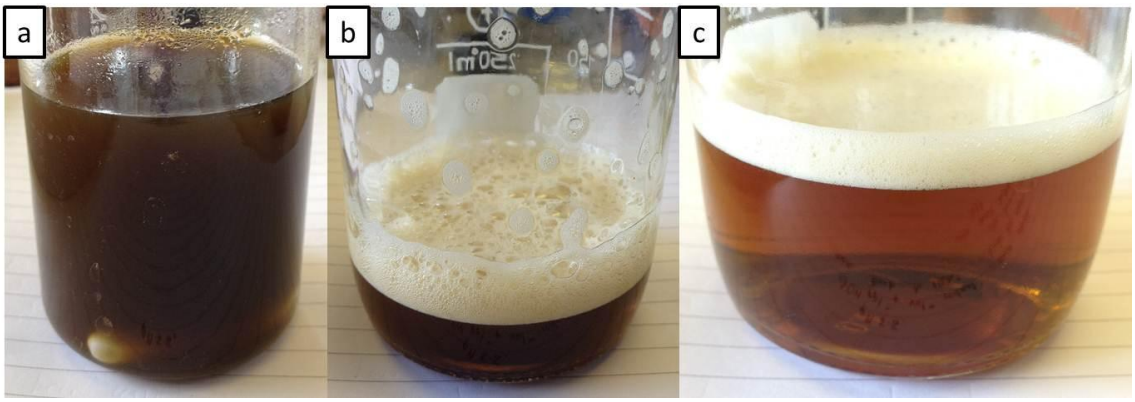

Figure 6.15. (a) Hay extract solution after adjusting to pH 5.5 and precipitating of the saccharides using ethanol; (b) after its volume was reduced, the same solution still generated foam upon shaking; (c) the solution still generated foam upon shaking after its volume was made back to 100 ml with deminaeralised water.

The volume of the pH 5.5 solution was then decreased to 100 ml using a rotary evaporator which left foaming of the solution upon shaking in a sealed unaffected. Ethanol (100 ml) was then added to the solution to precipitate the dissolved saccharides extracted from the original hay. The precipitated solids were filtered out of the solution using GF/C filter papers under vacuum. The filtrate volume was again decreased by removing the ethanol using a rotary evaporator and the solution is shown at this point in Figure 6.15 (b). The solution was then made back up to 100 ml using ultra-high purity water. At this point the solution was still brown, though less strongly coloured than the original extract solution and still produced foam when shaken in a sealed bottle. The solution at this point is shown in Figure 6.15 (c). The lignin was then precipitated by adjusting the solution to pH 1.5 using HCl. The precipitated lignin derivatives were filtered off using a GF/C filter paper and the volume of the solution was again reduced using rotary evaporation then made back up to 100 ml using demineralised water. The solution was now yellow in colour and gave no foam upon shaking in a sealed vessel.

The hay extract solution generated foam after neutralisation, continued to do so after removal of the saccharides in the solution and was suppressed only after lignin precipitation

and removal from the solution. The suppression of foam after lignin precipitation proves that the foaming in alkali hay extract solutions is due to lignin derivatives.

It is hypothesised that the rice straw extract solution foaming is also caused by lignin derivatives. The hypothesis that rice straw foaming is also due to lignin derivatives in solution comes from the fact that rice straw, as a grass, is compositionally similar to the hay (grass) used in the extractions. This means the rice straw when reacted with NaOH should generate foaming extract solutions *via* similar mechanisms. However due to time restrictions, the lignin removal was not repeated on the rice straw extract solutions. This is a potential area for further research in the future.

7 Chapter 7 – Examination of alkali plant extract foaming properties

7.1 Introduction

The research work presented in Chapter 4 demonstrated that reaction time, temperature and NaOH concentration have varying effects on the properties of alkali hay extract solutions. Chapter 5 extended the research by modelling effects of the reaction variables on alkali hay extract solution properties. The microstructures of alkali plant extract foams were examined using cryo SEM in Chapter 6, which found that particles are involved in the stabilisation of the extract foams. The components of the plant materials extracted into solution which generate foam were also identified (lignin derivatives extracted from hay and protein extracted from horse chestnut leaves).

Among the aims of the current research was to explore whether a correlation might be found between foamability of the extract solutions and other solution properties measured within the current research. Measurement of foaming of hay extract solutions has proven difficult and the data generated were noisy, including a lot of variability. Methods of foam measurement attempted included hand shaking the extract solutions, using a Teclis *Foamscan* as used by (Schmidt *et al.*, 2010) and using P&G proprietary tumbling tube equipment. Sparging and measuring foam height versus time, as in the Bikerman method Bikerman (1973b) was found to be the most promising method for measuring the foaming of alkali hay extract solutions (see section 3.7).

Sparging the extract solutions relies on the extract solutions having a higher capacity for generating stable foam at the base of the column with slower rate of collapse at the top of the column of foam. Experiments performed within the current research looked at the

initial rate of foam formation during sparge testing and differentiated extract solutions according to the volume of foam generated by the solution in time.

Though foamability testing using sparging was considered the best foam testing method available, it was cumbersome, requiring a lot of materials and time to test samples and generate data. A simpler measurement (or combination of measurements) of some other extract solution properties which could be used as a proxy for direct foamability measurement was desirable. Such a proxy measurement for foamability would allow understanding of the foaming capacity *potential* of alkali plant extract solutions more easily with less time and resources required for sample testing in future research.

The initial aim of the research in this chapter was to generate a model to describe the foaming of hay solutions by sparging, relating the reaction conditions used to generate the solution to its foamability. This attempt at modelling foamability of the hay extract solutions is presented in sections 7.2 - 7.2.8.

Section 7.3 looks for correlation between the foaming models constructed and the models of the responses Y_M, Y_A, Y_V, Y_S and Y_C generated in Chapter 5, to identify potential measurements of extract solution properties which might indicate which solutions will produce voluminous foams.

7.2 Modelling foaming ability of alkali extracted hay solution with reaction conditions

The hay batch used for the research presented in Chapter 5 was used for the first eight experiments in the foaming modelling research presented in this chapter (the data generated is referred to as 'data set 1'). A subsequent second round of eight experiments which took place later (generating foaming 'data set 2') used a second batch of hay, though

it was hypothesised that this would not impact the results and that foaming of hay extract solutions from one batch of hay would be similar to the next. Observations of variation in the foaming properties of the hay extracts produced from both batches are discussed in this chapter, by examining the foaming data sets and the models generated.

7.2.1 Experimental design

A factorial experimental design was chosen for the sparging experiments as it used 8 experiments to examine the effect of reaction time, temperature and NaOH concentration on the foamability of the alkali hay extract solutions. A 16 experiment response surface central composite experimental design could have been used as an alternative to the factorial design. However, using a response surface experimental design would have taken very much more time due to the large scale and hence large volumes of reactions solutions required for sparge testing. Due to time constraints and availability of materials, the 8 experiment factorial design was favoured. The reaction variables were reaction time in minutes (x_1), temperature in °C (x_2) and concentration of NaOH used in $molL^{-1}$ (x_3). Each of the variables was examined at two levels: low (-1), and high (1) as shown in Table 7.1.

Table 7.1. The reaction conditions used to prepare solutions for sparge testing.

Reaction	Coded variables			Uncoded Variables		
	Time	Temperature	[NaOH]	Time (mins.)	Temperature (°C)	[NaOH] ($molL^{-1}$)
1	-1	1	-1	5	60	0.25
2	-1	-1	1	5	20	3.75
3	1	1	1	30	60	3.75
4	1	-1	1	30	20	3.75
5	-1	1	1	5	60	3.75
6	1	-1	-1	30	20	0.25
7	-1	-1	-1	5	20	0.25
8	1	1	-1	30	60	0.25

The reactions were carried out in a random order to minimise bias.

As the models generated in Chapter 5 described the data measured for the reaction product solution properties with high levels of statistical significance the modelled extract solution properties were not measured again for the foamability modelling investigation in this chapter.

7.2.2 Foaming data analysis – data set one

The foam height versus time measurements from sparging the solutions were input into Microsoft Excel (2010) and the 'foamability index' calculated as the gradient of graphs of foam height versus time. See Appendix section 9.4.1 for an explanation of the units and calculation of foamability index. The foamability index was used rather than the foam height at seven minutes in an attempt to improve the quality of the data by taking an effective average of the foaming rate of the solutions during the seven minute measurements. Using the data for foaming over seven minutes reduces the effect of noise associated with individual foam height measurements and should improve data. The sparging conditions (air flow rate, nozzle used *etc.*) were kept constant for the various foaming experiments hence difference in the foamability index of the solutions would have only occured according to the foaming ability of the solutions.

Ideally the foaming measurements would have been repeated in triplicate on samples of the same alkali hay extract solution from each extraction. This would have required very large amounts of extracts solutions to be generated and needed a lot of time for the work to be carried out. Time constraints on the research meant this simply was not possible hence the foaming experiments were only carried out once.

A graph showing the foaming versus time for alkali hay extract solutions generated using various reaction conditions is shown in Figure 7.1.

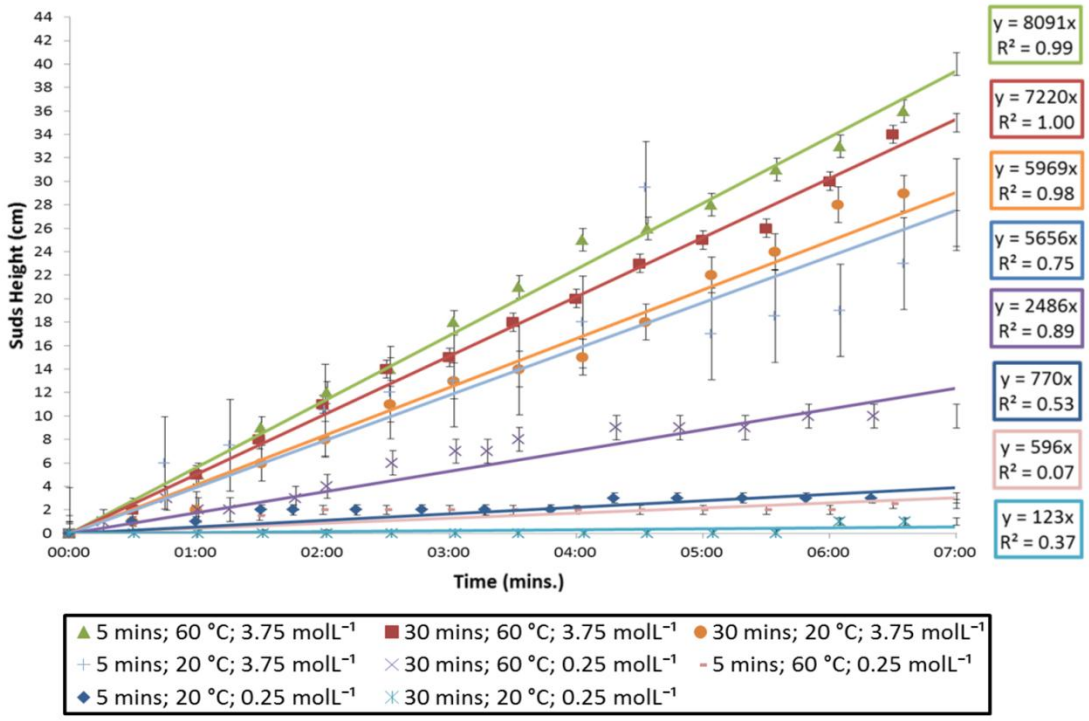

Figure 7.1. Foaming versus time for the initial eight experiments (data set 1).

In Figure 7.1 Excel was used to perform linear regression and apply a line of best fit to the data to allow the foamability index to be calculated from the gradient of the line. The error bars associated with the data show the estimated standard error for the data calculated using the STEYX function in excel which returns the standard error of the predicted *y*-value for each x in the linear regression performed by excel in calculating the R^2 for the data. This is useful for looking for significant differences between foamability of different solutions but is not an estimate of the error associated with the calculated foamability value. Repeated experiments would allow the standard error for the foamability indices to be estimated for the experiments.

On the whole the foaming data demonstrates that the hay extract solutions produced foam which increased in volume as it was sparged. Sometimes the foam volume did not increase smoothly which leads to noise in the data *e.g.* for the solution produced where extraction time = 5 minutes, temperature = 20 °C, and NaOH concentration = 3.75 $molL^{-1}$ (the light blue line), at four and a half minutes the foam volume is seen to have increased rapidly before

decreasing again when measured at 5 minutes. This increase and rapid decrease of foam volume was due to rapid expansion of a bubble within the foam which elevated the top surface of the foam more quickly. Once the rapidly expanding bubble burst, the top surface of the foam dropped back down to a more sensible level hence the apparently noisy data for this solution. A similar collapse of large bubbles in the foam is responsible for the foam volume decrease at 7 minutes for the solution produced with extraction time = 30 minutes, temperature = 20 °C, NaOH concentration = 3.75 $molL^{-1}$.

The gradients for the fitted lines for each experiment are equal to the foamability index of the experiment and are given in the corresponding coloured box on the right hand side of Figure 7.1. The R^2 values represent how well the fitted line represents the data for each experiment. The R^2 values range from being poor (R^2 = 0.07) for the experimental conditions, extraction time = 5 minutes, temperature = 60 °C, NaOH concentration = 0.25 $molL^{-1}$; to very good (R^2 = 0.99) for the experimental conditions, extraction time = 5 minutes, temperature = 60 °C, NaOH concentration = 3.75 $molL^{-1}$. The fit of the line to the experimental data is better for the solutions with the best foaming ability because these solutions demonstrated more consistent growth in their foam volumes. The foam height increased more slowly for solutions with lower foamability, due to the rate of foam collapse being larger hence the net foam volume increase in time was smaller leading to the line fitted to the data having a lower R^2.

Figure 7.1 demonstrates that foaming of hay solutions extracted with high concentration NaOH have better foamability than solutions extracted with low concentration NaOH. All of the extract solutions generated using 3.75 $molL^{-1}$ NaOH have higher foamability than those where 0.25 $molL^{-1}$ NaOH was used for extraction. Within the extractions using 3.75 $molL^{-1}$ NaOH better foamability of extracts generated by higher temperature is seen as the two

extractions at 60 °C give solutions with higher foamability than the 20 °C solutions. Improved foaming for solutions at higher temperatures is in agreement with the effect of higher temperature giving solutions with higher absorbance as observed in Chapter 4.

Regarding the foamability of the solutions from the two hay extractions performed at 60 °C with 3.75 $molL^{-1}$ NaOH, 5 minutes extraction time generated hay extract solution with similar foamability to the 30 minutes extraction time solution. The error bars for the measurement of the foamabilities of the two solutions indicate that they are different within their respective estimated standard errors. However it is suspected that the 5 minutes extraction, producing solutions with higher foamability than the 30 minutes solution would not be found to be a consistent result had the measurements been repeated. Variability leading to inaccuracy in the foaming measurements means this result could have occurred by chance. Extractions performed with 3.75 $molL^{-1}$ NaOH at 20 °C again produced solutions with similar foamabilities for 5 minutes and 30 minutes extraction times though this time 30 minutes extraction time gave marginally higher foamability.

The extractions performed with 0.25 $molL^{-1}$ NaOH showed the same increase in foamability of the solutions generated with higher extraction temperature, where the foamability of solutions generated at 60 °C was higher than solutions generated at 20° C reaction temperature. In the case of the 0.25 $molL^{-1}$ solutions 30 minutes extraction time did give solutions with higher foamability than the 5 minutes extraction time for the 60° C reactions. The foamability of hay extracts solutions generated using 0.25 $molL^{-1}$ NaOH at 20 °C solutions is so similar for the 5 and 30 minutes extraction times (both solutions generated little or no foam) that it is not possible to draw conclusions from the data.

By examining the foaming profiles of the solutions generated with varying reaction conditions it is apparent that higher NaOH concentration and higher extraction temperature

give solutions which generate more foam. The effect of extraction time is less clear though it is expected that that longer extraction times (up to 30 minutes) would give better foamability of the alkali hay extract solutions generated. The ordered foamability index of each of the extract solutions is listed with the corresponding reaction conditions given in Table 7.2.

Table 7.2. Reaction conditions used and foaming indices calculated from the foaming measurements.

Extraction conditions			Foamability index	
Time (mins.)	Temperature (°C)	[NaOH] ($molL^{-1}$)	Value (cm)	Std. error (cm)
5	60	3.75	8091	0.96
30	60	3.75	7220	0.78
30	20	3.75	5969	1.52
5	20	3.75	5656	3.92
30	60	0.25	2486	1.02
5	20	0.25	770	0.42
5	60	0.25	596	0.38
30	20	0.25	123	0.31

The foamability index was analysed with respect to the extraction conditions using JMP® software to generate a model to describe the effects of the reaction variables on the foamability of the hay extract solutions. Discussion of the model generated for the initial experiments examining foaming of the hay extract solutions is given in section 7.2.4.

7.2.3 The form of the model generated to describe foaming.

The model proposed for describing the measured foamability of the alkali hay extract solutions in terms of the reaction variables (reaction time, temperature and NaOH concentration) was based on Equation 7.1 and was generated by analysis of the experimental data in Table 7.2.

Equation 7.1. The form of the model generated from the foaming data.

$$Y_i = \beta_0 + \sum_{n=1}^{3} \beta_n X_n + \sum_{n \neq m=1}^{3} \beta_{nm} X_n X_m$$

Where Y_i is the predicted foamability index of the hay extract solutions, β_0 is the value of the fitted response at the centre of the experimental design (*i.e*. the coded variables are 0, 0, 0), β_n and β_m are the linear and β_{nm} the interaction regression terms respectively for the independent variables used in these experiments. $X_{n,m}$ refers to the coded values for the parameters used in the experiments, n and m refer to the reaction variables where n,m = 1 = reaction time, 2 = temperature of reaction, 3 = aqueous NaOH concentration used during the reaction.

7.2.4 Modelling data set one – initial eight experiment factorial design

The estimates of the regression terms in the model describing the foamability of the alkali hay extract solutions and their respective p-values are listed in Table 7.3.

Table 7.3. Regression term estimates for the foaming model generated from the foaming measurements in data set 1.

Parameter	Coefficient	Estimate	p =
Intercept	β_0	13705	0.08
Time	β_1	-687	0.75
Temperature	β_2	1376	0.56
[NaOH]	β_3	11481	0.10
Time*Temperature	β_{12}	169	0.78
Time*[NaOH]	β_{13}	-901	0.71
Temperature*[NaOH]	β_{23}	749	0.76

The data in Table 7.3 can be used to construct the foaming model in the form given by Equation 7.1. As an example of this the model generated by the data in Table 7.3 is fully expressed in Equation 7.2.

Equation 7.2. The predictive model describing the foamabilityof alkali hay extract solutions written out in full.

$$\text{Foamability index } = 13705 - 687 \times \left(\frac{\text{Time} - 17.5}{12.5}\right) + 1376 \times \left(\frac{\text{Temperature} - 40}{20}\right)$$
$$+ 11481 \times \left(\frac{[\text{NaOH}] - 2}{1.75}\right) - 169 \times \left(\frac{\text{Time} - 17.5}{12.5}\right) \times \left(\frac{\text{Temperature} - 40}{20}\right)$$
$$- 901 \times \left(\frac{\text{Time} - 17.5}{12.5}\right) \times \left(\frac{[\text{NaOH}] - 2}{1.75}\right)$$
$$+ 749 \times \left(\frac{\text{Temperature} - 40}{20}\right) \times \left(\frac{[\text{NaOH}] - 2}{1.75}\right)$$

The p-values for the regression terms in Table 7.3 indicate the statistical significance of the regression term where $p < 0.05$ indicates 95% confidence associated with the regression term. None of the terms have statistical significance as all regression terms have $p > 0.05$ indicating that none of the regression terms are statistically significant. Lack of statistical significance means conclusions cannot confidently be drawn about the effect of the reaction variables on the foaming of the extract solutions using data set one.

In order to examine how well the model describes foamability of the alkali hay extract solution in relation to the variation in the experimental data, a graph of experimental versus predicted foaming generated by JMP is included in Figure 7.2.

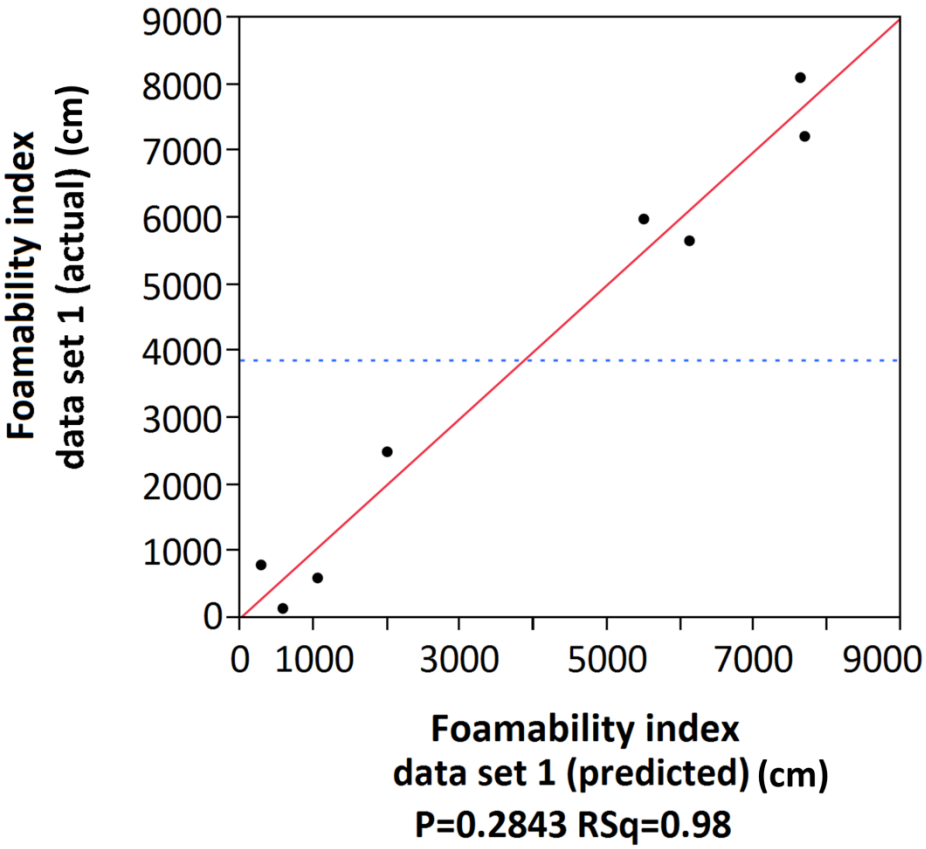

Figure 7.2. Actual foamability index vs. predicted foamability index for the data set 1.

Figure 7.2 shows that data points in the actual versus predicted graph for the sudsing data obtained in the initial eight experiments have an R^2 = 0.98 as would be required for a model where the model predicted values are closely related to the experimental values. However the lines indicating the 95% confidence interval for the graph are not visible in the graph as the confidence interval is very large due to the amount of available foaming data being limited. The variability of the foaming data limits the quality of the data and reduces the statistical significance of the model generated by the data analysis. The p-value for the graph is included on the *x*-axis and shows that p = 0.28 which demonstrates that there is no statistical significance associated with the model as a whole.

Therefore although the R^2 value for the graph of model predicted values of foaming versus the experimental values of foaming is ~1, the model is not able to be used with any statistical confidence to make predictions about foamability of the hay extract solutions

according to variations in the experimental conditions. Though the model cannot be used to make quantitative foaming predictions it is still usable to look for correlation with other extract solution properties and this is discussed in section 7.3.

7.2.5 Data set two – repeating the eight experiment factorial design

When data set 1, from the initial 8 experiment factorial design foamability study was analysed, the model generated was not statistically significant. Hence it was decided to repeat the experiments in order increase the available data, in an attempt to increase the statistical significance of the model hence confidence with which conclusions could be drawn from it.

At this point it is worth restating that the second round of experiments to measure foaming of the hay extract solutions (which generated 'data set 2') were performed on fresh extract solutions generated from a second batch of hay (not by re-measuring foaming of the original solutions). It was hypothesised that the two hay batches should behave similarly enough to allow a statistically significant model to be generated by combination of the two datasets. Even if this were not the case and batch to batch variability of the materials led to vastly different data, observations of foaming from the second round of experiments would generate knowledge of the likely applicability of the models to different batches of plant raw materials which itself would be insightful.

7.2.6 Foaming data analysis – data set two

The graphs showing foam height versus time measured for the extract solutions generated from the second batch of hay in the eight repeated experiments is shown in Figure 7.3.

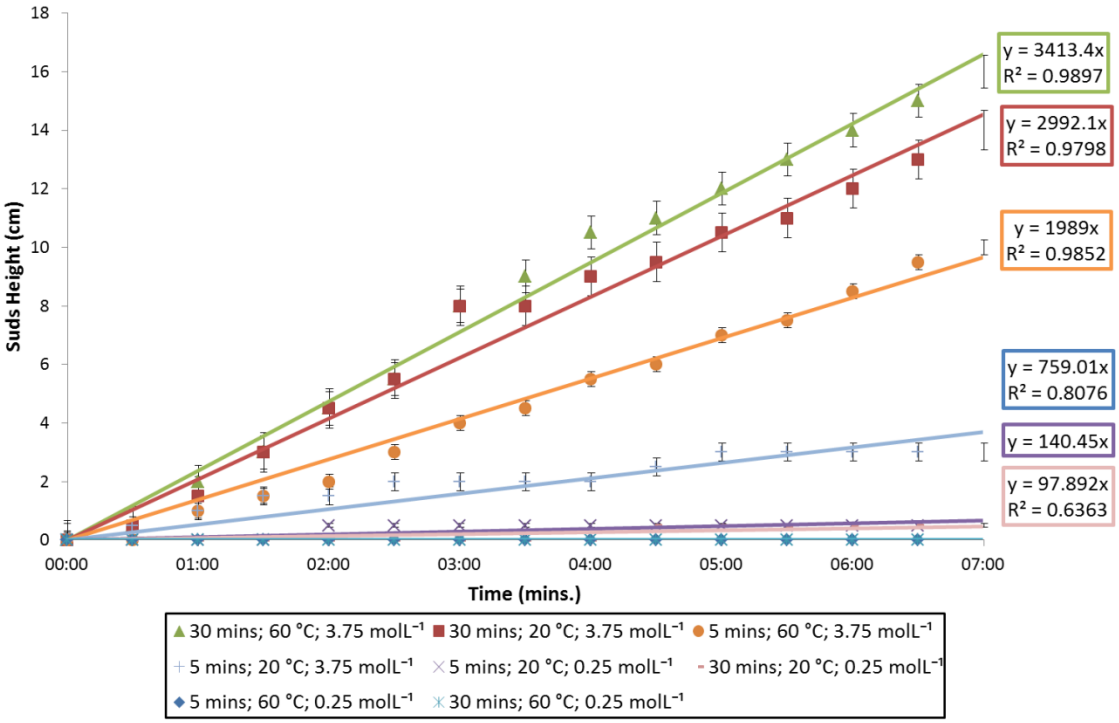

Figure 7.3. Foaming versus time for the eight repeated experiments.

Microsoft Excel was again used to perform linear regression on the data and a line of best fit applied to the foaming data from each extract solution. Again the error bars represent the estimated standard error for the foaming data (calculated using the STEYX function) rather than an estimate of the standard error associated with the foamability indices. The gradients for the fitted lines for each experiment are equal to the foamability index of the experiments and are given in the corresponding coloured boxes on the right hand side of Figure 7.3.

The broad trends seen when examining the foaming in the initial eight experiments were again observed in the repeated experiments. Higher NaOH concentration and extraction temperature gave hay extract solutions with higher foamability. The effect of extraction time was as expected with 30 minutes being clearly beneficial to generating solutions with increased foamability for the extractions performed using 3.75 $molL^{-1}$ NaOH both at 20 and 60 °C. The very low foamability of the 0.25 $molL^{-1}$ NaOH solutions again means

differentiation between the foaming of these solutions is not easy and no conclusions can necessarily be drawn.

An important observation regarding the level of foaming of the hay extract solutions used in generating data set 2, is that overall, the foaming of the extract solutions was very much lower than observed for the solutions in data set 1. The fact that all experiments generated solutions which had lower foamability suggests that this is not merely due to variability in the foaming measurements but that the switch to a new batch of hay led to the foaming of the extract solutions being significantly reduced overall.

The ordered foamability index of each experiment in data set 2 is listed with the corresponding reaction conditions is given in Table 7.4 and the information from data set 1 is reproduced also for ease of comparison.

Table 7.4. Reaction conditions used and foaming indices calculated from the foaming measurements in the repeated experiments.

Extraction conditions			Foamability index			
			Data set 1		Data set 2	
Time (mins)	Temp. (°C)	[NaOH] ($molL^{-1}$)	Value (cm)	Std. error (cm)	Value (cm)	Std. error (cm)
30	60	3.75	8091	0.96	3413	0.56
30	20	3.75	7220	0.78	2992	0.67
5	60	3.75	5969	1.52	1989	0.25
5	20	3.75	5656	3.92	759	0.30
5	20	0.25	2486	1.02	140	0.15
30	20	0.25	770	0.42	98	0.14
5	60	0.25	596	0.38	0	0.00
30	60	0.25	123	0.31	0	0.00

7.2.7 Modelling data set two – the repeated experiments

The estimates of the regression terms in the model describing the foamability of the alkali hay extract solutions generated in the repeated experiments and their associated p-values

are listed in Table 7.5 with the information from data set 1 reproduced for ease of comparison.

Table 7.5. Regression term estimates for the foaming model generated from the foaming measurements in data set 2.

		Estimated regression terms			
		Data set 1		Data set 2	
Parameters	Coefficient	Estimate	p =	Estimate	p =
Intercept	β_0	13705	0.08	4995	0.05
Time	β_1	-687	0.75	2038	0.12
Temperature	β_2	1376	0.56	986	0.23
[NaOH]	β_3	11480	0.10	4458	0.06
Time*Temperature	β_{12}	169	0.78	-96	0.53
Time*[NaOH]	β_{13}	-901	0.71	1850	0.14
Temperature*[NaOH]	β_{23}	749	0.76	945	0.27

The data in Table 7.5 for data set 2 can again be used to construct the relevant foamability model in the form given by Equation 7.1.

The p-values in Table 7.5 for the regression terms in the model generated by data set 2 again show that none of the estimated regression terms have statistical significance as all terms have $p > 0.05$. Hence, yet again no conclusion can confidently be drawn from the model generated by data set two describing the effect of the extraction variables on the foamability of hay extract solutions. One point of note however, is that though the p-values for the estimated regression terms in the model from data set 2 are not statistically significant the term for NaOH concentration has a p-value being relatively close to the significance cut off ($p = 0.06$ for NaOH concentraion).

In order to examine how well the model generated from foaming data set 2 describes foamability of the hay extract solution in relation to the variation in the experimental data, a graph of experimental versus predicted foamability for the model generated from data set 2, by JMP is included in Figure 7.4.

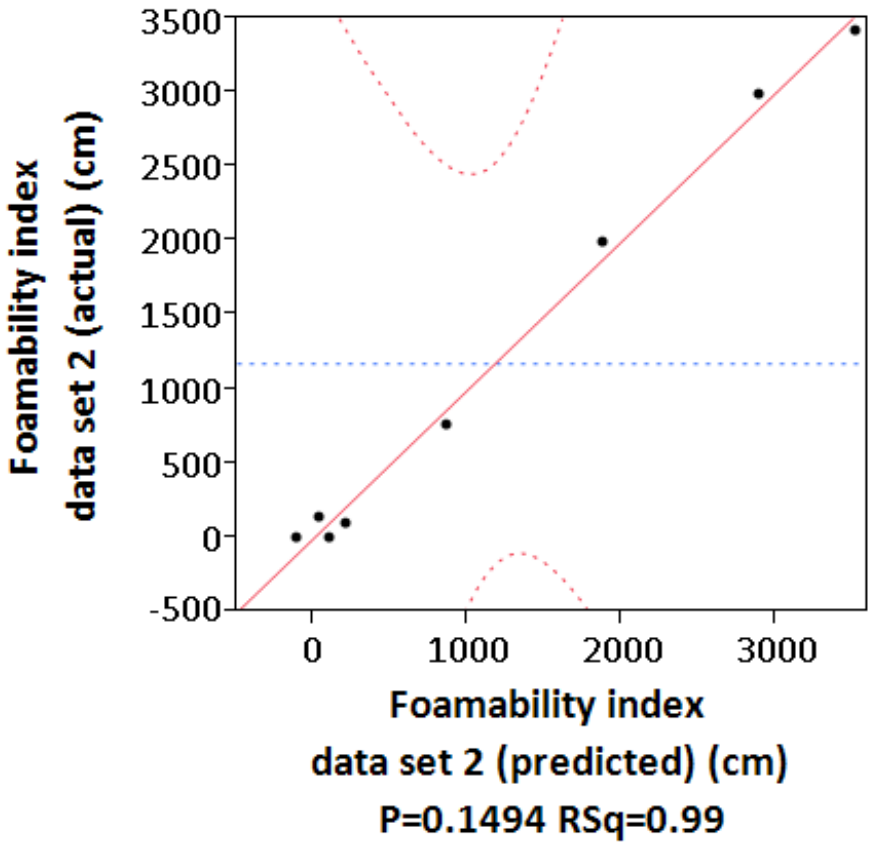

Figure 7.4. Actual sudsing vs. predicted for the 8 repeated experiments.

Figure 7.4 shows that data points in the actual versus predicted graph for the sudsing data set 2 have an $R^2 = 0.99$ as would be required for a model where the model predicted values are closely related to the experimental values. The red dashed lines indicating the 95% confidence interval are visible this time, though they are not very tightly positioned around the data points as the confidence interval is again large, again due to poor quality foaming data. The p-value for the graph is included on the *x*-axis and shows that p = 0.15 which is an improvement on the p-value for the same graph pertaining to data set 1 (where p = 0.28). This high p-value again means that there is no statistical significance associated with the model generated from the repeated experiment data. Hence the model generated from the foaming data set 2 is also not able to be used to confidently make predictions about foaming of the hay extract solutions according to variations in the experimental conditions.

Both the models generated by the initial eight and the repeated experiments were not statistically significant enough to confidently predict the foamability of alkali hay extract solutions in terms of the extraction conditions and their interactions. Despite this, insight into the effect of extraction conditions on foamability was still garnered from the foaming experiments themselves as explained in sections 7.2.2 and 7.2.6.

One important observation is that the foaming data generated for the two models shows the level of foaming in the repeated experiments was diminished compared to that of the initial experiments. This means that batch to batch material variation in the hay had a large effect on the level of foaming of the extracts produced from the hay. This difference in foaming is also important as it means combining the data in both sets is not likely to give a statistically significant predictive model of foamability of the alkali hay extract solutions. The combined data set is useful however in helping to better understand the relative importance of the extraction conditions in affecting the foamability of the product solutions. With this in mind the two data sets were combined and an attempt was made to construct a model from the combined data sets to see if any extraction conditions (or interactions) became statistically significant in affecting the foamability of the hay extract solutions. The model generated by the combined data also allowed examination of correlations between foaming and other extract solutions properties and this is discussed in section 7.2.8.

7.2.8 Combined data sets

Estimates of the regression terms and their associated p-values, in the model generated by combining data set 1 and data set 2, describing the foamability of alkali hay extract solutions are listed in Table 7.6. The estimated regression terms and p-values for the models generated from data set 1 and 2 are reproduced for ease of comparison.

Table 7.6. Regression term estimates and p-values for the foamability models generated from the foaming measurements in data set 1, 2 and both data sets combined.

		Estimated regression terms					
		Data set 1		Data set 2		Combined Data	
Parameters	Coefficient	Estimate	p =	Estimate	p =	Estimate	p =
Intercept	β_0	13705	0.08	4995	0.05	9350	0.001
Time	β_1	-687	0.75	2038	0.12	675	0.75
Temperature	β_2	1376	0.56	986	0.23	1181	0.58
[NaOH]	β_3	114801	0.10	4458	0.06	7969	0.007
Time*Temperature	β_{12}	169	0.78	-96	0.53	37	0.95
Time*[NaOH]	β_{13}	-901	0.71	1850	0.14	474	0.84
Temperature*[NaOH]	β_{23}	749	0.76	945	0.27	847	0.72

The data in Table 7.6 for the combined data sets can be used to construct the relevant foaming model in the form given by Equation 7.1.

The p-values for the regression terms in the model generated from the combined data set (16 experiments in total) given in Table 7.6, show that only one of the estimated regression terms has statistical significance as all $p > 0.05$ for all regression terms except [NaOH] where $p = 0.007$. Though the NaOH concentration term has statistical significance, this does not indicate that the model generated is in itself wholly statistically significant. What it does demonstrate is that combing the foaming data has improved the ability of the model generated to find reaction variables which have a statistically significant influence on foamability of the hay extract solutions. It is interesting that NaOH concentration was found to have a statistically significant effect on extract solution viscosity, solution absorbance and the % mass of hay extracted into solution, as discussed in Chapter 5. Potential relationships between these extract solution properties are discussed in section 7.3.

In order to examine how well the model generated from the combined foaming data (from all 16 experiments) is able to describe foamability of the hay extract solution relative to the experimental data, a graph of experimental versus predicted foamability index for the combined data is included in Figure 7.5.

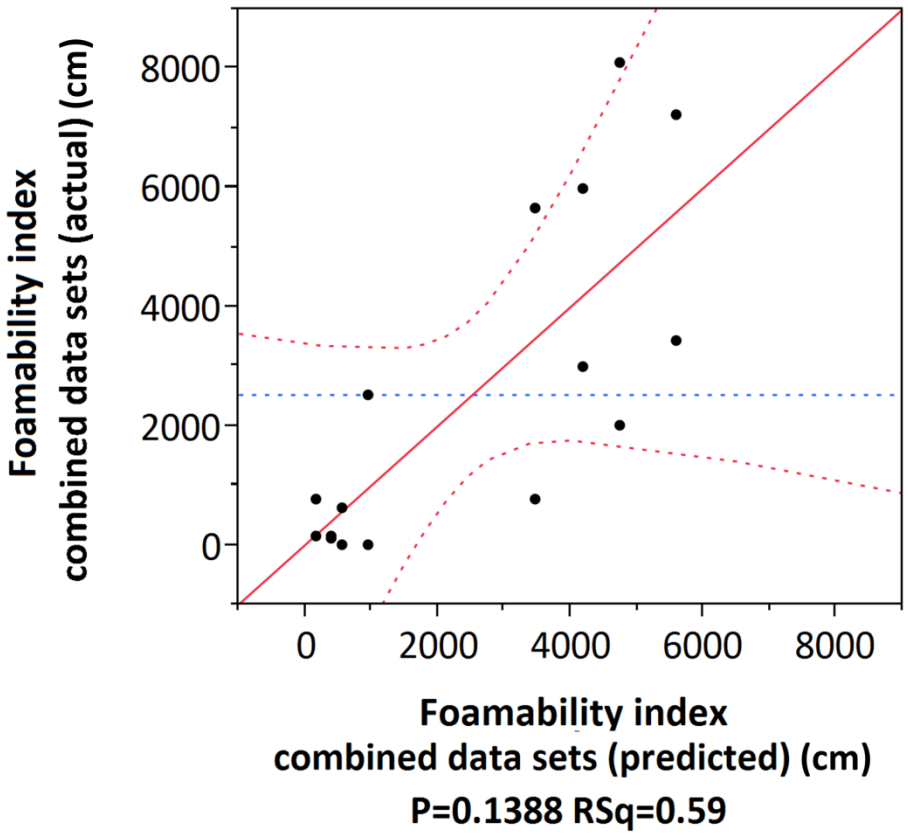

Figure 7.5. Actual foamability index vs. predicted for the combined data set of 16 experiments.

Figure 7.5 shows that data points in the actual versus predicted graph for the combined sudsing data have an $R^2 = 0.59$. A lower R^2 than those seen previously would be expected for a model based on two very different sets of data representing foaming measurements for solutions generated under the same extraction conditions. The disparity in the level of foaming between foaming data set 1 and 2 has led to the data points being more disperse in the actual versus predicted graph for the combined data set. The effect of increasing the number of experiments can also be observed as the red dashed lines representing the 95% confidence intervals for the model are now even more closely situated around the data points. The p-value for the graph is included on the *x*-axis and shows that p = 0.14. Though this is an improvement on the p-value for the models generated by data sets 1 and 2 (where p = 0.28 and p = 0.15 respectively) this high p-value again means that there is no statistical significance associated with the model generated from the combined experimental data.

Therefore as expected, the model generated from the combined data is not able to be used confidently to make predictions about foamability of the hay extract solutions according to variations in the experimental conditions.

In the case of foaming measurements random variation is large which means the available foaming data cannot be used to generate a robust model to describe the foamability of alkali hay extract solutions. More measurements of foaming would result in reduced noise to signal ratio associated with the foaming measurements which might ultimately make it possible to generate a model capable of predicting the foaming of alkali hay extract solutions when considering the reaction conditions used to generate the solutions.

Repeated foaming measurements were considered during the experimental planning however once foam is generated by sparging a solution it is not easily recombined with the solution. This means that by repeatedly sparging the hay extract solutions, the composition of the solution would potentially be altered due to preferential removal of sudsing materials with the generated foam. This removal of sudsing materials would mean that if the same solution was sparged more than once, the composition of the solution would be different each time with less and less surfactant in solution. In order to make repeated foaming measurements using the sparging rig, very large batches of hay extract solutions would have been required so that foaming measurements could be performed on multiple sub samples of the solutions. None of the models generated from the measured foaming data were statistically significant hence none were suitable for use in predicting foamability of alkali hay extract solutions with varying extraction conditions. Despite this, the models are still useful to try and find correlations with the extract solution properties measured and modelled in Chapter 5.

7.3 Correlations between foamability and physical properties of alkali hay extracts solutions

To search for correlation between the foamability of alkali hay extract solutions and the properties of the extract solutions measured in Chapter 5, predicted foamability values were generated using the models developed in this chapter at the reaction conditions used in Chapter 5. Though the models generated for foamability of the extract solutions are not robust enough to be used for reliable prediction of foamability of the hay extract solutions, they are still useful in terms of looking for correlation between foamability and other properties of hay extract solutions. JMP® software (Version 9.0.2, SAS Institute Inc., Cary, NC, 2010) was used to generate a correlation chart for the predicted foamability values and the various extract solution properties predicted by the models in Chapter 5. This correlation chart is reproduced in Figure 7.6, with the R values which represent the strength of the respective correlations listed in Table 7.7. While examining correlation between the various extract solutions properties it is worth stating that correlation does not necessarily imply causation, however, the correlations are combined with the evidence and information discussed in previous chapters to increase knowledge of the properties of alkali hay extract solutions.

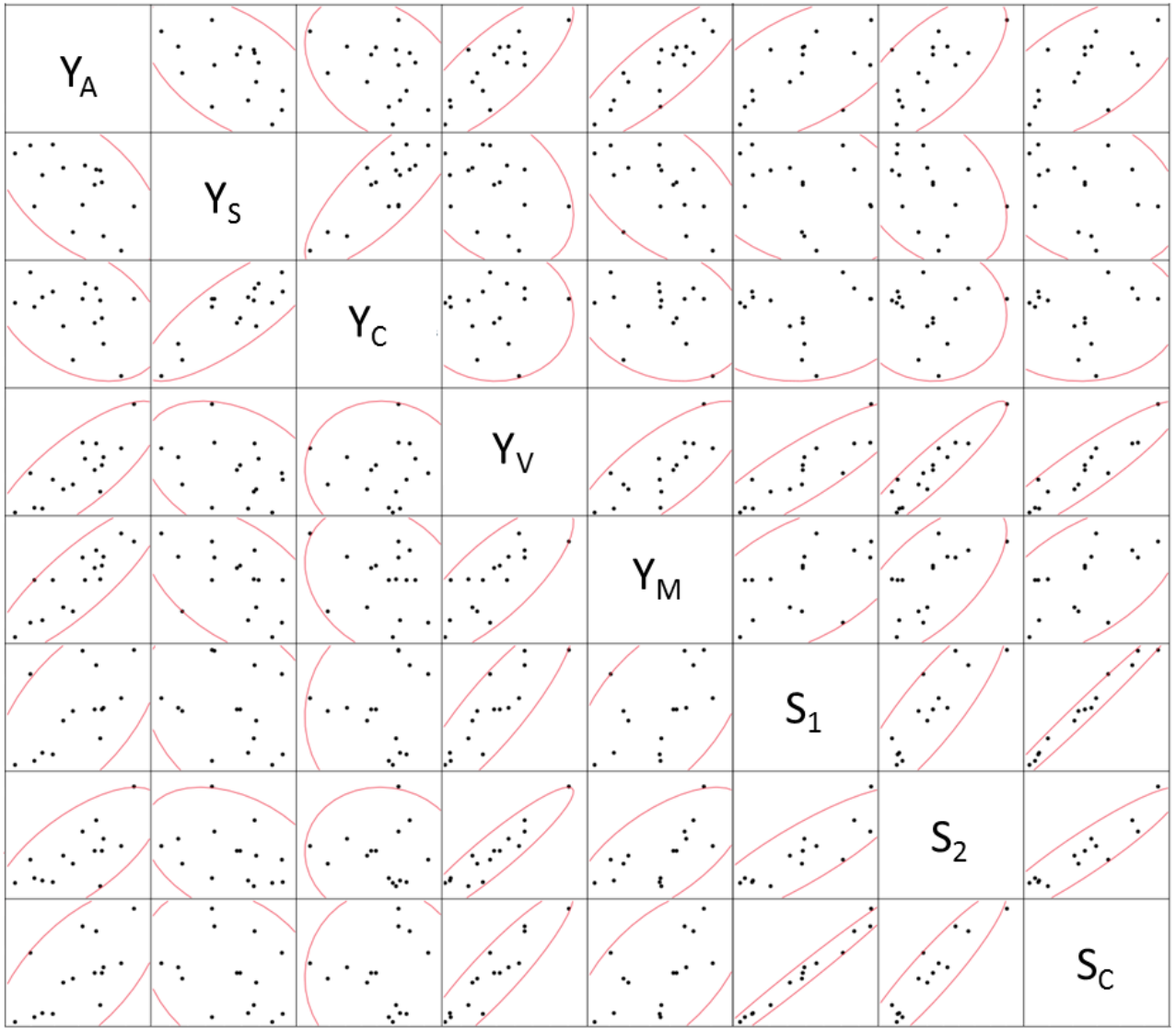

Figure 7.6. Correlation plots between the various properties of hay extract solutions measured in Chapter 5 and the foaming of the solutions.

Table 7.7. Correlations between alkali hay extract solution properties measured during the research presented within this thesis.

Y_A	-0.53	-0.38	0.79	0.85	0.59	0.69	0.63
-0.53	Y_S	0.81	-0.34	-0.52	-0.26	-0.37	-0.30
-0.38	0.81	Y_C	-0.03	-0.25	0.05	-0.05	0.02
0.79	-0.34	-0.03	Y_V	0.78	0.88	0.94	0.92
0.85	-0.52	-0.25	0.78	Y_M	0.53	0.66	0.58
0.59	-0.26	0.05	0.88	0.53	S_1	0.87	0.99
0.69	-0.37	-0.05	0.94	0.66	0.87	S_2	0.93
0.63	-0.30	0.02	0.92	0.58	0.99	0.93	S_C

In Figure 7.6 and Table 7.7 Y_A = hay extract solution absorbance at 286 nm; Y_S = hay extract solution surface tension; Y_C = hay extract solution contact angle on a polystyrene surface; Y_V = hay extract solution viscosity; Y_M = % mass extracted from the hay during reaction with NaOH; S_1 = hay extract solution foamability modelled from foaming data set 1; S_2 = hay solution foamability modelled from data set 2 and S_C = hay extract solution foamability modelled by combining data set 1 and 2.

Reading the chart in Figure 7.6 is straightforward; the first property of the alkali hay extract solution is crossed with the second property of the solution and the corresponding rectangle shows an ellipse around the data points which visually indicates correlation. The direction of the slope of ellipse indicates how the selected solution properties correlate (positive or negative) and the closer the ellipse is to being a single line, the stronger the correlation. The 'R value' which quantifies the strength of the correlation between the hay extract solution properties is given in the position in Table 7.7 which corresponds to the ellipse in Figure 7.6. R = 1 indicates a perfect correlation with decreasing values indicating weaker correlation.

The colours in Table 7.7 provide an easy visual indication of the strength of correlations between the extract solution properties. A white cell indicates no correlation → weak correlation where ($0 < R < 0.6$); red cells indicate a degree correlation is present ($0.6 < R < 0.7$); orange cells indicate moderate correlation ($0.7 < R < 0.8$) and green cells indicate strong correlation ($R > 0.8$) between the respective solutions properties. A positive R indicates positive correlation (as *x* increases *y* increases) and negative R indicates negative correlation (as *x* increases *y* decreases). By examining Figure 7.6 and Table 7.7 together, interesting observations can be made about the solutions formed by reaction of hay with NaOH.

7.3.1 Solution absorbance at 286 nm (Y_A)

Starting with hay extract solution absorbance at 286 nm, there are weak negative correlations with solution surface tension ($R(Y_A\text{-}Y_S) = -0.53$) and contact angle ($R(Y_A\text{-}Y_C) = -0.38$). The negative correlation indicates that as extract solution absorbance increases, the surface tension and contact angle of the solution decrease. This correlation agrees with the hypothesis that lignin derivatives which increase hay extract solution absorbance, having surfactant properties, should also decrease its surface tension and contact angle.

Hay extract solution absorbance at 286 nm has a moderate positive correlation to solution viscosity ($R(Y_A\text{-}Y_V) = 0.79$). This means that as the viscosity of the hay extract solution increases the solution absorbance increases also. This is an example of correlation not necessarily indicating causation as the lignin will not necessarily increase the solution viscosity directly (no evidence of alkali extracted lignin significantly increasing solution viscosities is found in the literature). This correlation, however, is in agreement with a previously stated hypothesis that more lignin chromophores would be extracted into solution as more material overall is extracted from the hay during the reactions with NaOH. Overall increase in the % mass extracted from the hay results in higher viscosity in the alkali extract product solutions hence the positive correlation between extract solution viscosity and absorbance.

For the same reason as is responsible for the absorbance/viscosity correlation, there is also a strong correlation found between hay extract solution absorbance and % mass extracted from the hay during the extractions ($R(Y_A\text{-}Y_M) = 0.85$).

As solution absorbance is due to lignin derivatives in solution and because foaming of the solutions is also due to lignin derivatives in solution, positive correlation would be expected

between solution absorbance and the foamability of the hay extract solutions. When looking at data set 1, absorbance shows a weak positive correlation ($R(Y_A\text{-}S_1) = 0.59$). Foaming data set 2 (S_2) and the combined foaming data (S_C) sets show somewhat stronger positive correlations to solution absorbance ($R(Y_A\text{-}S_2) = 0.69$ and $R(Y_A\text{-}S_C) = 0.63$ respectively). Correlation between extract solution absorbance and foamability is not conclusive proof of causation with respect to the foaming *i.e.* this alone does not conclusively prove foaming in the hay extract solutions is due to the same lignin chromophores that lead to increased solution absorbance. However if the correlation between absorbance and foamability was absent or was negative, it would have meant that the hypothesis that foaming is caused by lignin chromophores, was nullified. The correlation between absorbance and foamability contributes toward overall understanding of foaming of alkali hay extract solutions supporting the conclusion that lignin derivatives are responsible for foaming in hay extract solutions reached in Chapter 6.

7.3.2 Solution surface tension (Y_S)

Change in surface tension of solutions produced from NaOH extraction of hay performed under varying reaction conditions shows strong positive correlation with the contact angle of the solution ($R(Y_S\text{-}Y_C) = 0.81$). Correlation between surface tension and contact angle of the solution is expected as increased surface tension would mean increased contact angle for the solutions as contact angle is dependent on the surface tension according to Young's equation (Equation 3.2).

The solution surface tension shows weak negative correlation with solution viscosity ($R(Y_S\text{-}Y_V)_= -0.34$) and % mass loss ($R(Y_S\text{-}Y_M) = -0.52$) meaning that as the % mass extracted from the hay during reaction with NaOH and the product solution viscosity increase, the solution surface tension would be expected to decrease. These weak correlations occur

because more surfactants are extracted into solution (which leads to surface tension decrease) as the overall mass extracted from the hay increases (which in turn increases the solution viscosity).

The correlations between the solution surface tension and foaming are weak ($R(Y_S\text{-}S_1) = -0.26$; $R(Y_S\text{-}S_2) = -0.37$ and $R(Y_S\text{-}S_C) = -0.30$). The correlations are negative though, which means that as the surface tension of the solution increases the foamability of the solution would be expected to decrease. This is as expected for foaming solutions as lowered surface tension is beneficial for effective foaming hence increased surface tension would decrease foamability. It might be expected that the positive correlation between surface tension and foamability would be stronger but this expectation fails to acknowledge the importance of other solution properties which affect foamability (*e.g.* solution viscosity). Problems with variability in extract solution surface tension and foaming measurements which resulted in poor models being generated, would also weaken the observed correlations.

7.3.3 Solution contact angle measured on a polystyrene surface (Y_C)

The change in contact angle (Y_C) of product solutions from NaOH extraction of hay performed under varying reaction conditions, shows no correlation with the solution viscosity ($R(Y_C - Y_V) = -0.03$) and only weak negative correlation with % mass extracted from the hay during reaction ($R(Y_C\text{-}Y_M) = -0.25$). Stronger correlation between contact angle and solution viscosity was not necessarily expected because solution viscosity does not affect the contact angle of the solution (see Equation 3.2). Similarly % mass extracted from the hay would not directly affect contact angle of the extract solution hence the weakness of the correlation.

7.3.4 Solution viscosity (Y_V)

Solution viscosity showed moderate correlation with % mass extracted into solution ($R(Y_V - Y_M) = 0.78$) which was expected as more material extracted into solution increases the viscosity. Strong correlation between extract solution viscosity and foamability ($R(Y_V-S_1) = 0.88$; $R(Y_V – S_2) = 0.94$ and $R(Y_V – S_C) = 0.92$) was also evident. The strength of the correlation between the solution viscosity and the foamability of the solutions demonstrates that the solution viscosity plays a very important role in conferring foaming ability on the hay extract solutions. Moreover, increase in the solution viscosity means reduced film drainage rate in foams which means film thinning is slowed hence disproportionation and film rupture are impeded.

The strength of this correlation is another example of strong correlation not being indicative of causation. High solution viscosity does not cause foaming in solutions, the viscosity merely increases stability of any foam that is actually formed. Though the correlation between absorbance and foamability was weaker than that between viscosity and foaming, the fact still remains that lignin derivatives which affect absorbance *cause* foaming with the foam being *stabilised* due to increased solution viscosity. Solubilised saccharides are responsible for the extract solution viscosity increase which stabilises foam, though would not confer the ability to generate foam on the extract solution.

7.3.5 % Mass extracted into solution

The % mass extracted from the hay by the NaOH solutions shows positive correlation to the foaming of the solutions ($R(Y_M – S_1) = 0.53$, $R(Y_M – S_2) = 0.66$ and $R(Y_M – S_C) = 0.58$). This correlation exists for the reasons stated previously: more mass extracted from the hay by the NaOH means more surfactants in solutions which reduce surface tension, also, more mass extracted means increased solution viscosity which in turn stabilises foams.

7.3.6 Foaming (data set 1, 2 and combined)

The foamability of the hay extract solutions described by the models S_1, S_2 and S_C show strong positive correlations (for $R(S_1\text{-}S_2) = 0.87$;$R(S_1\text{-}S_C) = 0.99$ and $R(S_2\text{ -}S_C) = 0.93$). This is as expected because ideally the sudsing data would have been identical for both data set 1 and data set 2 and the sudsing of hay extract solution would respond similarly with similar changes to extraction conditions. The poor quality of the sudsing data generated by the sparging measurements and the fact that data set 2 was measured for a different batch of hay than data set 1 mean that there are differences between the absolute foaming values measured for extractions performed under the same conditions. As it stands models obtained correlate in such a way as to demonstrate that they at least behave similarly, so when foamability increased for an extraction according to the model generated for data set 1 it also increased according to the model generated by data set 2 and the combined data sets.

8 Chapter 8 - Conclusions

This research has potential importance to those interested in processing lignocellulosic material (such as hay) *via* alkali extraction as well as those working in FMCGs interested in finding in alternatives to oil based surfactants to generate foam in products. Response surface methodology was used to better understand a range of properties of NaOH extracted hay solutions and unique models were generated, models such as these were not found in the research currently published in the literature hence they contribute to the knowledge. Examination of the surface tension and contact angle of alkali extract solutions from lignocellulosic materials and application of cryo SEM to observe the microstructure of foams from these extract solutions is not found elsewhere in the literature hence the model generated for the solution contact angle and the SEM images are unique in their insights. Finally, the attempts of this research to understand the relationships between lignocellulosic extract solution properties and its foamability by looking for correlations also make this research novel.

The research methodology used in this thesis or experiments identified as potential future research opportunities could be usefully applied to many different plant raw materials to aid screening of which materials might be suitable for use in generating foaming solutions which might be incorporated into detergent formulations.

8.1 Single variable experiments

Hay extract solution absorbance plateaued with extraction time meaning longer extractions only increase the proportion of *accessible* lignin which is solubilised from hay for given reaction conditions. This means increasing extraction times would not improve extraction of foaming materials from hay *ad infinitum* and extraction time should be optimised in future research and when taking the research forward into process development at larger scales.

Increasingly concentrated NaOH solutions solubilised more material from hay however this trend did not continue up to the highest concentrations used in the extractions. At some concentration of NaOH (around 3.75 $molL^{-1}$), further increase did not dissolve more material from the hay as all of the accessible material was solubilised. That % mass extracted did not decrease with higher concentration NaOH even though absorbance was found to, demonstrated that higher concentration NaOH breaks down extracted lignin chromophores leading to decreased solution absorbance rather than actually extracting less lignin. This finding is interesting as examples of lignin breakdown by highly NaOH are found in the literature but not at the low temperatures used in the current research.

Higher extraction temperatures increased the amount of material solubilised from hay for a given extraction time and NaOH concentration. Extract solution absorbance also increased with extraction temperature, indicating that lignin chromophores were not broken down by the highest temperatures used in the current extractions (60 °C) which agreed with prior findings in the literature.

Extract solution viscosity increased with higher NaOH concentration used in the reactions. This result was complicated, as higher concentration NaOH has higher viscosity to begin with though extract solution viscosity was found to be higher than the corresponding unreacted NaOH viscosity in all cases. No pattern in the relative increase in solution viscosity and the concentration of NaOH used in the extraction was observed.

The findings of this Chapter assisted in the choice of extraction conditions for the rest of the research within this thesis the selected conditions were:

Table 8.1. Extraction conditions identified for use in the research beyond single variable experiments.

Extraction variable	Range
Time (minutes)	5 – 30
Temperature (°C)	ambient - 60
NaOH concentration ($molL^{-1}$)	0.25 – 3.75

8.2 Modelling extract solution properties with varying extraction conditions

Statistically significant models were generated for the % mass extracted from the hay (Y_M), the hay extract solution absorbance (Y_A), the hay extract solution viscosity (Y_V) and the hay extract solution contact angle (Y_C) responses (though the Y_C model required data screening to attain a satisfactory R^2 value).

Y_M was found to increase linearly with extraction temperature and NaOH concentration which confirmed the findings of Chapter 4 over the same variable ranges. A quadratic dependence was found for extraction time, leading to plateauing in Y_M at the longest extraction times.

Y_A was found to increase linearly with reaction time and temperature and have a quadratic relationship with NaOH concentration leading to a peak in solution absorbance at higher NaOH concentrations. Again these results agree with the findings of Chapter 4 over the same range of the reaction variables. Higher concentrations of NaOH lead to destruction of lignin derivatives (seen in Chapter 4) as well as potentially increased solubilisation of non-lignin materials from the hay (*e.g.* cellulose) which explains how % mass extracted can increase while the product solution absorbance peaks of around 3.75 $molL^{-1}$ NaOH.

Y_V had linear dependence on the reaction variables hence Y_V was maximised by using the most extreme reaction conditions examined in the research for Chapter 5. NaOH concentration was the most statistically significant influence on the extract solution viscosity over the other reaction variables.

Y_C was found to have a quadratic dependence on NaOH concentration with no statistically significant influence observed from any of the other extraction variables.

Interestingly, extract solution absorbance (Y_A) and contact angle models (Y_C) showed similarities in their dependence on NaOH concentration. The Y_A model increased for low to intermediate NaOH concentration and decreased for intermediate to high NaOH concentration. The solution contact angle initially decreased then increased over similar concentration ranges. Similarities in the Y_A and Y_C models occur due to variation in the concentration of lignin based surfactants in solution which increase solution absorbance and are also responsible for the extract solution contact angle being depressed.

A statistically significant model for the hay extract solution surface tension response (Y_S) could not effectively be generated using the pendant drop data available in the current research.

8.3 Cryo SEM examination of foams

Finding from that Pickering stabilisation was responsible for alkali plant extract foaming was a new and exciting contribution to the overall knowledge of foaming of alkali plant extract solutions. The other SEM images of Gelatin, Guinness and Kronenbourg also contribute to the knowledge and understanding of particle stabilised foam systems more generally, by imaging real world examples of the actual effects and arrangements of particles at interfaces within foams that are extensively described, without 'real' images being available, in the literature.

Particles were observed at foam interfaces and within the liquid bubble films with consistent tendencies to agglomerate and adsorb at and within the interface. Particles were pictured exhibiting behaviour such as Plateau border clogging which would contribute toward foam

stabilisation. Halos of particles were identified as consistent features in particle stabilised bubbles and networks of agglomerated particles, having appearances similar to those discussed in the literature have been observed and contribute evidence toward theories on foam/emulsion stabilisation by particles. The origins of foaming in the plant extract solutions was clarified through simple experiments confirming that foaming in hay extracts is due to lignin derivatives and proteins in horse chestnut leaf extract solutions.

8.4 Foaming of extract solutions

8.4.1 Modelling

Statistically significant models could not be generated to describe foamability of hay extract solutions relative to the extraction conditions used to generate the foaming solutions. Variability of the foaming measurements led to the two foamability models generated being poor when considered individually and even when the data sets were combined the model produced was not statistically significant. The learning from this research is that it is difficult to measure (and hence model) foamability of hay extract solutions and that batch to batch variation in the plant materials used for extractions to generate foaming solution makes modelling the foamability of the solutions difficult if not impossible.

Analysis of both sets of foaming data individually showed that higher NaOH concentration and higher extraction temperature gave solutions which generated more foam. Combining the data sets from both sets of measurements demonstrated that NaOH concentration *was* statistically significant in affecting foaming of hay extract solutions. The effect of extraction time was less clear overall though longer extraction times are likely to be beneficial in generating solutions with increased foamability by maximising the amount of extracted material for a specific NaOH concentration and extraction temperature.

8.4.2 Correlations between extract solution properties

Correlations between hay extract solution properties demonstrated that increased % mass extracted from hay correlates with increased solution absorbance, which in turn correlates with increased foamability of the extract solutions. Increased % mass extracted from hay also correlated with increased solution viscosity which in turn correlated strongly with increased foamability of the extract solutions. Solution surface tension showed inverse correlation with solution contact angle as expected though neither of these solution properties showed strong correlation with foaming of the solutions.

Correlations between extract solution properties suggest that better foamability of extract solutions would be achieved by maximising the amount of material extracted from hay, the solution viscosity and the amount of surfactant in hay extract solutions (leading to maximised solution absorbance). The research also demonstrated that NaOH concentration is the most important reaction variable in producing the extract solutions by reaction of hay with NaOH. NaOH concentration has been identified as affecting foaming and also those solution properties which themselves affect foamability of the extract solutions *i.e.* solution viscosity and absorbance at 286 nm. It seems that, without considering cost or environmental implications, the optimum NaOH concentration for extraction of hay to produce foaming solutions is around 3.75 $molL^{-1}$.

8.5 Future research

Opportunities for expansion on the research within this thesis have been identified and a summary is given below.

- To test the hypothesis that foaming would be higher for extract solutions generated above the lignin phase transition temperature (T > 120 °C) due to increased lignin extraction, reactions with NaOH could be performed at high temperature and

subsequent foaming measured. Also it would be interesting to see if the trend of increasing % mass extracted from hay continued at temperatures > 60 °C, as greater extraction of materials would generate more viscous solutions which would have higher foamability.

- To test the hypothesis that % mass extracted from hay by NaOH truly plateaus with reaction time, extractions performed for extended extraction times could be performed. This would also allow testing whether extract solution viscosity increases linearly with more extended extraction times also.
- Extractions should be performed at higher NaOH concentration than in the current research and analysis performed on the composition of the material extracted into solution. This would test the hypothesis that proportionally more non-lignin material (*e.g.* cellulose) is extracted from hay when using higher concentration NaOH. This is interesting because % mass extracted from hay is observed to increase linearly even though extract solution absorbance was observed to plateau when using higher NaOH concentration in extractions in Chapter 5.
- Further experimentation is required to test the hypothesis that oxygen degradation is the mechanism by which lignin in solution is broken down which results in the observed decreased solution absorbance at higher NaOH concentration. To test this would simply require extractions performed under both a nitrogen atmosphere and in air, to look for decrease in solution absorbance with high NaOH concentration used in the extractions performed with air present.
- Use of cryo AFM to examine hay extract foams would allow higher resolution imaging of the particles in the hay foam in its native state. This would allow identification of individual particles amongst agglomerates at foam interfaces and would generate yet more unique and interesting images of particle stabilised foam systems.

- Further cryo SEM examination of alkali plant extract foams using etching on the samples during their preparation would certainly increase the insight into the extract foam microstructures.
- To test the hypothesis that foaming in rice straw extract solution was due to lignin derivatives as in hay, lignin removal from rice straw extract solution should be performed as in section 6.4). This would allow observation of foam suppression and confirm the identity of the material responsible for rice straw extract foaming.
- Study of foamability of hay extract solutions should be performed using a single batch of hay for all experiments to generate the large volumes of solutions which would allow triplicate foaming measurements on the same extract solutions. This would increase the size of the foaming measurement data set. More data on foaming would help understand whether foamability of hay extract solutions can actually be modelled in a statistically significant manner using sparging. At the same time the other hay extract solution properties measured in the current research should be measured and models developed on the corresponding solutions to increase the effectiveness of the modelling of the solution properties and examination of their correlations with foaming.
- Batch by batch variation of plant raw materials could be further investigated by performing modelling studies on different batches of the same plant raw materials.
- Compositional analysis of the raw materials and extract solutions could be included in the input variables for the modelling studies which would give information on which of the specific components of the raw materials which are important in the models of each extract solution properties.

- Other plant raw materials might offer possibilities for producing foaming solutions and screening of other plant materials should be considered as strong colouration of hay extract solutions may make them less easily converted into useful material for incorporation into laundry detergent products. Such strongly coloured extracts make them likely to result in non-white foams being generated from laundry detergent foaming-additives generated from them. Non-white foams are unlikely to be desirable for consumers. Other plant raw materials might produce extracts which generate more acceptably coloured foam.
- Life cycle assessment would be necessary on any processes based on the current research to ensure sustainability and to find the balance required between maximising extraction from materials versus inefficient extraction and utilisation of residues elsewhere *e.g.* as animal feeds; or taken forward for processing through biofuels routes.

8.6 Application of the Principles of Green Chemistry

- The research described in this thesis is part of efforts by P&G to understand foaming of plant extract solutions with a view to using them to promote foaming in greener laundry detergent formulations. The research satisfies the principles of green chemistry as discussed in Table 8.2.

Table 8.2. How this project is in keeping with some of the principles of green chemistry.

Principle		Application
1	**Prevention *(of waste)***	Cellulose enriched residue from alkali extraction of foaming materials from plants, will be less recalcitrant to enzymatic attack than the original plant raw material hence may be valuable for use in biofuel production or inclusion in animal feeds. This means the residue could become a useful commodity and the concept of it being a 'waste material' is removed (Zimmerman and Anastas, 2006). With the right industrial cooperation, process residues could be used elsewhere to maximise the sustainability of the overall process (Deswarte *et al.*, 2007, Octave and Thomas, 2009).
2	**Atom Economy**	Maximising the usefulness of residues at each stage in a supply chain means traditionally considered 'efficient/maximised use' of the raw materials becomes less important. If the 'waste' from one process is used within another series of processes than minimising the volume of the waste stream from an individual process becomes less important. What remains important is maximising the usefulness of the residual material in each sequential process which will require coordinated efforts from the various stakeholders involved (Wilhelm, 2008). Less 'efficient' utilisation of materials as seen by conventional considerations, for a process step in isolation (*e.g.* foam enhancer extraction,) would become tolerable as more steps were added to a manufacturing chain which

		ensured maximum utilisation of raw materials overall.
3	**Less Hazardous Chemical Syntheses**	Surfactants are hazardous to the environmental both in production and use. If less surfactant was required in formulations, required synthesis of surfactant would be less which would decrease its hazards to the environment.
4	**Designing Safer Chemicals**	The sudsing materials produced from plant raw materials will contain bio-synthesised materials and will therefore be inherently biodegradable meaning they are less likely to be damaging to the environment than synthetic surfactants.
6	**Design for Energy Efficiency**	It is intended that the process to produce foam enhancers for detergents will not require energetic milling of the plant raw materials and reactions will be performed at ambient temperature if possible. (Milling was used within the current research to aid dispersion of raw materials in NaOH which was difficult on the lab scale if the plant material was not milled). By not milling the materials and not heating the reactions at manufacturing scale, the overall production process for foaming agents will require less energy. Decreased 'efficiency' of production will be tolerable if the residues can be utilised in other processes.

7	**Use of Renewable Feedstocks**	Plant raw materials used for producing the foam enhancing agents are required to be renewable, and not cultivated for use as foam enhancers in an environmentally damaging manner. The best feedstock would be biomass waste such as straw, leaves from forestry, husk or shells from rice production if possible.
9	**Catalysis**	Laundry detergent formulations incorporating plant based foam enhancers will use catalytic cleaning in the form of relatively small amounts of enzymes, or new catalytic bleaching technologies which could be used to improve cleaning performance where necessary.
10	**Design for Degradation**	Foam enhancers produced by alkali extraction of plant materials should be naturally biodegradable, more so than conventional oil based surfactants.
12	**Inherently Safer Chemistry for Accident Prevention**	Production of plant based foam enhancers will be done through simple reactions using aqueous NaOH at moderate temperature (ambient – 60 °C). By not using high temperatures or pressures in extractions, the safety of employees in producing the materials will be improved. By keeping the extractions simple and not using many different chemicals, the risks associated handling chemicals is reduced hence overall process safety will be higher.

This project represents a step on the road to reducing the reliance of the FMCG industry on oil based and unsustainably produced surfactants. P&G have demonstrated their intentions to use the research in this thesis within future 'greener' products by registering a patent related to the research (Hudson *et al*., 2009). This represents one part of on-going efforts by P&G and indeed, across the FMCG industry to use green chemistry in product development. It is unlikely that sweeping changes will be made in using green chemistry within FMCGs in the short term due to the many barriers to implementation that currently exist (Matus *et al.*, 2012). However, it will be the companies that have the foresight to invest resources in understanding the barriers to implementation of green chemistry and the science of how to overcome them, that will cultivate a more prosperous and sustainable future for their business and for the planet.

8.7 Final thoughts

The research in this thesis was successful in increasing the knowledge of foaming of alkali hay extract foaming. Extraction conditions conducive in promoting various properties of hay extract solutions have been identified through experimentation and data analysis. The findings provide a foundation upon which further research can be built by future researchers in order to continue the work toward improving the sustainability of laundry detergent products.

9 Chapter 9 - Appendices

9.1 Chapter 2

9.1.1 Foams

Foam is an emulsion where a gas is dispersed in the form of bubbles and the continuous liquid phase sits in films between these bubbles.

9.1.2 Surfactants

Surfactants are amphiphilic molecules having hydrophilic and hydrophobic portions within the same molecule as shown in Figure 9.1.

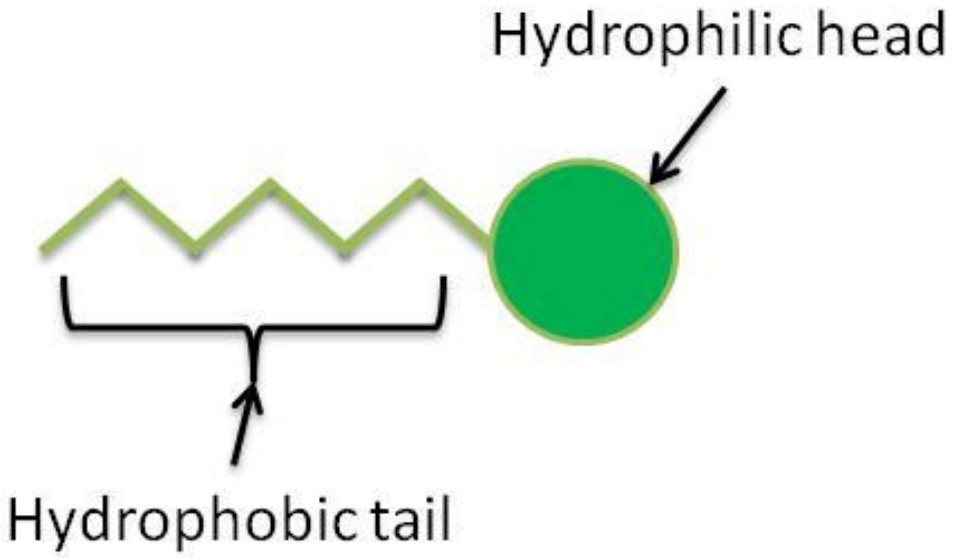

Figure 9.1. Schematic of a surfactant molecule.

Surfactants acts to lower surface tension of liquids. Lowering surface tension by a surfactant decreases the energy penalty associated with increased interfacial area of oily/greasy stains as they are broken down during washing, which makes them useful for cleaning in detergents.

Surface tension is the energy required to increase the interfacial area of a liquid. Molecules within the bulk of a liquid experience attraction in all directions, however at the interface with air for example, the forces experienced by the molecules are imbalanced. Molecules at the interface experience a net force perpendicular to the interface itself which act to pull the molecules back into the solution resisting the growth of an interface as shown schematically in Figure 9.2.

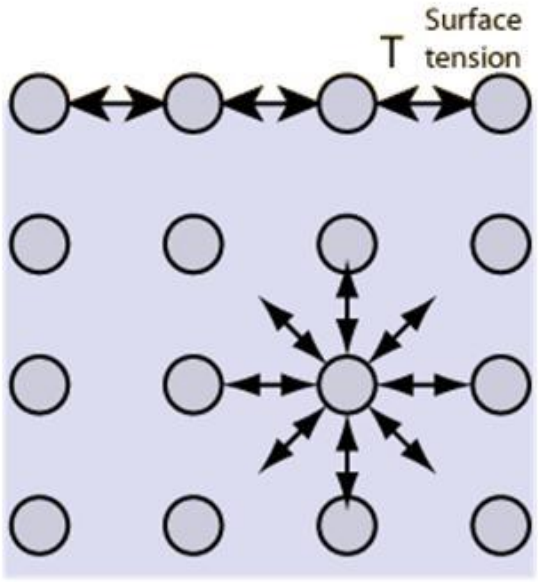

Figure 9.2. Schematic of surface tension of a liquid.

When surfactant is dissolved in solution the surfactant molecules diffuse to the interface and as the surfactant concentration increases so does the coverage of surfactants at the interface as seen in the lower part of Figure 9.3.

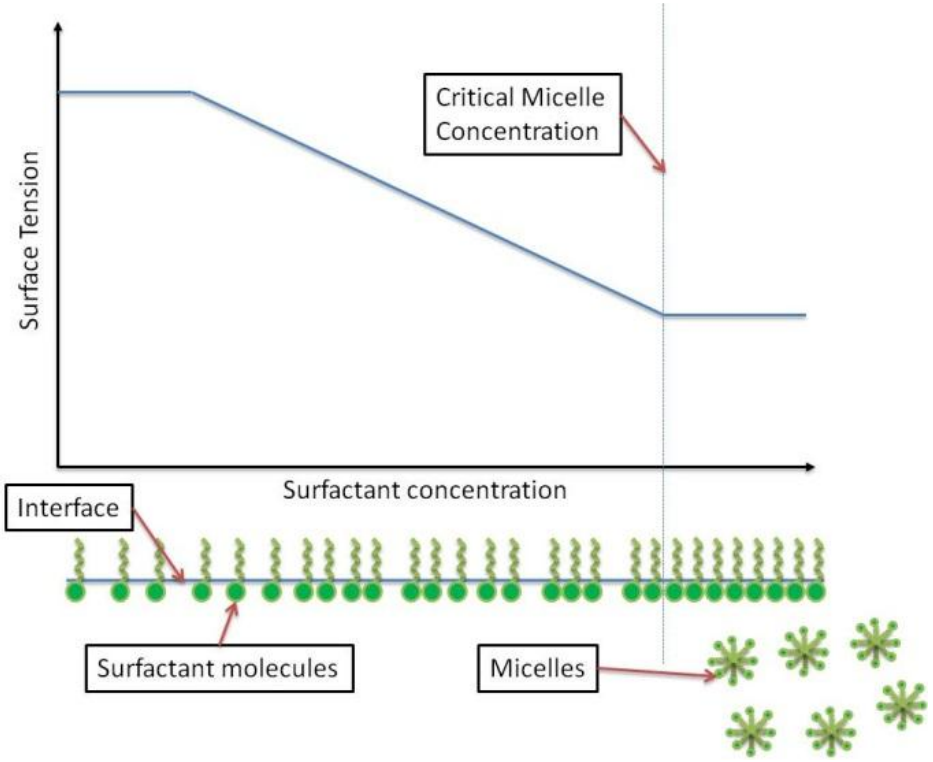

Figure 9.3. Adsorption of surfactant molecules at the interface and micelle formation with increasing surfactant concentration.

Coverage of the interface by surfactant molecules disrupts the cohesive forces between the liquid molecules, reducing the surface tension. The schematic chart in Figure 9.3 shows surface tension change is small for very low surfactant concentrations where the coverage of surfactant at the interface is low. As the concentration of surfactant at the interface builds up, the surface tension decreases further. Decrease in surface tension continues with surfactant concentration increase up to the critical micelle concentration (CMC). The CMC is the concentration of surfactant at which micelles form in solution as shown at the bottom of Figure 9.3.

At concentrations of surfactant greater than the CMC, further adsorption of surfactant at the interface is not possible as the interface is saturated with surfactant. After saturation surfactant concentration increase in solution no longer leads surface tension decrease and any extra surfactant molecules aggregate to form micelles. Micelles are aggregated surfactant molecules where the hydrophobic portion is shielded from the aqueous phase

and maximises contact with the hydrophobic portions of other molecules. This minimises the interaction energy between the hydrophobic tails and the aqueous phase. The hydrophilic portions of the molecules align to maximize contact with the aqueous phase – again minimising the overall energy of the system.

The amphiphilic nature of surfactants allows them to interact with both water and oily/greasy stains on fabrics. The surfactant molecules will attach to molecules in these stains and increase the solubility of these molecules in the wash water. When the oily molecules are solubilised they can be removed from the washing system when the fabrics are rinsed leaving clean fabrics behind. At air water interfaces surfactants will align and orientate themselves with their hydrophilic portion within the aqueous phase and the hydrophobic portion aligned out of the water into the air. The air in a bubble is not hydrophilic hence it is energetically more favourable for the hydrophobic portions of the surfactant molecules to be orientated into the air and hydrophilic portions to be orientated into the aqueous solution.

9.1.3 The Marangoni effect

The Marangoni effect arises due to surface tension gradients coming from varying surfactant concentration in different areas of a curved bubble interface (Franke and Pahl, 1997). Figure 9.4 shows surfactant molecules adsorbed at the interface of a bubble.

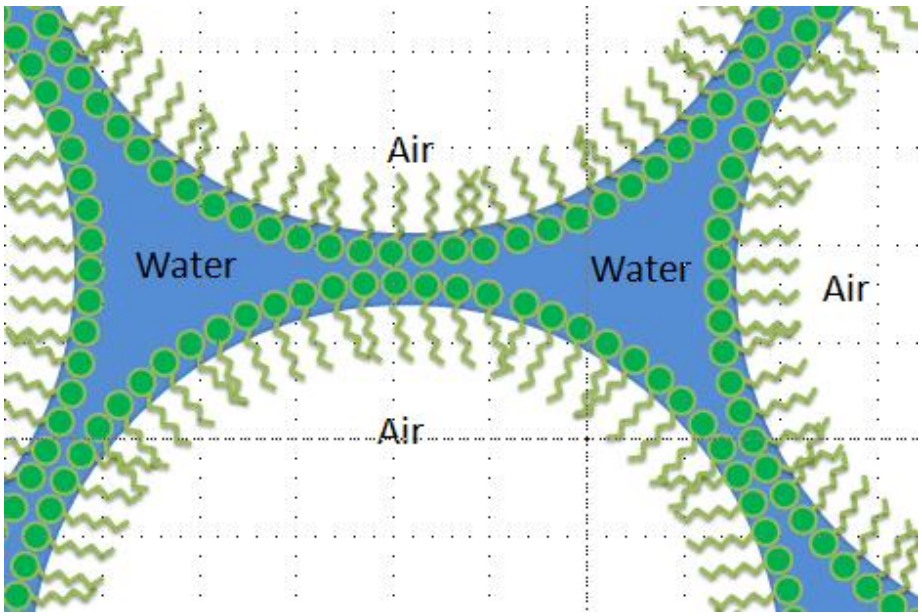

Figure 9.4. The arrangement of surfactant molecules at the interface in foams.

As bubbles form, their interfacial area increases rapidly which spreads out the surfactant molecules at the interface – effectively decreasing the surfactant concentration at the interface. Lowering the amount of surfactant at the interface locally increases the surface tension. Areas of low surfactant concentration have higher surface tension than areas with higher concentration of surfactant. Surfactants at the interface set up surface tension gradients in films and give bubbles stability (Garrett, 1993). These surface tension gradients effectively 'drag' liquid with the expanding interface stopping it rupturing. Ultimately equilibrium between the surface tension across the bubble surface is restored again when the interface is covered in surfactant once more. Surfactants therefore stabilise bubbles by distributing surface tension across the whole bubble. Distribution of tension within the interface keeps a bubble stable during expansion and allows more liquid flow into films as they expand. After formation of a thin liquid film, thermal motion of surfactant molecules and the influence of gravity on a liquid within a film cause liquid drainage. Liquid drainage in thin films can lead to surfactant concentration variation at the interface, as can diffusion/movement of the surfactant molecules around/into and out of the interface.

Surfactants diffuse at an interface in such a way as to minimise the energy of the system hence stabilising the bubble.

9.1.4 'Conventional' (oil derived, small molecule) surfactant foams

Foams are generated when stable bubbles accumulate and become interlinked. Bubbles are made up of films of water between layers of surfactant molecules adsorbed at the interface between the water and air inside/outside the film. Where the films of multiple bubbles intersect is called a 'Plateau border'. Most of the water in the continuous phase of a foam will be found in the Plateau border. Foams made from surfactants in water are gas-like in that their volume is proportional to temperature and pressure; liquid-like in that they can flow without breaking and take the shape of the vessel they are contained in and solid-like in that under small shear, forces bubbles in foams distort without rearrangement.

Foams can form by agitation/whipping or sparging of solutions containing some kind of foaming agent (pure solutions do not give stable foams). Small molecule surfactants are particularly effective at generating foam as they migrate to the interface rapidly which is an important factor in generating stable foams. If a surfactant molecule cannot migrate to the interface rapidly then as a bubble forms, and the area of the interface increases, surfactant may not be able to adsorb at the interface rapidly enough to maintain surface tension equilibrium. If surfactant is not present as the surface expands the tension will increase to the point where catastrophic foam rupture will occur and no stable bubble will form. When surfactants migrate to an air-water interfaces to form a bubble, they form an electrostatic double layer where repulsion between surfactant molecules cause a disjoining pressure between the molecules which overcomes the Van der Waals forces trying to pull the molecules together.

Optimum foam formation and stability for a given surfactant occurs at surfactant concentration slightly higher than the CMC of the surfactant in the conditions used. The CMC of the surfactant is related to the hydrophilicity/hydrophobicity of the surfactant and decreases with increasing chain length in the hydrophobic alkyl chain of surfactants (Lin, 1972, Zhang and Marchant, 1996) as illustrated in the schematic in Figure 9.5.

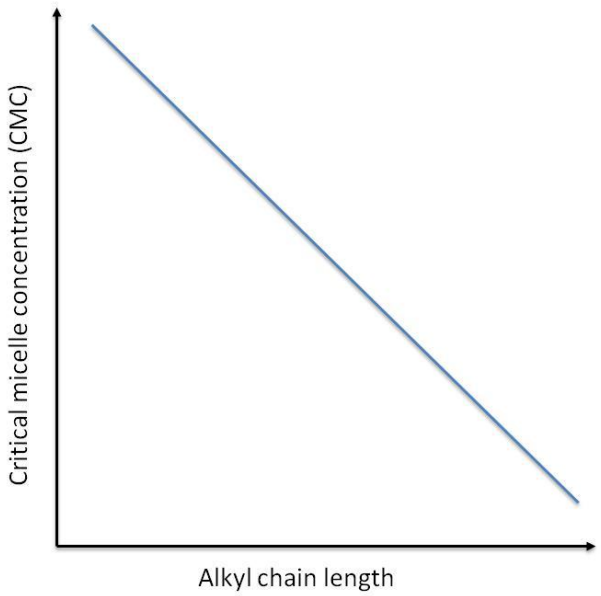

Figure 9.5. CMC vs alkyl chain length for small surfactants.

With increasing alkyl chain length (increasing hydrophobicity), the surfactants adsorb more strongly at the interface which aids foam stability. Increasing alkyl chain length in surfactant molecules also means they adsorb at the interface more slowly. Slower adsorption at the interface impedes stable foam formation. Foams are inherently unstable and are constantly trying to change to a lower energy configuration.

9.1.5 Foam coarsening/disproportionation

Foam coarsening is another effect that disrupts foam stability. Coarsening is when the overall average bubble size in a foam increases as the foam ages. This can occur when smaller bubbles coalesce and form larger bubbles or when the gas in smaller bubbles diffuses through the continuous (liquid) phase of the foam and into larger bubbles.

Gas diffusion from smaller to larger bubbles leads to the larger bubbles becoming larger and the smaller bubbles eventually disappearing, this is called 'disproportionation'. Gas diffusion from smaller to larger bubbles occurs when the gas is soluble in the continuous phase of the foams. The 'Young-Laplace effect' whereby the pressure of the gas inside smaller bubbles is higher than in the larger bubbles (Stevenson, 2010) leads to dissolution of gas from the smaller bubbles into the continuous phase where it then diffuses into the larger bubbles driving foam coarsening. Figure 9.6 shows two bubbles and their associated pressure difference.

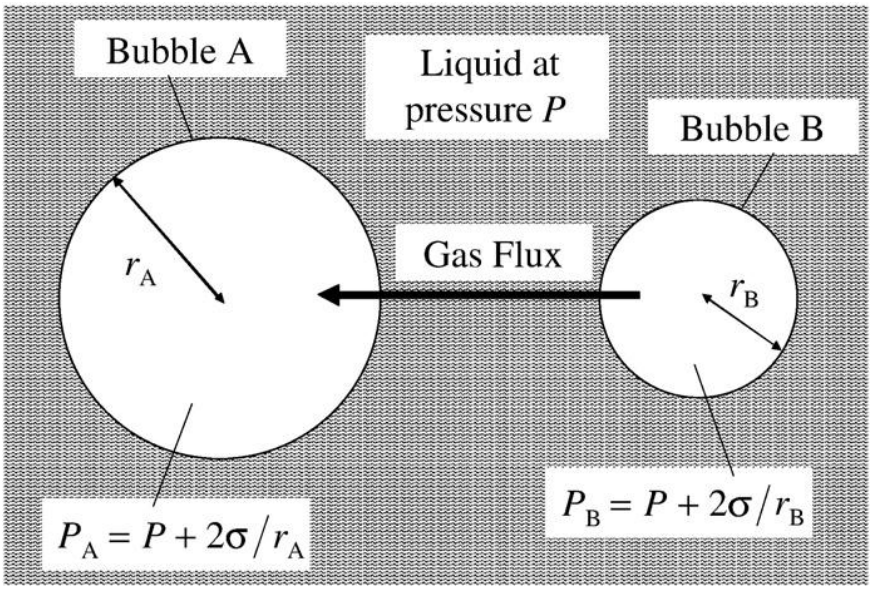

Figure 9.6. Inter-bubble gas diffusions due to pressure differences within the bubbles. (Reproduced from Stevenson, 2010)

The pressure in each bubble is given by equation Equation 9.1:

Equation 9.1. The pressure inside a spherical bubble

$$P_x = P + \frac{2\sigma}{r_x}$$

Where P_x is the pressure inside bubble x (where x is A or B); P is the pressure in the liquid continuous phase; σ is the surface tension of the interface and r_x is the radius of bubble x.

The diffusion of gas out of bubbles is possible as the surfactants at the interface are in a dynamic state where molecules desorb and are rapidly replaced. On these short time scales, loss of gas molecules from within the bubbles through the gap created by desorbing surfactant molecules occurs, hence diffusion of the gas out of the bubble. Foam coarsening is similar to Ostwald ripening in liquid emulsions where larger droplets increase in size at the expense of smaller droplets.

Stabilisation of foams against coarsening can be achieved by changing the nature of the bubbles in the foams. One way of changing the nature of the bubbles within the foam is producing foams with a uniform bubble size. If this is achieved then the Laplace pressure inside the bubbles should be the same for all bubbles therefore coarsening by diffusion of gas from smaller to larger bubbles would not occur. This has been observed and reported in the literature though bubbles at the surface of accumulations of such individual bubbles do not benefit from stability of surrounding bubbles with equal gas pressure and hence themselves are not truly stable (Vignes-Adler and Weaire, 2008). Another way to stabilise against coarsening is to reduce the solubility of the gas phase in the liquid phase which limits gas diffusion between bubbles. For laundry detergent applications producing uniform bubbles or reducing gas solubility to stabilise foams is impossible.

9.1.6 Particle stabilised foams

Pickering stabilisation is named after Percival Spencer Umfreville Pickering who first described stabilisation of emulsion by adsorbed particles in 1907 (Pickering, 1907). Pickering stabilisation is the stabilisation of emulsions and foams by particles. Pickering stabilisation of foams is extensively examined in the literature (Murray and Ettelaie, 2004, Sethumadhavan *et al.*, 2004, Blute *et al.*, 2007, Mileva and Exerowa, 2008, Sani and Mohanty, 2009, Dickinson, 2010, Rodrigues *et al.*, 2011) and can lead to very stable foams. The stability of Pickering stabilised bubbles can be such that distortion of the bubbles or manipulation of the bubbles can be performed to the extent where ellipsoidal and even toroidal armoured bubbles (where the surface is covered /'armoured' by particles) have even been described by Bala Subramaniam *et al.* (2005). Particles with the right surface energy/contact angle at the interface and high enough surface area (*i.e*. small enough particle size) adsorb and form a layer around the outside of the dispersed (gas) phase. The energy of separation of the particle from the interface is very high. High energy of detachment of particles from the interface effectively makes the particles irreversibly bound (Binks, 2002).

If a droplet or bubble is to shrink then any particles adsorbed at the interface must be at least partially removed from the surface, which is very difficult given the high energy required to remove the particles. Therefore adsorption of particles at the interface makes droplets or bubbles quite stable to shrinkage as would happen if gas were to diffuse out of the bubble so disproportionation through gas diffusion out of bubble cells can be severely restricted and the stability of such bubbles can be indefinite (Du *et al.*, 2003).

The optimum contact angle for particles to be strongly adsorbed at an interface is 90° hence the hydrophobic/hydrophilic balance of the particle must be right (similar to the hydrophilic-

lipophilic balance for surfactants). The particles' required hydrophobicity means that they are likely to aggregate in the aqueous phase which can slow or impede their ability to adsorb rapidly at an interface (Murray and Ettelaie, 2004). Elsewhere in the literature the stabilising effect of particles is attributed to 'clogging' Plateau borders hence impeding liquid drainage from films or increasing the apparent viscosity of the liquid held within the films which again would reduce film drainage and hence lead to increased foam stability (Sethumadhavan *et al.*, 2001).

9.2 Chapter 3

9.2.1 The sparging nozzle

The bubbles were produced using a glass sparging nozzle made by Steve Williams within the School of Chemistry at the University of Birmingham. The sparging nozzle was made with a number 1 glass frit which has pores sizes in the range 100 – 160 µm. The nozzle was mounted in the sparging rig using the rubber bung/connector shown schematically in Figure 9.7.

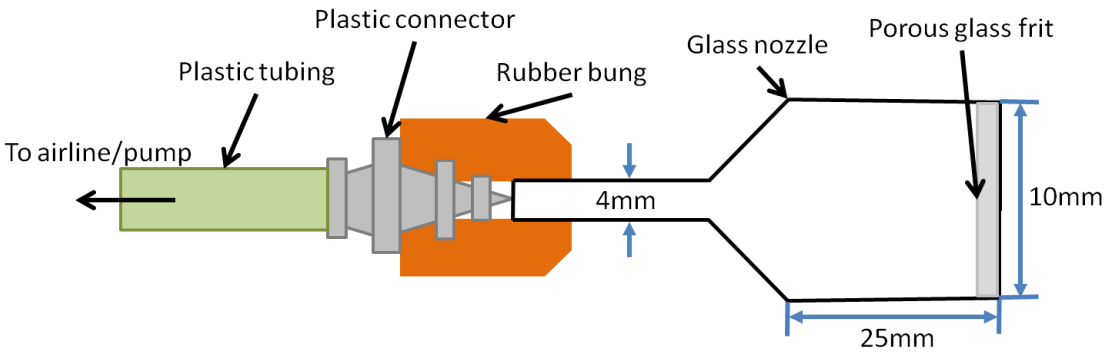

Figure 9.7. The configuration used for inserting the glass sparging nozzle into the sparging rig shown in Figure 3.7

9.2.2 UV-vis absorbance of solutions

UV-vis spectroscopy is used to examine the absorbance of electromagnetic radiation by a solution across a range of wavelengths in the ultraviolet (*UV*) and visible (*vis*) regions.

Absorbance of light by solutions occurs as the electrons of the dissolved substances absorb photons of light and become excited. Excitation of the electrons occurs when the energy required for the electron excitations is the same as the energy of incident photons of light (Atkins, 1996). A UV-vis spectrometer is able to expose solutions to light of narrow energy ranges (wavelengths) and measure at the amount of light absorbed/transmitted by solutions. This absorbance of the solution is characteristic of the amount of light absorbing material dissolved in the solution according to *Beer-Lambert Law.*

Equation 9.2. The Beer-Lambert law.

$$\text{Beer} - \text{Lambert Law: Absorbance} = \log\frac{I_0}{I} = \varepsilon cl$$

Where I_0 = the intensity of the incident light; I is the intensity of the light emerging from the sample; ε = the molar absorptivity of the dissolved substance (a measurement of how strongly a chemical species absorbs light at a given wavelength); c = the concentration of the absorbing substance; l = the path length of the cell used for the measurement (= 1 cm).

For the purposes of examining the solutions generated during this research the reaction conditions during alkali extraction of hay was varied and the UV-vis absorbance of the reaction products was measured. The exact species responsible for the solutions absorbance was unknown and is unlikely to be a single identifiable molecule therefore generating a calibration curve to allow quantitative measurements of the amounts of materials dissolved in solution was not possible.

9.2.3 Viscosity measurement

The viscosity for solutions generated by NaOH extraction of hay was found to not vary with shear rate be above around 30 s^{-1} as shown in Figure 9.8, hence the viscosity of the solutions was measured at 94s^{-1}. (Note the use of a logarithmic scale for the *x*-axis (shear rate).

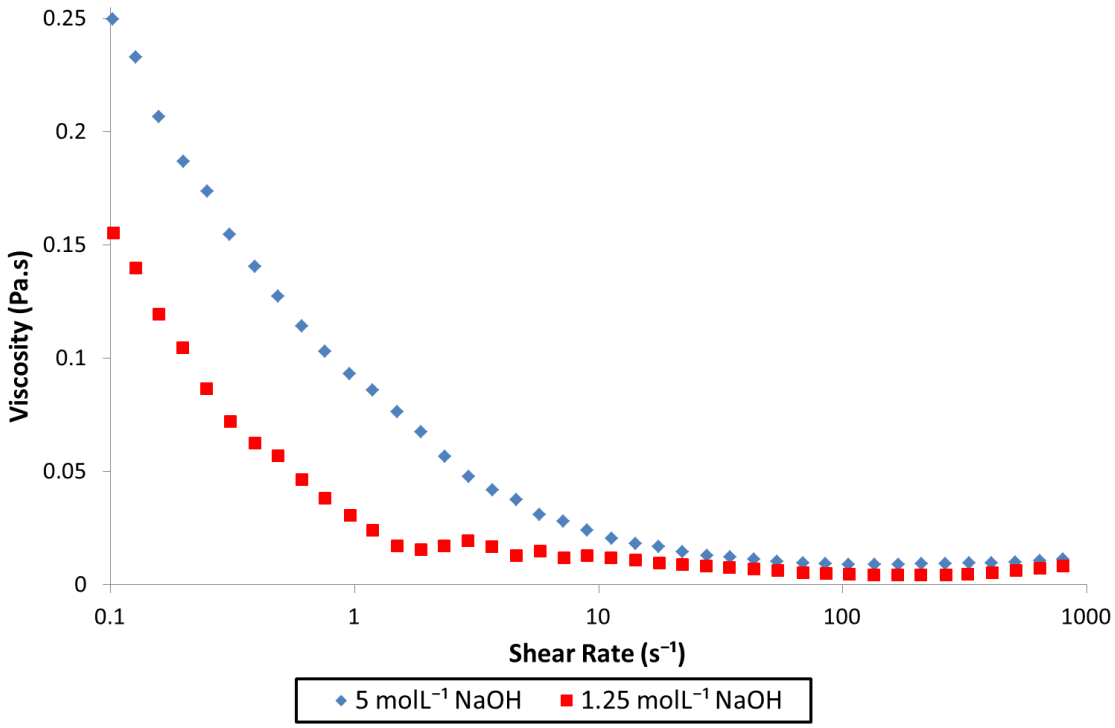

Figure 9.8. Viscosity vs. shear rate for alkali hay extract solutions.

9.2.4 Scanning electron microscopy

The principles of scanning electron microscopy (SEM) are similar to those of optical microscopy, though a focussed electron beam is used to irradiate samples instead of light. Electromagnet coils and electric potentials are used to manipulate an electron beam similarly to glass optics being used to manipulate light in optical microscopy. Using electrons instead of light means SEM achieves a much higher resolution (< 100 nm) than optical microscopy (maximum of ~0.5 μm). The limit of spatial resolution is defined as the minimum distance that can separate two objects and the objects can still be distinguished as separate.

The limit of resolution is dependent on the wavelength being used to image the objects according to Abbe's equation (Zhou *et al.*, 2007):

Equation 9.3. Abbe's equation linking resolution with wavelength of imaging radiation.

$$d = \frac{0.612\lambda}{n \sin \alpha}$$

Where d = effective resolution distance; λ = wavelength of the imaging radiation; n = index of refraction medium between point source and lens relative to free space; α = half the angle of the cone of light from specimen plane accepted by the objective (half aperture in radians). Abbe's equation demonstrates that resolution is proportional to wavelength of the imaging radiation, hence smaller wavelengths of radiation will result in the ability to resolve smaller objects.

Electrons have a wavelength associated with them due to wave-particle duality and their wavelength is calculated according to Equation 9.4:

Equation 9.4. The de Broglie equation.

$$\lambda_e = \frac{h}{m_e v}$$

Where λ_e = the wavelength of the electrons; h = the planck's constant (= 6.63 x 10^{-34} Js); m_e = the mass of an electron (= 9.11 x 10^{-31} kg); v = the velocity of the electrons. Electrons can have wavelengths of the order of picometres (10^{-12} m), whereas light has a wavelength of the order of nanometres (10^{-9} m). Therefore, according to Abbe's equation the resolution of SEM is considerably higher than for optical microscopy. The resolution of SEM can be increased by using higher velocity electrons in the incident beam (higher velocity gives shorter wavelength electrons), which can be straightforwardly generated by using a higher accelerating potential on the electron beam though. However higher energy electrons can cause sample degradation especially in delicate samples. Images are generated when

electrons from the beam are scattered or dislodge other sample electrons after interaction with the sample. The scattered/dislodged electrons are captured by a detector to generate an image.

9.2.5 Atomic force microscopy

Atomic force microscopy (AFM) uses a high resolution scanning probe microscope with resolution possible down to the atomic scale in favourable experimental set-ups and samples (Binnig *et al.*, 1987). AFM was used within this project as the resolution of cryo-SEM used to examine the foams was not sufficient to see the microstructure in sub-micron particles identified in SEM images. It was the aim that AFM could probe these sub-micron particles and give more detail about whether these particles were themselves agglomerates.

An AFM measures force between a surface and an atomically sharp probe tip which is rastered in the *x*-*y* plane across a surface with the deflection of the cantilever in the z axis precisely monitored and controlled using a laser/photodetector, with piezoelectric feedback to control the height (or force) of the probe (Hansma and Pietrasanta, 1998).

AFM can be run in contact mode (where contact between the tip and the surface is maintained), non-contact mode (where the tip is maintained at a specified distance from the surface) and intermittent contact (tapping) mode. Tapping mode was used for the dried alkali hay extract foam samples in this research and involves the cantilever being deflected up and down, oscillating near to the resonant frequency of the cantilever. Interactions between the tip and surface mean that the amplitude of oscillation decreases as the probe approaches the surface. The piezoelectric actuator is controlled in order to maintain the amplitude of oscillation of the probe by moving it up and down as it passes over the surface (Bowen *et al.*, 2009). A schematic demonstrating the probe used by an AFM is shown in Figure 9.9.

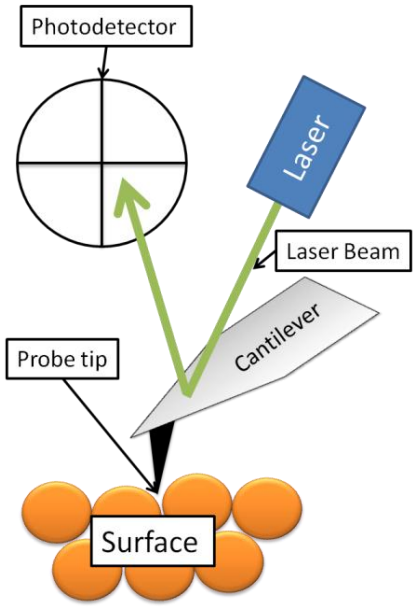

Figure 9.9. A basic AFM set-up.

AFM resolution is limited by the size of the probe/sample volume of interaction, hence better resolution comes from smaller probes. AFM can be performed at atmospheric pressure in air, or even submerged in a liquid, unlike conventional or cryogenic SEM. Disadvantages of AFM include slow image formation due to the need for rastering over the sample area, limited sample area size and limitations on resolution which arise due to the quality of scanning tips (Morita, 2007). A specific disadvantage of AFM when used within this project was that samples had to be presented in dried form rather than the original wet foam sample. AFM was still used with this in mind, as it was considered possible that the particles observed in the frozen wet foam during cryogenic SEM, would still be apparent in AFM imaging.

9.2.6 ANOVA of the models in Chapter 5 and Chapter 7

ANOVA is the analysis of the variance associated with the models generated and gives statistical information on how well the models developed described the measured experimental data (*i.e.* compare how closely the models would have predicted the measured

experimental values measured). Results of ANOVA are given in the ANOVA tables and discussed in Chapter 5 and Chapter 7.

An explanation of the terms found in the ANOVA tables is given below:

- The sum of squares

The sum of squares is the sum of the square of the difference between the individual measurements and the average measurement of the respective responses. It is calculated using Equation 9.5:

Equation 9.5. Calculation of the sum of squares used in ANOVA.

$$\text{sum of squares} = \sum_{i=1}^{n} (y_i - \bar{y})^2$$

The total sum of squares (C.total) for a model takes a contribution from the measurements made and the model itself, from the lack of fit of the model (*i.e.* how the experimental data deviate from the model) and from pure errors. The size of the sum of squares will vary according to the size of the measurements made.

- Degree of freedom (DF)

The number of independent pieces of information that go into the estimate of a parameter is called the degrees of freedom.

- R^2

Gives a measure of how well the experimental data fits the model generated. $R^2 = 1$ would indicate that the model perfectly described the experimental data. For the current research $R^2 > 0.8$ indicates a robust model.

- R^2 adjusted

The R^2 adjusted value penalises a model for inclusion of unnecessary terms within a model. This is useful as the R^2 value for a model can be artificially improved by simply including more terms in the model, whereas the adjusted R^2 value would penalise the model for this. R^2 should be close to the R^2 adjusted value for a robust model.

- (Prob> F) for analysis of variance

If the model generated is able to describe the experimental data in a statistically significant manner (*i.e.* if the model is robust) then Prob> F will have a value < 0.05 indicating statistical significance of the description of the data by the model. This is a measure of how the level of confidence in how well the model can describe the experimental data when using the relevant reaction parameters in the model.

- (Prob> F) for lack of fit

If there is a lack of fit between the experimental data and the model it will be shown as the lack of fit having statistical significance and Prob> F will have a value < 0.05. This is a measure of confidence in stating that there is no lack of fit of the model to the data at points between those where experimental measurements of the response were made.

- p-value

p-values indicate significance/confidence or otherwise of a particular parameter relevant to the generated models. Generally, if the p-value is < 0.05 then whichever term the p-value is describing can be deemed statistically significant with 95% confidence.

9.3 Chapter 5

9.3.1 Actual versus predicted plots for the models

Plots of actual value of the measured response versus the value predicted by the models were generated using the JMP® software (Version 9.0.2, SAS Institute Inc., Cary, NC, 2010). and are given below in Figure 9.10 - Figure 9.15.

The red dashed lines represent the 95% confidence intervals, the solid red line represents the line where the measured and predicted values are equal and the blue line represents the average measured response.

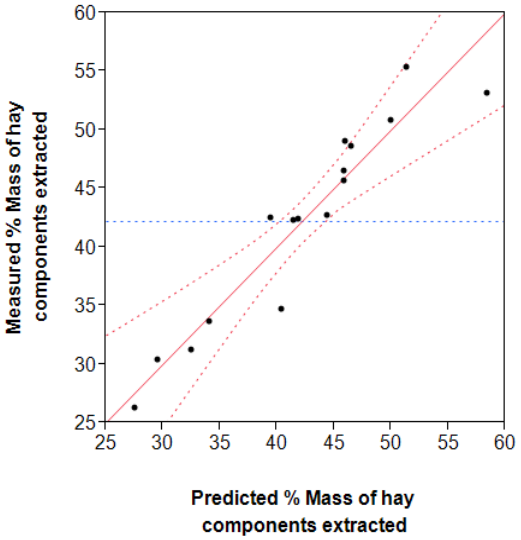

Figure 9.10. % Mass extracted from hay

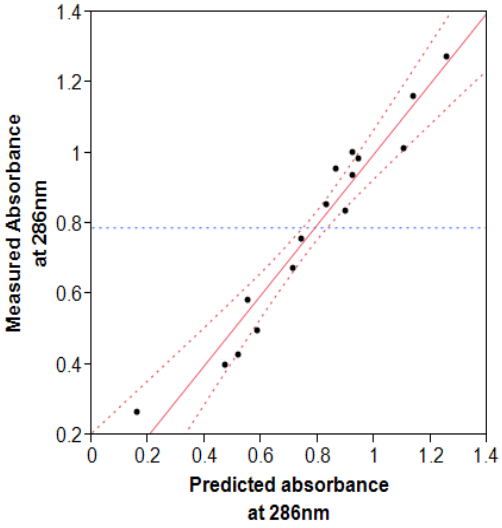

Figure 9.11. Absorbance at 286 nm

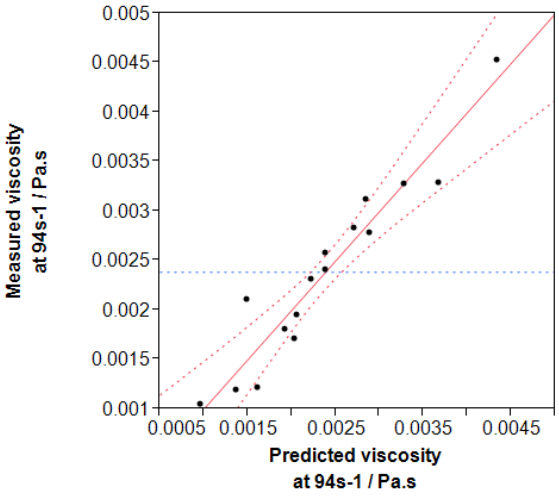

Figure 9.12. Viscosity

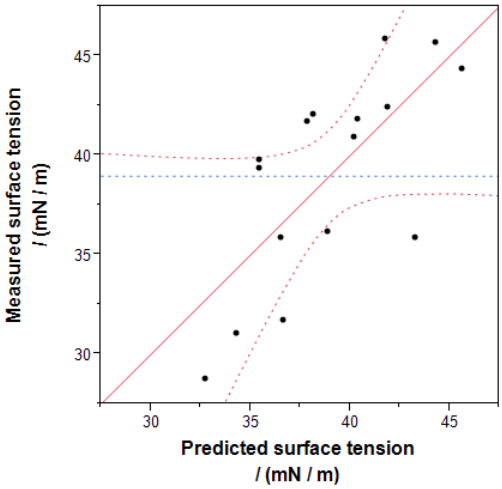

Figure 9.13. Surface tension

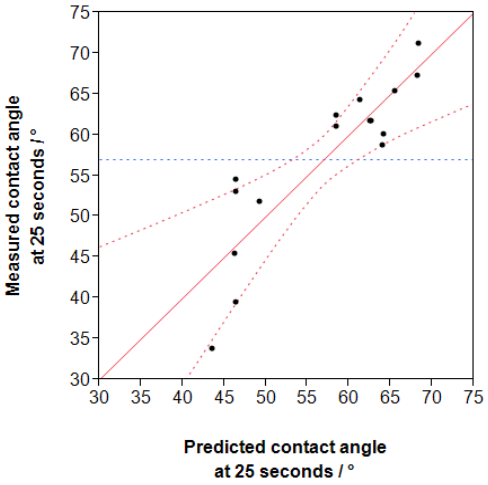

Figure 9.14. Contact angle

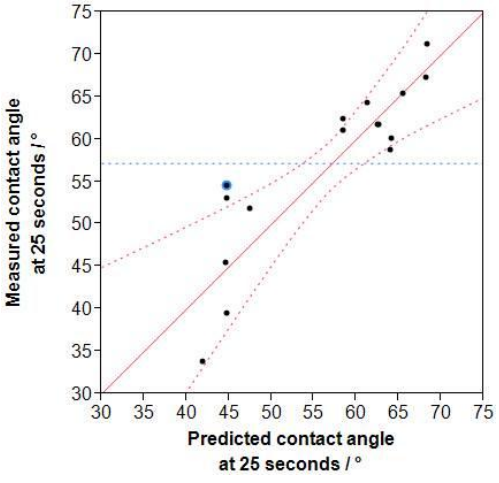

Figure 9.15. Predicted contact angle with highlighted data point removed to improve the model.

9.3.2 Residual plots for the models

A residual error (residual) is the amount by which the measured experimental data differs from the value predicted by the model for a particular measurement. A larger residual indicates that the model does not describe a particular data point well. Residuals from the measurements performed should have a random appearance if no systematic experimental error was occurring during experimentation and measurement. If a systematic experimental error was occurring over time (*e.g.* a calibration drift in a measurement) then the residual plots could show this by showing a pattern to them thus residual plots allow quick and easy checking of the data for problems.

The residual plots given below were generated using the JMP® software (Version 9.0.2, SAS Institute Inc., Cary, NC, 2010). The *x*-axis row number simply refers to the position of the data point in the table. The *y*-axis shows the magnitude of the residual for the data point. Residual plots for each of the responses are given on the next page.

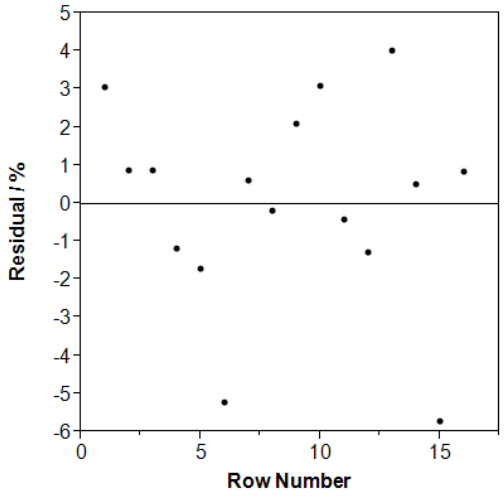

Figure 9.16. % Mass extracted from hay residuals plot.

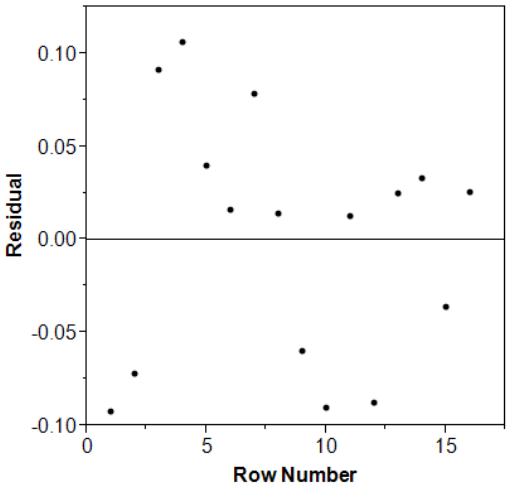

Figure 9.17. Absorbance at 286 nm residuals plot.

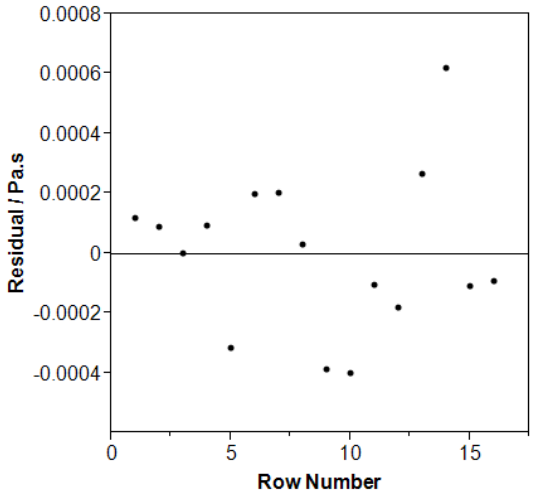

Figure 9.18. Viscosity residuals plot.

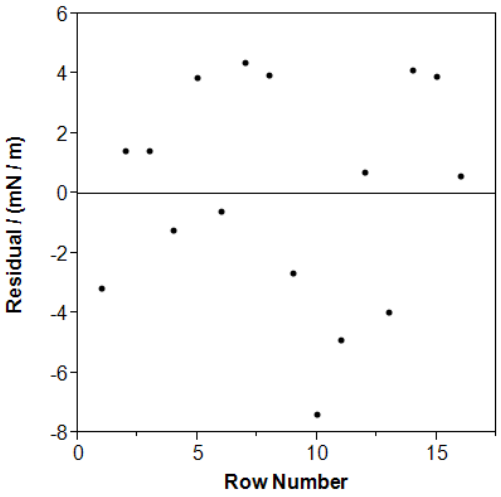

Figure 9.19. Surface Tension residuals plot.

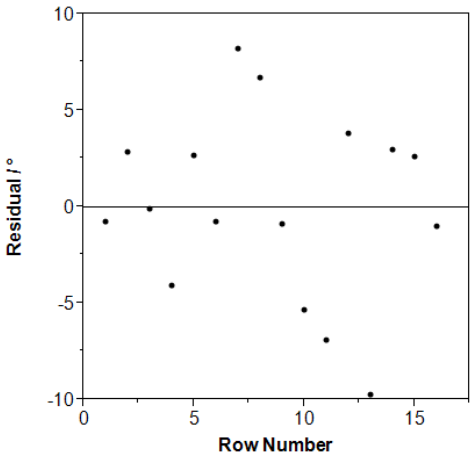

Figure 9.20. Contact angle residuals plot.

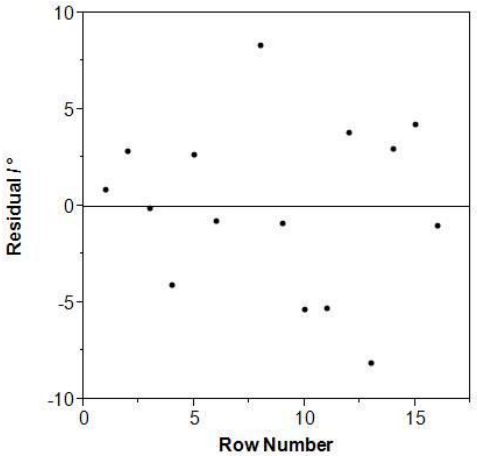

Figure 9.21. Contact angle with data point removed residuals plot.

9.4 Chapter 7

9.4.1 Foamability index calculation

Excel handles time as a decimal fraction in order to make calculations using time easier. This means that 00:00:00 or 24:00:00 are equal to 1. Excel handles the time 18:00:00 as = 0.75 because it is three quarters of one whole 24 hour period.

The calculation of the gradients which represent the foamability index of the hay extract solutions in Chapter 7 is the form:

$$foamability\ index = \frac{foam\ height_{t2} - foam\ height_{t1}}{t_2 - t_1}$$

Where t_1 = decimal fraction time 1 and t_2 = decimal fraction time 2. As t_1 and t_2 are decimal fractions representing proportions of a 24 hours period they are dimensionless. This means the foamability index has dimensions of length only, hence the units of foamability index are cm.

10 References

AJANOVIC, A. 2011. Biofuels versus food production: Does biofuels production increase food prices? *Energy,* 36**,** 2070-2076.

AKIN, D. 2008. Plant cell wall aromatics: influence on degradation of biomass. *Biofuels, Bioproducts & Biorefining,* 2**,** 288-303.

ALVAREZ, N. J., WALKER, L. M. & ANNA, S. L. 2009. A non-gradient based algorithm for the determination of surface tension from a pendant drop: Application to low Bond number drop shapes. *Journal of Colloid and Interface Science,* 333**,** 557-562.

ANASTAS, P. T. & KIRCHHOFF, M. M. 2002. Origins, current status, and future challenges of green chemistry. *Accounts of Chemical Research,* 35**,** 686-94.

ANASTAS, P. T. & WARNER, J. C. 1998. *Green Chemistry: Theory and Practice, 30,* New York, Oxford University Press.

ANASTAS, P. T. & ZIMMERMAN, J. B. 2003. Peer Reviewed: Design Through the 12 Principles of Green Engineering. *Environmental Science & Technology,* 37**,** 94A-101A.

ARDITTY, S., SCHMITT, V., LEQUEUX, F. & LEAL-CALDERON, F. 2005. Interfacial properties in solid-stabilized emulsions. *European Physical Journal B,* 44**,** 381-393.

ARISOY, M. 1998. The effect of sodium hydroxide treatment on chemical composition and digestibility of straw. *Turkish Journal of Veterinary and Animal Sciences,* 22**,** 165-170.

ATKINS, P. W. 1996. *The Elements of Physical Chemistry, Page 436*, Oxford University Press.

BALA SUBRAMANIAM, A., ABKARIAN, M., MAHADEVAN, L. & STONE, H. A. 2005. Colloid science: Non-spherical bubbles. *Nature,* 438**,** 930-930.

BANIPAL, P. K., CHAHAL, A. K., SINGH, V. & BANIPAL, T. S. 2010. Rheological behaviour of some saccharides in aqueous potassium chloride solutions over temperature range 288.15 to 318.15K. The *Journal of Chemical Thermodynamics,* 42**,** 1024-1035.

BANIPAL, P. K., SINGH, V., CHAHAL NEE HUNDAL, A. K. & BANIPAL, T. S. 2011. Effect of sodium acetate on the rheological behaviour of some mono-, di-, and tri-saccharides in aqueous solutions over the temperature range 288.15 to 318.15K. *The Journal of Chemical Thermodynamics,* 43**,** 290-299.

BARNES, H. A., HUTTON, J. F. & WALTERS, K. 1991. *An Introduction to Rheology, Page 12*, Elsevier.

BATCHELOR, S. N., DIXON, S. & WHIETOAK, C. J. 2007. *Laundry Composition*, WO2007147698.

BETSCHART, A. & KINSELLA, J. E. 1973. Extractability and solubility of leaf protein. The *Journal of Agricultural and Food Chemistry,* 21**,** 60-65.

BETTIOL, J.-L. P., MOSS, M. A. J., THOEN, C. A. J. K., BOYER, S. L., SHOWELL, M. S. & JEFFREY, J. 1998. *Amylase-containing detergent compositions*. United States patent application 5783546.

BEVERUNG, C. J., RADKE, C. J. & BLANCH, H. W. 1999. Protein adsorption at the oil/water interface: characterization of adsorption kinetics by dynamic interfacial tension measurements. *Biophysical Chemistry,* 81**,** 59-80.

BIKERMAN, J. J. 1973a. *Foams, 13, 14*, Springer-Verlag.

BIKERMAN, J. J. 1973b. *Foams, 77 - 79,* New York, Springer-Verlag.

BIKOVA, T. & TREIMANIS, A. 2004. UV-absorbance of oxidized xylan and monocarboxyl cellulose in alkaline solutions. *Carbohydrate Polymers,* 55**,** 315-322.

BILLA, E., KOUKIOS, E. G. & MONTIES, B. 1998. Investigation of lignins structure in cereal crops by chemical degradation methods. *Polymer Degradation and Stability,* 59**,** 71-75.

BINKS, B. P. 2002. Particles as surfactants--similarities and differences. *Current Opinion in Colloid & Interface Science,* 7**,** 21-41.

BINNIG, G., GERBER, C., STOLL, E., ALBRECHT, T. R. & QUATE, C. F. 1987. Atomic resolution with atomic force microscope. *Surface Science,* 189–190**,** 1-6.

BINOD, P., SINDHU, R., SINGHANIA, R. R., VIKRAM, S., DEVI, L., NAGALAKSHMI, S., KURIEN, N., SUKUMARAN, R. K. & PANDEY, A. 2010. Bioethanol production from rice straw: An overview. *Bioresource Technology,* 101**,** 4767-74.

BLUTE, I., PUGH, R. J., VAN DE PAS, J. & CALLAGHAN, I. 2007. Silica nanoparticle sols: 1. Surface chemical characterization and evaluation of the foam generation (foamability). *Journal of Colloid and Interface Science,* 313**,** 645-655.

BOWEN, W. R., HILAL, N. & KNOVEL 2009. *Atomic force microscopy in process engineering : introduction to AFM for improved processes and products, 10,* Burlington, MA, Butterworth-Heinemann.

BRADFORD, M. M. 1976. A rapid and sensitive method for the quantitation of microgram quantities of protein utilizing the principle of protein-dye binding. *Analytical Biochemistry,* 72**,** 248-254.

BRANDT, K. K., HESSELSOE, M., ROSLEV, P., HENRIKSEN, K. & SORENSEN, J. 2001. Toxic effects of linear alkylbenzene sulfonate on metabolic activity, growth rate, and microcolony formation of Nitrosomonas and Nitrosospira strains. *Applied and Environmental Microbiology,* 67**,** 2489-98.

BROUWER, S. J. & WINT, M. J. 2000. *Powder detergent composition and method of making*, WO1997033961.

BURNS, M. E., GRAYDON, A. R., LABEQUE, R., PERKINS, C. M., SADLOWSKI, E. S. & WILLIAMS, B. K. 2003. *Bleach compositions*, US20030040451.

CASSMAN, K. & LISKA, A. 2007. Food and fuel for all: realistic or foolish? *Biofuels, Bioproducts & Biorefining,* 1**,** 18-23.

CHAUDHRY, A. S. 1998. Nutrient composition, digestion and rumen fermentation in sheep of wheat straw treated with calcium oxide, sodium hydroxide and alkaline hydrogen peroxide. *Animal Feed Science and Technology,* 74**,** 315-328.

CHAUDHRY, A. S. 2000. Rumen degradation in sacco in sheep of wheat straw treated with calcium oxide, sodium hydroxide and sodium hydroxide plus hydrogen peroxide. *Animal Feed Science and Technology,* 83**,** 313-323.

CHAUDHRY, A. S. & MILLER, E. L. 1996. The effect of sodium hydroxide and alkaline hydrogen peroxide on chemical composition of wheat straw and voluntary intake, growth and digesta kinetics in store lambs. *Animal Feed Science and Technology,* 60**,** 69-86.

CHEN, H., TANG, T. & AMIRFAZLI, A. 2012a. Fabrication of polymeric surfaces with similar contact angles but dissimilar contact angle hysteresis. *Colloids and Surfaces A,* 408**,** 17-21.

CHEN, W., WANG, W.-P., ZHANG, H.-S. & HUANG, Q. 2012b. Optimization of ultrasonic-assisted extraction of water-soluble polysaccharides from Boletus edulis mycelia using response surface methodology. *Carbohydrate Polymers,* 87**,** 614-619.

CHIESA, S. & GNANSOUNOU, E. 2011. Protein extraction from biomass in a bioethanol refinery - Possible dietary applications: Use as animal feed and potential extension to human consumption. *Bioresource Technology,* 102**,** 427-436.

COLLINS, P. M. & FERRIER, R. J. 1995. *Monosaccharides : their chemistry and their roles in natural products,* Chichester, Wiley.

CORLEY, R. H. V. 2009. How much palm oil do we need? *Environmental Science & Policy,* 12**,** 134-139.

DE LA TORRE UGARTE, D. & HE, L. 2007. Is the expansion of biofuels at odds with the food security of developing countries? *Biofuels, Bioproducts & Biorefining.,* 1**,** 92-102.
DEJAEGHER, B. & VANDER HEYDEN, Y. 2011. Experimental designs and their recent advances in set-up, data interpretation, and analytical applications. *Journal of Pharmaceutical and Biomedical Analysis,* 56**,** 141-158.
DESWARTE, F., CLARK, J., WILSON, A., HARDY, J., MARRIOTT, R., CHAHAL, S., JACKSON, C., HESLOP, G., BIRKETT, M., BRUCE, T. & WHITELEY, G. 2007. Toward an integrated straw-based biorefinery. *Biofuels, Bioproducts & Biorefining,* 1**,** 245-254.
DICKINSON, E. 2010. Food emulsions and foams: Stabilization by particles. *Current Opinion in Colloid & Interface Science,* 15**,** 40-49.
DONOHOE, B., DECKER, S., TUCKER, M., HIMMEL, M. & VINZANT, T. 2008. Visualizing lignin coalescence and migration through maize cell walls following thermochemical pretreatment. *Biotechnology and Bioengineering,* 101**,** 913-925.
DRENNAN, M. J., ALTAWASH, M. & LESTRANGE, J. L. 1982. Sodium-Hydroxide Treatment of Straw .1. Effect of Straw Treatment on the Intake and Performance of Cattle. *Irish Journal of Agricultural and Food Research,* 21**,** 249-259.
DU, Z., BILBAO-MONTOYA, M. P., BINKS, B. P., DICKINSON, E., ETTELAIE, R. & MURRAY, B. S. 2003. Outstanding Stability of Particle-Stabilized Bubbles. *Langmuir,* 19**,** 3106-3108.
DUTTA, S., DE, S., SAHA, B. & ALAM, M. I. 2012. Advances in conversion of hemicellulosic biomass to furfural and upgrading to biofuels. *Catalysis Science & Technology*, 2, 2025-2036.
EDSER, C. 2006. Charting palm oil's progress towards sustainability. *Focus on Surfactants,* 2006**,** 1-2.
EDSER, C. 2007. Let's concentrate (on laundry detergents). *Focus on Surfactants,* 2007**,** 1-2.
EUROMONITOR INTERNATIONAL 2011a. Category Briefing: Laundry Care in China. Euromonitor International.
EUROMONITOR INTERNATIONAL 2011b. Category Briefing: Laundry Care in India. Euromonitor International.
EVANS, A., STREZOV, V. & EVANS, T. J. 2010. Sustainability considerations for electricity generation from biomass. *Renewable & Sustainable Energy Reviews,* 14**,** 1419-1427.
EVANS, D. E. & BAMFORTH, C. W. 2009. *In: Beer*, *8,* CHARLES, W. B., INGE, R. & GRAHAM, S. (eds.). San Diego: Academic Press.
FERNÁNDEZ, S. S., PADILLA, A. P. & MUCCIARELLI, S. 1999. Protein extraction from Atriplex lampa leaves: Potential use as forage for animals used for human diets. *Plant Foods for Human Nutrition,* 54**,** 251-259.
FIRATLIGIL-DURMUS, E. & EVRANUZ, O. 2010. Response surface methodology for protein extraction optimization of red pepper seed (Capsicum frutescens). *LWT - Food Science and Technology,* 43**,** 226-231.
FOX, D., GRAY, P., DUNN, N. & MARSDEN, W. 1987. Factors affecting the enzymic susceptibility of alkali and acid pretreated sugar-cane bagasse. *Journal of Chemical Technology and Biotechnology,* 40**,** 117-132.
FOYLE, T., JENNINGS, L. & MULCAHY, P. 2007. Compositional analysis of lignocellulosic materials: Evaluation of methods used for sugar analysis of waste paper and straw. *Bioresource Technology,* 98**,** 3026-3036.
FRANKE, D. & PAHL, M. H. 1997. Breakdown of a foam lamella. *Chemical Engineering and Processing,* 36**,** 175-183.
GARRETT, P. R. 1993. Recent developments in the understanding of foam generation and stability. *Chemical Engineering Science,* 48**,** 367-392.

GAUTIER, F., DESTRIBATS, M., PERRIER-CORNET, R., DECHEZELLES, J.-F., GIERMANSKA, J., HEROGUEZ, V., RAVAINE, S., LEAL-CALDERON, F. & SCHMITT, V. 2007. Pickering emulsions with stimulable particles: from highly- to weakly-covered interfaces. *Physical Chemistry Chemical Physics,* 9**,** 6455-6462.

GRAHAM, D. E. & PHILLIPS, M. C. 1979. Proteins at liquid interfaces : I. Kinetics of adsorption and surface denaturation. *Journal of Colloid and Interface Science,* 70**,** 403-414.

GUAN, X. & YAO, H. 2008. Optimization of Viscozyme L-assisted extraction of oat bran protein using response surface methodology. *Food Chemistry,* 106**,** 345-351.

GUO, X., ZOU, X. & SUN, M. 2010. Optimization of extraction process by response surface methodology and preliminary characterization of polysaccharides from Phellinus igniarius. *Carbohydrate Polymers,* 80**,** 344-349.

HANSMA, H. G. & PIETRASANTA, L. 1998. Atomic force microscopy and other scanning probe microscopies. *Current Opinion in Chemical Biology,* 2**,** 579-584.

HARBERS, L. H., KREITNER, G. L., DAVIS, G. V., RASMUSSEN, M. A. & CORAH, L. R. 1982. Ruminal Digestion of Ammonium Hydroxide-Treated Wheat Straw Observed by Scanning Electron-Microscopy. *Journal of Animal Science,* 54**,** 1309-1319.

HENDRIKS, A. T. W. M. & ZEEMAN, G. 2009. Pretreatments to enhance the digestibility of lignocellulosic biomass. *Bioresource Technology,* 100**,** 10-18.

HIRST, E. L. 1962. The Structure of the Hemicelluloses. *Pure Applied Chemistry,* 5**,** 53-56.

HOLT, S. A., MCGILLIVRAY, D. J., POON, S. & WHITE, J. W. 2000. Protein Deformation and Surfactancy at an Interface. The *Journal of Physical Chemistry B,* 104**,** 7431-7438.

HOLTZAPPLE, M. T., DAVISON, R. R. & NAGWANI, M. 1997. *Calcium hydroxide pretreatment of biomass*, US5693296.

HOORFAR, M., KURZ, M. A. & NEUMANN, A. W. 2005. Evaluation of the surface tension measurement of axisymmetric drop shape analysis (ADSA) using a shape parameter. *Colloids and Surfaces A,* 260**,** 277-285.

HROMADKOVA, Z., EBRINGEROVA, A. & MALOVIKOVA, A. 2005. The Structural, Molecular and Functional Properties of Lignin-Containing Beechwood Glucuronoxylan. *Macromolecular Symposia,* 232**,** 19-26.

HSU, F.-L. G., ZHU, Y. P., PADRON, T. & WOELFEL, K. J. 2006. *Liquid laundry detergent with polyanionic ammonium surfactant*, WO2005026302 A1.

HUDSON, P., LANT, N., BROOKER, A. & SOMMERVILLE-ROBERTS, N. 2009. *Cleaning composition containing hemicellulose*, EP 2 336 283 B1.

HUNTER, T. N., PUGH, R. J., FRANKS, G. V. & JAMESON, G. J. 2008. The role of particles in stabilising foams and emulsions. *Advances in Colloid and Interface Science,* 137**,** 57-81.

HUSBAND, F. A., GARROOD, M. J., MACKIE, A. R., BURNETT, G. R. & WILDE, P. J. 2001. Adsorbed Protein Secondary and Tertiary Structures by Circular Dichroism and Infrared Spectroscopy with Refractive Index Matched Emulsions. *Journal of Agricultural and Food Chemistry,* 49**,** 859-866.

IBRAHIM, M. M., EL-ZAWAWY, W. K., ABDEL-FATTAH, Y. R., SOLIMAN, N. A. & AGBLEVOR, F. A. 2011. Comparison of alkaline pulping with steam explosion for glucose production from rice straw. *Carbohydrate Polymers,* 83**,** 720-726.

JARAMILLO-CARMONA, S., FUENTES-ALVENTOSA, J. M., RODRÍGUEZ-GUTIÉRREZ, G., WALDRON, K. W., SMITH, A. C., GUILLÉN-BEJARANO, R., FERNÁNDEZ-BOLAÑOS, J., JIMÉNEZ-ARAUJO, A. & RODRÍGUEZ-ARCOS, R. 2008. Characterization of Asparagus Lignin by HPLC. *Journal of Food Science,* 73**,** C526-C532.

JONES, O. G. & MCCLEMENTS, D. J. 2011. Recent progress in biopolymer nanoparticle and microparticle formation by heat-treating electrostatic protein–polysaccharide complexes. *Advances in Colloid and Interface Science,* 167**,** 49-62.

JORGENSEN, L., VAN DE WEERT, M., VERMEHREN, C., BJERREGAARD, S. & FROKJAER, S. 2004. Probing structural changes of proteins incorporated into water-in-oil emulsions. *Journal of Pharmaceutical Sciences,* 93**,** 1847-1859.

KANAI, R. & EDWARDS, G. E. 1999. *In: C4 Plant Biology*, *49-87,* ROWAN, F. S. & RUSSELL, K. M. (eds.). San Diego: Academic Press.

KASTURI, C., SCHAFER, M. G., SIVIK, M. R., KLUESENER, B. W., SCHEPER, W. M., BERGER, P. S. & BODET, J.-F. 2005. *Detergent composition comprising polymeric suds volume and suds duration enhancers*, US6903064.

KNILL, C. J. & KENNEDY, J. F. 2003. Degradation of cellulose under alkaline conditions. *Carbohydrate Polymers,* 51**,** 281-300.

KNORR, J. R. E., NJ), , HEPLER, B. S. B. B., NJ), & HOLMGREN, M. S., NJ). 2001. *Laundry detergent composition containing level protease enzyme*. US6235697.

KOH, L. P. & WILCOVE, D. S. 2009. Oil palm: disinformation enables deforestation. *Trends in Ecology & Evolution,* 24**,** 67-8.

KOSCHUH, W., POVODEN, G., THANG, V. H., KROMUS, S., KULBE, K. D., NOVALIN, S. & KROTSCHECK, C. 2004. Production of leaf protein concentrate from ryegrass (Lolium perenne x multiflorum) and alfalfa (Medicago sauva subsp. sativa). Comparison between heat coagulation/centrifugation and ultrafiltration. *Desalination,* 163**,** 253-259.

KRISTENSEN, J., THYGESEN, L., FELBY, C., JORGENSEN, H. & ELDER, T. 2008. Cell-wall structural changes in wheat straw pretreated for bioethanol production. *Biotechnology for Biofuels.*

KUDRYASHOVA, E. V., MEINDERS, M. B., VISSER, A. J., VAN HOEK, A. & DE JONGH, H. H. 2003. Structure and dynamics of egg white ovalbumin adsorbed at the air/water interface. *European Biophysics Journal,* 32**,** 553-562.

LAPIERRE, C., JOUIN, D. & MONTIES, B. 1989. On the molecular origin of the alkali solubility of Gramineae lignins. *Phytochemistry,* 28**,** 1401-1403.

LAWTHER, J. M., SUN, R. C. & BANKS, W. B. 1996a. Effects of extraction conditions and alkali type on yield and composition of wheat straw hemicellulose. *Journal of Applied Polymer Science,* 60**,** 1827-1837.

LAWTHER, J. M., SUN, R. C. & BANKS, W. B. 1996b. Rapid isolation and structural characterization of alkali-soluble lignins during alkaline treatment and atmospheric refining of wheat straw. *Industrial Crops and Products,* 5**,** 97-105.

LELAND, W. 2006. Revising the Pareto Chart. *The American Statistician,* 60**,** 332-334.

LESTARI, D., MULDER, W. & SANDERS, J. 2010. Improving Jatropha curcas seed protein recovery by using counter current multistage extraction. *Biochemical Engineering Journal,* 50**,** 16-23.

LIMAGE, S., SCHMITT, M., VINCENT-BONNIEU, S., DOMINICI, C. & ANTONI, M. 2010. Characterization of solid-stabilized water/oil emulsions by scanning electron microscopy. *Colloids and Surfaces A,* 365**,** 154-161.

LIN, I. J. 1972. Hydrophile-lipophile balance (hlb) of fluorocarbon surfactants and its relation to the critical micelle concentration (cmc). The *Journal of Physical Chemistry,* 76**,** 2019-2023.

LU, J. R., SU, T. J. & THOMAS, R. K. 1999. Structural Conformation of Bovine Serum Albumin Layers at the Air–Water Interface Studied by Neutron Reflection. *Journal of Colloid and Interface Science,* 213**,** 426-437.

LU, J. R., SU, T. J., THOMAS, R. K., PENFOLD, J. & WEBSTER, J. 1998. Structural conformation of lysozyme layers at the air/water interface studied by neutron reflection. *Journal of the Chemical Society, Faraday Transactions,* 94**,** 3279-3287.

MA, T., WANG, Q. & WU, H. 2010. Optimization of extraction conditions for improving solubility of peanut protein concentrates by response surface methodology. *LWT - Food Science and Technology,* 43**,** 1450-1455.

MACDONALD, D., BAKHSHI, N., MATHEWS, J., ROYCHOWDHURY, A., BAJPAI, P. & MOO-YOUNG, M. 1983. Alkali treatment of corn stover to improve sugar production by enzymatic hydrolysis. *Biotechnology and Bioengineering,* 25**,** 2067-2076.

MARCOMINI, A., FILIPUZZI, F. & GIGER, W. 1988. Aromatic surfactants in laundry detergents and hard-surface cleaners: Linear alkylbenzenesulphonates and alkylphenol polyethoxylates. *Chemosphere,* 17**,** 853-863.

MARTIN, A. H., GROLLE, K., BOS, M. A., STUART, M. A. C. & VAN VLIET, T. 2002. Network Forming Properties of Various Proteins Adsorbed at the Air/Water Interface in Relation to Foam Stability. *Journal of Colloid and Interface Science,* 254**,** 175-183.

MARTINEZ, J., VIVES-REGO, J. & SANCHEZ-LEAL, J. 1989. The effect of chemical structure and molecular weight of commercial alkylbenzenes on the toxic response of Daphnia and naturally occurring bacteria in fresh and seawater. *Water Research,* 23**,** 569-572.

MATUS, K. J. M., CLARK, W. C., ANASTAS, P. T. & ZIMMERMAN, J. B. 2012. Barriers to the Implementation of Green Chemistry in the United States. *Environmental Science & Technology*, 46 (20), 10892 - 10899.

MCCARTNEY, D. H., BLOCK, H. C., DUBESKI, P. L. & OHAMA, A. J. 2006. Review: The composition and availability of straw and chaff from small grain cereals for beef cattle in western Canada. *Canadian Journal of Animal Science,* 86**,** 443-455.

MCMURRY, J. 2004. *Organic Chemistry,* Belmont, CA, Brooks/Cole.

MEINDERS, M. B. J. & DE JONGH, H. H. J. 2002. Limited conformational change of β-lactoglobulin when adsorbed at the air–water interface. *Biopolymers,* 67**,** 319-322.

MILEVA, E. & EXEROWA, D. 2008. Amphiphilic nanostructures in foam films. *Current Opinion in Colloid & Interface Science,* 13**,** 120-127.

MILLS, C., GAO, C., WILDE, P. J., RIGBY, N. M., WIJESINHA-BETTONI, R., JOHNSON, V. E., SMITH, L. J. & MACKIE, A. R. 2009. Partially Folded Forms of Barley Lipid Transfer Protein Are More Surface Active. *Biochemistry,* 48**,** 12081-12088.

MONTGOMERY, D. C. 1997. *Design and Analysis of Experiments, 37,110*, John Wiley & Sons.

MORITA, S. 2007. *Roadmap of scanning probe microscopy [Electronic book], 19,* Berlin ; New York, Springer.

MORRISON, I. M. 1973. Isolation and analysis of lignin-carbohydrate complexes from Lolium multiflorum. *Phytochemistry,* 12**,** 2979-2984.

MORRISON, I. M. 1974a. Lignin-carbohydrate complexes from Lolium perenne. *Phytochemistry,* 13**,** 1161-1165.

MORRISON, I. M. 1974b. Structural investigations on lignin-carbohydrate complexes of lolium-perenne. *Biochemical Journal,* 139**,** 197-204.

MOSIER, N., WYMAN, C., DALE, B., ELANDER, R., LEE, Y. Y., HOLTZAPPLE, M. & LADISCH, M. 2005. Features of promising technologies for pretreatment of lignocellulosic biomass. *Bioresource Technology,* 96**,** 673-686.

MUETZEL, S. & BECKER, K. 2006. Extractability and biological activity of tannins from various tree leaves determined by chemical and biological assays as affected by drying procedure. *Animal Feed Science and Technology,* 125**,** 139-149.

MURRAY, B. S. & ETTELAIE, R. 2004. Foam stability: proteins and nanoparticles. *Current Opinion in Colloid & Interface Science,* 9**,** 314-320.

NADJI, H., BRUZZÈSE, C., BELGACEM, M. N., BENABOURA, A. & GANDINI, A. 2005. Oxypropylation of Lignins and Preparation of Rigid Polyurethane Foams from the Ensuing Polyols. *Macromolecular Materials and Engineering,* 290**,** 1009-1016.

NADJI, H., DIOUF, P. N., BENABOURA, A., BEDARD, Y., RIEDL, B. & STEVANOVIC, T. 2009. Comparative study of lignins isolated from Alfa grass (Stipa tenacissima L.). *Bioresource Technology,* 100**,** 3585-3592.

NAGY, S., TELEK, L., HALL, N. T. & BERRY, R. E. 1978. Potential food uses for protein from tropical and subtropical plant leaves. *Journal of Agricultural and Food Chemistry,* 26**,** 1016-1028.

OCTAVE, S. & THOMAS, D. 2009. Biorefinery: Toward an industrial metabolism. *Biochimie,* 91**,** 659-664.

OLARTE, M. V. 2001. *Base-catalyzed depolymerization of lignin and hydrodeoxidation of lignin model compounds for alternative fuel production.* Doctor of Philosophy, Georgia Institute of Technology

PAL, A. & CHAUHAN, N. 2009. Volumetric, viscometric, and acoustic behaviour of diglycine in aqueous saccharide solutions at different temperatures. *Journal of Molecular Liquids,* 149**,** 29-36.

PICKERING, S. U. 1907. CXCVI.-Emulsions. *Journal of the Chemical Society, Transactions,* 91**,** 2001-2021.

PROCTER AND GAMBLE. 2012. *Products & Packaging* [Online]. Available: http://www.pg.com/en_US/sustainability/environmental_sustainability/products_packaging/index.shtml [Accessed 12th September 2012].

RATHMANN, R., SZKLO, A. & SCHAEFFER, R. 2010. Land use competition for production of food and liquid biofuels: An analysis of the arguments in the current debate. *Renewable Energy,* 35**,** 14-22.

RODRIGUES, J. A., RIO, E., BOBROFF, J., LANGEVIN, D. & DRENCKHAN, W. 2011. Generation and manipulation of bubbles and foams stabilised by magnetic nanoparticles. *Colloids and Surfaces A,* 384**,** 408-416.

ROJAS, O. J., BULLÓN, J., YSAMBERTT, F., FORGIARINI, A., SALAGER JEAN, L. & ARGYROPOULOS DIMITRIS, S. 2007. *In: Materials, Chemicals, and Energy from Forest Biomass*, *182-199*. American Chemical Society.

ROLFES, T. R. 1999. *Laundry detergent bar containing soap, and methylester sulfonate surfactants*, US5972861.

ROUNTABLE ON SUSTAINABLE PALM OIL. 2012. *Who is RSPO?* [Online]. Available: http://www.rspo.org/en/who_is_rspo [Accessed Accessed 10th August 2012].

SAAD, S. M. I., POLICOVA, Z. & NEUMANN, A. W. 2011. Design and accuracy of pendant drop methods for surface tension measurement. *Colloids and Surfaces A,* 384**,** 442-452.

SAHA, B. C. & COTTA, M. A. 2007. Enzymatic hydrolysis and fermentation of lime pretreated wheat straw to ethanol. *Journal of Chemical Technology and Biotechnology,* 82**,** 913-919.

SAHA, B. C. & COTTA, M. A. 2008. Lime pretreatment, enzymatic saccharification and fermentation of rice hulls to ethanol. *Biomass & Bioenergy,* 32**,** 971-977.

SAIDUR, R., ABDELAZIZ, E. A., DEMIRBAS, A., HOSSAIN, M. S. & MEKHILEF, S. 2011. A review on biomass as a fuel for boilers. *Renewable & Sustainable Energy Reviews,* 15**,** 2262-2289.

SANI, A. M. & MOHANTY, K. K. 2009. Incorporation of clay nano-particles in aqueous foams. *Colloids and Surfaces A,* 340**,** 174-181.

SAOUTER, E. 2002. Laundry Detergents: Cleaner Clothes and a Cleaner Environment. *Corporate Environmental Strategy,* 9**,** 40-51.

SAULNIER, L., MAROT, C., CHANLIAUD, E. & THIBAULT, J.-F. 1995. Cell wall polysaccharide interactions in maize bran. *Carbohydrate Polymers,* 26**,** 279-287.

SCHMIDT, I., NOVALES, B., BOUE, F. & AXELOS, M. A. 2010. Foaming properties of protein/pectin electrostatic complexes and foam structure at nanoscale. *Journal of Colloid and Interface Science,* 345**,** 316-324.

SELIG, M. J., VIAMAJALA, S., DECKER, S. R., TUCKER, M. P., HIMMEL, M. E. & VINZANT, T. B. 2007. Deposition of Lignin Droplets Produced During Dilute Acid Pretreatment of Maize Stems Retards Enzymatic Hydrolysis of Cellulose. *Biotechnology Progress,* 23**,** 1333-1339.

SETHUMADHAVAN, G., NIKOLOV, A. & WASAN, D. 2004. Stability of films with nanoparticles. *Journal of Colloid and Interface Science,* 272**,** 167-171.

SETHUMADHAVAN, G. N., NIKOLOV, A. D. & WASAN, D. T. 2001. Stability of Liquid Films Containing Monodisperse Colloidal Particles. *Journal of Colloid and Interface Science,* 240**,** 105-112.

SHAFIEE, S. & TOPAL, E. 2009. When will fossil fuel reserves be diminished? *Energy Policy,* 37**,** 181-189.

SHAFIEE, S. & TOPAL, E. 2010. A long-term view of worldwide fossil fuel prices. *Applied Energy,* 87**,** 988-1000.

SHAO, Z. & ZHANG, Y. 1996. Biological cryo atomic force microscopy: a brief review. *Ultramicroscopy,* 66**,** 141-152.

SHELUDKO, A. 1967. Thin liquid films. *Advances in Colloid and Interface Science,* 1**,** 391-464.

SHULGA, G., SHAKELS, V., SKUDRA, S. & BOGDANOVS, V. Modified lignin as an environmentally friendly surfactant. *In:* 8th International Scientific and Practical Conference, 2011. 276-281.

SILVA, E. A. B. D., ZABKOVA, M., ARAÚJO, J. D., CATETO, C. A., BARREIRO, M. F., BELGACEM, M. N. & RODRIGUES, A. E. 2009. An integrated process to produce vanillin and lignin-based polyurethanes from Kraft lignin. *Chemical Engineering Research and Design,* 87**,** 1276-1292.

SIMÃO, J. P. F., EGAS, A. P. V., CARVALHO, M. G., BAPTISTA, C. M. S. G. & CASTRO, J. A. A. M. 2008. Heterogeneous studies in pulping of wood: Modelling mass transfer of alkali. *Chemical Engineering Journal,* 139**,** 615-621.

SPIERTZ, J. H. J. & EWERT, F. 2009. Crop production and resource use to meet the growing demand for food, feed and fuel: opportunities and constraints. *NJAS - Wageningen Journal of Life Sciences,* 56**,** 281-300.

STEIN, K. 2007. Food vs biofuel. *Journal of the American Dietetic Association,* 107**,** 1870, 1872-6, 1878.

STEVENS, E. S., A. KLAMCZYNSKI, A. & GLENN, G. M. 2010. Starch-lignin foams. *Express Polym Lett,* 4**,** 311-320.

STEVENSON, P. 2010. Inter-bubble gas diffusion in liquid foam. *Current Opinion in Colloid & Interface Science,* 15**,** 374-381.

SUBRAMANIAM, A. B., MEJEAN, C., ABKARIAN, M. & STONE, H. A. 2006. Microstructure, Morphology, and Lifetime of Armored Bubbles Exposed to Surfactants. *Langmuir,* 22**,** 5986-5990.

SUN, R., LAWTHER, J. M. & BANKS, W. B. 1995. Influence of alkaline pre-treatments on the cell wall components of wheat straw. *Industrial Crops and Products,* 4**,** 127-145.

SUN, R., LAWTHER, J. M. & BANKS, W. B. 1997. A tentative chemical structure of wheat straw lignin. *Industrial Crops and Products,* 6**,** 1-8.

SUN, R., TOMKINSON, J., MAO, F. C. & SUN, X. F. 2001. Physicochemical characterization of lignins from rice straw by hydrogen peroxide treatment. *Journal of Applied Polymer Science,* 79**,** 719-732.

SUN, R., TOMKINSON, J., SUN, X. F. & WANG, N. J. 2000. Fractional isolation and physico-chemical characterization of alkali-soluble lignins from fast-growing poplar wood. *Polymer,* 41**,** 8409-8417.

SUN, X. F., XU, F., SUN, R. C., FOWLER, P. & BAIRD, M. S. 2005. Characteristics of degraded cellulose obtained from steam-exploded wheat straw. *Carbohyd Research,* 340**,** 97-106.

SUN, Y. & CHENG, J. 2002. Hydrolysis of lignocellulosic materials for ethanol production: a review. *Bioresource Technology,* 83**,** 1-11.

SVENDSEN, A., PATKAR, S. A., GORMSEN, E., OKKELS, J. S. & THELLERSEN, M. 1999. *Lipase variants*. US5869438.

TALBOT, J., TARJUS, G., VAN TASSEL, P. R. & VIOT, P. 2000. From car parking to protein adsorption: an overview of sequential adsorption processes. *: Physicochemical and Engineering Aspects,* 165**,** 287-324.

TAN, K. T., LEE, K. T., MOHAMED, A. R. & BHATIA, S. 2009. Palm oil: Addressing issues and towards sustainable development. *Renewable & Sustainable Energy Reviews,* 13**,** 420-427.

THIRMAL, C. & DAHMAN, Y. 2012. Comparisons of existing pretreatment, saccharification, and fermentation processes for butanol production from agricultural residues. The *Canadian Journal of Chemical Engineering,* 90**,** 745-761.

VANHOLME, R., MORREEL, K., RALPH, J. & BOERJAN, W. 2008. Lignin engineering. *Current Opinion in Plant Biology,* 11**,** 278-285.

VIGNES-ADLER, M. & WEAIRE, D. 2008. New foams: Fresh challenges and opportunities. *Current Opinion in Colloid & Interface Science,* 13**,** 141-149.

WANG, K. & SUN, R. C. 2012. *In: Industrial Crops and Products*, *33-34,* TOFANICA, B. M. (ed.). Elsevier.

WANG, Z. & NARSIMHAN, G. 2007. Rupture of Draining Foam Films Due to Random Pressure Fluctuations. *Langmuir,* 23**,** 2437-2443.

WARNE, M. S. & SCHIFKO, A. D. 1999. Toxicity of laundry detergent components to a freshwater cladoceran and their contribution to detergent toxicity. *Ecotoxicology and Environmental Safety,* 44**,** 196-206.

WETZSTEIN, M. & WETZSTEIN, H. 2011. Four myths surrounding U.S. biofuels. *Energy Policy,* 39**,** 4308-4312.

WICKE, B., SIKKEMA, R., DORNBURG, V. & FAAIJ, A. 2011. Exploring land use changes and the role of palm oil production in Indonesia and Malaysia. *Land Use Policy,* 28**,** 193-206.

WIEPRECHT, T., XIA, J., HEINZ, U., DANNACHER, J. & SCHLINGLOFF, G. 2003. Novel terpyridine-manganese(II) complexes and their potential to activate hydrogen peroxide. *Journal of Molecular Catalysis A: Chemical,* 203**,** 113-128.

WIERENGA, P. A. & GRUPPEN, H. 2010. New views on foams from protein solutions. *Current Opinion in Colloid & Interface Science,* 15**,** 365-373.

WIERENGA, P. A., MEINDERS, M. B. J., EGMOND, M. R., VORAGEN, F. A. G. J. & DE JONGH, H. H. J. 2003. Protein Exposed Hydrophobicity Reduces the Kinetic Barrier for Adsorption of Ovalbumin to the Air−Water Interface. *Langmuir,* 19**,** 8964-8970.

WIERENGA, P. A., VAN NORÉL, L. & BASHEVA, E. S. 2009. Reconsidering the importance of interfacial properties in foam stability. *Colloids and Surfaces A,* 344**,** 72-78.

WILHELM, W. W. 2008. My biomass, your biomass, our solution. *Biofuels, Bioproducts & Biorefining,* 2**,** 8-11.

XIAO, B., SUN, X. F. & SUN, R. 2001. Chemical, structural, and thermal characterizations of alkali-soluble lignins and hemicelluloses, and cellulose from maize stems, rye straw, and rice straw. *Polymer Degradation and Stability,* 74**,** 307-319.

XU, F., GENG, Z. C., LIU, C. F., REN, J. L., SUN, J. X. & SUN, R. C. 2008. Structural characterization of residual lignins isolated with cyanamide-activated hydrogen peroxide from various organosolvs pretreated wheat straw. *Journal of Applied Polymer Science,* 109**,** 555-564.

YANG, B. & WYMAN, C. E. 2008. Pretreatment: the key to unlocking low-cost cellulosic ethanol. *Biofuels, Bioproducts & Biorefining,* 2**,** 26-40.

YING, G. G. 2006. Fate, behavior and effects of surfactants and their degradation products in the environment. *Environmental International,* 32**,** 417-31.

ZHANG, T. & MARCHANT, R. E. 1996. Novel Polysaccharide Surfactants: The Effect of Hydrophobic and Hydrophilic Chain Length on Surface Active Properties. *Journal of Colloid and Interface Science,* 177**,** 419-426.

ZHOU, W., WANG, Z. L. & SPRINGERLINK 2007. *Scanning microscopy for nanotechnology : techniques and applications, 2-39,* New York ; London, Springer.

ZHU, C. & LIU, X. 2013. Optimization of extraction process of crude polysaccharides from Pomegranate peel by response surface methodology. *Carbohydrate Polymers,* 92**,** 1197-1202.

ZIMMERMAN, J. B. & ANASTAS, P. T. 2006. *In: Sustainability Science and Engineering*, *201-221,* ABRAHAM, M. A. (ed.). Elsevier.